

Université
de Toulouse

THÈSE

En vue de l'obtention du
DOCTORAT DE L'UNIVERSITÉ DE TOULOUSE

Délivré par :
Institut National Polytechnique de Toulouse (INP Toulouse)

Discipline ou spécialité :
Génie des procédés et de l'environnement

Présentée et soutenue par :
Weifeng SHEN

le : vendredi 21 septembre 2012

Titre :
Conception des procédés de distillation extractive continue basée sur des critères de faisabilité thermodynamique de la distillation extractive discontinue

Ecole doctorale :
Mécanique, Énergétique, Génie civil et Procédés (MEGeP)

Unité de recherche :
Laboratoire de Génie Chimique, UR 5503

Directeur(s) de Thèse :

Vincent GERBAUD

Rapporteurs :

Prof. Peter LANG
Prof. Jean-Michel RENAUME

Membre(s) du jury :

Prof. Xavier JOULIA
Prof. Michel MEYER
Ing. Olivier BAUDOUIN

Abstract

We study the continuous extractive distillation of minimum and maximum boiling azeotropic mixtures A-B with a heavy or a light entrainer E, intending to assess its feasibility based on thermodynamic insights. The ternary mixtures belong to the 1.0-1a and 1.0-2 class ternary diagrams, each with two sub-cases depending on the univolatility line location. The column has three sections, rectifying, extractive and stripping. Differential equations are derived for each section composition, depending on operating parameters: distillate product purity and recovery, reflux ratio R and entrainer – feed flow rate ratio F_E/F for the heavy case; bottom product purity and recovery, reboil ratio S and entrainer – feed flow rate ratio for the light entrainer case. For the case with a heavy entrainer fed as a boiling liquid above the main feed, the feasible product and operating parameters R and F_E/F ranges are assessed under infinite reflux ratio conditions by using the general feasibility criterion enounced by Rodriguez-Donis et al. (Ind. Eng. Chem. Res, 2009, 48(7), 3544–3559). For the 1.0-1a class, there exists a minimum entrainer - feed flow rate ratio to recover the product, and also a minimum reflux ratio. The minimum entrainer - feed flow rate ratio is higher for the continuous process than for the batch because of the additional requirement in continuous mode that the stripping profile intersects with the extractive profile. For the 1.0-2 class both A and B can be distilled. For one of them there exists a maximum entrainer - feed flow rate ratio. The continuous process also has a minimum entrainer - feed flow rate ratio limit for a given feasible reflux ratio.

For the case with a light entrainer fed as saturated vapor below the main feed, the feasible product and operating parameters S and F_E/F ranges are assessed under infinite reflux ratio conditions by using the general feasibility criterion enounced by Rodriguez-Donis et al. (Ind. Eng. Chem. Res, 2012, 51, 4643–4660). Compared to the heavy entrainer case, the main product is removed from the column bottom. Similar results are obtained for the 1.0-1a and 1.0-2 class mixtures whether the entrainer is light or heavy. With a light entrainer, the batch insight about the process feasibility holds for the stripping and extractive sections. Now, an additional constraint in continuous mode comes from the necessary intersection between the rectifying and the extractive sections.

This work validates the proposed methodology for assessing the feasibility of continuous extractive distillation processes and enables to compare entrainers in terms of minimum reflux ratio and minimum entrainer feed flow rate ratio.

Keywords

Extractive distillation – feasibility – thermodynamic insight – univolatility line - unidistribution line - reflux ratio – entrainer - feed flow rate ratio – reboil ratio – heavy entrainer – light entrainer

Résumé

Nous étudions la faisabilité du procédé de distillation extractive continue pour séparer des mélanges azéotropiques A-B à température de bulle minimale ou maximale, avec un tiers corps E lourd ou léger. Les mélanges ternaires A-B-E appartiennent aux classes 1.0-1-a et 1.0-2 qui se subdivisent chacune en deux sous-cas selon la position de la courbe d'univolatilité. La colonne de distillation a trois sections, rectification, extractive, épuisement. Nous établissons les équations décrivant les profils de composition liquide dans chaque section en fonction des paramètres opératoires: pureté et taux de récupération du distillat, taux de reflux ratio R et rapport des débits d'alimentation F_E/F dans le cas d'un tiers corps lourd; pureté et taux de récupération du produit de pied, taux de rebouillage S et rapport des débits d'alimentation F_E/F dans le cas d'un tiers corps léger.

Avec un tiers corps lourd alimenté comme liquide bouillant au dessus de l'étage d'alimentation du mélange A-B, nous identifions le distillat atteignable et les plages de valeurs faisables des paramètres R et F_E/F à partir du critère général de faisabilité énoncé par Rodriguez-Donis et al. (Ind. Eng. Chem. Res, 2009, 48(7), 3544–3559). Pour la classe 1.0-1a, il existe des rapports F_E/F et reflux ratio minimum. Le rapport F_E/F est plus important pour le procédé continu que pour le procédé discontinu parce que la faisabilité du procédé continu nécessite que les profils d'épuisement et extractifs s'intersectent. Pour la classe 1.0-2, les deux constituants A et B sont des distillats potentiels, l'un sous réserve que le rapport F_E/F reste inférieur à une valeur limite maximale. Le procédé continu exhibe également une valeur minimale de F_E/F à un taux de reflux ratio donné, contrairement au procédé discontinu.

Avec un tiers corps léger alimenté comme vapeur saturante sous l'étage d'alimentation du mélange A-B, nous identifions le produit de pied atteignable et les plages de valeurs faisables des paramètres S et F_E/F à partir du critère général de faisabilité énoncé par Rodriguez-Donis et al. (Ind. Eng. Chem. Res, 2012, 51, 4643–4660). Comparé au cas des tiers corps lourds, le produit principal est obtenu en pied. Autrement, les comportements des classes 1.0-1a et 1.0-2 sont analogues entre les tiers corps léger et lourd. Avec un tiers corps léger, le procédé continu ajoute la contrainte que les profils de rectification et extractifs s'intersectent. La contrainte d'intersection des profils d'épuisement et extractif est partagée par les deux modes opératoires continu et discontinu.

Ce travail valide la méthodologie proposée pour évaluer la faisabilité du procédé de distillation extractive continue et permet de comparer les tiers entre eux en termes de taux de reflux ratio minimum et de rapport de débit d'alimentation minimal.

Mots-clés

Distillation extractive - courbes d'univolatilité - taux de reflux ratio - taux de solvant - entraîneur lourde - entraîneur léger

Acknowledgements

My deepest gratitude goes first and foremost to my supervisor Mr. Vincent GERBAUD, Chargé de recherche CNRS, for his constant encouragement and guidance. I really admire his wonderful and intriguing personality, his preciseness, patience, persistence, high requirements and great interest on research, his mind always abounded with new and effective idea, his courage to explore extensive different fields. He has walked me through all the stages of this thesis no matter weekends and evenings, without his consistent and illuminating instruction, this thesis would not have reached its present form.

I should like to acknowledge with deep gratitude the assistance and guidance given to me by Miss Hassiba BENYOUNES, lecturer of Université Des Sciences et Technologies. Oran, Algeria. I would also like to highlight the contribution of Ms. Ivonne Rodriguez-Donis, Prof. of Instituto Superior de Tecnologías y Ciencias Aplicadas, Cuba. It has been a pleasure collaborating with them and I sincerely appreciate their warm and cordial personalities. My heartfelt thanks are also due to their patience, encouragement, and professional instructions during my research activities.

I am also indebted to prof. Peter LANG of Budapest University of Technology and Economics, Faculty of Mechanical Engineering, Hungary, and prof. Jean Michel RENEAUME of Université de Pau et des Pays de l'Adour, France. Both of them are reviewers of this thesis. I thank them for spending time to give constructive suggestions, and kindly eliminate many of the errors in it, which are of help and importance in making the thesis a reality.

I am also honored by the presence of prof. Xavier JOULIA, co-founder and board member of Prosim Company who has so kindly accepted to be a part of the jury. Likewise, I would like to thank Mr. Michel MEYER, excellent professor of laboratoire de Génie Chimique, Dr. Olivier BAUDOUIN, head of process operation at Prosim. All of them have graciously accepted to be a member of the jury.

Last but not the least, my gratitude also extends to my dear colleagues and friends: Ali, Juliette, Sofia, Eduardo, Guillermo, László, Raul, Ferenc, ElAwady, Anthony, Moises, Meryem, Jean-Stephane, Fernando, René, Marco, Sayed, Nishant, Jesus, Marianne, Mary, Tibor, Adama, Marie, Mayra, Nguyen, Marie Roland and many others, without them I cannot have so happy, colorful, and wonderful life in France.

Weifeng SHEN

Toulouse

Table of contents

Chapter Content

1. GENERAL INTRODUCTION	1
GENERAL INTRODUCTION	2
2. STATE OF THE ART, METHODOLOGY, OBJECTIVES	7
2.1 INTRODUCTION	8
2.2 PHASE EQUILIBRIUM	8
2.2.1 <i>Phase equilibrium equations</i>	8
2.2.2 <i>Activity coefficient model</i>	9
2.2.3 <i>Non ideality of the mixture</i>	11
2.2.4 <i>Residue curve</i>	13
2.2.5 <i>Unidistribution and relative volatility</i>	14
2.2.6 <i>Ternary VLE diagrams classification</i>	19
2.3 THE DISTILLATION PROCESS AND ITS IMPROVEMENT	22
2.3.1 <i>Highly integrated distillation columns</i>	23
2.3.2 <i>Vapor recompression distillation</i>	24
2.3.3 <i>Petlyuk arrangements</i>	25
2.4 NONIDEAL MIXTURES SEPARATION	26
2.4.1 <i>Pressure-swing distillation</i>	27
2.4.2 <i>Azeotropic distillation</i>	29
2.4.3 <i>Reactive distillation</i>	30
2.4.4 <i>Salt-effect distillation</i>	31
2.4.5 <i>Extractive distillation</i>	31
2.5 LITERATURE STUDIES ON EXTRACTIVE DISTILLATION	32
2.5.1 <i>Extractive Batch Column configurations</i>	32
2.5.2 <i>Continuous Column configurations</i>	34
2.5.3 <i>Entrainer design</i>	35

2.5.4	<i>Key operating parameters</i>	36
2.6	METHODOLOGY FOR EXTRACTIVE DISTILLATION PROCESS FEASIBILITY IN RESEARCH	36
2.6.1	<i>Ternary systems studied in extractive distillation</i>	37
2.6.2	<i>Batch extractive process operation policies and strategy</i>	41
2.6.3	<i>Thermodynamic insight on extractive distillation feasibility</i>	45
2.6.4	<i>Topological features related to process operation</i>	46
2.6.5	<i>Extractive process feasibility assessed from intersection of composition profiles and differential equation</i>	53
2.6.6	<i>Extractive process feasibility from pinch points analysis</i>	54
2.6.7	<i>Feasibility validation by rigorous simulation assessment</i>	56
2.7	RESEARCH OBJECTIVES	57
3.	EXTENSION OF THERMODYNAMIC INSIGHTS ON BATCH EXTRACTIVE DISTILLATION TO CONTINUOUS OPERATION. AZEOTROPIC MIXTURES WITH A HEAVY ENTRAINER	61
3.1	INTRODUCTION	62
3.2	COLUMN CONFIGURATION AND OPERATION	62
3.3	FEASIBILITY STUDY METHODOLOGY	63
3.3.1	<i>Thermodynamic feasibility criterion for 1.0-1a and 1.0-2 ternary diagram classes</i>	63
3.3.2	<i>Computation of section composition profiles</i>	66
3.3.3	<i>Methodology for assessing the feasibility</i>	68
3.4	RESULTS AND DISCUSSION	70
3.4.1	<i>Separation of minimum boiling temperature azeotrope with heavy entrainers (Class 1.0-1a)</i>	70
3.4.2	<i>Separation of maximum boiling temperature azeotropes with heavy entrainers (class 1.0-2)</i>	83
3.5	CONCLUSIONS	96
4.	EXTENSION OF THERMODYNAMIC INSIGHTS ON BATCH EXTRACTIVE DISTILLATION TO CONTINUOUS OPERATION. AZEOTROPIC MIXTURES WITH A LIGHT ENTRAINER	95
4.1	INTRODUCTION	100
4.2	STATE OF THE ART WITH LIGHT ENTRAINER	101
4.3	COLUMN CONFIGURATION AND OPERATION	103
4.4	EXTRACTIVE DISTILLATION FEASIBILITY ASSESSMENT	104
4.5	FEASIBILITY STUDY METHODOLOGY	106
4.5.1	<i>Thermodynamic feasibility criterion for 1.0-1a and 1.0-2 ternary diagram classes</i>	106
4.5.2	<i>Calculation of reboil ratio vs. entrainer - feed flow rate ratio diagrams</i>	109

4.6	RESULTS	116
4.6.1	<i>Separation of Maximum Boiling Temperature Azeotropes with light Entrainers (Class 1.0-1a).</i>	116
4.6.2	<i>Separation of Minimum Boiling Temperature Azeotropes with Light Entrainers (class 1.0-2).</i>	127
4.7	CONCLUSIONS	138
5.	CONCLUSIONS, PERSPECTIVE	143
5.1	CONCLUSIONS.....	144
5.2	PERSPECTIVE	150
6.	APPENDIX: NOMENCLATURE, REFERENCE	151
6.1	NOMENCLATURE.....	152
6.2	REFERENCES	155

Figure content

<i>Figure 2.1. Typical homogeneous mixtures without azeotrope.....</i>	11
<i>Figure 2.2. Typical homogeneous mixtures with maximum boiling azeotrope, a negative deviation from Raoult's law</i>	12
<i>Figure 2.3. Typical homogeneous mixtures with minimum boiling azeotrope, a positive deviation from Raoult's law</i>	12
<i>Figure 2.4. Typical homogeneous minimum boiling heteroazeotrope.....</i>	12
<i>Figure 2.5 Condition of tangency between a residue curve and its corresponding distillate curve.....</i>	14
<i>Figure 2.6 Feasible patterns of the VLE functions for binary mixtures of components 1 and 2: (a) equilibrium line $y(x)$, (b) distribution coefficients $K_i(x)$ and $K_j(x)$, (c) relative volatility $\alpha_{ij}(x)$ and (d) distribution coefficient trajectories for a mixture 1-2-3 with minimum-boiling azeotrope 1-2 (Kiva et al., 2003).</i>	17
<i>Figure 2.7 Unidistribution and univolatility line diagrams for the most probable classes of ternary mixtures according to Reshetov's statistics (Kiva et al., 2003).</i>	18
<i>Figure 2.8 Azeotropic ternary mixture: Serafimov's 26 topological classes and Reshetov's statistics (Hilmen et al., 2002). (o) unstable node, (Δ) saddle, (\bullet) stable.....</i>	20
<i>Figure 2.9 Occurrence of classes from published data for ternary mixtures based on Reshetov's statistics 1965-1988 (Kiva et al., 2003).</i>	21
<i>Figure 2.10 Ternary zeotropic mixtures Classes of diagrams of K-ordered regions for unilateral and bilateral univolatility α-lines, respectively; 123, 132, 213, ..., indices of K-ordered regions.....</i>	22
<i>Figure 2.11. (a) Schematic diagram of HIDiC (Fukushima et al., 2006) and (b) HIDiC concentric tube column (From PSE's Gproms manual, gP-B-611--051028 DR).....</i>	23
<i>Figure 2.12 Schematic diagram of (1) direct vapor recompression distillation (1: distillation column, 2: compressor, 3: reboiler–condenser and 4: expansion valve) and (2) external vapor recompression distillation (1: distillation column, 2,3: heat exchangers, 4: compressor and 5: expansion valve). (from Jogwar and Daoutidis, 2009).</i>	24
<i>Figure 2.13 Schematic diagram of the fully thermally coupled (Petlyuk) arrangement (a) replaces the conventional arrangements with a prefractionator and a main column, and only a single reboiler and a single condenser is needed and (b) dividing wall configuration by moving the prefractionator into the same shell (from Halvorsen and Skogestad, 2011).</i>	25
<i>Figure 2.14 Effect of pressure on the azeotropic composition and corresponding continuous pressure-swing distillation processes (from Gerbaud and Rodriguez-Donis, 2010).</i>	28
<i>Figure 2.15 Indirect separation (a) and direct (b) azeotropic continuous distillation under finite for a 1.0-2 class mixture (from Gerbaud and Rodriguez-Donis, 2010).</i>	30

Figure 2.16 Configurations of extractive batch distillation column in rectifier and stripper	33
Figure 2.17. Flowsheet of typical extractive distillation with (a) heavy entrainer and (b) light entrainer.....	34
Figure 2.18 Configurations for the heterogeneous distillation column considering all possibilities for both the entrainer recycle and the main azeotropic feed. (from Rodriguez-Donis et al. 2007)	35
Figure 2.19 Topological features related to extractive distillation process operation of class 1.0-1a when using a heavy entrainer (Rodriguez-Donis et al., 2009a).	47
Figure 2.20 Topological features related to the extractive distillation process operation of class 1.0-2 when using a heavy entrainer.....	52
Figure 2.21 The equilibrium stage: (a) component mass flows and (b) stream energy flows	56
Figure 3.1 Configurations of extractive distillation column: (a) continuous (b) batch.....	63
Figure 3.2 Thermodynamic features of 1.0-1a mixtures with respect to batch extractive distillation. Separation of a minimum boiling azeotrope with a heavy entrainer.....	64
Figure 3.3 Thermodynamic features of 1.0-2 mixtures with respect to batch extractive distillation. Separation of a maximum boiling azeotrope with a heavy entrainer.	65
Figure 3.4 Separation of acetone-heptane using toluene: (a) 1.0-1a class residue curve map (rcm) and batch extractive profile map (b) ($F_E/V=0.01, R=\infty$) (c) ($F_E/V=1, R=\infty$) and (d) ($F_E/V=1, R=10$).....	71
Figure 3.5 Extractive distillation of acetone – heptane with toluene (1.0-1a class). Entrainer - feed flow rate ratio as a function of the reflux ratio.	72
Figure 3.6 Extractive distillation of acetone – methanol with water (1.0-1a class). Entrainer - feed flow rate ratio as a function of the reflux ratio to recover 98%mol acetone (A).	74
Figure 3.7 Rectifying, extractive and stripping composition for four operating parameter points taken from Figure 3.5 (b) point Y_{U2} , (b) point Y_{F1} , (c) point Y_{U2} and (d) point Y_{U3}	75
Figure 3.8 Rigorous simulation result to recover acetone at $F_E/F=1, R=20$ and $F_E/F=20, R=20$, compared with calculated profiles: (a-d) stripping section, (b-e) extractive section and (c-f) rectifying section.	77
Figure 3.9 Separation of acetone-methanol using chlorobenzene: (a) 1.0-1a class residue curve map (rcm) and batch extractive profile map (b) ($F_E/V=0.01, R=\infty$) (c) ($F_E/V=2, R=\infty$) and (d) ($F_E/V=2, R=5$).....	79
Figure 3.10 Extractive distillation of acetone – methanol with chlorobenzene (1.0-1a class). Entrainer - feed flow rate ratio as a function of the reflux ratio to recover 98%mol methanol (B).....	80
Figure 3.11 Rectifying, extractive and stripping composition for two operating parameter points taken from Figure 3.10 (b) point Y_{F1} and (b) point Y_{U1}	81
Figure 3.12 Rigorous simulation result to recover methanol at: (a) $R=1, F_E/F=10$; (b) $R=1, F_E/F=20$; (c) $R=20, F_E/F=10$ and (c) $R=20, F_E/F=20$	83
Figure 3.13 chloroform-vinyl acetate using butyl acetate: (a) 1.0-2 class residue curve map (rcm) and batch extractive profile map (b) ($F_E/V=0.1 < (F_E/V)_{max}, R=15$).....	84
Figure 3.14 Extractive distillation of chloroform – vinyl acetate with butyl acetate (1.0-2 class). Entrainer - feed flow rate ratio as a function of the reflux ratio to recover 98%mol chloroform (A).	85

Figure 3.15 Comparison of three different entrainers to recover Chloroform (A) from the mixture chloroform – vinyl acetate. (a) Univolatility curve location. (b) Toluene, (c) Cyclohexane and (d) Butyl acetate feasible regions.	87
Figure 3.16 Extractive distillation of chloroform – vinyl acetate with butyl acetate (1.0-2 class). Entrainer - feed flow rate ratio as a function of the reflux ratio to recover 98%mol vinyl acetate (B).....	88
Figure 3.17 Rigorous simulation result to recover vinyl acetate (B) at $F_E/F=5$, $R=5$ and $F_E/F=0.1$, $R=5$, compared with calculating profiles: (a-d) stripping section, (b-e) extractive section and (c-f) rectifying section.	89
Figure 3.18 acetone-chloroform using benzene: (a) 1.0-2 class residue curve map (rcm) and batch extractive profile map (b) $(F_E/V=0.1 < (F_E/V)_{max}$, $R=60$).	91
Figure 3.19 Extractive distillation of acetone – chloroform with benzene (1.0-2 class). Entrainer - feed flow rate ratio as a function of the reflux ratio to recover 98%mol acetone (A).....	93
Figure 3.20 Extractive distillation of acetone – chloroform with benzene (1.0-2 class). Entrainer - feed flow rate ratio as a function of the reflux ratio to recover 98%mol chloroform (B).....	94
Figure 3.21 Rectifying, extractive and stripping composition for four operating parameter points taken from Figure 3.20 (a) point Y_{U1} , (b) point Y_{F1} , (c) point Y_{U2} and (d) point Y_{U3}	95
Figure 4.1 Configurations of extractive distillation column: (a) batch (b) continuous.....	104
Figure 4.2. Thermodynamic features of 1.0-1a mixtures with respect to batch extractive distillation. Separation of a maximum boiling azeotrope with a light entrainer.	106
Figure 4.3. Thermodynamic features of 1.0-2 mixtures with respect to batch extractive distillation. Separation of a maximum boiling azeotrope with a light entrainer.	108
Figure 4.4. 1.0-1a class residue curve map of propanoic acid – DMF maximum boiling azeotrope separation using light entrainer MIBK.	117
Figure 4.5. Entrainer - entrainer - feed flow rate ratio F_E/F as a function of the reboil ratio S . Propanoic acid – MIBK – DMF Separation to recover A (propanoic acid).	118
Figure 4.6. The influence of the reboil ratio on stripping section composition profiles.	119
Figure 4.7. Operating parameter scene explanation. Points taken from Figure 4.5: (b) point Y_{F1} , (a) point Y_{U1} , (c) point Y_{F2} and (d) point Y_{U2}	121
Figure 4.8. Rigorous simulation result to recover A (propanoic acid) at $F_E/F=1$, $S=15$, compared with calculated profiles: (a) rectifying section, (b) extractive section and (c) stripping section.	123
Figure 4.9. 1.0-1a class residue curve map of water – ethylene diamine maximum boiling azeotrope separation using light entrainer acetone.	126
Figure 4.10. Entrainer - entrainer - feed flow rate ratio F_E/F as a function of the reboil ratio S . Water – EDA – acetone separation to recover B (EDA).	126
Figure 4.11. 1.0-2 class residue curve map of ethanol - water minimum boiling azeotrope separation using light entrainer methanol.....	129
Figure 4.12. Entrainer - entrainer - feed flow rate ratio F_E/F as a function of the reboil ratio S . Ethanol-water-methanol separation: (a) to recover A (ethanol) (b) to recover B (water).	129

Figure 4.13. 1.0-2 class residue curve map of MEK – benzene minimum boiling azeotrope separation using light entrainer acetone.	131
Figure 4.14. Entrainer - entrainer - feed flow rate ratio F_E/F as a function of the reboil ratio S . MEK-benzene- acetone separation: (a) to recover A (MEK) (b) to recover B (benzene).....	132
Figure 4.15 Operating parameter scene explanation. Points taken from Figure 13b: (a) point Y_{F1} , (b) point Y_{U1}	133
Figure 4.16. Influence of the reboil ratio on the extractive section composition profiles.....	135
Figure 4.17. Rigorous simulation result to recover MEK (a-c) or Benzene (d-f) at $S=15$, $F_E/F=1$ compared with simplified composition profiles: (a-d) stripping section, (b-e) extractive section and (c-f) rectifying section.....	136

Table content

Table 2.1 The most important literature concerning extractive distillation separation of binary azeotropic and low relative volatility mixtures in a batch rectifier with light, intermediate or heavy entrainer.	39
Table 2.2 The study case related to extractive distillation separation of binary azeotropic and low relative volatility mixture in a batch rectifier with light, intermediate or heavy entrainer.	40
Table 2.3. The operating steps and limiting parameters of extractive distillation in configuration BED-I separating binary azeotropic and low relative volatility mixture in a batch rectifier with light, intermediate or heavy entrainer (Varga, 2006).	43
Table 2.4. The operating stages and limiting parameters of azeotropic extractive distillation in configuration BES-I separating binary azeotropic and low relative volatility mixture in a batch rectifier with light, intermediate or heavy entrainer (Varga, 2006).....	44
Table 2.5 Summary of possible systems studied in the PhD thesis manuscript.	59
Table 3.1 Operating parameters for all study cases.	69
Table 3.2 Column operating specifications for rigorous simulation.....	70
Table 3.3 Operating parameters corresponding to Figure 3.5.....	73
Table 3.4 Operating parameters corresponding to Figure 3.6.....	74
Table 3.5. Operating parameters corresponding to Figure 3.7a,b,c,d.....	76
Table 3.6 Operating parameters corresponding to Figure 3.8a,b,c.....	78
Table 3.7 Operating parameters corresponding to Figure 3.8 d,e,f.....	78
Table 3.8 Operating parameters corresponding to Figure 3.10.....	81
Table 3.9 Operating parameters corresponding to Figure 3.14.....	85
Table 3.10 Operating parameters corresponding to Figure 3.16.....	88
Table 3.11 Operating parameters corresponding to Figure 3.17a,b,c.....	90
Table 3.12 Operating parameters corresponding to Figure 3.17 d,e,f.	90

<i>Table 3.13 Operating parameters corresponding to Figure 3.19.....</i>	<i>93</i>
<i>Table 3.14. Operating parameters corresponding to Figure 3.20.....</i>	<i>94</i>
<i>Table 3.15. Operating parameters corresponding to Figure 3.21.....</i>	<i>96</i>
<i>Table 4.1. operating parameters for all case study involving possible products.</i>	<i>115</i>
<i>Table 4.2. Column operating specifications for rigorous simulation</i>	<i>116</i>
<i>Table 4.3 Operating parameters corresponding to Figure 4.5.....</i>	<i>118</i>
<i>Table 4.4 Operating parameters corresponding to Figure 4.7.....</i>	<i>122</i>
<i>Table 4.5 Operating parameters corresponding to Figure 4.8a,b,c.....</i>	<i>124</i>
<i>Table 4.6 Operating parameters corresponding toFigure 4.10.</i>	<i>127</i>
<i>Table 4.7 Operating parameters corresponding to Figure 4.12.....</i>	<i>130</i>
<i>Table 4.8 Operating parameters corresponding to Figure 4.14a.....</i>	<i>133</i>
<i>Table 4.9 Operating parameters corresponding to Figure 4.15a,b.</i>	<i>134</i>
<i>Table 4.10 Operating parameters corresponding to Figure 4.17a,b,c.....</i>	<i>138</i>

General introduction

GENERAL INTRODUCTION

Distillation is the most widely used industrial method for separating liquid mixtures in many chemical and other industry fields like perfumery, medicinal and processing. The first clear evidence of distillation can be dated back to first century AD. Being the leading process for the purification of liquid mixtures, distillation columns consume about 40% of the energy used to operate plants in the refining and bulk chemical process industries according the U.S Dept of Energy. Azeotropic and low relative volatility mixtures often occur in separating industry and their separation cannot be realized by conventional distillation. Extractive distillation is then a suitable alternative process. Extractive distillation has been studied for many decades with a rich literature. Some main subjects studied include: column with all possible configurations; process operation policies and strategy; process design, synthesis, optimization; determining separation sequencing; entrainer design and selection, feasibility studies and so on. Among those topics, feasibility is always a critical issue as it is necessary to assess process feasibility before making the design specifications. Feasibility studies also contribute to a better understanding of complex unit operations such as the batch extractive distillation.

Upon the feasibility study, the design of conventional and azeotropic distillation is connected to thermodynamics, in particular the volatility of each compound and azeotrope. Furthermore, residue curve maps analysis allows assessing the feasibility under infinite reflux ratio conditions with the finding of the ultimate products under direct or indirect split conditions. However, distillation runs under finite reflux ratio conditions and finding which products are achievable and the location of the suitable feed composition region is more complicated because we must consider the dependency of composition profile on reflux ratio. This affects the range of composition available to each section profiles, due to the occurrence of pinch points, which differ from the singular points of the residue curve map. The identification of possible cut under key parameters reflux ratio, reboil ratio and entrainer - feed flow rate ratio has been the main challenge for an efficient separation of azeotropic mixtures.

Extractive distillation is a powerful and widely used technique for separating azeotropic and low relative volatility mixtures in pharmaceutical and chemical industries. Given an azeotropic mixture A-B (with A having a lower boiling temperature than B), an entrainer E is added to interact selectively with the original components and alter their relative volatility, thus enhancing the original separation. It differs from azeotropic distillation by the fact that the third-body solvent E is fed continuously in another column position than feed mixture. For decades a single feasibility rule holds in industry: extractive distillation should be operated by

choosing a miscible, azeotrope, relatively non-volatile component. The solvent forms no new azeotrope and the original component with the greatest volatility separates out as the top (bottom) product. The bottom (top) product consists of a mixture of the solvent and the other component.

Combining knowledge of residue curve maps and of the univolatility and unidistribution curves location Rodriguez-Donis et al (2009a, 2009b, 2010, 2012a, 2012b) published a general feasibility criterion for extractive distillation under infinite reflux ratio. The volatility order is set by the univolatility curves. Using illustrative examples covering all sub cases, but exclusively operated in batch extractive distillation, those authors found that Serafimov's classes covering up to 53% of azeotropic mixtures were suited for extractive distillation: 0.0-1 (low relative volatility mixtures), 1.0-1a, 1.0-1b, 1.0-2 (azeotropic mixtures with light, intermediate or heavy entrainers forming no new azeotrope), 2.0-1, 2.0-2a, 2.0-2b and 2.0-2c (azeotropic mixtures with an entrainer forming one new azeotrope). For all suitable classes, the general criterion under infinite reflux ratio could explain the product to be recovered and the possible existence of limiting values for the entrainer - feed flow rate ratio for batch operation: a minimum value for the class 1.0-1a, a maximum value for the class 1.0-2, etc. The behavior at finite reflux ratio could be deduced from the infinite behavior and properties of the residue curve maps, and some limits on the reflux ratio were found. However precise finding of the limiting values of reflux ratio or of the entrainer - feed flow rate ratio required other techniques.

The feasibility always relies upon the intersection for the composition profiles in the various column sections (rectifying, extractive, stripping). Whatever the operation parameter values (reflux ratio, flow-rates...), the process is feasible if the specified product compositions at the top (x_D) and at the bottom (x_W) of the column can be connected by a single or by a composite composition profile. Here in this thesis we use geometrical analysis to evaluate profile intersection but mathematical ones could be used as well.

Several column configurations can be used for extractive distillation both in batch and continuous. In batch mode, both batch extractive distillation (BED) and simple batch distillation (SBD) processes can be performed either in rectifier, or in middle-vessel column, or in stripping column. With a heavy entrainer fed above the main feed, the batch column is a rectifier, with an extractive and a rectifying section and the product is removed as distillate from the top. With a light entrainer here we quote and apply the batch stripper column from Rodriguez-Donis et al., (2011), the original binary mixture (A+B) is initially charged into the column top vessel and it is fed to the first top tray as a boiling liquid. Light entrainer is introduced continuously at an intermediate tray leading to two column sections: extractive and stripping section. In the

continuous process, we consider the classical configuration, with the entrainer fed above the main feed, giving rise to three sections, rectifying, extractive and stripping ones.

In extractive distillation, the entrainer is conventionally chosen as a heavy (high boiling) component, however, there are some cases when its use is not recommended such as if a heat sensitive or a high boiling component mixture has to be separated. Besides, different entrainers can cause different components to be recovered or recovered overhead in extractive distillation. Therefore finding potential entrainers is critical since an economically optimal design made with an average design using best entrainer can be much less costly, Theoretically, any candidate entrainer satisfying the feasibility and optimal criteria can be used no matter it is heavy, light, or intermediate entrainer. Literature studies on intermediate entrainer or light entrainer, even though not too much, validate this assumption.

The presentation of this work focuses on four chapters:

Chapter 2 is a literature review to present the state of the art on the extractive distillation. This chapter introduces several issues related to our thesis: phase equilibrium, ternary diagram classifications, the principles of distillation and its improvement studies, possible method to separate non ideal mixtures, the state of art on extractive distillation, the general methodology used in this thesis, the objective, and organization of the thesis are shown at the end of this chapter. As this thesis is mainly concerned with feasibility studies, the most important methods are discussed in this part.

In Chapter 3, a systematic study is performed for the extractive distillation separation of azeotropic mixtures with a heavy entrainer belonging to 1.0-1a and 1.0-2 classes. The occurrence of two types of A-B azeotropic mixtures (minimum or maximum boiling temperature) and of two possible intersection of the univolatility line $\alpha_{AB}=1$ with the binary sides gives rise to four sub cases. Firstly, the column configuration is discussed. Then, the section composition profiles equations are derived for a heavy entrainer. Then a methodology in three steps is presented. In step1, based on batch feasibility knowledge, the feasibility of batch and continuous separation is studied under finite reflux ratio and entrainer - feed flow-rate, Insights gained from the batch extractive distillation criterion are extended to the feasible operation of the continuous process, with focus on the product cut sequence and operating parameter limit values. In step 2, assuming a given product purity and recovery, the feasible ranges of values of the operating parameters, reflux ratio R and entrainer - feed flow rate ratio F_E/F are determined for the batch and continuous processes, and compared with the help of diagrams F_E/F vs. R in continuous mode and F_E/V vs. R in batch mode.

Comparison of three entrainers leading to the same class of diagram and sub-case is performed to check that the feasible conditions ranges are entrainer dependent, in particular the minimum reflux ratio and the minimum entrainer entrainer - feed flow rate ratio. In step 3, rigorous simulations verify the results of step 2, by providing rigorous values of the product purity and recovery.

Chapter 4 focuses on the extractive distillation feasibility studies with a light entrainer to separate minimum or maximum boiling azeotropic mixtures. The corresponding ternary diagram belongs to the 1.0-1a and 1.0-2 Serafimov's class. Knowledge of the residue curve map and of the location of the univolatility curve $\alpha_{AB}=1$ can help assess which product is removed in the distillate. Contrary to the heavy entrainer case (Chapter 3), the main product is removed from the column bottom. The batch extractive process is a stripping column and the continuous process considers that the entrainer is fed below the main feed. The heavy entrainer methodology is now adapted to the light entrainer case. The section composition profile equations are reformulated in terms of the reboil ratio S and entrainer - feed flow rate ratio F_E/F , also considering the entrainer physical state (saturated vapor or boiling liquid). The analyses of each of the four sub cases follow the same three step methodology used in the previous chapter: section profiles and methodology used, thermodynamic feasibility criterion analysis, calculation of reboil ratio vs. entrainer feed flow rate ratio diagrams and rigorous simulation, discussion and conclusion.

The last chapter deals with conclusion and future studies that can be drawn. Appendix collected some definitions of common terms in extractive distillation, the table data used in result discussion.

State of the art, methodology, objectives

2.1 INTRODUCTION

We first recall phase equilibrium issues to introduce the concepts of residue curve map and their classifications along with the concepts of the volatility and distribution curves. Then we survey distillation processes and their use for the separation of non ideal mixtures. We insist on extractive distillation key literature and review methods used to assess the feasibility of this process.

2.2 PHASE EQUILIBRIUM

2.2.1 Phase equilibrium equations

The phase equilibrium behavior is the foundation of chemical mixture components separation by distillation. The basic relationship for every component in the vapor and liquid phases of a system at equilibrium is the equality of fugacities in all phases. In an ideal liquid solution the liquid fugacity of each component in the mixture is directly proportional to the mole fraction of the component. However, because of the no ideality in the liquid solution of the systems studied in the following chapters, activity coefficient representing the deviation of the mixture from ideality methods are used to describe the liquid phase behavior. For the vapor phase, ideal gas behavior is assumed leading to the gas fugacity equal to the partial pressure. Thus the basic vapor-liquid equilibrium equation is modified as:

$$f_i^l = x_i \gamma_i f_i^{0,l} = f_i^v = y_i P \quad (2.1)$$

With the liquid phase reference fugacity $f_i^{0,l}$ being calculated from:

$$f_i^{0,l} = \varphi_i^{0,v}(T, P_i^0) P_i^0 \theta_i^0 \quad (2.2)$$

Where

$\varphi_i^{0,v}$ is the fugacity coefficient of pure component i at the system temperature (T) and saturated vapor pressure, as calculated from the vapor phase equation of state (for ideal vapor phase: $\varphi_i^{0,v} = 1$).

P_i^0 is the saturated vapor pressure of component i at the system temperature.

θ_i^0 is the Poynting correction for pressure $\exp\left(\frac{1}{RT} \int_{P_i^*}^P V_i^{0,l} dP\right)$.

At low pressures, the Poynting correction is near unity and can be ignored. Thus the overall vapor–liquid phase equilibrium (VLE) relationship for most of the mixture systems in the following chapters can be described as the following equation:

$$y_i P = x_i \gamma_i P_i^* \quad (2.3)$$

When setting the condition $\gamma_i=1$, equation (2.3) is the so-called Raoult's Law. The computation of the liquid activity coefficient γ_i requires thermodynamic models given in the next section.

Calculation of the saturated vapor pressure for a pure component is needed in Equation (2.3) for the VLE relationship. The extended Antoine equation can be used to compute liquid vapor pressure as a function of the system temperature T:

$$\ln P_i^0 = C_{1i} + \frac{C_{2i}}{T + C_{3i}} + C_{4i} T + C_{5i} \ln T + C_{6i} T^{C_{7i}} \quad (2.4)$$

Where C_{1i} to C_{7i} are the model parameters, model parameters for many components are available in the literature or from the pure component databank of the Aspen Physical Property System.

2.2.2 Activity coefficient model

The UNIFAC, UNIQUAC, Wilson, NRTL activity coefficient model are recommended methods for highly non ideal chemical systems, The UNIFAC, UNIQUAC, NRTL model can be used for VLE, LLE and LLVE applications while the Wilson model can only be used for VLE application. (Kontogeorgis and Folas, 2010, Vidal, 2003). We use the UNIFAC model in this study to predict the VLE of each of the mixtures studied. In each case it was verified that the UNIFAC predictions agreed with available experimental data (Gmehling et al., 2004). The UNIFAC model is a semi-empirical method for the prediction of non-electrolyte activity estimation in non ideal mixtures. It is constituted by two parts: a combinatorial γ_i^C and a residual component γ_i^R . For the molecule i, the equation for the UNIFAC model is:

$$\ln \gamma_i = \ln \gamma_i^C + \ln \gamma_i^R \quad (2.5)$$

The combinatorial component of the activity γ_i^C is contributed to by several terms in its equation, and is the same as for the UNIQUAC model

$$\ln \gamma_i^C = \ln \frac{\phi_i}{x_i} + \frac{z}{2} q_i \ln \frac{\theta_i}{\phi_i} - q_i \ln t_i - q_i \sum_j \frac{\theta_j}{t_j} + l_i + q_i - \frac{\phi_i}{x_i} \sum_j x_j l_j \quad (2.6)$$

Where

$$\theta_i = \frac{q_i x_i}{\sum_k q_k x_k} \quad (2.7)$$

$$\theta'_i = \frac{q'_i x_i}{\sum_k q'_k x_k} \quad (2.8)$$

$$\phi_i = \frac{r_i x_i}{\sum_k r_k x_k} \quad (2.9)$$

$$l_i = \frac{z}{2}(r_i - q_i) + 1 - r_i \quad (2.10)$$

$$t'_i = \sum_k \theta'_k \exp\left(a_{ij} + c_{ij} \ln T + d_{ij} T + \frac{e_{ij}}{T^2}\right) \quad (2.11)$$

$$z = 10 \quad (2.12)$$

The residual component of the activity γ_i^R is due to interactions between groups present in the equation

$$\ln \gamma_i^R = \sum_{k=1}^m v_k^{(i)} \left[\ln \Gamma_k - \ln \Gamma_k^{(i)} \right] \quad (2.13)$$

Where $\Gamma_k^{(i)}$ is the activity of an isolated group in a solution consisting only of molecules i,

$$\ln \Gamma_k = Q_K \left[1 - \ln \left(\sum_{j=1}^m \bar{\theta}_j \varphi_{jk} \right) - \sum_{j=1}^m \left(\frac{\bar{\theta}_j \varphi_{jk}}{\sum_{n=1}^m \bar{\theta}_n \varphi_{nj}} \right) \right] \quad (2.14)$$

Where:

$$\bar{\theta}_j = \frac{Q_j x_j}{\sum_{n=1}^m Q_n x_n} \quad (2.15)$$

$$X_j = \frac{\sum_{i=1}^c v_j^i x_i}{\sum_{i=1}^c \sum_{k=1}^m v_k^i x_i} \quad (2.16)$$

$$\phi_{jk} = \exp\left(-\frac{U_{jk} - U_{kk}}{RT}\right) = \exp\left(-\frac{a_{jk}}{T}\right) \quad (2.17)$$

2.2.3 Non ideality of the mixture

In most distillation systems, the predominant non ideality occurs in the liquid phase because of molecular interactions. Equation (2.3) contains the liquid phase activity coefficient of the component j. When chemically dissimilar components are mixed together (for example, oil molecules and water molecules), there exists repulsion or attraction between dissimilar molecules. If the molecules repel each other, they exert a higher partial pressure than if the mixture was ideal. In this case the activity coefficients are greater than unity (called a “positive deviation” from Raoult’s law). If the molecules attract each other, they exert a lower partial pressure than in an ideal mixture. Activity coefficients are less than unity (negative deviations). Activity coefficients are usually calculated from experimental data or from the aforementioned models regressed on experimental data. Azeotropes occur in a number of non ideal systems. An azeotrope exists when the liquid and vapor compositions are the same ($x_i=y_i$) at a given azeotrope temperature. There are several types of azeotropes, *Figure 2.1-Figure 2.4* sketch typical phase graphical representations of the VLE.

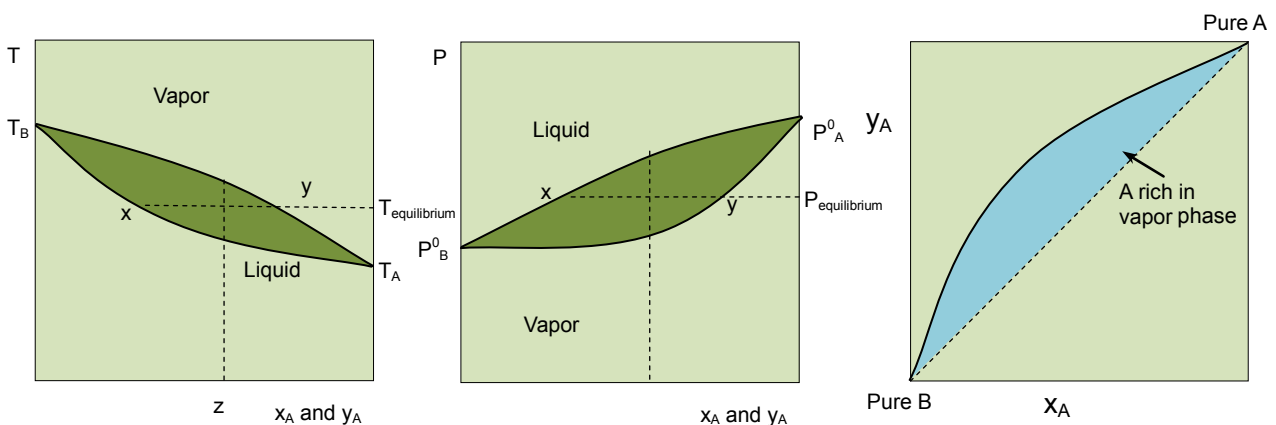


Figure 2.1. Typical homogeneous mixtures without azeotrope

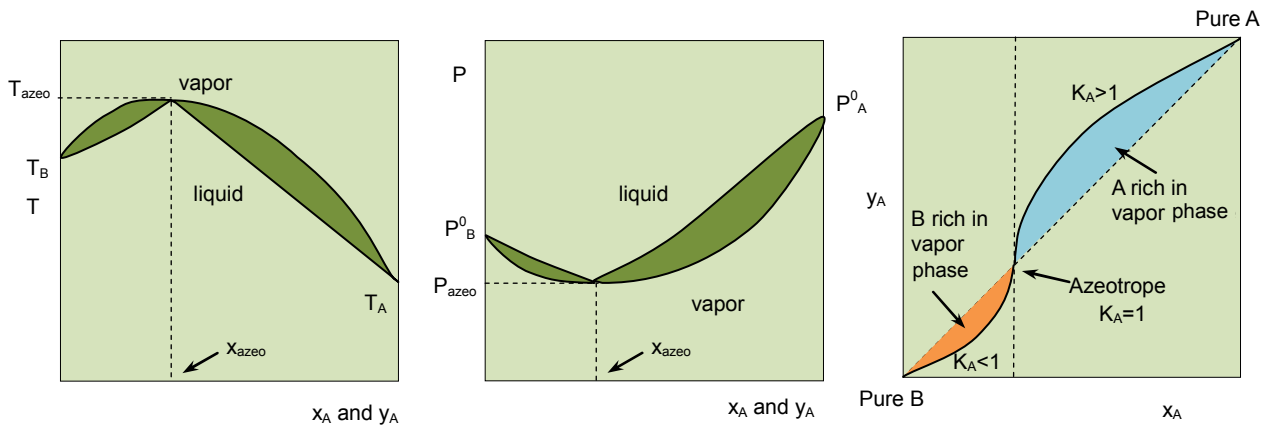


Figure 2.2. Typical homogeneous mixtures with maximum boiling azeotrope, a negative deviation from Raoult's law

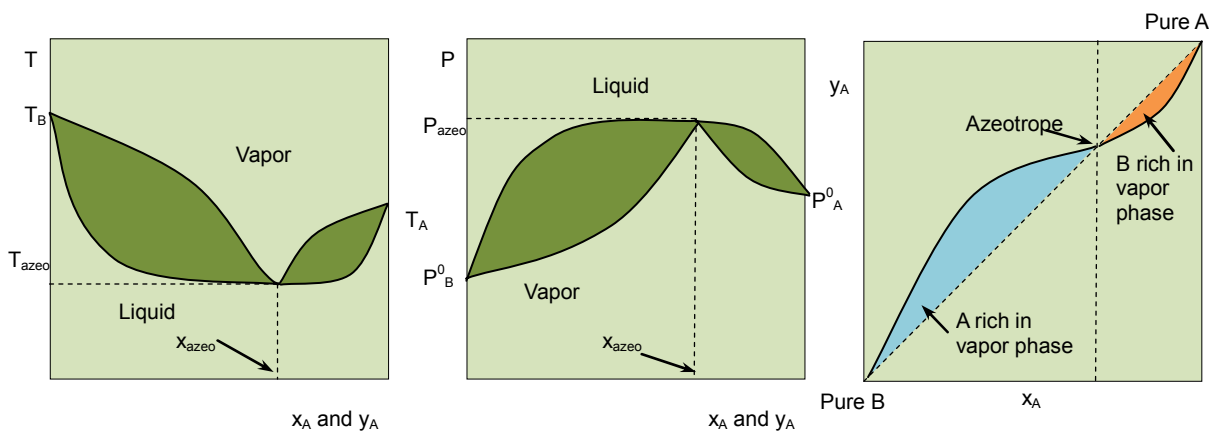


Figure 2.3. Typical homogeneous mixtures with minimum boiling azeotrope, a positive deviation from Raoult's law

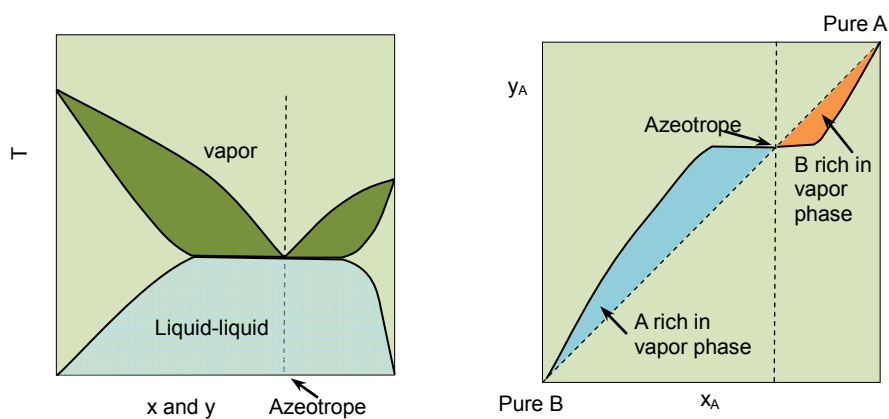


Figure 2.4. Typical heteroazeotrope mixtures with minimum boiling azeotrope

The left part of Figure 2.1-Figure 2.4 shows a combined graph of the bubble and dew temperatures, pressure and the vapor-liquid equilibrium phase mapping, which gives a complete representation of the VLE. In addition, the right part gives the equilibrium phase mapping y vs. x alone. Each of these diagrams uniquely characterizes the type of mixture. Negative deviations (attraction) can give a higher temperature boiling

mixture than the boiling point of the heavier component, called a maximum-boiling azeotrope (Figure 2.2). Positive deviations (repulsion) can give a lower temperature boiling mixture than the boiling point of the light component, called a minimum boiling azeotrope (Figure 2.3).

2.2.4 Residue curve

A residue curve map (RCM) is a collection of the liquid residue curves in a simple one-stage batch distillation originating from different initial compositions. The RCM technique is considered as powerful tool for the flow-sheet development and preliminary design of conventional multi-component separation processes. It has been extensively studied since 1900. Using the theory of differential equations, Doherty and his colleagues (e.g. Doherty and Malone, 2001a) explored the topological properties of residue curve map (RCM) which are summarized in two recent articles (Kiva et al., 2003, Hilmen et al., 2002b). The simple RCM was modeled by the set of differential equations.

$$\frac{dx_i}{dh} = x_i - y_i^* \quad (2.18)$$

Where h is a dimensionless time describing the relative loss of the liquid in the still-pot and $dh=dV/L$. x_i is the mole fraction of species i in the liquid phase, and y_i is the mole fraction of species i in the vapor phase. The y_i values are related with the x_i values using equilibrium constants K_i .

The singular points of the differential equation are checked by computing the associated eigenvalues. Within a non-reactive residue curve map, a singular point can be a stable or an unstable node or a saddle, depending on the sign of the eigenvalues related to the residue curve equation.

For non-reactive mixtures, there are three stabilities:

- Unstable node (denoted [un] with a symbol of white circle): The singular point eigenvalues are all positive. It has a boiling point that is the lowest of the region of distillation. The residue curves move away from the unstable node with increasing temperature.
- Stable node (denoted [sn] with a symbol of solid circle): Singular points whose own values are all negative. It has a boiling point that is the highest of the region of distillation. The residue curves move towards the stable node. Moving away from stable node along a residue curve, the temperature is decreasing.
- Saddle point (denoted [s] with a symbol of triangle): Singular points are intermediate boiling temperature points, which have at least one eigenvalue positive and the other negative. Some

residue curves away from a saddle point decreasing temperature and others with increasing temperature.

Some significant properties of residue curves are the following:

1. The singular points of residue curves networks are either pure component or azeotropes.
2. The Stability of singular points is an unstable node, a saddle point or a node stable and it depends on their respective boiling temperature.
3. In a simple distillation (Rayleigh's distillation), the product follows a sequence of decreasing temperature. Thus, the unstable node will be the first distillate, followed by the saddle point and finally the node stable.
4. The orientation of the residue curve, that is to say, the changing composition of the boiling liquid, is in line with increasing temperature from the unstable node to the stable node.
5. Under total reflux ratio, the composition profile in a packed distillation column exactly follows the residue curve. Thus, in a column of infinite length at total reflux ratio, the distillate is the unstable node (direct split) or the bottom product is the stable node (indirect split).
6. The residue curve equation indicates that the equilibrium vector ($y - x$) is tangent to the residue curve at point x (Figure 2.5), hinting at the still path direction in simple distillation.
7. Each residue curve is related to a vapor in equilibrium, which is named the distillate curve. The vapor curve is always located on the convex side of the corresponding residue curve (Figure 2.5).

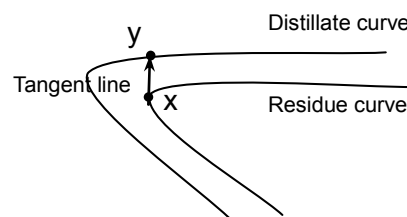


Figure 2.5 Condition of tangency between a residue curve and its corresponding distillate curve.

8. Two residue curves do not intercept.

2.2.5 Unidistribution and relative volatility

The distribution coefficient and relative volatility are well-known characteristics of the vapor–liquid equilibrium. The distribution coefficient K_i is defined by

$$K_i = \frac{y_i}{x_i} \quad (2.19)$$

K_i characterizes the distribution of component i between the vapor and liquid phases in equilibrium. $K_i=1$ defines the unidistribution curve. The vapor is enriched with component i if $K_i>1$, and is impoverished with component i if $K_i<1$ compared to the liquid. The higher K_i , the greater the driving force (y_i-x_i) and the easier the distillation. The ratio of the distribution coefficient of components i and j gives the relative volatility. The relative volatility is a very convenient measure of the ease or difficulty of separation in distillation. The volatility of component j relative to component i is defined as:

$$\alpha_{ij} = \frac{y_j/x_j}{y_i/x_i} \quad (2.20)$$

The relative volatility characterizes the ability of component i to transfer (evaporate) into the vapor phase compared to the ability of component j . Component i is more volatile than component j if $\alpha_{ij}>1$, and less volatile if $\alpha_{ij}<1$. For ideal and nearly ideal mixtures, the relative volatilities for all pair of components are nearly constant in the whole composition space. The situation is different for non ideal and in particular azeotropic mixtures where the composition dependence can be complex.

A large value of relative volatility α implies that components i and j can be easily separated in a distillation column. Values of α_{ij} close to 1 imply that the separation will be very difficult, requiring a large number of trays and high reflux ratio (high energy consumption). For binary systems, the relative volatility of light to heavy component is simply called α :

$$\alpha = \frac{y/x}{(1-y)/(1-x)} \quad (2.21)$$

$$y = \frac{\alpha x}{1+(\alpha-1)x} \quad (2.22)$$

Where x and y are the mole fractions of the light component in the liquid and vapor phases respectively. Rearrangement of equation (2.21) leads to the very useful y - x relationship equation (2.22) that can be employed when α is constant in a binary system. If the temperature dependence of the vapor pressure of both components is the same, relative volatility α will be independent of temperature. This is true for many components over a limited temperature range, particularly when the components are chemically similar. Distillation columns are frequently designed assuming constant relative volatility because it greatly

simplifies the vapor-liquid equilibrium calculations. Relative volatilities usually decrease somewhat with increasing temperature in most systems.

Unidistribution and univolatility line diagrams can be used to sketch the VLE diagrams and represent the geometry of the simple phase transformation trajectories. The qualitative characteristics of the distribution coefficient and relative volatility functions are typical approaches for the thermodynamic topological analysis. Kiva et al., (2003) considered the behavior of these functions for binary mixtures. The composition dependency of the distribution coefficients is qualitative and quantitative characteristics of the VLE for the given mixture. The patterns of these functions determines not only the class of binary mixture (zeotropic, minimum-or maximum-boiling azeotrope, or biazetropic), but also the individual behavior of the given mixture, as it is shown in Figure 2.6.

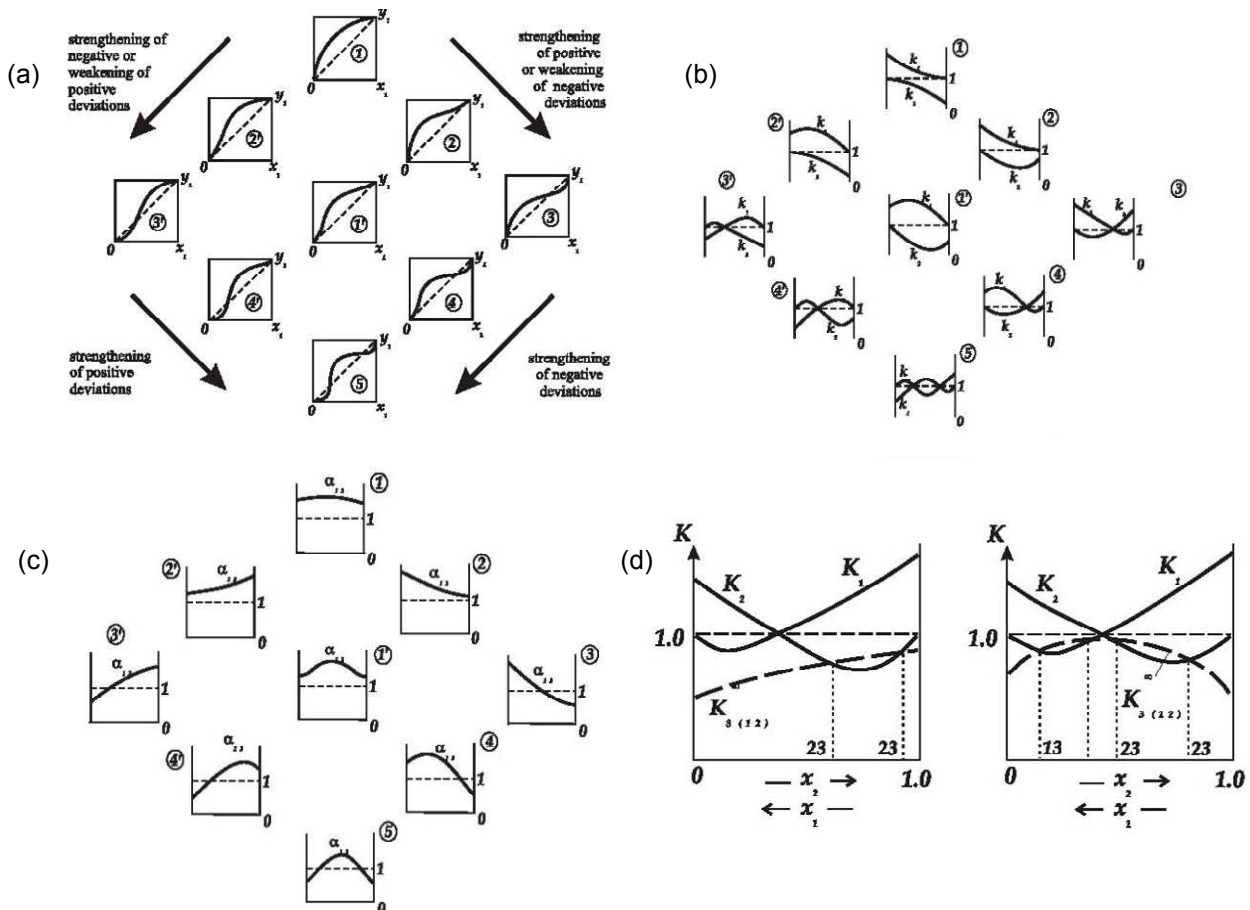


Figure 2.6. Feasible patterns of the VLE functions for binary mixtures of components 1 and 2: (a) equilibrium line $y(x)$, (b) distribution coefficients $K_i(x)$ and $K_j(x)$, (c) relative volatility $\alpha_{ij}(x)$ and (d) distribution coefficient trajectories for a mixture 1-2-3 with minimum-boiling azeotrope 1-2 (Kiva et al., 2003).

The composition dependence of the distribution coefficients of a ternary mixture of components 1, 2 and 3 can be represented by three surfaces $K_1(x)$, $K_2(x)$ and $K_3(x)$. The system of unidistribution lines $K_i(x)=1$ was analyzed in the composition space:

- The existence of a binary azeotrope gives rise to two unidistribution lines, and the existence of a ternary azeotrope gives rise to three unidistribution lines.
- The point of pure component i may (or may not) give rise to a unidistribution line of component i .
- A given residue curve map corresponds to a given set of feasible diagrams of unidistribution lines.

In a similar way to the distribution coefficient, the relative volatility features can be represented by isovolatility lines. Then the system of univolatility lines where $\alpha_{ij}=1$ was proposed. It is evident that the point of a binary azeotrope Az_{ij} gives rise to an α_{ij} univolatility line and that the point of a ternary azeotrope gives rise to the three univolatility lines (Kiva et al., 2003).

These features are represented in Figure 2.7 for the most probable classes (see the next section for the ternary diagram classification and probable occurrence).

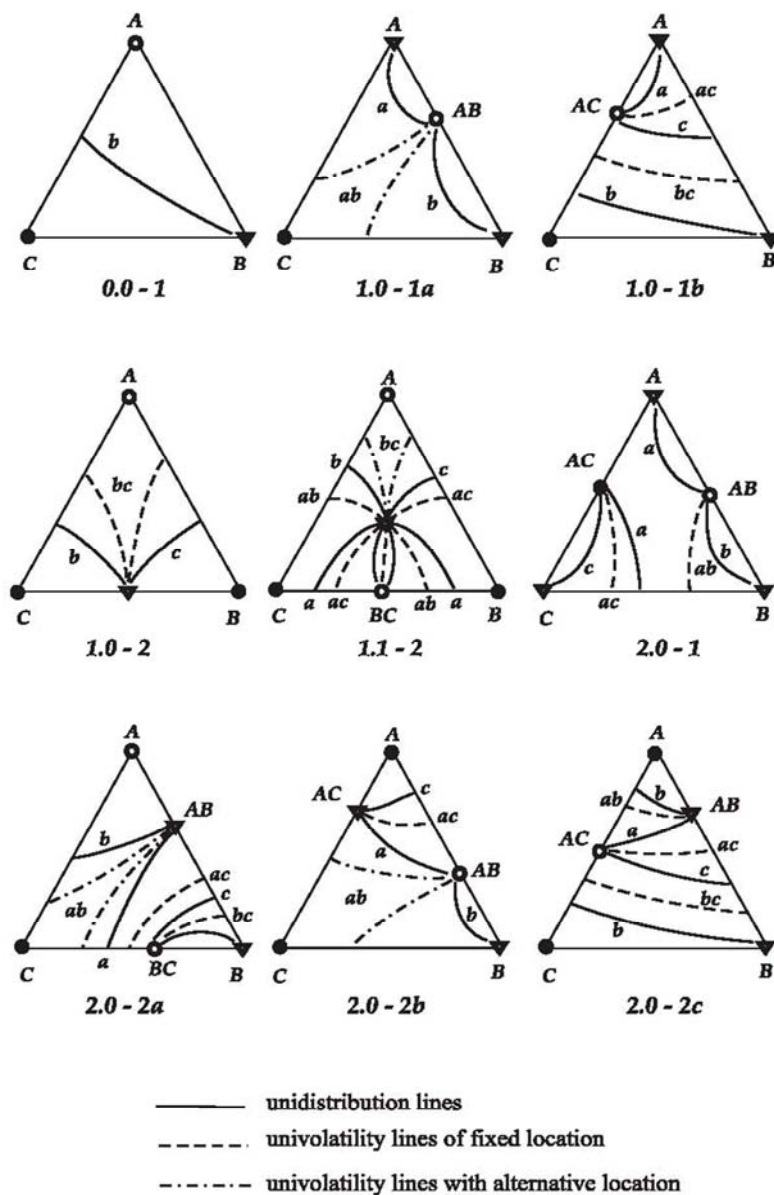


Figure 2.7 Unidistribution and univolatility line diagrams for the most probable classes of ternary mixtures according to Reshetov's statistics (Kiva et al., 2003).

Analysis of feasible diagrams of unidistribution and univolatility lines is given by Kiva et al., (2003). The main aim of their work was to consider feasible structures of the residue curve maps in more detail, and in fact this study helped to popularize more refined classification of the ternary diagrams. The diagrams of unidistribution lines were used as a main tool for analysis of tangential azeotrope and biazeotrope (Serafimov, 1996). Recently, Rodriguez-Donis et al (2009, 2010) studied how univolatility lines split the composition triangle into regions of certain order of volatility of components and defined a general feasibility

criterion for extractive distillation under infinite reflux ratio. In this work we consider unidistribution and univolatility line diagrams for the purpose of sketching the volatility order region and thus of assessing the feasible structures which will give possible products and offer information of possible limitation of entrainer feed.

2.2.6 Ternary VLE diagrams classification

The study of the thermodynamic classification of liquid-vapor phase equilibrium diagrams for ternary mixtures and its topological interpretation has a long history. Considering a ternary diagram A-B-E formed by a binary mixture A-B with the addition of an entrainer E, the classification of azeotropic mixtures in 113 classes was first proposed by Matsuyama (1978), then it was extended to 125 classes (Foucher et al., 1991a). After the work of Hilmen et al.(2002b), it became known that a more concise classification existed since the 70's: Serafimov classification. As explained by Hilmen (2000), Serafimov extended the work of Gurikov and used the total number of binary azeotropes M and the number of ternary azeotropes T as classification parameters. Serafimov's classification denotes a structure class by the symbol "M.T" where M can take the values 0, 1, 2 or 3 and T can take the values 0 or 1. These classes are further divided into types and subtypes denoted by a number and a letter. As a result of this detailed analysis, four more feasible topological structures, not found by Gurikov, were revealed. Thus Serafimov's classification includes 26 classes of feasible topological structures of VLE diagrams for ternary mixtures. Both the classifications of Gurikov and Serafimov consider topological structures and thus do not distinguish between antipodal (exact opposite) structures since they have the same topology. Thus, the above classifications include ternary mixtures with opposite signs of the singular points and opposite direction of the residue curves (antipodal diagrams). Serafimov's classification is presented graphically in Figure 2.8. The transition from one antipode to the other (e.g. changing from minimum-to maximum-boiling azeotropes) can be made by simply changing the signs of the nodes and inverting the direction of the arrows and the correspondence between Matsuyama and Serafimov's classification is detailed in Kiva et al. (2003)and Hilmen (2000).

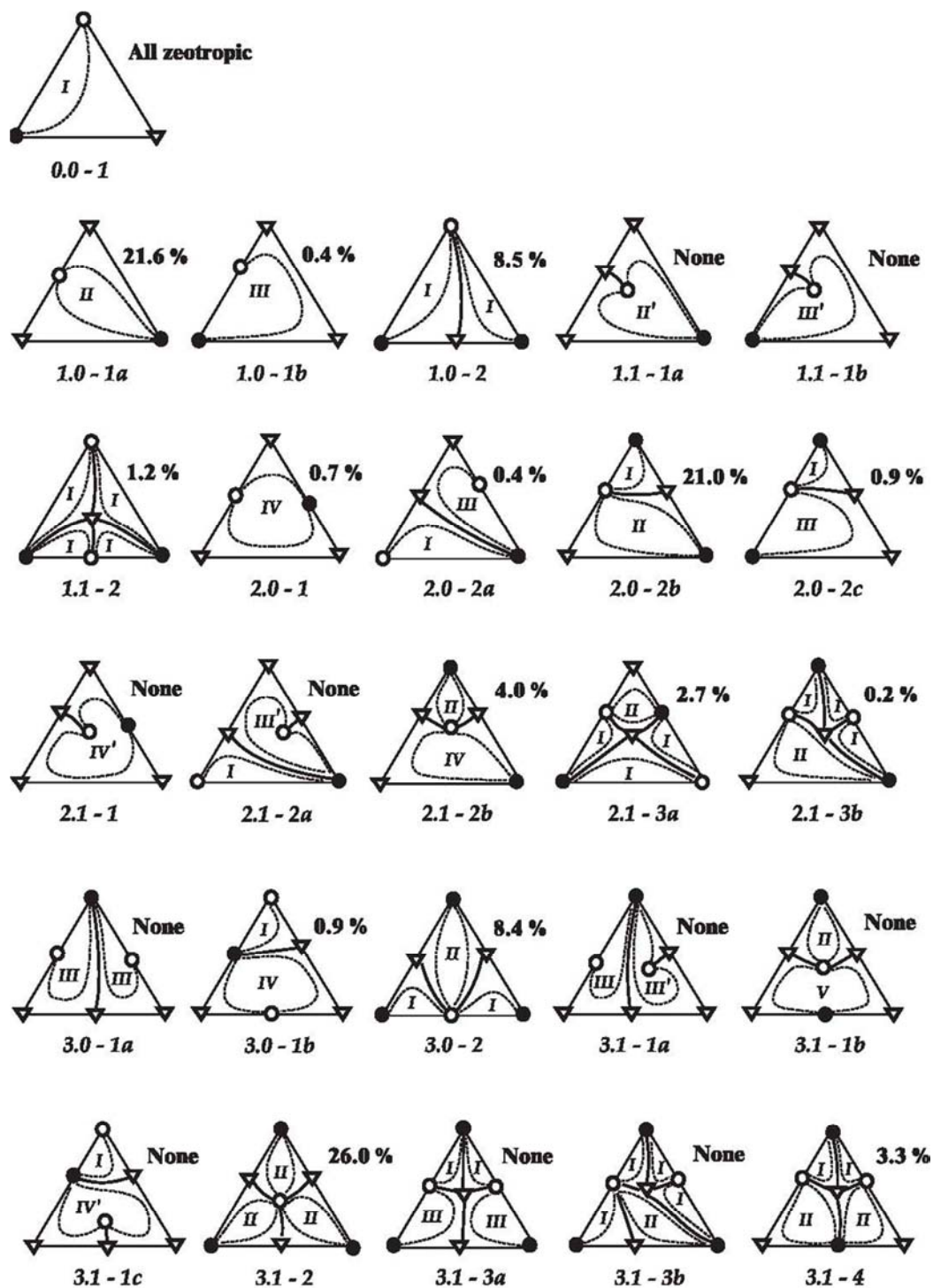


Figure 2.8 Azeotropic ternary mixture: Serafimov's 26 topological classes and Reshetov's statistics (Hilmen et al., 2002). (o) unstable node, (Δ) saddle, (\bullet) stable

As illustrated in Figure 2.7, the concentration simplex of these mixtures in the presence of an inflection on conjugated tie and inverted tie lines consists of at least two regions characterized by different ranges for the phase equilibrium ratio K_i , where i is the component number. The region of the concentration simplex in

which the decreasing order of K_i remains the same concerning azeotrope ternary mixture was called the K-ordered region. These regions were separated from each other by univolatility α -lines.

The studies on the frequency of occurrences of different types of phase diagrams for ternary azeotropic mixtures were presented by Reshetov and Kravchenko (2007). All 26 Serafimov's classes are topologically and thermodynamically feasible but their occurrence is determined by the probability of certain combinations of molecular interactions. The statistics on the physical occurrence of these 26 classes were provided to Kiva et al. (2003) by Reshetov (1998) but the original source is not available. The hereafter called "Reshetov's statistics" are based on thermodynamic data for 1609 ternary systems from which 1365 are azeotropic. The database covers data published from 1965 to 1998. The results in Figure 2.8 show that 16 out of the 26 Serafimov's classes were reported in the literature. Although Reshetov's statistics do not necessarily reflect the real occurrence in nature they can be used as an indicator of common azeotropic classes that are worthy of further investigation. A graphical representation of the occurrence of the various classes and types of ternary mixtures is given in Figure 2.9.

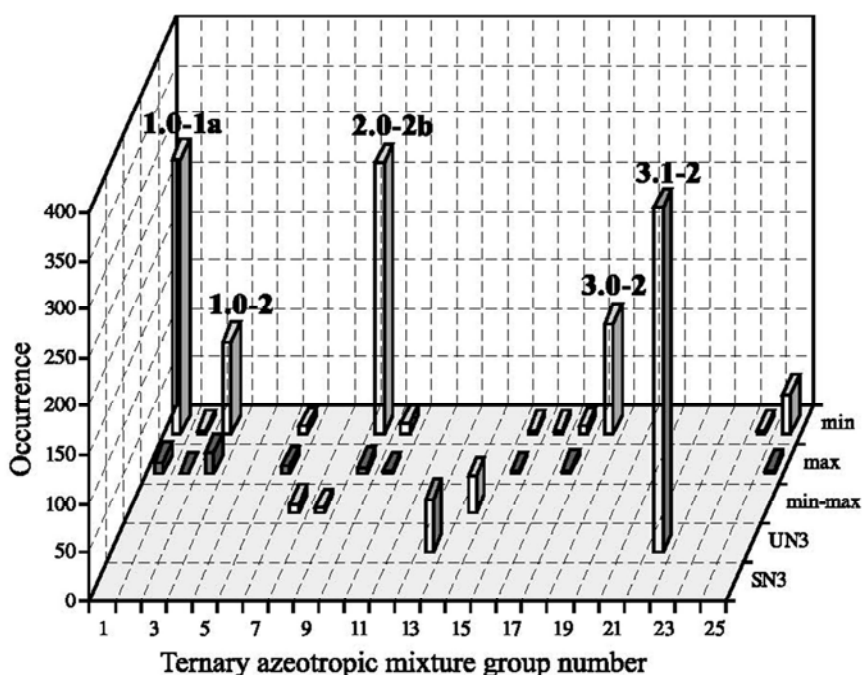


Figure 2.9 Occurrence of classes from published data for ternary mixtures based on Reshetov's statistics 1965-1988 (Kiva et al., 2003).

The Figure 2.10 illustrates diagrams of K-ordered regions and their corresponding occurrence over the studied azeotrope mixtures classes found by the Reshetov and Kravchenko (2007).

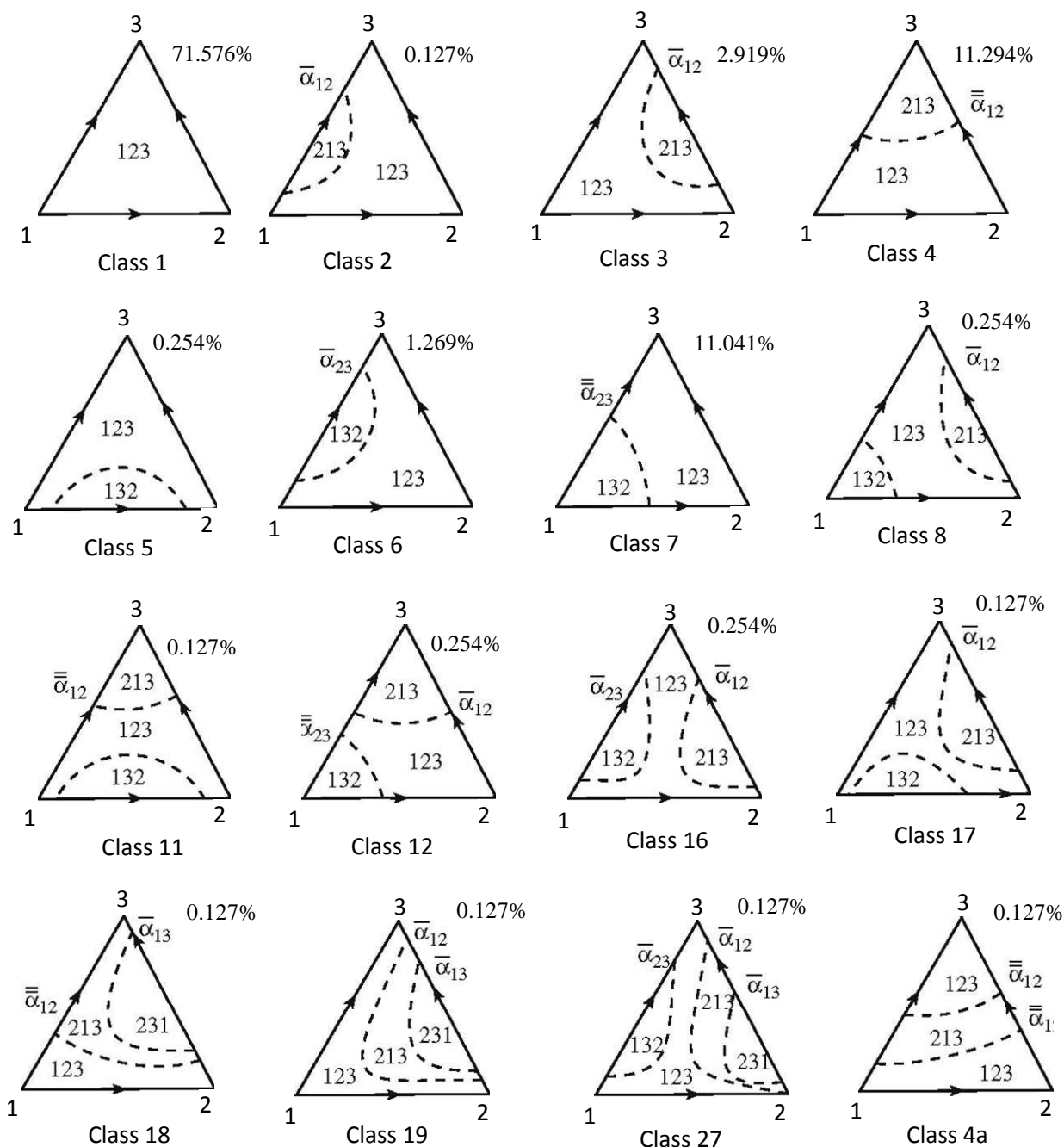


Figure 2.10 Ternary zeotropic mixtures Classes of diagrams of K -ordered regions for unilateral and bilateral univolatility α -lines, respectively; 123, 132, 213, ..., indices of K -ordered regions.

2.3 THE DISTILLATION PROCESS AND ITS IMPROVEMENT

Distillation is the most widely used industrial method for separating liquid mixtures in many chemical and other industry fields like perfumery, medicinal and food processing, the first clear evidence of distillation can be dated back to first century AD (Forbes, 1970). Being the leading process for the purification of liquid mixtures, the distillation process is driven by the differences between the vapor and liquid phase

compositions of the mixture arising from successive partial vaporization and condensation steps (Geankoplis, 2003). Distillation operations are responsible for 40% of the energy used in the chemical process industries.

The technology that can significantly reduce the energy requirement will represent a major breakthrough, and give significant competitive edge to the companies that adopt it. Regarding its high energy consumption, which comes from the vaporization of the liquid and is related both to the mixture charge and to the reflux ratio inside the column, progress has been made by the use of HIDiC (highly integrated distillation columns) (Skogestad et al., 1992, 1997; Nakaiwa et al., 2001, 2003), vapor recompression column (Jogwar et al., 2009) and other Petlyuk-like columns (Wolff and Skogestad, 1995; Halvorsen and Skogestad, 1999; Vitoria et al. 2008; Halvorsen and Skogestad, 2011).

2.3.1 Highly integrated distillation columns

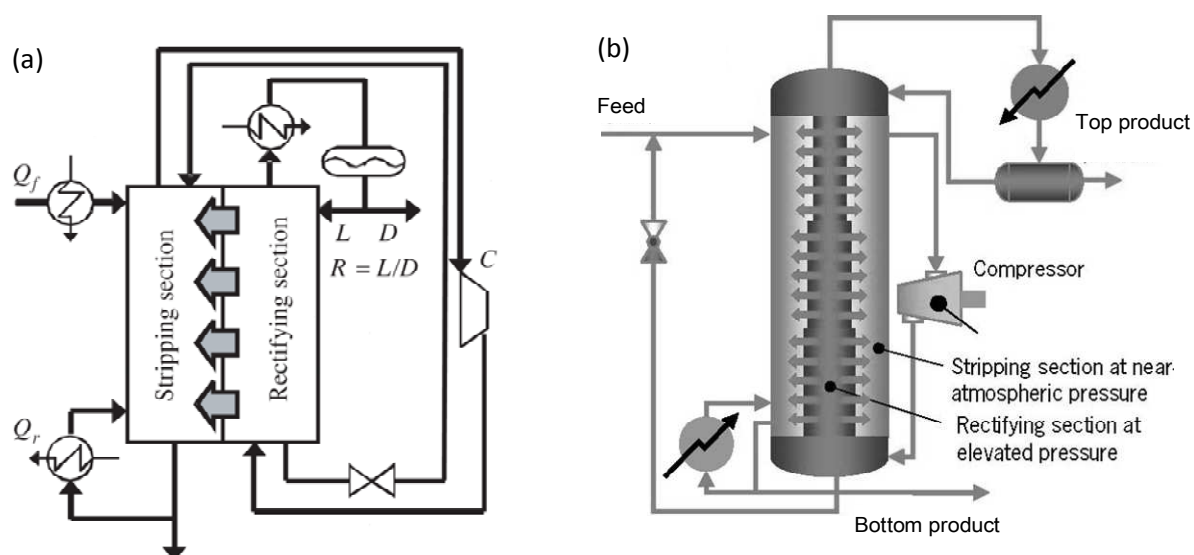


Figure 2.11.(a) Schematic diagram of HIDiC (Fukushima et al., 2006) and (b) HIDiC concentric tube column (From PSE's Gproms manual, gP-B-611--051028 DR)

The ideal HIDiC, which is enlightened from compressor, is a technology combining rectifying and stripping columns in an annular (or similar suitable) arrangement so that they exchange heat along their lengths, and elevated pressure in the rectifying section. Hence it is able to operate without a reboiler or a condenser. It was firstly introduced by Nakaiwa et al. (1996). Both simulation studies (Nakaiwa et al, 2000, 2001, 2003) and experimental validation in a HIDiC pilot plant (Naito K. et al., 2000) were carried out using the model system benzene/toluene, Nakaiwa et al. proposed the new configuration through manipulations of pressure difference between the rectifying and stripping sections and feed thermal condition. Energy savings of HIDiC can reach nearly 50%. However, despite the obvious potential, this very promising concept has not

yet developed into successful industrial-scale applications. This is partly because it is difficult to test its applicability to specific mixtures to be separated, leading to a high perceived risk in deploying such innovative technology. In particular, the practical deployment of HiDiC technology is hampered by the difficulty of proving that it is possible to start up and operate the unit as intended. There is a relatively narrow window of feasible operation, outside which the HiDiC system is either not fully efficient or suffers from liquid drying in certain regions. The main conclusions from the feasibility by Jansens et al. (2001), Olujic et al. (2003) were that HiDiC is especially attractive for close boiling mixtures.

2.3.2 Vapor recompression distillation

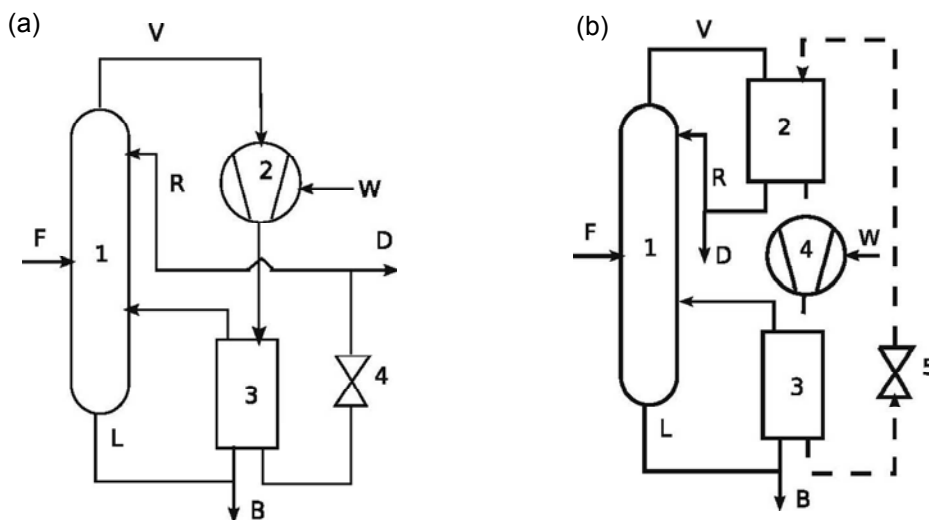


Figure 2.12 Schematic diagram of (1) direct vapor recompression distillation (1: distillation column, 2: compressor, 3:reboiler–condenser and 4: expansion valve)and (2)external vapor recompression distillation (1: distillation column, 2,3: heat exchangers, 4: compressor and 5: expansion valve).(From Jogwar and Daoutidis, 2009).

Vapor recompression distillation is an energy integrated distillation configuration which works on the principle of a heat pump. The vapor coming from the top of the distillation column is compressed in a compressor and is then used to transfer energy in a combined reboiler–condenser leading to the so-called direct vapor recompression distillation (Figure 2.12a). On the other hand, an external refrigerant can also be used to facilitate the energy transfer between the top vapor stream and the bottom liquid stream, leading to the so-called external vapor recompression distillation (Figure 2.12b).Direct vapor recompression is commonly used, whereas external vapor recompression is generally preferred when the column fluid is corrosive or is not a good refrigerant (Jogwar & Daoutidis 2009).

Muhrer et al. (1990) proposed a specific vapor recompression columns control scheme. Compared to conventional columns, heat input control was replaced by compressor control. The pressure loops were found to be faster than the composition loops. Hence, the pressure loop can be adjusted for relatively tight control independently from the composition loops. This simple conclusion can be universally used for most vapor recompression columns if they are satisfying their two requirements: the composition time constants of column must be 5 times larger than the pressure time constant, and the time constants of reboiler of conventional and vapor recompression columns should be nearly the same. For most columns vapor recompression distillation systems the two requirements can be satisfied. Jogwar & Daoutidis (2009) developed a systematic modeling framework which explicitly captures the difference between the different material and energy flows. A case of propane–propylene separation was considered to demonstrate the effectiveness of the proposed control strategy.

2.3.3 Petlyuk arrangements

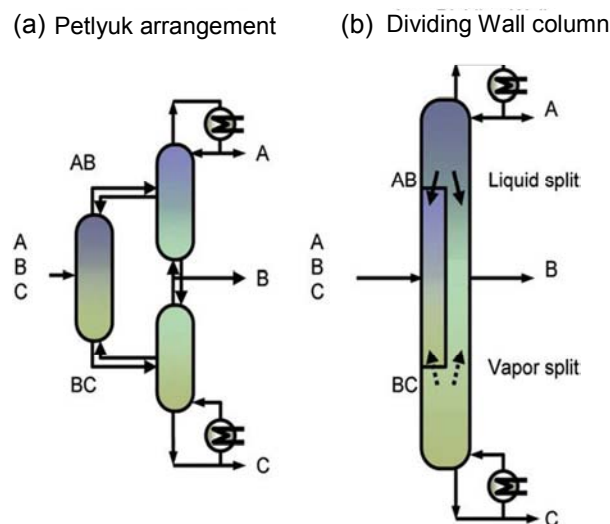


Figure 2.13 Schematic diagram of the fully thermally coupled (Petlyuk) arrangement (a) replaces the conventional arrangements with a pre-fractionator and a main column, and only a single reboiler and a single condenser is needed and (b) dividing wall configuration by moving the pre-fractionator into the same shell (from Halvorsen and Skogestad, 2011).

Petlyuk arrangements may reduce internal vapour flow rate ratio, and thereby the need for external heating and cooling. The basis for the configuration is the pre-fractionator arrangement in Figure 2.13, where the reboiler and condenser of the pre-fractionator column are removed and replaced with directly connected vapour and liquid streams. This is called a full thermallycoupled arrangement. The dividing wall column (DWC) is an implementation of the fully thermally coupled Petlyuk column arrangement (Petlyuk et al., 1965) in a single shell. Kaibel (1987) firstly introduced a distillation column with vertical partitions to separate a feed

mixture into 3 or 4 pure fractions in a single distillation step and column. The internal separation wall prevents lateral mixing of liquid and vapor in the central part of the column, forming feed and outlet sections. This is particularly advantageous when heat sensitive components are to be separated. The potential energy savings are 20-40%, compared to other conventional arrangements (Halvorsen and Skogestad, 2011). Although the DWC has many advantages, its application in chemical process industries has been still limited to 80 industrial columns for zeotropic mixtures. This is due to the lack of proper control strategy to monitor the internal flow on each side of the wall.

All these new arrangements (HiDiC, vapor recompression distillation and Petlyuk arrangements) aim at making the column operate closer to the ideal reversible system by reducing the thermodynamic losses. Whereas the HiDiC approach with internal heat exchange between sections focuses on increasing the efficiency of a single binary distillation column, the Petlyuk like arrangements columns are used for multicomponent separations.

2.4 NONIDEAL MIXTURES SEPARATION

The separation in distillation processes are based on the differences on the vapor and liquid phase compositions of the mixture arising from successive partial vaporization and condensation steps, distillation process is a method for separating various components of a liquid solution depending upon the distribution of these components between a vapor phase and a liquid phase. However, in case of a close-boiling (low relative volatility) mixture, these differences in the compositions of the vapor and the liquid phase become small. The separation of non ideal mixtures, azeotropic ones and low relative volatility ones, is the second major incentive for distillation research. Low relative volatility mixtures require many vaporization or condensations steps, columns and bigger reflux ratio and process often becomes uneconomical both in equipment investment and operating cost by conventional distillation. Azeotrope mixtures also require advanced techniques to facilitate separation.

The most common non-conventional distillation alternatives involve changing the operating pressure (pressure-swing distillation) or adding of a so-called entrainer, either with the load (azeotropic distillation) or at another location than the load (extractive distillation). All of these special techniques are ultimately based on the same differences in the vapor and liquid compositions as ordinary distillation, but, in addition, they rely on some additional mechanism to further modify the vapor-liquid behavior of the key components. These enhanced techniques can be classified according to their effect on the relationship between the vapor and

liquid compositions: 1. Azeotropic distillation and pressure-swing distillation are methods that cause or exploit azeotrope formation or behavior to alter the boiling characteristics and separability of the mixture. 2. Extractive distillation and salt distillation are methods that primarily modify liquid-phase behavior to alter the relative volatility of the components of the mixture. 3. Reactive distillation is a method that uses chemical reaction to modify the composition of the mixture or, alternatively, use existing vapor-liquid differences between reaction products and reactants to enhance the performance of a reaction.

2.4.1 Pressure-swing distillation

Pressure-swing distillation is a method for separating a pressure-sensitive azeotrope that utilizes two columns operated in sequence at two different pressures if concentration of the azeotrope changes significantly with pressure (Seader and Henley, 1998). Generally, the composition of component A (light in the azeotropic mixture) increases as pressure decreases, possibly until disappearance of the azeotrope allowing the use of a conventional distillation process. In a ternary mixture separation, there may exist distillation boundaries involving azeotrope(s) as seen on residue curve maps. By changing the pressure we can cross these boundaries because they vary with pressure along with the azeotropic composition. Between the boundaries at two different pressures, there is a region from where different products can be obtained at the different pressures. If all products obtained at different pressures are pure components or pressure sensitive binary azeotrope(s) this region is considered as the operating region of pressure swing distillation (Modla et al., 2010). In pressure-swing distillation process, two columns operate at different pressures, each column supplied with the azeotropic composition at a pressure which is different from the other to obtain a possible pure component in each column. For the case of mixture with T_{\max} azeotrope, the less volatile component are obtained at first column top and more volatile one from the second column (Figure 2.14). The opposite result occurs for the mixture with a T_{\min} azeotrope (Gerbaud et al., 2010).

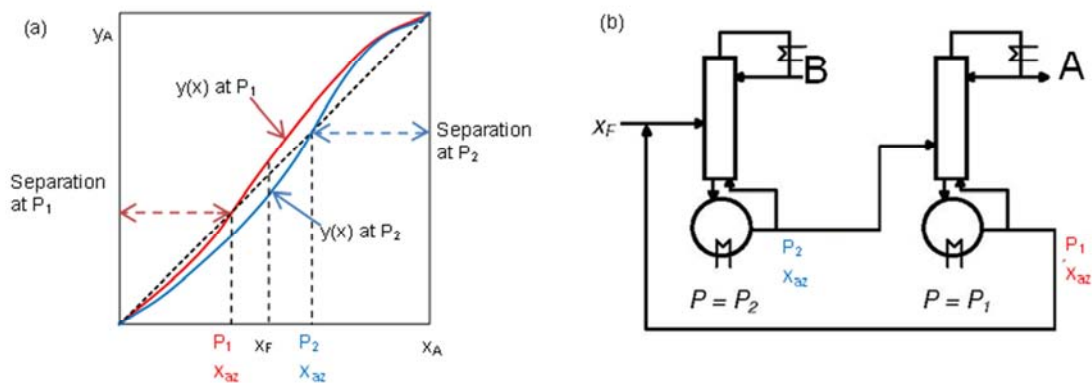


Figure 2.14 Effect of pressure on the azeotropic composition and corresponding continuous pressure-swing distillation processes (from Gerbaud and Rodriguez-Donis, 2010).

Lewis (1928) appears to be the first one to exploit the pressure sensibility to distillate azeotropic mixtures. Since then pressure-swing distillation has been known as a readily thermally integrated method to separate azeotropic mixtures. In 1992, Knapp and Doherty proved that pressure-swing is not restricted to binary mixtures with pressure-sensitive azeotrope, and it can be extended to separate mixtures in which the desired products lie in different distillation regions. They can be separated by a new pressure-swing process when one end of the distillation boundary is a pressure-sensitive azeotrope. Thus pressure-insensitive binary azeotropes can be separated using novel entrainers that form pressure-sensitive distillation boundaries. The separations of ethanol from water and acetone from methanol were used to demonstrate the new pressure-swing technique. These examples exhibit some interesting behavior such as (1) a region of multiplicity in the number of trays required to achieve the same separation at fixed reflux ratio, (2) a maximum reflux ratio above which no feasible column exists, (3) a separation where the unexpected component is the distillate due to a reversal of the relative volatility as the pressure changes, and (4) a non-azeotropic separation that becomes easier as the pressure is increased. An optimal-control algorithm was employed to determine desirable campaigns, and to schedule pressure switch-over policies (Phimister and Seider, 2000). The column achieves production rates near 89% of the maximum throughput of a single column in the continuous process and shows superior performance when compared to reverse-batch operation. Based on the analysis of batch stripping/batch rectifying distillation regions, assuming maximal separation, Modla et al. (2010) studied the feasibility of the separation of ternary homoazeotropic mixtures with pressure swing batch distillation (PSBD) in different column configurations: one column (batch stripper (BS) and rectifier (BR) and double column configurations (double column batch stripper (DCBS) and rectifier (DCBR)). The separation steps were also determined for the corresponding column configurations.

2.4.2 Azeotropic distillation

Azeotropic distillation usually refers to the specific technique of adding a third component along with the main feed. In some senses, adding an entrainer is similar to extractive distillation. Azeotropic processes have been well studied and the feasibility assessment only relies upon residue curve map analysis whereas for extractive distillation, the volatility order region must be known, as well. The separation of a minimum boiling azeotrope AB with a light entrainer E forming no new azeotrope is considered. The ternary diagram belongs to the 1.0-2 class (Figures 2.8 and 2.15). Both A and B are stable nodes but they are located in different batch distillation regions. Residue curves begin at the unstable entrainer vertex (E) and end at the stable A or B. In batch both azeotropic components can be distilled if the boundary is curved enough (Bernot et al., 1990, Doherty and Malone, 2001). In continuous only A or B is obtained from the column, regarding continuous process, research has focused on advances in the methodologies for the synthesis, design, analysis and control of separation sequences involving homogeneous and heterogeneous azeotropic towers. Maps of residue curves and distillation lines were studied (Widagdo and Seider, 1996), as well as geometric methods for the synthesis and design of separation sequences, trends in the steady-state and dynamic analysis of homogeneous and heterogeneous towers, the nonlinear behavior of these towers, and strategies for their control. Emphasis is placed on the methods of computing all of the azeotropes associated with a multicomponent mixture, on the features that distinguish azeotropic distillations from their non azeotropic counterparts, on the possible steady-state multiplicity, and on the existence of maximum and minimum reflux ratio bounds. Important considerations in the selection of entrainers are examined (Foucher et al., 1991b). For the synthesis of separation trains, when determining the feasible product compositions, the graphical methods are clarified, especially the conditions under which distillation boundaries can be crossed and bounding strategies under finite reflux ratio.

The azeotropic distillation column usually follows three rules:

1. The temperature decreases from bottom to top of the column.
2. The material balance must be satisfied and the rule indicates that the points of feed, distillate, and boiler are aligned in the composition diagram. If there are multiple power supplies, the global feed is calculated in advance by a lever arm rule.
3. Applying the principles of total reflux ratio feasibility, the compositions of the distillate and boiler are located approximately on a residue curve.

Figure 2.15 shows the separation of an azeotropic ternary system belongs to the class Serafimov 1.0-2. Two distillation regions are separated by a separatrix connecting the saddle point azeotrope and unstable node entrainer in Figure 2.15. The feeds F_1 and F_2 enter in different locations, and the composition of the global feed F_G is aligned with that of the column bottom SL , and the distillate D . x_D and x_N are connected by a composition profile which approximately follows the residue curve map. For indirect separation, the column bottom SL is located near the stable node B (Figure 2.15a). For direct separation, the distillate D is located near the unstable node E (Figure 2.15b).

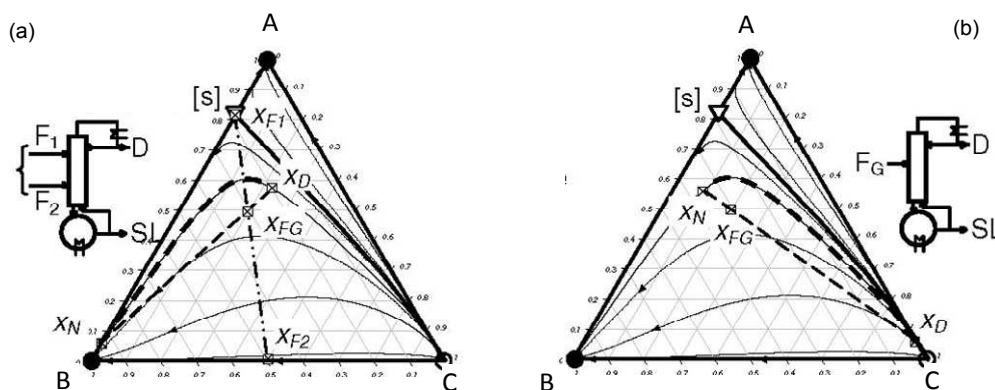


Figure 2.15 Indirect separation (a) and direct (b) azeotropic continuous distillation under finite for a 1.0-2 class mixture (from Gerbaud and Rodriguez-Donis, 2010).

2.4.3 Reactive distillation

Reactive distillation (RD) is a process where the chemical reactor is also the column. The entrainer reacts preferentially and reversibly with one of the original mixture components. The reaction product is distilled out from the non-reacting component and the reaction is reversed to recover the initial component. This can result insignificant reductions in both energy and equipment in systems that have appropriate chemistry and appropriate vapor–liquid phase equilibrium. This technique is attractive in those systems where certain chemical and phase equilibrium conditions exist and it is especially useful for equilibrium-limited reactions such as esterification and ester hydrolysis reactions. Conversion can be increased far beyond what is expected by the equilibrium due to the continuous removal of reaction products from the reactive zone. This helps to reduce capital and investment costs and may be important for sustainable development since that shifts the chemical equilibrium to produce more product and thus a lower consumption of resources (Luyben and Yu, 2009).

Although invented in 1921, the industrial application of reactive distillation did not take place before the 1980s. Being a relatively new field, research on various aspects such as modeling and simulation, process

synthesis, column hardware design, non-linear dynamics and control is in progress. The suitability of RD for a particular reaction depends on various factors such as volatilities of reactants and products along with the feasible reaction and distillation temperature. Hence, the use of RD for every reaction may not be feasible. A commentary paper (Malone and Doherty, 2000) on RD exposes an effective way of decomposing the design and development of reactive distillation involves four stages: (1) feasibility and alternatives, (2) conceptual design and evaluation, (3) equipment selection and hardware design, and (4) operability and control.

2.4.4 Salt-effect distillation

The salt effect distillations a method of extractive distillation in which a salt is dissolved in the mixture of liquids to be distilled. The salt dissociates in the mixture and alters the relative volatilities sufficiently so that the separation becomes possible. Hence salt effect on vapor-liquid equilibrium relationships provides a potential technique of extractive distillation for systems difficult or impossible to separate by normal rectification in a related process. The salt is fed into the distillation column at a steady rate by adding it to the reflux ratio stream at the top of the column. It dissolves in the liquid phase, and since it is non-volatile, flows out with the heavier bottoms stream. The bottom is partially or completely evaporated to recover the salt for reuse. An example is the dehydration of ethanol using potassium acetate solution (Furter, 1968). One advantage of salt-effect distillation over other types of azeotropic distillation is the potential for reduced costs associated with energy usage.

2.4.5 Extractive distillation

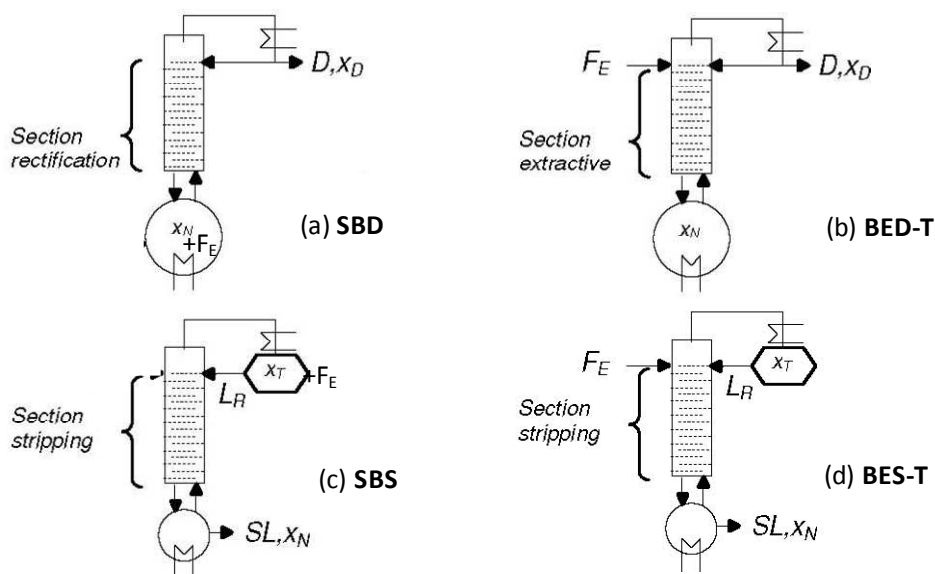
Extractive distillation is a powerful and widely used technique for separating azeotropic and low relative volatility mixtures in pharmaceutical and chemical industries. Given an azeotropic mixture A-B (with A having a lower boiling temperature than B), an entrainer E is added to interact selectively with the original components and alter their relative volatility, thus enhancing the original separation. It differs from azeotropic distillation by the fact that the third-body solvent E is fed continuously in another column position other than mixture feed. For decades a single feasibility rule holds in industry for separating minimum boiling azeotrope: extractive distillation is defined as involving a miscible, heavy component. The solvent forms no new azeotrope and the original component with the greatest volatility separates out as the top product. The bottom product consists of a mixture of the solvent and the other component fed to the recovering column. An example is the dehydration of ethanol with ethylene glycol. The extractive process allows distilling ethanol, a saddle of the 1.0-1a class diagram.

2.5 LITERATURE STUDIES ON EXTRACTIVE DISTILLATION

Extractive distillation has been studied for many decades with a rich literature, some main subjects studied include: (1) column with all possible configurations (Davidyan et al., 1994, Phimister and Seider, 2000, Stéger et al., 2005b, Hua et al., 2007) and a systematic study on column configurations of continuous heterogeneous extractive distillation was published by Rodriguez-Donis et al. (2007a); (2) process operation policies and strategy (Demicoli and Stichlmair, 2003, Safrit and Westerberg, 1997, Lelkes et al., 1998); (3) process design, synthesis, optimization (Doherty and Calderola, 1985, Pham and Doherty, 1990a, Barreto et al., 2011); (4) determining the separation sequencing (Bernot et al., 1991, Ulrich and Morari, 2003); (5) entrainer design and selection (Wahnschafft and Westerberg, 1993a, Thomas and Karl Hans, 1994, Van Dyk and Nieuwoudt, 2000); (6) feasibility studies (Knapp and Doherty, 1994, Rodriguez-Donis et al., 2009a, Rodriguez-Donis et al., 2011).

2.5.1 Extractive Batch Column configurations

Several column configurations can be used for extractive distillation both in batch and continuous. In batch mode, batch extractive distillation (BED) is a process where the mixture to be separated is charged into the still whereas entrainer (E) is fed continuously. When the entrainer is added to the mixture to be separated at the beginning of the process, it belongs to solvent-enhanced batch distillation (SBD). Both BED and SBD processes can be performed either in rectifier, or in middle-vessel column, or in stripping column (see Figure).



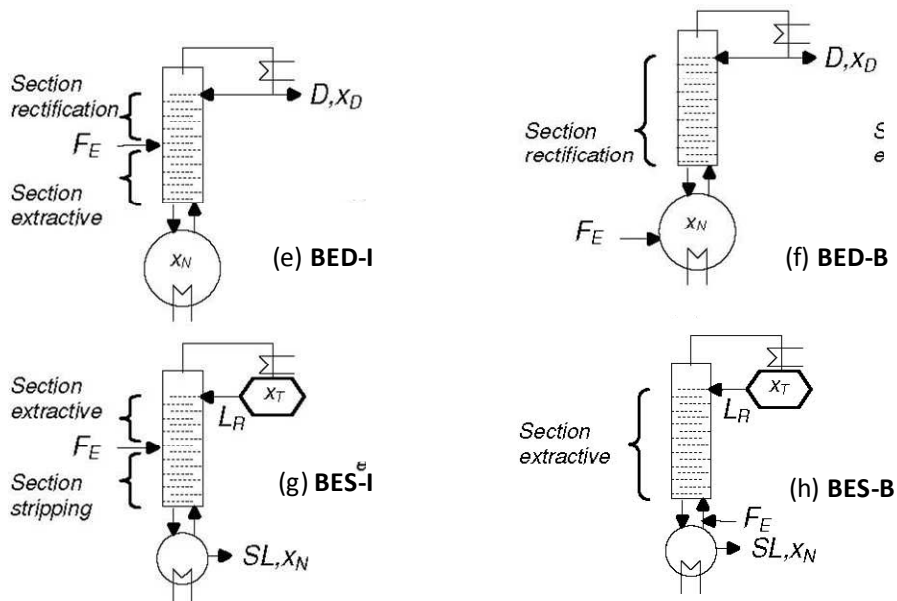


Figure 2.16 Configurations of extractive batch distillation column in rectifier and stripper

According to the position of the entrainer feed, four configurations in a rectifier can be considered:

- A single rectifying section exists (Figure 2.16a, b).
 - o both the entrainer and feed are premixed to the boiler in batch mode (SBD configuration).
 - o the entrainer is fed to the boiler continuously (BED-B configuration).
- extractive and rectifying section exist (Figure 2.16e).
 - o the entrainer is fed to the intermediate section in continuous mode (configuration BED-I).
- a single extractive section exists (BED-T configuration) (Figure 2.16f).
 - o the entrainer is fed to the condenser in continuous mode (configuration BED-I).

Correspondingly, depending on the location of the feed configurations in a stripper (reverse extractive column) can be considered (see Figure 2.16 c, d, g, h):

- A single stripping section (Figure 2.16c,d).
 - o both the entrainer and feed are premixed to the condenser (SBS configuration).
 - o both feed and entrainer are fed to the condenser, the entrainer is fed continuously (BES-B configuration).
- extractive and rectifying section (Figure 2.16g).
 - o the entrainer is fed to the intermediate section in continuous mode (configuration BES-I).
- a single extractive section exists (Figure 2.16h).

- o the feed is fed to the condenser and the entrainer is fed to the boiler in continuous mode (configuration BES-B).

Steger et al. (2005) emphasize that the most commonly applied configuration is the rectifier as controlling a batch rectifier is less complex than controlling a stripper.

2.5.2 Continuous Column configurations

A typical extractive distillation process is shown in Figure 2.17, which includes an extractive distillation column where the solute, A, is obtained as the distillate and the mixture of raffinate, B, and solvent is exits from the bottom. A solvent recovery column comes next where the purified raffinate, B is obtained as distillate and the solvent is recovered from the bottom and recycled to the extractive distillation column is also shown. The study on extractive distillation summarizes in following sections.

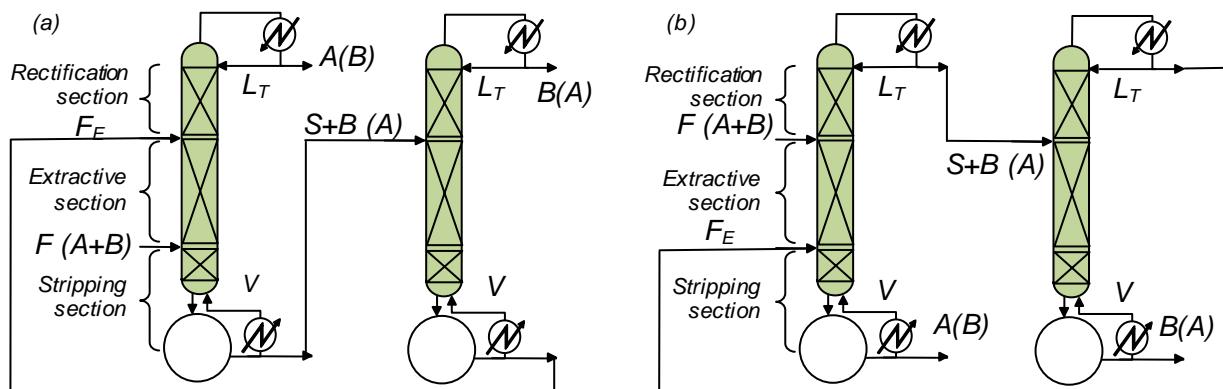


Figure 2.17. Flowsheet of typical extractive distillation with (a) heavy entrainer and (b) light entrainer

Rodriguez-Donis et al (2007) investigated the feasibility of heterogeneous extractive distillation process in a continuous column considering several feed point strategies for the entrainer recycle stream and for the main azeotropic feed (Figure 2.18).

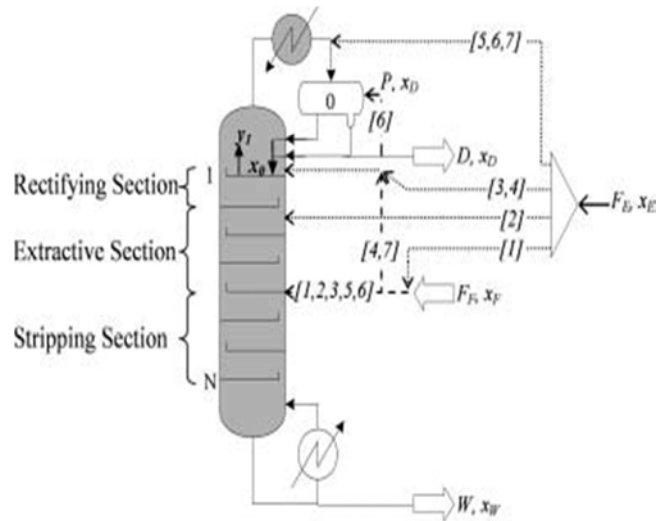


Figure 2.18 Configurations for the heterogeneous distillation column considering all possibilities for both the entrainer recycle and the main azeotropic feed. (From Rodriguez-Donis et al. 2007)

Depending on these choices, the heterogeneous distillation column is composed of one, two, or three column sections. Unlike homogeneous extractive distillation, a reflux policy composed by a single or both decanted liquid phases is considered. They also looked at the impact of the external feeding influence on the composition of the top column liquid stream, which knowledge was required to assess the feasibility. Figure 2.18 try to display superstructure for the extractive distillation column considering all possibilities for both the entrainer recycle and the main azeotropic feed (Rodriguez-Donis et al., 2007). Taking into account the seven configurations combining the entrainer recycle stream and the main azeotropic feed. The heteroazeotropic distillation column is the aggregation of several parts among (i) a condenser and a decanter together, (ii) a rectifying section from the top of the column down to the entrainer recycle feed, (iii) an extractive section between the two feeds, and (iv) a stripping section from the main azeotropic feed to the bottom, including the boiler. Choosing the main azeotropic feed location (intermediate or column top) and the entrainer recycle strategy (mixed with the azeotropic feed or with the top liquid reflux or sent to an intermediate column point of the column or to the decanter) leads to any of the seven configurations.

2.5.3 Entrainer design

The effectiveness of an extractive distillation process relies on the choice of extractive agent. Although many heuristic methods have been developed to assist in the choice of solvent, they are mostly qualitative. A more effective method for selecting solvents is computer-aided molecular design (CAMD). In this method the required properties of a solvent are specified, and its structure is then calculated through the use of group contribution methods (Van Dyk and Nieuwoudt, 2000b). Entrainer design study has been rich in the literature.

A potential candidate entrainer is often related to three major properties: (1) pure solvent properties such as boiling point, vapor pressure, molar volume, and critical properties (Marrero and Gani, 2001, Heins, 1994); (2) process properties such as relative volatility, solvent solubility power, phase stability criterion performance index (Pretel et al., 1994), and (3) recent criteria related to sustainability: environment properties such as LC₅₀ (Song and Song, 2008), environmental waste, impact, health, and safety issues (Weis and Visco, 2010). The entrainer is conventionally chosen in industrial practice as a heavy (high boiling) component (Seader et al., 1998, Luyben and Chien, 2010, Lang et al., 1994, Rodriguez-Donis et al., 2009a). However, there are some cases when its use is not recommended such as if a heat sensitive, high boiling component mixture is to be separated. Different entrainers can cause different components to be recovered overhead in extractive distillation, potential entrainers is critical since an economically optimal design made with an average design using best entrainer can be much less costly. Besides, the entrainer must also be easy to recover from the regeneration column. Inspired by Laroche et al., (1991), the work by Rodriguez-Donis et al. (2009a, 2009b, 2010, 2012a, 2012b) showed that a feasible extractive process is achievable in batch for heavy, light, or intermediate entrainer and even for entrainers that form new azeotropes. Extending that insight to continuous is the main objective of our PhD Thesis.

2.5.4 Key operating parameters

Both minimum entrainer - feed flow rate ratio and minimum reflux ratios can be used as indicators of a flowsheet's energy requirements. Levy and Doherty (1986) used tangent pinch points to calculate minimum reflux ratios for class 1.0-1a. Knapp and Doherty, (1994) determined for 1.0-1a class (min T azeotrope with a heavy entrainer) the minimum entrainer - feed flows using a geometric method involving bifurcations of the finite difference equations describing the middle section of the column. In addition to minimum reflux ratio, there may be a maximum reflux ratio above which separation cannot be achieved. These bounds for the reflux ratio depend on the entrainer feed flow rate ratio. The range of feasible choices for the reflux ratio decreases with decreasing entrainer - feed flow rate ratio. Below a minimum entrainer - feed flow rate ratio the extractive effect is no longer sufficient for separation and a feasible reflux ratio policy cannot be found.

2.6 METHODOLOGY FOR EXTRACTIVE DISTILLATION PROCESS FEASIBILITY IN RESEARCH

The design of all distillation processes is connected to thermodynamics, in particular to the boiling point of each compound and azeotrope. For conventional or azeotropic distillation, residue curve maps

analysis allows assessing the feasibility under infinite reflux ratio conditions with the finding of the ultimate products under direct or indirect split conditions (Doherty and Malone, 2001).

The initial feasibility study related to well-known design tools: residue curve maps analysis and liquid phase diagrams, since they can represent good approximations to actual equilibrium behavior and can be used to predict composition changes in separation processes under infinite reflux ratio conditions, residue curve maps (RCMs), were first defined and used by Schreinemakers (1901). A past review article (Fien and Liu, 1994) presented the use of ternary diagrams including RCMs for the feasibility analysis, flowsheet development, and preliminary design of both homogeneous and heterogeneous azeotropic systems separation processes. Residue curve maps of reactive and extractive distillation units are used by (Jiménez et al., 2001) for a simultaneous analysis, this graphical techniques reveal the sensitivity of design options by giving us a visual representation over the whole composition space and assist the engineer to detect separation constraints. Pham and Doherty (1990b) conducted a residue curve map analysis for ternary heterogeneous mixtures to aid in the sequencing of heterogeneous distillation columns. However, distillation runs under finite reflux ratio (reboil ratio in reverse extractive distillation) conditions, finding which products are achievable and the location of the suitable feed composition region is more complicated (Wahnschafft et al., 1992, Fidkowski et al., 1993, Pöllmann and Blass, 1994) because the dependency of composition profile on reflux ratio (reboil ratio) needs to be considered. That affects the range of composition available to each section profiles, due to the occurrence of pinch points, which differ from the singular points of the residue curve map (Levy et al., 1985, Doherty and Caldarola, 1985, Bausa et al., 1998, Urdaneta et al., 2002).

The design of extractive distillation columns is further complicated by the occurrence of a middle extractive section, and the process often shows counterintuitive operational properties. The separation maximum and efficiency are not necessarily improved by increasing the reflux ratio (Knapp and Doherty, 1994) and batch extractive distillation studies further demonstrated the importance of selecting a suitable entrainer feed flow rate ratio (Lelkes et al., 1998a). As detailed later, those issues are related to the knowledge of univolatility curve location and of volatility order region. It was needed in complement to RCM analysis for studying the feasibility of extractive distillation processes.

2.6.1 Ternary systems studied in extractive distillation

Ternary systems are studied in this thesis on the basis of Serafimov's classification that includes 26 classes of feasible topological structures of VLE diagrams for ternary mixtures (Serafimov, 1996). The

entrainer E is conventionally defined by its boiling temperature with respect to the binary mixture A-B to separate: a heavy entrainer E has a boiling temperature higher than A and B, an intermediate entrainer E has a boiling temperature between the A and B, a light entrainer E has a boiling temperature lower than A and B. In industry, extractive distillation entrainer is usually chosen as a heavy (high boiling) component (Seader, J. D., et al., 1998, Luyben and Chien, 2010, Lang et al., 1994, Rodriguez-Donis et al., 2009a). Theoretically, any candidate entrainer satisfying the feasibility and optimal criteria enounced by Rodriguez-Donis et al.(2009a) can be used no matter it is heavy, light, or intermediate entrainer. Literature studies on intermediate entrainer or light entrainer validate this assumption (Lelkes et al., 2002, Hunek et al., 1989, Laroche et al., 1992, Lang et al., 1999b, Varga et al., 2006, Rodriguez-Donis et al., 2011). Apart from Laroche et al., 1990, 1992, continuous extractive distillation studies have always considered a heavy entrainer to split a minimum boiling azeotrope which belongs to class 1.0-1a (Knapp and Doherty, 1994a, Luyben, 2008a, 2008b, Brüggemann and Marquardt, 2004). Laroche et al., 1991 also considered light and intermediate entrainers.

Steger et al., 2005 compared several systems of batch extractive distillation in a rectifier. Varga (2006 PhD thesis) surveyed batch extractive distillation studies in a stripper. These works give a useful guide to the separation of mixtures binary homogeneous azeotropic mixtures by batch extractive distillation. Table 2. and

Table 2.2 update the information on literature for each ternary system.

Table 2.1 The most important literature concerning extractive distillation separation of binary azeotropic and low relative volatility mixtures in a batch rectifier with light, intermediate or heavy entrainer.

Extractive distillation of ternary mixture systems								
Entrainer type	heavy			intermediate		light		
Mixture type	minimum	maximum	low alpha	minimum	maximum	minimum	maximum	low alpha
Serafimov class	1.0-1a	1.0-2	0.0-1	1.0-1b	1.0-1b	1.0-2	1.0-1a	0.0-1
Volatility order	Az>A>B>E	A>B>Az>E	A>B>E	Az>A>E>B	A>E>B>Az	E>Az>A>B	E>A>B>Az	E>A>B
Related Literature								
	Yatim, 1993,	Lang et al., 2000a	Lang et al., 1994	Rev et al., 2003	Bernot et al., 1990	Hunek et al., 1989	Varga et al., 2006	Varga et al., 2006
	Lang et al., 1994, Laroche et al., 1992	Lang et al., 2000b	Rodriguez-Donis et al. 2009b	Varga, 2003	Lelkes et al., 2002	Laroche et al., 1992	Rodriguez-Donis et al. 2012a	Rodriguez-Donis et al. 2012a
	Knapp and Doherty, 1994a,	Rodriguez-Donis et al. 2009a		Rodriguez-Donis et al. 2012b	Rodriguez-Donis et al. 2012b	Lelkes, 1998		
	Lang et al., 1995,					Lelkes et al., 1998b		
	Lelkes et al., 1998a, 1998b,					Lang et al., 1999		
	Milani, 1999,					Varga et al., 2006		
	Brüggemann and Marquardt, 2004,					Rodriguez-Donis et al. 2012a		
	Luyben, 2008a,2008b,							
	Rodriguez-Donis et al. 2009a							

Table 2.2 The study case related to extractive distillation separation of binary azeotropic and low relative volatility mixture in a batch rectifier with light, intermediate or heavy entrainer.

Extractive distillation of ternary mixture systems								
Entrainer type	heavy			intermediate		light		
Mixture type	minimum	maximum	low alpha	minimum	maximum	minimum	maximum	low alpha
Serafimov class	1.0-1a	1.0-2	0.0-1	1.0-1b	1.0-1b	1.0-2	1.0-1a	0.0-1
Volatility Order	Az>A>B>E	A>B>Az>E	A>B>E	Az>A>E>B	A>E>B>Az	E>Az>A>B	E>A>B>Az	E>A>B
Case study [A ; B ; E]								
	acetone methanol water	acetone chloroform benzene	ethyl acetate benzene butanol	methyl acetate cyclohexane carbon tetrachloride	chloroform ethyl acetate 2-chlorobutane	ethanol water methanol	water ethylene diamine methanol	chlorobenzene ethylebenzene 4-methylheptane
	acetone methanol isopropanol	acetone chloroform toluene	heptane toluene phenol	methanol Toluene triethylamine		ethanol toluene acetone	chloroform acetone dichloromethane	
	acetone methanol ethanol	vinyl acetate Butyl acetate chloroform	heptane toluene chlorobenzene			methyl ethyl ketone(A) enzene(B) acetone(E)	methyl isobutyl ketone(A) propanoic acid dimethylformami de	
	acetone methanol chlorobenzene		ethyl acetate benzene hexanol					

2.6.2 Batch extractive process operation policies and strategy

Process operation policies and strategy concern batch extractive distillation process. The batch extractive distillation realization and the role played by the different steps in the process are analyzed and are presented by Lelkes et al. (1998), on the basis of this analysis several operational policies. Usually, batch extractive distillation (BED) proceeds in four operation steps: (1) infinite reflux ratio operation to reach steady state inside the column, (2) infinite reflux ratio operation with continuous entrainer feeding, (3) finite reflux ratio, leading to the distillation of one of the original component while feeding continuously the entrainer, and (4) conventional distillation for the separation of the zeotropic binary mixture retained into the still. The original $R=\text{const.}$ policy is modified by shortening the second preparatory step of the BED ($R=\infty$, $F>0$). The possibilities of performing a constant distillate composition ($x_{D,A}=\text{const.}$) policy are discussed. In their article about improved operational policies for batch extractive distillation columns, Safrit and Westerberg (1997) studied the sensitivities to various column operation parameters, in particular the entrainer - feed flow rate ratio policy, bottoms flow rate ratio policy, and the switching time between operational steps. They showed that these variables do have a large effect on the final solution and should be solved as in an optimal process. While the optimal policies for the entrainer and bottoms flow rate ratio were not obvious, the value of the switching time that maximized the final profit for the simulations run was very near to the value of the time in which the accumulated profit was maximized in the main operational step (distillate recovery step). The problem solution was very sensitive to assumed product value and operational costs. They also found that the still path steering algorithm provides a good first approximation to the bottoms flow rate ratio policy for certain types of objective functions. Demicoli and Stichlmair (2003), presented an experimental investigation of the separation of a zeotropic ternary mixture via total reflux ratio operation and of the separation of an azeotropic binary mixture via batch-wise extractive distillation. Lang et al. (2006) proposed a new operational policy which was successfully applied in the industry, as well. They started the continuous E feeding already during the heating-up of the column.

Step 1 feasibility obeys the residue curve map analysis results, because the residue curve then describes the liquid composition in the column. Steps 2 and 3 are the extractive steps, and their feasibility is determined by the existence of an extractive composition profile that links the rectifying profile to the instantaneous still composition, following Lelkes' model. Under feasible operating parameters, both profiles intersect close to the extractive stable node (SN_{extr}) that, under a sufficiently high entrainer/vapor flow rate ratio and number of extractive trays, is commonly located near the binary side of the entrainer and the

original component, which is drawn as distillate product. The other azeotropic component remains in the still with the entrainer at the end of step 3. This intersection-finding methodology has been used to study the separation of minimum and maximum azeotropic mixtures and that of close-boiling mixtures by feeding a heavy, light, and intermediate entrainer in extractive distillation (Rodriguez-Donis et al., 2009a, 2009b, 2010, 2012a, 2012b).

The necessary operating steps of the process and the limiting operating parameters in a batch rectifier or a batch stripper with intermediate entrainer feeding are determined and compared in Table 2.3 and Table 2.4 for each case reported in Table 2.2. These results can be useful in other separation problems. The limiting parameters include: the reflux ratio R , the entrainer - feed flow rate ratio F / V , the number of theoretical stages in rectifying and extractive section.

Table 2.3. The operating steps and limiting parameters of extractive distillation in configuration BED-I separating binary azeotropic and low relative volatility mixture in a batch rectifier with light, intermediate or heavy entrainer (Varga, 2006).

Extractive distillation of ternary mixture systems								
Entrainer type	heavy			intermediate		light		
Mixture	minimum	maximum	low alpha	minimum	maximum	minimum	maximum	low alpha
Serafimov class	1.0-1a	1.0-2	0.0-1	1.0-1b	1.0-1b	1.0-2	1.0-1a	0.0-1
Volatility Order	Az>A>B>E	A>B>Az>E	A>B>E	Az>A>E>B	A>E>B>Az	E>Az>A>B	E>A>B>Az	E>A>B
Analysis of Operating steps with configuration BED-I								
Adding entrainer in advance	-	-	-	-	necessary	necessary	necessary	necessary
Startup	$R=\infty ; F=0$	$R=\infty ; F=0$	$R=\infty ; F=0$	$R=\infty ; F=0$	$R=\infty ; F=0$	$R=\infty ; F=0$	$R=\infty ; F=0$	$R=\infty ; F=0$
Purification	$R=\infty ; F>0$	$R=\infty ; F>0$	$R=\infty ; F>0$	$R=\infty ; F>0$	-	-	-	-
1st product	$R<\infty ; F>0$	$R<\infty ; F>0$	$R<\infty ; F>0$	$R<\infty ; F>0$	$R<\infty ; F>0$	$R<\infty ; F>0$	$R<\infty ; F>0$	$R<\infty ; F>0$
	{A}	{A}	{A}	{A}	{AE}	{EA}	{EA}	{EA}
2nd product	$R<\infty ; F=0$	$R<\infty ; F=0$	$R<\infty ; F=0$	$R<\infty ; F=0$	$R<\infty ; F=0$	$R<\infty ; F=0$	$R<\infty ; F=0$	$R<\infty ; F=0$
	{B}	{B}	{B}	{E}	{E}	{E}	{E}	{E}
3rd product	remainder: {E}	remainder: {E}	remainder: {E}	remainder: {B}	remainder: {B}	remainder: {B}	remainder: {B}	remainder: {B}
Reloading					{AE}	{EA}	{EA}	{EA}
4th product					$R<\infty ; F=0$	$R<\infty ; F=0$	$R<\infty ; F=0$	$R<\infty ; F=0$
					{A}	{E}	{E}	{E}
5th product					remainder: {E}	remainder: {A}	remainder: {A}	remainder: {A}
Limitation parameters								
Reflux ratio	min	min	min	min	min	min ; max	min ; max	min
N_{Rect} (rect. stage)	min ; max	min	min	min ; max	min	min ; max	min ; max	min ; max
N_{Extr} (extr. stage)	min	min ; max	min	min	-	max	max	max
F/V (entrainer - feed flow rate ratio)	min	max	min	min	min	max	min	-

Table 2.4. The operating stages and limiting parameters of azeotropic extractive distillation in configuration BES-I separating binary azeotropic and low relative volatility mixture in a batch rectifier with light, intermediate or heavy entrainer (Varga, 2006).

Extractive distillation of ternary mixture systems									
Entrainer type:	heavy			intermediate		light			
Mixture:	minimum	maximum	low alpha	minimum	maximum	minimum	maximum	low alpha	
Volatility Order	Az>A>B>E	A>B>Az>E	A>B>E	Az>A>E>B	A>E>B>Az	E>Az>A>B	E>A>B>Az	E>A>B	
Analysis of Operating steps with configuration BES-I									
Operating steps – BES-I	1 / Startup	$s=\infty ; +F$	$s=\infty ; +F$	$s=\infty ; +F$	$s=\infty ; +F$	$s=\infty ; F=0$	-	$s=\infty ; F=0$	$s=\infty ; +F$
	2 / purification	-	-	-	-	$s=\infty ; F>0$	-	$s=\infty ; F>0$	-
	3 / production	$s<\infty ; F>0$ {B/E}	$s<\infty ; F>0$ {B/E}	$s<\infty ; F>0$ {B/E}	$s<\infty ; F>0$ {B/E}	$s<\infty ; F>0$ {B}	-	$s<\infty ; F>0$ {B}	$s<\infty ; F>0$ {B}
	4 / cutting	$s<\infty ; F>0$	$s<\infty ; F>0$	$s<\infty ; F>0$	$s<\infty ; F=0$	$s<\infty ; F=0$	-	$s<\infty ; F=0$	$s<\infty ; F=0$
	5 / production	$s<\infty ; F=0$ {E} remainder: A	$s<\infty ; F=0$ {E} remainder: A	$s<\infty ; F=0$ {E} remainder: A	$s<\infty ; F=0$ {E} remainder: A	$s<\infty ; F=0$ {E} remainder: A	-	$s<\infty ; F=0$ {A} remainder: E	$s<\infty ; F=0$ {A} remainder: E
	reloading	{B/E}	{B/E}	{B/E}	{B/E}	-	-	-	-
	6 / production	$s<\infty ; F=0$ {E} remainder: B	$s<\infty ; F=0$ {E} remainder: B	$s<\infty ; F=0$ {E} remainder: B	$s<\infty ; F=0$ {B} remainder: E	-	-	-	-

2.6.3 Thermodynamic insight on extractive distillation feasibility

Almost all the literature relied upon the feasibility rule that a heavy entrainer forming new azeotrope was suitable to separate a minimum boiling azeotrope. The corresponding ternary diagram belongs to the 1.0-1a Serafimov's class (occurrence 21.6%). As Laroche et al. (1991, 1992) showed for the 1.0-1a class, knowledge of the residue curve map and of the location of the univolatility curve $\alpha_{AB}=1$ can help assess which product is removed in the distillate when using a light, intermediate or heavy entrainer. With a heavy entrainer, A (or B) can be distilled by using a direct sequence if the univolatility curve intersects the A-E edge (the B-E edge). This helped to explain some counterintuitive observation that sometimes the intermediate boiling compound B within the A-B-E mixture is removed in the distillate.

The important separation of a maximum boiling azeotrope with a heavy entrainer corresponds to the 1.0-2 class (occurrence 8.5%) was not studied in continuous operation but it was studied in batch by using composition profiles (Lang et al., 2000a, 2000b).

Completion and extension of thermodynamic insight to other mixture classes was published by Rodriguez-Donis et al (2009a, 2009b, 2010, 2012a, 2012b) who combined knowledge of the thermodynamic properties of residue curve maps and of the univolatility and unidistribution curves location. They expressed a general feasibility criterion for extractive distillation under infinite reflux ratio:

“Homogeneous extractive distillation of a A-B mixture with entrainer E feeding is feasible if there exists a residue curve connecting E to A or B following a decreasing (a) or increasing (b) temperature direction inside the region where A or B are the most volatile (a) or the heaviest (b) component of the mixture”.

The volatility order is set by the univolatility curves which knowledge is therefore critical. Using illustrative examples covering all sub cases, but exclusively operated in batch extractive distillation, Rodriguez-Donis and colleagues found that Serafimov's classes covering up to 53% of azeotropic mixtures were suited for extractive distillation : 0.0-1 (low relative volatility mixtures), 1.0-1a, 1.0-1b, 1.0-2 (azeotropic mixtures with light, intermediate or heavy entrainers forming no new azeotrope), 2.0-1, 2.0-2a, 2.0-2b and 2.0-2c (azeotropic mixtures with an entrainer forming one new azeotrope). For all suitable classes, the general criterion under infinite reflux ratio could explain the product to be recovered and the possible existence of limiting values for the entrainer - feed flow rate ratio for batch operation: a minimum value for the class 1.0-1a, a maximum value for the class 1.0-2, etc. The behavior at finite reflux ratio could be deduced from the infinite reflux ratio behavior and properties of the residue curve maps, and some limits on

the reflux ratio were found. However precise finding of the limiting values of reflux ratio or of the entrainer - feed flow rate ratio required other techniques, summarized now, more details will be given in Chapters 3 and 4.

Batch distillation process studies have added new insights to both batch and continuous distillation operation. The design of pressure swing batch distillation process has been recently revisited with precise feasibility criteria based on thermodynamic properties of ternary diagrams (Wozny and Repke, 2007; Modla and Lang, 2008, Modla et al., 2010, Modla, 2010, Modla, 2011). Batch azeotropic distillation exhaustive feasibility rules for homogeneous (Rodriguez-Donis et al., 2001) and heterogeneous mixtures (Rodriguez-Donis et al. 2001, 2002, Skouras et al., 2005, Lang and Modla, 2006) have increased the number of mixture classes suited for azeotropic batch distillation, prompted the search of novel operation modes, like double columns (Denes et al., 2009) and helped the selection of the proper load composition region in continuous operation. Regarding extractive distillation, continuous mode studies have relied for decades upon a simple feasibility rule (Laroche et al., 1991, Knapp and Doherty, 1990, 1994): for the separation of a minimum (resp. maximum) boiling azeotropic mixture A-B, one should add a heavy (resp. light) entrainer E that forms no new azeotrope. The corresponding ternary mixture A-B-E belongs to the 1.0-1a class (Kiva et al., 2003), which occurrence amounts to 21.6% of all azeotropic ternary mixtures (Hilmen et al. 2000). In Chapters 3 and 4 we study how batch insight can be used for assessing continuous extractive distillation feasibility for classes 1.0-1a and 1.0-2 (min T and max T azeotropic mixtures with a heavy or light entrainer).

2.6.4 Topological features related to process operation

The general feasibility criterion enounced previously strictly holds for infinite reflux ratio operation, corresponding to steps 1 and 2 of the batch extractive distillation process. For finite reflux ratio (step 3), things are more complicated and can only be exhaustively studied from the computation of extractive singular points as was done for the minimum boiling azeotrope separation with a heavy entrainer (class 1.0-1a) via batch homogeneous extractive rectification (the BED process) (Frits et al., 2006). Figure 2.19 displays the qualitative topological features of the class 1.0-1a diagram.

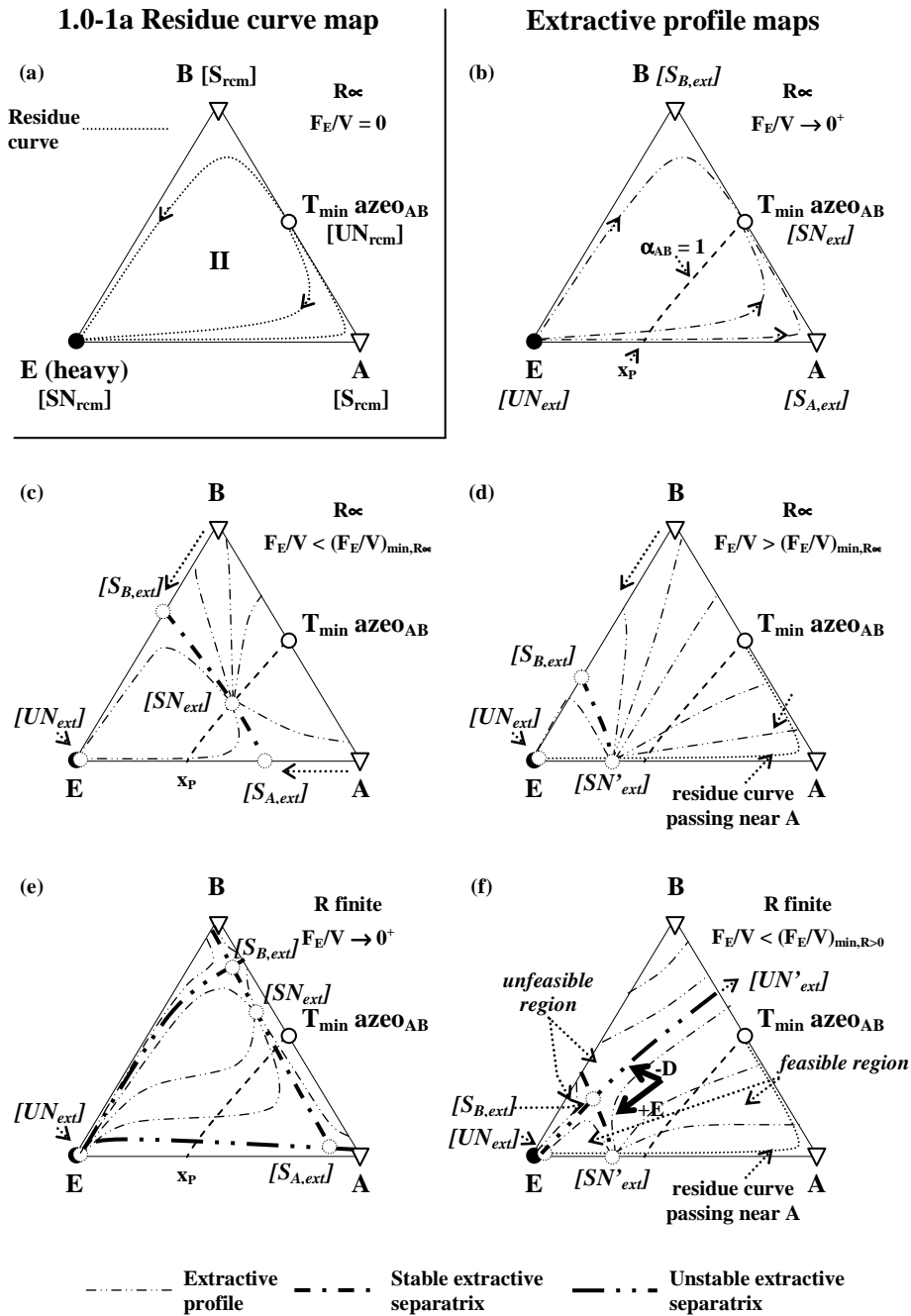


Figure 2.19 Topological features related to batch extractive distillation process operation of class 1.0-1a when using a heavy entrainer (Rodriguez-Donis et al., 2009a).

Feasible and unfeasible regions for the composition in the extractive section of the column are deduced from the analysis of the extractive composition profile map, similarly to residue curve map (rcm) analysis. Those regions are bounded by extractive stable and unstable separatrices crossing at saddle extractive singular points (Knapp and Doherty, 1994a). For the class 1.0-1a, the pinch point of the extractive composition profiles is a stable extractive node SN_{ext} issued from the original minimum boiling azeotrope. Saddle extractive points $S_{i, ext}$ are emerged from the rcm saddle points (A and B vertices). An extractive

unstable node UN_{extr} is located at the entrainer vertex. We now discuss the conclusions of Frits et al., from the perspective of a univolatility concept (Frits et al., 2006).

At infinite reflux ratio with no entrainer feeding (BED process step1), the rcm holds (Figure 2.19a). The column has a single rectifying section, and the composition profile in a tray column follows strictly a residue curve assuming constant molar overflow hypothesis and infinite number of trays. The rcm analysis states that the minimum boiling azeotrope, being the unique rcm unstable node, is obtained at the top of the column.

At infinite reflux ratio, as soon as the entrainer entrainer - feed flow rate ratio is turned on ($F_E/V=0^+$) (BED process step 2), two column sections occur: a rectifying one above the feed and an extractive one the feed. The rectifying section composition profiles are residue curves, as shown in Figure 2.19a. Figure 2.19b sketches the extractive composition profiles map. Extractive singular points have the opposite stability of the rcm singular points by comparing Figure 2.19a and Figure 2.19b, as explained in the literature (Knapp and Doherty, 1994b). Of utmost importance is the univolatility curve $\alpha_{AB}=1$ that starts at the azeotrope $T_{min\ azeo_{AB}}$ and intersects the A-E edge at x_p . The general criterion that we have enounced previously holds for component A, which is then the first product cut of the BED process, provided that adequate reflux ratio and entrainer - feed flow rate ratio values are set. Note that since components A, B, and E are extractive singular points, the A-E, B-E, and A-B edges are, respectively, unstable, unstable, and stable extractive separatrices.

At infinite reflux ratio while F_E/V increases (Figure 2.19c), SN_{extr} moves along $\alpha_{AB}=1$, $S_{A,extr}$ and $S_{B,extr}$ moves along the binary edges (A-E and B-E, respectively), toward the vertex E. Extractive stable separatrices that link $S_{A,extr}$ - SN_{extr} - $S_{B,extr}$ move inside the composition triangle toward E with no effect on feasibility.

Close to a limiting value $F_E/V_{min,R^\infty}$, SN_{extr} and $S_{A,extr}$ merge and the extractive composition profiles are attracted to a new extractive stable node SN_{extr}' located below the A-E edge. $F_E/V_{min,R^\infty}$ is defined as the value for which the process becomes feasible: Extractive composition profiles ending at SN_{extr}' cross a rectifying profile that can reach the vicinity of the expected product (A) (Figure 2.19d).

At a finite reflux ratio with $F_E/V=0^+$ (Figure 2.19e), SN_{extr} no longer belongs to the univolatility curve but starts closer to component B on the B- $T_{min\ azeotrope}$ AB segment and moves inside the triangle along with the both saddles $S_{A,extr}$ and $S_{B,extr}$. The stable extractive separatrices $S_{A,extr}$ - SN_{extr} and $S_{B,extr}$ - SN_{extr} are the sequel of the A-B edge moving inside the triangle. UN_{extr} also moves slightly inside and sets with $S_{A,extr}$ and $S_{B,extr}$, two extractive unstable separatrices with significant curvature. Those separatrices end outside the

triangle toward unstable nodes UN_{extr}' and UN_{extr} . They are the sequel of the A-E and B-E edges, extractive unstable separatrixes at infinite R, moving inside the triangle at finite reflux ratio (Figure 2.19e).

As F_E/V increases at finite R, the extractive unstable separatrix $UN_{extr}-S_{A,extr}-UN_{extr}'$ near the A-E edge quickly disappears (Figure 2.19e). In the meantime (Figure 2.19f), $S_{B,extr}$ moves toward the vertex E inside the triangle. Consequently, the extractive unstable separatrix $UN_{extr}-S_{B,extr}-UN_{extr}'$ remains. Besides, the extractive stable separatrix also remains, joining $S_{B,extr}$ to SN_{extr}' and SN_{extr}' located outside the ternary composition space through the B-E edge. At finite reflux ratio, there exists $F_E/V_{min,R} > 0 > F_E/V_{min,R=\infty}$ above which SN_{extr} and $S_{A,extr}$ have merged and the extractive composition profiles are attracted to a new extractive stable node SN_{extr}' located below the A-E edge (Figure 2.19f). This allows one to connect the still composition via a composite extractive and rectifying profile to the vicinity of A, and the process becomes feasible again. However, the extractive unstable separatrix $UN_{extr}-S_{B,extr}-UN_{extr}'$ remains and now sets unfeasible composition regions located above it (Figure 2.19f) that prevent the total recovery of component A from the column. Notice also that there exists a minimum reflux ratio R_{min} at a given F_E/V , for which the still composition path lies entirely inside the unfeasible regions. This condition is accomplished when the unstable separatrix $UN_{extr}-S_{B,extr}-UN_{extr}'$ is tangent to the still path.

Hence finite reflux ratio operation is feasible if $F_E/V > F_E/V_{min,R} > 0$ and $R > R_{min}$. Now, as component E is fed to the column, the composition profile moves toward component E and away from the distillate that is close to component A (Figure 2.19f). Besides, the size of the unfeasible region increases as R decreases. Therefore, recommended operation is to start at low reflux ratio and increase the reflux ratio, preventing the column composition (or still path) from crossing the unstable separatrix $UN_{extr}-S_{B,extr}-UN_{extr}'$ and lie inside the unfeasible region.

Differential profiles do not hint at the number of theoretical trays in each column section. In practice, if the number of theoretical trays in each column section is large enough, composition profiles reach close enough to their nodes. So, there exist a minimum number of theoretical trays in both sections and also a maximum in the rectifying section. Indeed, the residue curve starts at the $T_{min} azeo_{AB}$ and too many rectifying trays would force the rectifying profile to approach to component A (the expected product) but, then turn away from component A toward the $T_{min} azeo_{AB}$.

In summary, we state that a priori knowledge of the residue curve shape and the location of the univolatility curve $\alpha_{AB}=1$ intersection with a diagram edge allows one to predict the distillate product obtained

by extractive distillation as a first cut. Second, the existence of an unstable separatrix (coming from an extractive saddle opposite to the distillate) must be tracked down, because it sets an unfeasible composition region that prevents total product recovery under finite reflux ratio operation.

In contrast to class 1.0-1a, applied to for the ternary diagram 1.0-2 that concerns the separation of maximum boiling azeotropes using heavy entrainers at infinite reflux ratio with no entrainer feeding (BED process step1), process operation insights on class 1.0-2 extractive distillation are evident if we recall the key features of class 1.0-1a (Figure 2.19), namely, under infinite R and $F_E/V=0+$, rcm stability of the singular points is reversed for the extractive profile map. Figure 2.20 shows the similar feature for residue curve map (Figure 2.20a) and extractive map (Figure 2.20b). The column has a single rectifying section, the composition profile in a tray column follows strictly a residue curve assuming constant molar overflow hypothesis and infinite number of trays. The rcm analysis states that both original components A and B are unstable nodes; the entrainer (E) is the stable node, while the maximum boiling azeotrope T_{max} azeotrope AB is a saddle point. The rcm stable separatrix, which is also called the basic distillation region boundary, links the azeotrope to E. Separation of components A and B is theoretically impossible by conventional azeotropic distillation adding E initially into the still, because components A and B are located in different distillation regions, separated by the rcm stable separatrix.

Under infinite R and $F_E/V \sim 0^+$ (see Figure 2.20b), the maximum boiling azeotrope $azeo_{AB}$ is a saddle S_{extr} and A and B are stable extractive nodes ($SN_{A,extr}$ and $SN_{B,extr}$, respectively), whereas E is an unstable extractive node (UN_{extr}). There will always be an unstable extractive separatrix between UN_{extr} (vertex E) and S_{extr} (T_{max} azeotrope AB).

All the general features of the topology of the extractive composition profile map and its difference relative to class 1.0-1a are now discussed as follow, depending on the intersection of the $\alpha_{AB}=1$ curve with the triangle edges.

Figure 2.20c shows the extractive composition profile maps for a higher value of F_E/V but lower than $(F_E/V)_{max}$ while R is infinite. S_{extr} moves inside the ternary composition space, precisely along the univolatility line $\alpha_{AB}=1$. Furthermore, the stable extractive nodes $SN_{A,extr}$ and $SN_{B,extr}$ move toward E over the binary edges A-E and B-E, respectively. Therefore, a stable extractive separatrix $SN_{B,extr}-S_{extr}-SN_{A,extr}$ and an unstable extractive separatrix $UN_{extr}-S_{extr}-UN_{extr}'$, similar to those shown in Figure 2.19e,f exist, even for

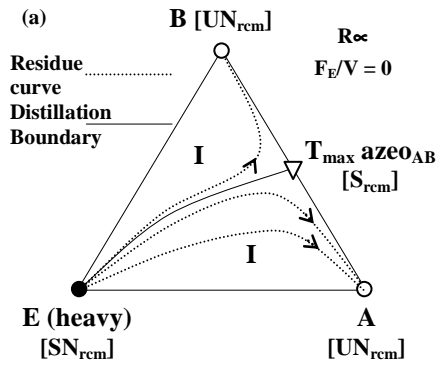
infinite reflux ratio. Logically, under finite reflux ratio, the unstable extractive separatrix $UN_{\text{extr}}-S_{\text{extr}}-UN'$ will move toward the selected distillate product (A or B), reducing the size of their respective feasible regions.

Further increases in F_E/V allow the fusion of S_{extr} and $SN_{A, \text{extr}}$. All extractive composition profiles then reach the unstable node $SN_{B, \text{extr}}$ (Figure 2.20d). This shows the significance of the univolatility line in the synthesis of the homogeneous extractive distillation process, because it sets limiting values of $(F_E/V)_{\text{max}}$. Here, the $\alpha_{AB}=1$ line sets a maximum value $(F_E/V)_{\text{max}, B, R=\infty}$ to recover component A.

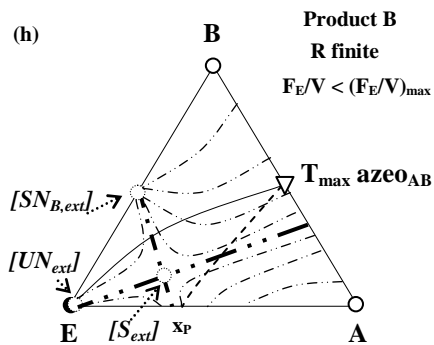
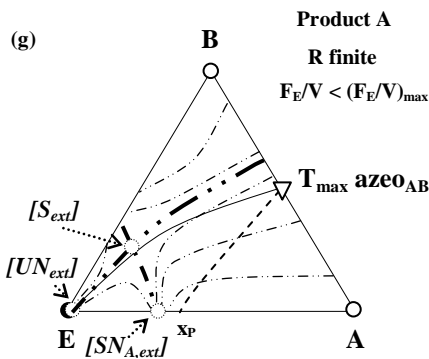
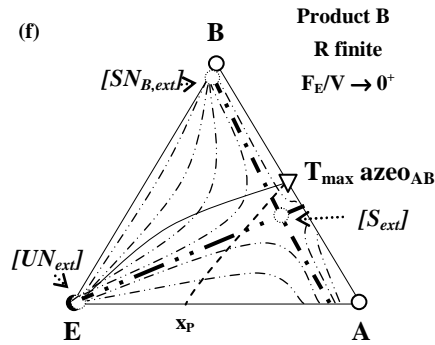
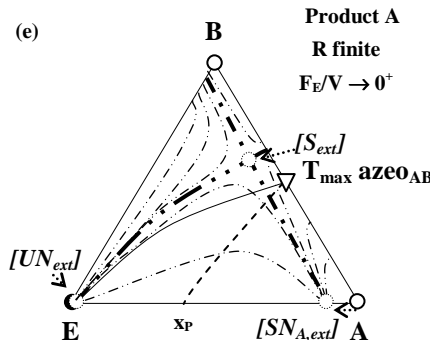
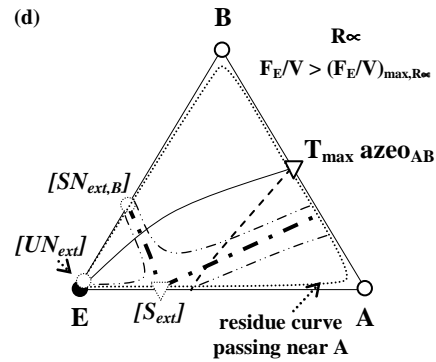
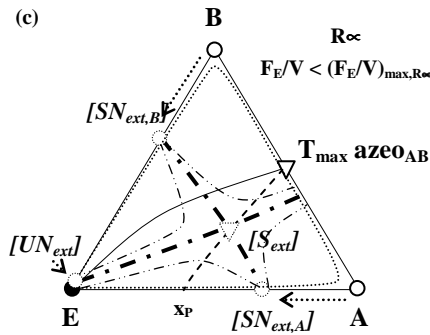
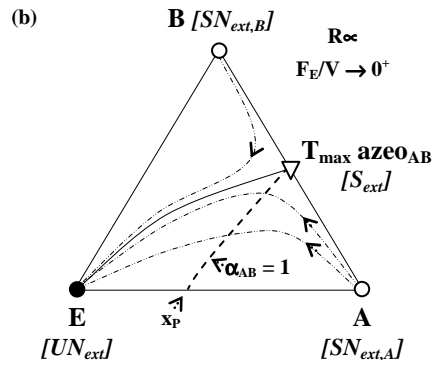
Under finite reflux ratio, extractive profiles are dependent on the distillate composition. Therefore, rectifying and extractive composition profile maps must be computed for both possible distillates x_{DA} and x_{DB} for different F_E/V and R conditions (Figure 2.20e-g for product A and Figure 2.20f-h for product B).

For Figure 2.20e, g, the ternary saddle S_{extr} moves toward vertex B inside the composition triangle and the stable node $SN_{B, \text{extr}}$ are located outside the composition triangle. That reflux ratio allows one to set the extractive separatrix on the left of the rectifying separatrix, an optimal reflux ratio exists for a given F_E/V . The occurrence of an unstable extractive separatrix prevents complete recovery of the distillate, because an unfeasible region of growing size arises as R decreases. On contrast, for Figure 2.20f-h, the ternary saddle S_{extr} moves toward vertex B inside the composition triangle and the stable node $SN_{A, \text{extr}}$ is located outside the composition triangle. Figure 2.20 displays the qualitative topological features of the class 1.0-2 diagram.

1.0-2 Residue curve map



Extractive profile maps



Extractive profile
 Stable extractive separatrix
 Unstable extractive separatrix

Figure 2.20 Topological features related to the extractive distillation process operation of class 1.0-2 when using a heavy entrainer.

2.6.5 Extractive process feasibility assessed from intersection of composition profiles and differential equation

The feasibility always relies upon intersection for composition profiles in the various column sections (rectifying, extractive, stripping), joining the top and bottom composition, whatever the operation parameter values (reflux ratio, flow-rates...)(Frits et al., 2006). The process is feasible if the specified product compositions at the top (x_D) and the bottom (x_W) of the column can be connected by a single or by a composite composition profile.

A single composition profile belongs to one column section and a composite composition profile is composed by two or three column section composition profiles connected at some punctual composition. The number of section depends on the column configuration. The column section profiles are described by the general finite differential model (Van Dongen and Doherty, 1985), and extended by Lelkes et al. (1998) for the BED:

$$\frac{dx_i}{dh} = \pm \frac{V}{L} \cdot [y(x) - y_i^*] \quad (2.23)$$

where V and L are the vapor and liquid flow-rates within the column, the vapor composition y^* in equilibrium with x is computed by the liquid-vapor equilibrium relation and the actual vapor composition y is computed from the mass balance in each column section, depending on choice of the column configuration (Rodriguez-Donis et al., 2007b). The V/L and y equation for each section will be detailed in Chapters 3 and 4.

The differential equation is a continuous model derived via a truncated series expansion of a staged model. As differential model, it is well suited for the study of singularities (stable or unstable node, saddle) and eventual boundaries of the liquid composition profile maps that may affect feasibility under various operating conditions, feasibility and limiting parameter values like minimum reflux ratio (reboil ratio). To assess intersection of composition profiles are easier with continuous composition profiles from the differential model than with discrete composition profiles from distillation line calculations as investigated in earlier works (Pham et al., 1989). The differential model is, however, neither related to theoretical or real stages, nor it is based on mass transfer equations. It cannot be used to evaluate a finite number of stages within some column section like with the distillation line calculations under higher than minimum reflux ratio conditions. Finally, it contains the same driving force $y-y^*$ as occurs in the well-known NTU-HTU mass transfer model.

This differential equation is an initial value problem that should be solved by starting the computation.

The double sign \pm shown in equation (2.23) is to be actualized according to the direction (top down or bottom up) considering that column height h is equal to zero at the top. Therefore, equation (2.23) must be used in computing the liquid composition profile of a rectifying, extractive and stripping column section with an adequate definition of the initial point for x , and the direction of the solution and the mass balance equation for y . The driving force applied in equation (2.23) is to be understood at a given column height h . This is valid even at the very top of the column. The composition of the vapor emerging from the column top, and the imagined vapor composition that would be in equilibrium y^* with the countercurrent liquid x_0 are in the same relation. Therefore, the composition of this countercurrent liquid x_0 is a good candidate to be an initial point for the higher (rectifying or extracting) column section and the equation is solved top down. Otherwise, if the bottom composition x_w is known then it can be directly applied as the initial value, and equation (2.23) is solved bottom up in the lowest (stripping) column section keeping negative sign.

Thus, computation of the top (rectifying or extractive) column section composition profile should be started from the composition of the liquid flowing on the top of the column if there are at least two column sections. This is called 'the top liquid composition', and denoted by x_0 . The x_0 is identical to the composition of the reflux ratio stream x_R if there is not external feed mixed with the liquid reflux ratio. This x_R , in turn, is identical to the distillate composition x_D if there is no decanter (homogeneous extractive case). If there is a liquid phase distribution then, the composition of the reflux ratio stream x_R is determined by the compositions x_D and the distributed liquid phases, and the reflux ratio R , together. Besides, if there is some external liquid feed sent to the top of the column then it should be accounted as a feed mixed to the reflux ratio stream. The top liquid composition x_0 is then determined by the mass balance of mixing the external feed stream to the reflux ratio stream, the reader can find more details in the work on heterogeneous extractive continuous distillation by Rodriguez-Donis et al., (2007b). Finally, if there are three sections in the column then the rectifying and stripping composition profiles begin at x_R and x_w , respectively, whereas for exploring the range of potentially valid extractive composition profiles (the intermediate column section) a series of composition profiles should be computed started from several points in the composition triangle.

2.6.6 Extractive process feasibility from pinch points analysis

The identification of possible cut under key parameters reflux ratio, reboil ratio and entrainer - feed flow rate ratio has been the main challenge for an efficient separation of azeotropic mixtures. Several

achievements have been realized by the use of an algebraic criterion (Levy et al. 1986) or of mathematical approaches either by using bifurcation theory (Knapp and Doherty, 2004); by interval arithmetic (Frits et al. 2006) or by a combined bifurcation-short cut rectification body method (Brüggemann and Marquardt, 2008).

Extending its method for single feed azeotropic distillations (Levy et al. 1985), Levy et al. (1986) proposed an algebraic trial-and-error tangent pinch points procedure for determining the minimum reflux ratio without the necessity of lengthy iteration schemes involving column profile calculations. The method consisted in finding the value of reflux ratio which makes the feed pinch point, the saddle pinch point, and the controlling feed composition collinear but was restricted to ternary mixtures.

After studying the sequence extractive column and entrainer regeneration column for the separation of the acetone – methanol azeotrope with water (Knapp and Doherty, 1990), Knapp and Doherty (1994) used bifurcation theory to analyze the 1.0-1a class behavior and related the feasibility to the appearance of saddle-node bifurcation points and branching points. Feasible processes required that a ternary saddle originating from a pure component exists whereas the appearance of a ternary unstable node on the pinch branch originating at the azeotrope led to an unfeasible separation. They also proposed some heuristics to set the operational values of R and F_E , once their minimal value was known. They also published more general diagrams, issued from bifurcation theory, without providing illustrative example for each.

Frits et al. (2006) used an interval arithmetic-based branch-and-bound optimizer to find limiting flows based on the existence and location of singular points and separatrices in profile maps and applied it to the same 1.0-1a mixture as Knapp and Doherty (acetone-methanol-water), but for batch extractive distillation. Agreeing with the findings of Knapp and Doherty (1994), they found a feasible process under infinite reflux ratio above a minimal entrainer - feed flow rate ratio which corresponded to the merging of a stable pinch point originating from the azeotrope with a saddle point originating from a pure component. Finite reflux ratio analysis showed that the pinch points moved inside the composition triangle and brought unfeasible regions which are described later.

Brüggemann and Marquardt (2008) exploited a fully-automated shortcut design procedure to determine the limit values. The method is based on the approximation of all column profiles by so-called rectification body method (RBM) which is constructed from nonlinear analysis of the pinches of each section (Bausa et al., 1998). Like Knapp and Doherty (1994) they also set some operational constraint to determine the quasi-optimal values once the minimal values of R and F_E are known. All was incorporated into a general

algorithm for the determination of the optimal values of the entrainer - feed flow rate ratio and the reflux ratio. Several ternary mixtures were used for illustration, all of them belonging to the 1.0-1a class, but a quaternary mixture with two azeotropes and an entrainer forming no new azeotrope was shown. Kossack et al. (2008) then used the RBM method as a second screening criterion for evaluating the extractive distillation entrainer candidates. Fast and efficient, the method bears some critics when the profiles are highly curves because each rectification body has straight boundaries (Lucia et al., 2008).

Finally, one should notice the recent publication of a unique non iterative method for finding the possible splits at finite reflux ratio of azeotropic distillation based on the identification of the common terminal points of pinch branches in each column section (Petlyuck et al., 2011, 2012). Its extension to extractive distillation is in preparation.

Although these methods are invaluable to get the accurate limiting values, they have mostly been illustrated for mixtures belonging to the 1.0-1a class, namely the separation of minimum (resp. maximum) boiling azeotrope with heavy (light) entrainers. None of them considering the relationship between reboil ratio and entrainer - feed flow rate ratio when recover product in bottom, which will summarize in following parts.

2.6.7 Feasibility validation by rigorous simulation assessment

Rigorous simulation validation is carried out with ProSim Plus® and Aspen Plus® for continuous column based on the MESH equilibrium distillation column model, The MESH equilibrium distillation model involves contacting of vapor and liquid in one or more equilibrium stages, in this process one or more feed stream enter a stage and one or more stream leave the stage, energy may be added or withdrawn from the stage, importantly the thermodynamic equilibrium is required to exist on this stage, which assumes the streams leaving any stage are in equilibrium with each other, The M equations are the material balance equations, E stands for equilibrium equations, S stands for mole fraction summation equations, and H refers to the heat or enthalpy balance equations.

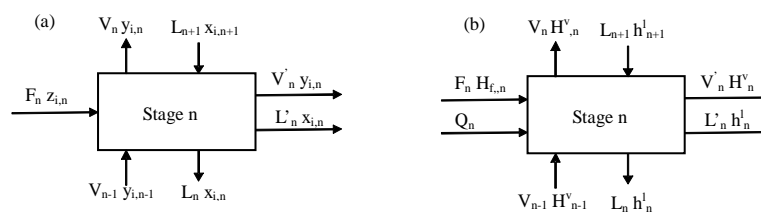


Figure 2.21 The equilibrium stage: (a) component mass flows and (b) stream energy flows

The mass balance across the stage is:

$$F_n z_{i,n} + L_{n+1} x_{i,n+1} + V_{n-1} y_{i,n-1} = (V_n + V'_n) y_{i,n} + (L_n + L'_n) x_{i,n} \quad i = 1, 2, \dots, n \quad (2.24)$$

There must be equilibrium on the stage:

$$y_{i,n} = K_{i,n} x_{i,n} \quad i = 1, 2, \dots, n \quad (2.25)$$

Where $K_{i,n}$ is the vapor-liquid equilibrium for component i , in general,

$$K_i = f(T, P, x_i, x_j, \dots) \quad i, j = 1, 2, \dots, n \quad (2.26)$$

Also, the summation of mole fractions must equal unity:

$$\sum_i x_{i,n} = 1 \quad \sum_i y_{i,n} = 1 \quad (2.27)$$

Finally, an enthalpy balance must prevail on the stage:

$$Q_n + F_n H^v_{f,n} + L_{n+1} h'_{n+1} + V_{n-1} H^v_{n-1} = (V_n + V'_n) H^v_n + (L_n + L'_n) h'_{n,n} \quad (2.28)$$

Where

$$H^v = f(T, P, y_i, y_j, \dots) = \text{vapor enthalpy} \quad i, j = 1, 2, \dots, n \quad (2.29)$$

$$h' = f(T, P, x_i, x_j, \dots) = \text{liquid enthalpy} \quad i, j = 1, 2, \dots, n \quad (2.30)$$

The simulation aims at adjusting the operating parameters by taking into account the overall optimization of other process parameter (number of theoretical stages, position of the feed and solvent and so on). Given the pressure and the column configuration, the degree of freedom of the MESH model is equal to 2, and the partial flow rate ratio of the desired component (at the top or at the bottom) is fixed. Then, the heat duties are deduced from the model resolution. The purity achieved is used to see the feasibility under the given condition of reflux ratio and entrainer - feed flow rate ratio. To ease the simulation convergence, achievable product compositions deduced from the simplified feasibility analysis based on composition profile are set in our calculation are used as initialization points.

2.7 RESEARCH OBJECTIVES

The operational stability of separation processes is a crucial factor to the economic success of such processes. This is especially true for extractive distillation columns that often show counterintuitive operational properties. Due to the extractive effect and the existence of a maximum reflux ratio the

separation is not necessarily improved by increasing the reflux ratio which is a common property of conventional distillation. Furthermore the range of feasible reflux ratios may be small. In this case explain control mechanisms are required. Therefore it is sometimes useful to sacrifice cost-optimality of a steady-state design in favor of better operational stability (Brüggemann and Marquardt, 2002). Thus, exploring a feasible region based on two key parameters: reflux ratio and entrainer - feed flow rate ratio, is an important issue when a chemical process is designed. Feasibility studies also contribute to the better understanding of complex unit operations such as extractive distillation. Both minimum solvent flow rate ratio and minimum reflux ratios can be used as indicators of a flowsheet's energy requirements. The limitations of entrainer - feed flows and operating reflux ratios give essential guidance for design and operation of extractive distillations.

Chapter 2 presented a survey of works on extractive distillation. Although the literature is extremely large regarding applications of extractive distillation, by using a heavy entrainer to separate a minimum boiling azeotrope, the number of works truly addressing issues like feasibility, design are rare, even more in continuous mode than in batch as only a few authors, Laroche in 1991 and 1992, Knapp in 1994, Brüggemann in 2004, Luyben in 2008 and co-workers, have truly contributed to better understand the continuous extractive distillation process. In batch extractive distillation, systematic studies starting in 1993 by Yatim et al. (1993) and continued by Blokes et al. (1998), and then followed by Rodriguez-Donis and co-workers, have surveyed all possible separation by batch extractive distillation. A transposition to continuous operation has not been done so far. Other issues have also been discussed, like the column configurations coming from the different entrainer feed location.

We select the feasibility method based on the thermodynamic insight gathered on batch distillation studied by Rodriguez-Donis et al (2009a, 2009b, 2010, 2012a, 2012b). Those authors combined knowledge of the thermodynamic properties of residue curve maps and of the univolatility and unidistribution curves location. They expressed a general feasibility criterion for extractive distillation under infinite reflux ratio (reboil ratio). Nevertheless, it was never systematically checked for continuous operation, which is our main focus. Based on thermodynamic criteria and topological features of ternary diagram should indeed be valid concepts for continuous distillation as well. Then, with the help of these theories and systematic calculations of rectifying, extractive, stripping section composition profiles, feasibility ranges for the two key parameters, entrainer - feed flow rate ratio and reflux ratio, can be determined and later validated by rigorous simulation.

We apply that methodology and we focus in chapter 3 on the separation of minimum and maximum azeotropic mixtures with a heavy entrainer, which refers to the 1.0-1a (occurrence 21.6%) and 1.0-2 (occurrence 8.5%) classes respectively. The 1.0-1a case has been the most studied in the literature but not with the thermodynamic insights of the general feasibility criterion for extractive distillation which covers all cases of product. Detailed study about the 1.0-2 case continuous extractive distillation has not been reported in the literature.

The case with a light entrainer is then presented in Chapter 4 has been studied in batch recently by Rodriguez-Donis et al., (2012a) but no systematic study of continuous extractive distillation process has been done so far.

Table 2.5 displays the systems for all the possible separating cut of class 1.0-1a and 1.0-2.

Table 2.5 Summary of systems studied.

Study cases		Minimum boiling azeotrope		Maximum boiling azeotrope	
		Product A	Product B	Product A	Product B
Heavy entrainer	univolatility line α_{AB} reach AE edge	1.0-1a case a A (acetone) – B (heptane) + E (toluene)		1.0-2 case (a) A (chloroform) – B (vinyl acetate) + E (butyl acetate)	
	univolatility line α_{AB} reach BE edge		1.0-1a case b A (acetone) - B (methanol) + E (chlorobenzene)	1.0-2 case (b) A (acetone) - B (chloroform) + E (benzene)	
Light entrainer	univolatility line α_{AB} reach AE edge	1.0-1a case a A (propanoic acid) – B (DMF) + E (MIBK)		1.0-2 case (a) A (ethanol) – B (water) + E (methanol)	
	univolatility line α_{AB} reach BE edge		1.0-1a case b A (water) – B (EDA) + E (acetone)	1.0-2 case (b) A (MEK) – B (benzene) + E (acetone)	

Extension of Thermodynamic Insights on Batch Extractive
Distillation to Continuous Operation. Azeotropic Mixtures with a
Heavy Entrainer

3.1 INTRODUCTION

In this chapter we study the batch and continuous extractive distillation of minimum and maximum boiling azeotropic mixtures with a heavy entrainer. Until the work of Rodriguez-Donis et al. (2009b), almost all the literature relied upon the feasibility rule that a heavy entrainer forming new azeotrope was suitable to separate a minimum boiling and a maximum azeotrope. The corresponding ternary diagram belongs to the 1.0-1a and 1.0-2Serafimov's class ternary diagrams, each with two sub-cases depending on the univolatility line location. Knowledge of the residue curve map and of the location of the univolatility curve $\alpha_{AB}=1$ can help assess which product is removed in the distillate. The feasible product and operating parameters reflux ratio (R) and entrainer - feed flow rate ratio (F_E/F , F_E/V) ranges are assessed under infinite reflux ratio conditions by using the general feasibility criterion enounced by Rodriguez-Donis et al. (2009).

From basic mass balance analysis, feasibility of an extractive distillation under finite reflux ratio conditions requires that the top and bottom product compositions are connected each other through the liquid composition profiles x_i in each section. Once a target product composition is set, the process feasibility depends on parameters like the feed heat condition (q), the feed stage location, the total number of stages, the column holdup, the vapor flow rate ratio, the condenser cooling duty, the boiler heat duty but the two most important and that we consider, remain the reflux ratio (reboil ratio) and the entrainer - feed flow rate ratio. The main content of the chapter is constituted by the following parts: the column configuration, section profiles and methodology utilized, thermodynamic feasibility criterion, calculation of reflux ratio vs. entrainer - feed flow rate ratio diagrams, result discussion and conclusion.

3.2 COLUMN CONFIGURATION AND OPERATION

Extractive distillation can be operated either in batch mode or in continuous mode. Because we consider a heavy entrainer (boiling temperature above that of both A and B), the entrainer stream is fed above the main feed in continuous configuration (Figure 3.1a) or above the boiler in batch (Figure 3.1b).

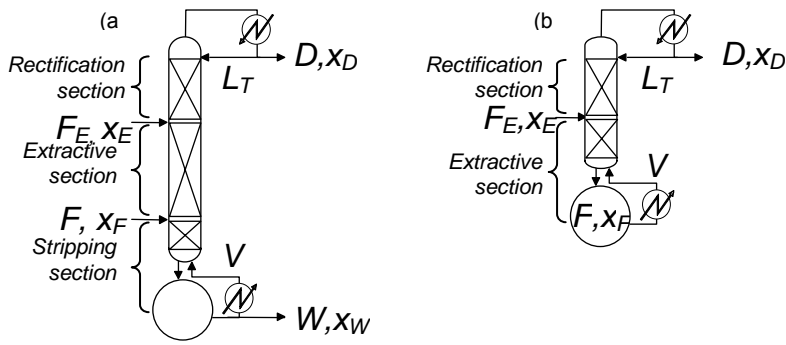


Figure 3.1 Configurations of extractive distillation column: (a) continuous (b) batch.

We consider the classical configuration displayed in Figure 3.1a, with the entrainer fed above the main feed, giving rise to three sections, rectifying, extractive and stripping ones.

Extractive batch distillation is a semi-batch process, as the main feed F is loaded initially into the boiler, whereas the entrainer is fed continuously. In the case of a heavy entrainer, the batch column is a rectifier, with an extractive and a rectifying section (Figure 3.1b) and the product is removed as distillate from the top.

3.3 FEASIBILITY STUDY METHODOLOGY

Our methodology aims at extending thermodynamic insight for batch extractive distillation to continuous distillation. The main difference lies in the existence of a stripping section for the continuous column configuration, compared to the batch column configuration (Figure 3.1). The key parameters remain the reflux ratio R and the solvent to feed flow-rate ratio F_E/F for continuous operation mode or F_E/V , where V is the vapor flow-rate going up from the boiler, for the batch process.

3.3.1 Thermodynamic feasibility criterion for 1.0-1a and 1.0-2 ternary diagram classes.

The thermodynamic insights published by Rodriguez-Donis et al. (2009a) and validated for batch extractive distillation are used for the 1.0-1a and 1.0-2 ternary mixture class studied here. Based on the verification of the general feasibility criterion, they provide the expected product, the possible occurrence of limiting values for the reflux ratio and the entrainer - feed flow rate ratio F_E/V .

Figure 3.2 displays the essential features of the 1.0-1a class, corresponding to the separation by extractive distillation of a minimum boiling azeotropic mixture A-B with a heavy entrainer E, the underlined letter indicates the possible distillate (e.g. A in ABE):

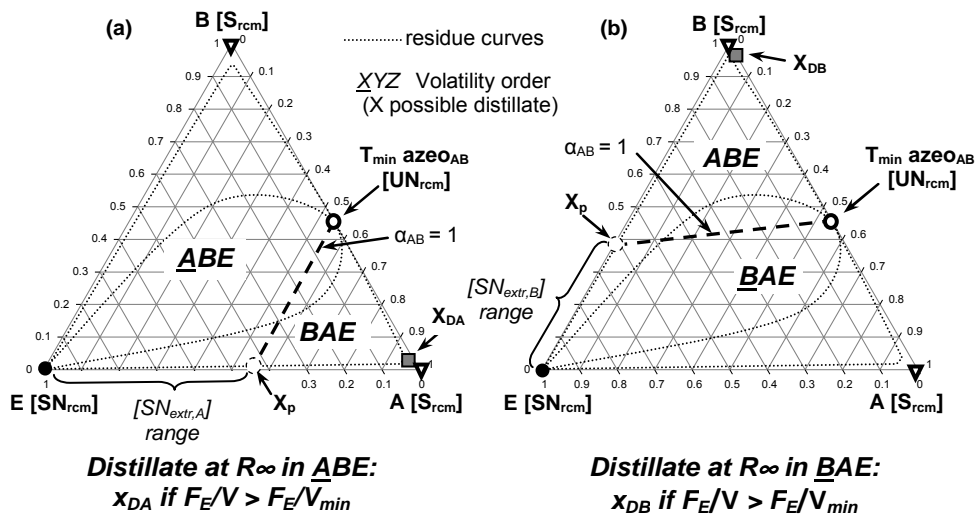


Figure 3.2 Thermodynamic features of 1.0-1a mixtures with respect to batch extractive distillation. Separation of a minimum boiling azeotrope with a heavy entrainer.

With a heavy entrainer, the light original component A and the heavy original component B are both residue curve map (rcm) saddles and they form a minimum boiling azeotrope $T_{\min} \text{azeo}_{AB}$, which is an unstable node. The heavy entrainer E is a stable node. The univolatility curve $\alpha_{AB} = 1$ changes the volatility order of its concerned compounds, and volatility orders are ABE or BAE depending on the side (Kiva et al., 2003). Two sub cases arise. In Figure 3.2a, the $\alpha_{AB} = 1$ curve intersects the binary side A-E at the point x_p . A is the expected product in the distillate because it satisfies the general feasibility criterion under infinite reflux ratio for batch distillation (Rodriguez-Donis et al, 2009a): it is the most volatile in the region ABE where it is connected to E by a residue curve of decreasing temperature from E to A. In Figure 3.2b, the $\alpha_{AB} = 1$ curve intersects the binary side B-E and now B is the expected product.

As detailed in chapter 2, analysis of the composition profile maps and pinch points under infinite reflux ratio have shown that the extractive distillation process is feasible only if the entrainer - feed flow rate ratio F_E/V is greater than a minimal value $(F_E/V)_{\min}$. F_E/V is the governing parameter of the extractive composition profile Equation 3.8 that holds for batch distillation. Below $(F_E/V)_{\min}$, the terminal point of the extractive section profiles, extractive $SN_{\text{extr},A}$, lies on the univolatility curve. Above $(F_E/V)_{\min}$, SN_{extr} leaves the univolatility curve to lie near the $[x_p; E]$ segment (Knapp and Doherty, 1994, Frits et al., 2006, Rodriguez-Donis et al., 2009a). Then the extractive profile can cross a rectifying profile, which is approximated by a residue curve under infinite reflux ratio and which reaches the vicinity of the product, e.g. A. We use illustrative examples: separation of the minimum boiling azeotropes acetone A (56.3°C) – heptane B (98.4°C) ($x_{\text{azeo},A} = 0.93$ at 55.8°C) with toluene E (110.6°C), so that $\alpha_{AB} = 1$ curve intersects the binary side A-E (Figure 3.2b); and acetone A (56.3°C) – methanol B (64.1°C) ($x_{\text{azeo},A} = 0.78$ at 55.4°C) with chlorobenzene E (131.7°C), so that $\alpha_{AB} = 1$ curve intersects the binary side B-E.

Figure 3.3 displays the essential features of the 1.0-2 class corresponding to the separation by extractive distillation of a maximum boiling azeotropic mixture A-B with a heavy entrainer E:

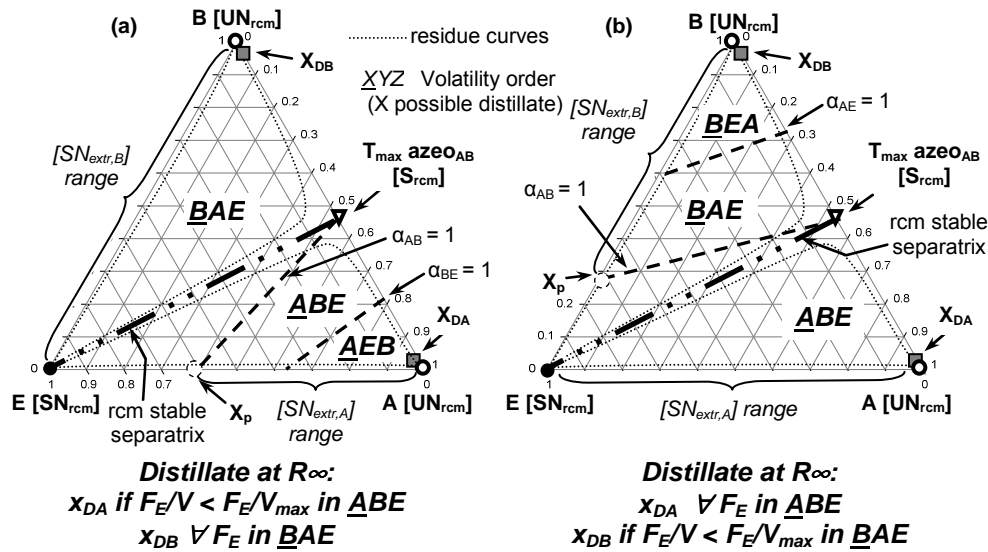


Figure 3.3 Thermodynamic features of 1.0-2 mixtures with respect to batch extractive distillation. Separation of a maximum boiling azeotrope with a heavy entrainer.

The 1.0-2 class diagram displays a rcm stable separatrix, which divides the composition space into two distillation regions. With a heavy entrainer, it connects the stable node E to the saddle maximum boiling azeotrope $T_{max\ azeo_{AB}}$. Both components A and B are unstable nodes. The size of the volatility order regions BAE (+BEA eventually) and ABE (+ AEB eventually) depends on the $\alpha_{AB} = 1$ univolatility curve location (Figure 3.3). The other univolatility curve ($\alpha_{BE} = 1$ Figure 3.3a or $\alpha_{AE} = 1$ Figure 3.3b) may exist (Kiva et al., 2003) but does not affect the extractive distillation feasibility and the product finding (Rodriguez-Donis et al., 2009a).

Regarding extractive distillation feasibility, both A and B are connected by a residue curve of decreasing temperature to E which nears the triangle edge in the ternary diagram. Therefore they can both be distillate products, depending on the location of the global feed composition $x_{F, av.}$, either in \underline{BAE} and \underline{BEA} (B product) or in \underline{ABE} and \underline{AEB} (A product). To add more explanations, we recall that under infinitesimal entrainer - feed flow rate ratio, the rcm singular points become the singular points of the extractive profile map with an opposite stability for the heavy entrainer case (Knapp and Doherty, 1994, Frits et al., 2006). Then for the 1.0-2 class, increasing the entrainer - feed flow rate ratio, the extractive profile singular points originating from A and B, $SN_{extr,A}$ and $SN_{extr,B}$ move towards the entrainer vertex (Rodriguez-Donis et al., 2009a). In Figure 3.3a, $SN_{extr,B}$ can go up to E and there is no limiting flow rate ratio. But $SN_{extr,A}$ disappears at point x_P when it merges with the saddle extractive S_{ext} originating at the $T_{max\ azeo_{AB}}$, so there is a maximum flow rate ratio $(F_E/V)_{max}$ to obtain A as product by extractive distillation. The opposite occurs in Figure 3.3b.

That behavior is directly related to the volatility order regions, which explains how the general criterion was set up. The exact value of F_E/V can be readily calculated.

1.0-2 class illustration is done for the separation of the maximum boiling azeotropes chloroform A (61.2°C)– vinyl acetate B (72.5°C) ($x_{azeo,A}=0.28$ at 75.1°C) with butyl acetate E (126°C), so that $\alpha_{AB}=1$ curve intersects the binary side A-E (Figure 3.3a); and acetone A (56.3°C) – chloroform B (61.2°C) ($x_{azeo,A}=0.37$ at 65.1°C) with benzene (81.1°C) E, so that $\alpha_{AB}=1$ curve intersects the binary side B-E (Figure 3.3b).

We expect the general feasibility criterion for batch mode to hold for the intersection of the extractive and rectifying section of the continuous distillation column, as those already exist in batch distillation column.

3.3.2 Computation of section composition profiles

Initial studies extended methods developed for single feed azeotropic distillation columns to double feed columns for the analysis of extractive distillation processes by looking at the composition profiles in each column section (Levy et al., 1986, Wahnschafft and Westerberg, 1993). The finding of pinch points for each section profiles allowed determining the limiting values of the operating parameters.

Earlier works (Levy et al., 1985, 1986) relied upon plate by plate calculations, leading to discrete profiles which segments numbers matched equilibrium tray numbers in each section. Inspired by the differential approach of Lelkes et al. (1998) for batch extractive distillation, a complete set of differential expression of the composition profiles was published by Rodriguez-Donis et al. (2007) for continuous heterogeneous extractive distillation. The computing of section composition profile allows checking whether they intersect each other, then a composition profile connects the top and bottom composition and the process is deemed feasible. The differential model is based on the following simplifying assumptions: (1) theoretical plates, (2) saturated liquid feeds, (3) constant molar flow rate ratio in the three respective column sections.

Liquid composition profile in each column section depends on the azeotropic mixture feed flow rate ratio (F) and composition (x_F), the entrainer - feed flow rate ratio (F_E), and composition (x_E), the specified recovery ratio of the primary key component (η), the temperature (T), the distillate composition (x_D , component-rich phase composition), the operating pressure (P), the reflux ratio (R). Given these operating variables, the other overall operating parameters can be computed such as vapor (V), distillate (D), and bottom product (W) flow rate ratio, the bottom product composition (x_W) and the liquid flow rate ratio in each column section: L_R , L_E , and L_W for the rectifying, extractive, and stripping section, respectively. These unknowns are determined by mass balance envelope, taking into account the combinations general column configuration displayed in Figure 3.1:

$$W = F_F + F_E - D \quad (3.1)$$

$$D = \frac{\eta_A \cdot F \cdot x_{F,A}}{x_{D,A}} \quad (3.2)$$

$$x_W = \frac{F \cdot x_F + F_E \cdot x_E - D \cdot x_D}{x_{D,A}} \quad (3.3)$$

Let's recall the general differential model equation:

$$\frac{dx_i}{dh} = \pm \frac{V}{L} \cdot [y(x) - y_i^*] \quad (3.4)$$

Here V is deduced from R and D:

$$V = D(R+1) \quad (3.5)$$

Then, from mass balance over each column section we can obtain the particular expressions for these column sections stripping, extractive and rectifying occurring in the column configuration (Fig 2.1a).

Stripping section:

$$\frac{dx_i}{dh} = \frac{S}{S+1} \left[\left(1 + \frac{1}{S}\right) x_i - \frac{1}{S} \cdot x_W - y_i^* \right] \quad (3.6)$$

y_i^* is the composition of the vapor in equilibrium with x_i and is computed by using a proper thermodynamic model, S is the reboil ratio equal to V/W.

Extractive section:

$$\frac{dx_i}{dh} = \frac{R+1}{R + \left(\frac{F_E}{F}\right)\left(\frac{F}{D}\right)} \left[\left(\frac{R}{R+1} + \frac{1}{R+1} \left(\frac{F_E}{F}\right)\left(\frac{F}{D}\right) \right) x_i + \frac{1}{R+1} x_D - \frac{1}{R+1} \left(\frac{F_E}{F}\right)\left(\frac{F}{D}\right) x_E - y_i^* \right] \quad (3.7)$$

R is the reflux ratio equal to L_T/D . Simple mass balance can show that this expression is equivalent to the one for batch distillation that was used by Rodriguez-Donis et al. (2009) to validate their general feasibility criterion under infinite reflux ratio for extractive distillation:

$$\frac{dx_i}{dh} = \frac{R+1}{R + (R+1)\left(\frac{F_E}{V}\right)} \left[\left(\frac{R}{R+1} + \left(\frac{F_E}{V}\right) \right) x_i + \frac{1}{R+1} x_D - \left(\frac{F_E}{V}\right) x_E - y_i^* \right] \quad (3.8)$$

Rectifying section:

$$\frac{dx_i}{dh} = \frac{R+1}{R} \left[\left(\frac{R}{R+1} \right) x_i + \frac{1}{R+1} x_D - y_i^* \right] \quad (3.9)$$

In these equations, setting S, the reboil ratio, or R, the reflux ratio, as infinite and F_E , the entrainer feed flow rate ratio, equal to zero leads to the residue curve equation:

$$\frac{dx_i}{dh} = x_i - y_i^* \quad (3.10)$$

The straightforward calculation method is to select a column configuration and values for the reflux ratio and the entrainer - feed flow rate ratio. Assuming a direct (fixed x_D) or indirect (fixed x_W) split and a recovery rate, the other product is computed from the overall mass balance as the main feed x_F and the entrainer feed x_E compositions and flow rate ratio are known. The rectifying liquid composition profile is computed top down from the reflux ratio composition which here, in a homogeneous process, is equal to x_D (see Rodriguez-Donis et al., 2007 for a complete discussion about heterogeneous variants). The stripping liquid composition profile is computed bottom up from x_W . The extractive distillation profile is computed from any composition belonging to either the rectifying or the stripping composition profile, which choice is user dependent. Limiting reflux ratio or entrainer - feed flow rate ratio values can then be found after tedious and lengthy calculations.

3.3.3 Methodology for assessing the feasibility.

We propose a three step methodology to assess the feasibility of continuous extractive distillation:

1-Knowledge of the existence of limiting values for the entrainer - feed flow rate ratio in batch mode, namely a value for F_E/V ; minimal for 1.0-1a class and maximal for the 1.0-2 class is transformed into a limiting entrainer entrainer - feed flow rate ratio value for continuous mode F_E/F by means of equation:

$$\left(\frac{F_E}{F}\right) = (R + 1) \cdot \left(\frac{F_E}{V}\right) \cdot \left(\frac{D}{F}\right) \quad (3.11)$$

This equation shows that the limiting value for F_E depends on R and on D. As the distillate composition x_D is chosen to compute the composition profiles, setting a distillate recovery enables to compute D from mass balance, given the main and entrainer feed composition and flow rate ratio. Table 3.1 summarizes these data for all mixtures.

2- Keeping the same x_D and distillate recovery rate in step 1, continuous composition profiles maps are computed for all three sections from equations 3.9 (rectifying section), 3.7 (extractive section) and 3.6 (stripping section). The stripping section is expected to differentiate the continuous from the batch mode. They allow to sketch entrainer - feed flow rate ratio vs. reflux ratio diagrams.

3- Rigorous simulation with a MESH equilibrium distillation column model either with ProSim Plus 3.1 (Prosim SA, 2009) or Aspen Plus 11.1 (Aspen, 2011) software is run to check the feasibility. Considering the reflux ratio and the entrainer - feed flow rate ratio and composition, those simulations provide the exact distillate and bottom compositions along with the stage compositions and flows of liquid and vapour and temperatures. Those simulations consider energy balances, although they are not expected to play a significant part in feasibility.

Table 3.1 Operating parameters for all study cases.

Case study		A	B	E		
Class1.0-1a case (a): A (acetone) – B (heptane) + E(toluene)						
<i>product:</i> A (acetone)	Feed x_F	0.9	0.1	0	Distillate flow rate ratio,D	0.9
	Entrainer x_E	0	0	1	Bottom flow rate ratio,W	10.1
	Distillate x_D	0.98	0.01	0.01	Feed flow rate ratio,F	1
	Bottom, x_w	0.0018	0.009	0.9892	Continuous entrainer - feed flow rate ratio, F_E/F	10
	Product recovery, η_b	0.98	0	0	Reflux ratio,R	20
	Global feed $x_{F,av.}$	0.0818	0.0092	0.909	Batch entrainer - feed flow rate ratio, F_E/V	0.53
Class1.0-1a case (b): A (acetone) - B (methanol) + E (chlorobenzene)						
<i>product:</i> B (methanol)	x_F	0.1	0.9	0	D	0.9
	x_E	0	0	1	W	10.1
	x_D	0.01	0.98	0.01	F	1
	x_w	0.0090	0.0018	0.9892	F_E/F	10
	η_b	0	0.98	0	R	10
	$x_{F,av.}$	0.0092	0.0818	0.9090	F_E/V	1.0-1
Class1.0-2 case (a): A (chloroform) – B (vinyl acetate) + E (butyl acetate)						
<i>product:</i> A (chloroform)	x_F	0.9	0.1	0	D	0.8909
	x_E	0	0	1	W	10.11
	x_D	0.99	0.005	0.005	F	1
	x_w	0.0018	0.0094	0.9888	F_E/F	10
	η_b	0.98	0	0	R	15
	$x_{F,av.}$	0.0818	0.0091	0.9091	F_E/V	0.7015
<i>product:</i> B (vinyl acetate)	x_F	0.1	0.9	0	D	0.8909
	x_E	0	0	1	W	10.11
	x_D	0.005	0.99	0.005	F	1
	x_w	0.0094	0.0018	0.9888	F_E/F	10
	η_b	0	0.98	0	R	15
	$x_{F,av.}$	0.0091	0.0818	0.9091	F_E/V	0.7015

Table 3.1 (next) Operating parameters for all study cases.

Class1.0-2 case (b): A (acetone) - B (chloroform) + E (benzene)						
<i>product.</i> A (acetone)	x_F	0.9	0.1	0	D	0.9
	x_E	0.1	0	0.9	W	10.1
	x_D	0.98	0.01	0.01	F	1
	x_w	0.1008	0.0090	0.8902	F_E/F	10
	ηb	0.98	0	0	R	15
	$x_{F,av.}$	0.1728	0.0091	0.8181	F_E/V	0.694
<i>product.</i> B (chloroform)	x_F	0.1	0.9	0	D	0.9
	x_E	0	0.1	0.9	W	10.1
	x_D	0.01	0.98	0.01	F	1
	x_w	0.0090	0.1008	0.8902	F_E/F	10
	ηb	0	0.98	0	R	15
	$x_{F,av.}$	0.0091	0.1728	0.8181	F_E/V	0.694

Table 3.2 displays the extractive distillation column features. No optimization of the separation is performed as it should be done along with the entrainer regeneration column (Luyben, 2008), not considered here. The number of trays in the extractive section is set so that the terminal point of the extractive section composition profile approaches to the extractive section stable node.

Table 3.2 Column operating specifications for rigorous simulation

Specifications	Class1.0.1-a		Class1.0.2 Case a and b
	Case a	Case b	
Tray number, N	22	22	40
Entrainer tray, N_{FE}	7	7	5
Feed tray, N_F	14	14	15
x_F , mole fraction (A,B,E)	{0.9; 0.1; 0.0}	{0.1; 0.9; 0.0}	{0.1; 0.9; 0.0}
x_E , mole fraction (A,B,E)	{0.0; 0.0; 1.0}	{0.0; 0.0; 1.0}	{0.0; 0.0; 1.0}

Results are displayed in terms of entrainer entrainer - feed flow rate ratio vs. reflux ratio diagrams F_E/F vs. R in continuous mode and F_E/V vs. R in batch mode.

3.4 RESULTS AND DISCUSSION

3.4.1 Separation of minimum boiling temperature azeotrope with heavy entrainers (Class 1.0-1a).

In this section, we consider the separation of a minimum boiling azeotrope with a heavy entrainer. The ternary mixture belongs to Serafimov's class 1.0-1a. For the extractive process, two sub-cases arise, whether the univolatility curve $\alpha_{AB} = 1$ reaches the A-E or the B-E side (Rodriguez-Donis et al. 2009a).

3.4.1.1. Subcase1.0-1a case (a): $\alpha_{AB} = 1$ Curve Reaching the Binary Side A-E.

The example of such a separation is the minT azeotrope acetone A - heptane B with toluene as the entrainer taken from Rodriguez-Donis et al (2009).

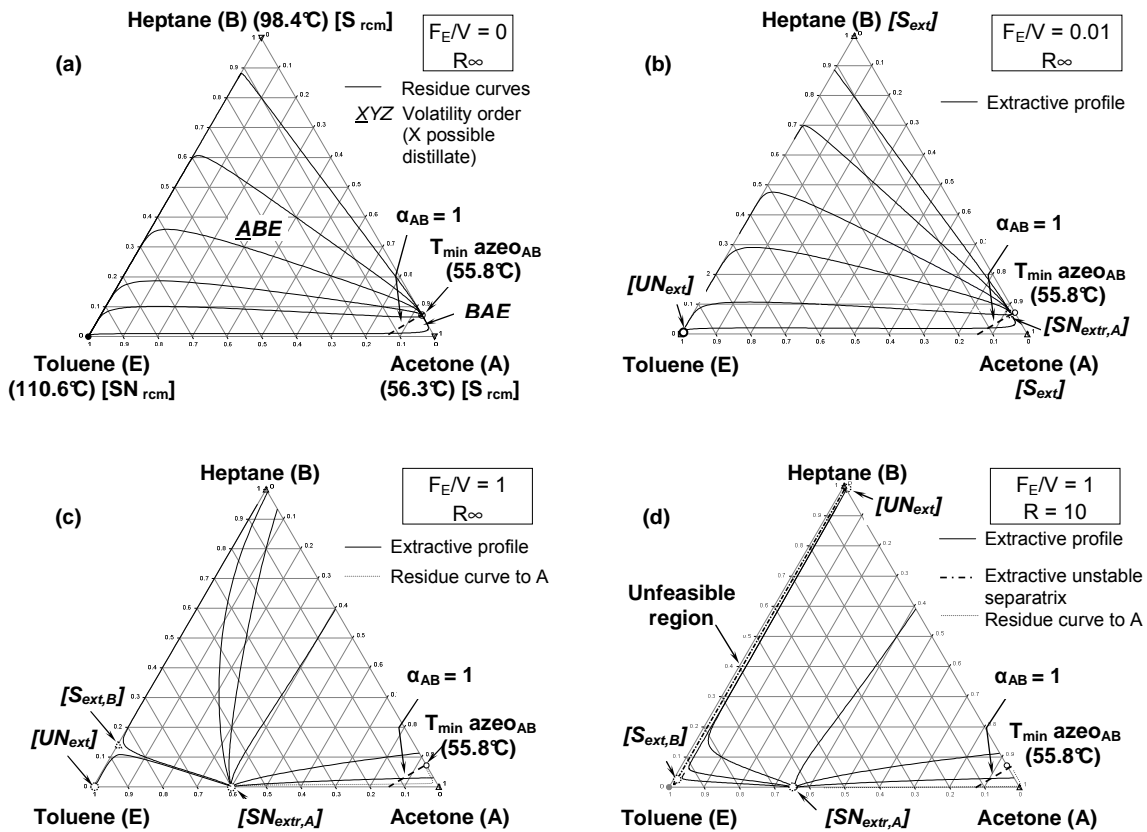


Figure 3.4 Separation of acetone-heptane using toluene: (a) 1.0-1a class residue curve map (rcm) and batch extractive profile map (b) ($F_E/V=0.01$, $R=\infty$) (c) ($F_E/V=1$, $R=\infty$) and (d) ($F_E/V=1$, $R=10$).

Figure 3.4a displays the residue curve map. An infinitely small increase in entrainer - feed flow rate ratio, $F_E/V=0.01$ highlights the extractive profile map features (Figure 3.4b): the extractive profile singular points stability is now opposite to the rcm one (Knapp and Doherty, 1994). Profiles shape are close to rcm ones. As F_E increases, the extractive stable node SN_{extr} moves along the univolatility curve until it merges near the A-E edge with the extractive saddle originating in A, for F_E/V_{min} . Then above F_E/V_{min} (Figure 3.4c), $SN_{extr,A}$ lies near the A-E edge and the extractive process is now feasible as with A becoming the unique possible distillate cut, because all the extractive composition profiles reach $SN_{extr,A}$ and can intersect a rectifying section profile, namely a residue curve as R is infinite, nearing A. In the mean while the saddle $S_{extr,B}$ originated from B has moved along the B-E edge towards E, but the whole triangle is feasible. If reflux ratio becomes finite (Figure 3.4d), $S_{extr,B}$ and UN_{extr} move inside the triangle, giving rise to an unstable extractive separatrix, which in turn defines an unfeasible region: near the B-E edge, the extractive profile no longer reaches $SN_{extr,A}$ and A is not the distillate product. At very low reflux ratio, the unfeasibility region overcomes the $SN_{extr,A}$ and the process is no longer feasible.

Figure 3.5a records the range of entrainer - feed flow rate ratio F_E/V vs. reflux ratio R for which the extractive batch or continuous processes are feasible to get A as product with the x_D purity (region limited by the dotted line).

Table 3.3 summarizes operating parameters corresponding to Figure 3.5. To extend that batch mode insight to continuous mode, we follow the methodology enounced above. According Equation 3.11, the occurrence of a minimum value for F_E/V to get a feasible batch process translates into a minimum value for F_E/F but which depends on R . The minimal value was related in batch to the need of having an extractive section profile intersecting the rectifying one. For continuous configuration (Figure 3.1a), the feasibility also requires that the extractive section profile intersects the stripping section profile to reach the bottom product x_W , computed from mass balances (Table 3.1). That is systematically checked by computing the continuous profiles for various F_E/F and R couples. Figure 3.5a and Figure 3.5b display the feasibility results for the batch process and the continuous process, displayed in terms of F_E/V vs. R (Figure 3.5a) and F_E/F vs. R (Figure 3.5b). The same parameters showed in Table 3.1 are used for both graphs, in particular the same desired purity. Even though the y-axis scales rotated to each other by Equation 3.11, one notices that the shape of the feasible region is unlike depending on the y-axis variable. This occurs because according to Equation 3.11 when F_E/V is fixed, F_E/F is not directly proportional to $R+1$ but also to D/F .

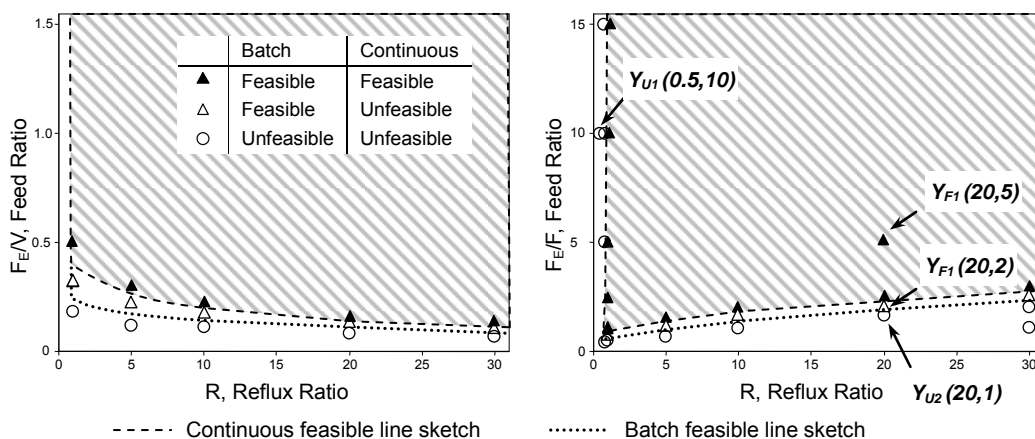


Figure 3.5 Extractive distillation of acetone – heptane with toluene (1.0-1a class). Entrainer - feed flow rate ratio as a function of the reflux ratio.

Table 3.3 Operating parameters corresponding to Figure 3.5.

Specification	Class 1.0-1a case A-E side with heavy entrainer							Feasibility	
	A	B	E	Reflux ratio	Reboil ratio	F_E/F	F_E/V	Batch	Continuous
Name	acetone	heptane	Toluene	30	7.75	3	0.12	yes	yes
Boiling T(°C)	56.3	98.4	110.6	30	11.27	2	0.08	no	no
X_F	0.9	0.1	0	30	9.18	2.5	0.11	yes	no
X_E	0	0	1	20	6.22	2.5	0.15	yes	yes
X_D	0.98	0.01	0.01	20	7.63	2	0.12	yes	no
Other Specification				20	9.88	1.5	0.09	no	no
F	1			10	4	2	0.23	yes	yes
D	0.9			10	5.17	1.5	0.17	yes	no
η	0.98			10	7.33	1	0.11	no	no
				5	2.82	1.5	0.31	yes	yes
				5	4	1	0.21	yes	no
				5	6.86	0.5	0.12	no	no
				1	1.6	0.8	0.5	yes	yes
				1	2.29	0.5	0.31	yes	no
				1	3.2	0.3	0.18	no	no
				0.8	0.28	5	3.47	no	no

One notices that the range of feasible reflux ratio to get the desired product purity enlarges as the entrainer - feed flow rate ratio increases. Besides, both batch and continuous feasible regions are bounded by a minimal value. We have explained above the batch limit F_E/V_{\min} . For a given reflux ratio, there exists a minimum entrainer - feed flow rate ratio F_E/F_{\min} related to the batch minimum F_E/V_{\min} by Equation 3.11. For both processes, the range of feasible reflux ratio to get the desired product purity enlarges as the entrainer - feed flow rate ratio increases. A closer look at the points delimiting the minimum entrainer - feed flow rate ratio on both graphs shows the key result that the minimal value is higher for the continuous process when the same purity is targeted. At $R=20$, the batch process is feasible for $F_E/V = 0.12$ (equivalent to $F_E/F = 2.0$), whereas the continuous process is feasible above $F_E/F = 2.5$ (equivalent to $F_E/V = 0.15$). That is caused by the additional stripping profile in the continuous process which must intersect the extractive profile to make the separation feasible.

Figure 3.6 emphasizes the universality of that behavior for all 1.0-1a class mixtures. It refers to the separation of the acetone-methanol minT azeotropic mixture with heavy water (1.0-1a) studied by Knapp and Doherty (1994) in continuous and Lelkes et al. (1998) in batch. The column specifications are given in Knapp et al. (1990). Calculations are done with $x_{D,Acetone}=0.98$ as acetone (A) is the product because $\alpha_{AB} = 1$ reaches the A-E side. For that mixture, the minimal reflux ratio increases a significant 2.5 fold for the continuous process at $R=20$: the batch process is feasible for $F_E/V = 0.13$ (equivalent to $F_E/F = 2.5$), whereas the continuous process is feasible above $F_E/F = 4.5$. The corresponding data are summarized in Table 3.4.

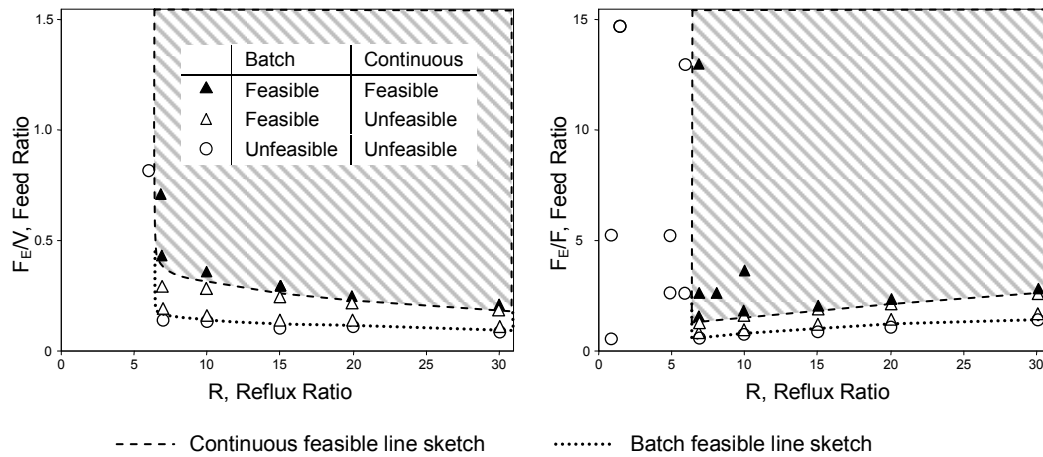


Figure 3.6 Extractive distillation of acetone – methanol with water (1.0-1a class). Entrainer - feed flow rate ratio as a function of the reflux ratio to recover 98%mol acetone (A).

Table 3.4 Operating parameters corresponding to Figure 3.6.

Class 1.0-1a case A-E side with heavy entrainer								Feasibility	
Specification	A	B	E	Reflux ratio	Reboil ratio	F_E/F	F_E/V	Batch	Continuous
Name	acetone	methanol	water	30	7.75	5.5	0.2	yes	yes
Boiling T(°C)	56.3	64.5	100	20	4	4.5	0.24	yes	yes
X_F	0.9	0.1	0	15	3.46	4	0.28	yes	yes
X_E	0	0	1	10	4	3.5	0.35	yes	yes
X_D	0.98	0.01	0.01	7	2	25	3.47	yes	yes
F	1			7	0.25	5	0.69	yes	yes
D	0.9			7	2.91	3	0.42	yes	yes
η	0.98			30	9.18	3	0.11	yes	no
				20	7.63	4	0.21	yes	no
				20	3.05	2.5	0.13	yes	no
				15	5.82	3.5	0.24	yes	no
				15	7.53	2	0.14	yes	no
				10	5.12	2	0.2	yes	no
				10	5.87	1.5	0.15	yes	no
				7	5.33	2	0.28	yes	no
				7	1.08	1.3	0.18	yes	no
				30	4.35	2.5	0.09	no	no
				20	6.22	2	0.11	no	no
				15	2.38	1.5	0.1	no	no
				10	1.23	1.3	0.13	no	no
				7	4.27	1	0.14	no	no
				6	7.75	25	3.97	no	no
				6	0.22	5	0.79	no	no

Figure 3.7 displays the composition profiles computed for all three sections from equations 3.6, 3.7 and 3.9 at four operating parameter points taken from Figure 3.5. It shows that the continuous process is not feasible under conditions for which the batch process is, because the additional stripping profile in the continuous process must intersect the extractive profile to make the separation feasible. For Y_{u1} ($R=0.5$, $F_E/F=10$) the process is unfeasible for both batch and continuous mode because the rectifying profile falls short of intersecting the extractive section profile. That later ends on a stable node SN_{extr} shifted towards the vertex E as F_E/F is large (Figure 3.7a). For Y_{F1} ($R=20$, $F_E/F=5$), the process is feasible for both processes as

all section profiles intersect and the specified purity 0.98 is reached (Figure 3.7b). For Y_{U2} ($R=20$, $F_E/F=2$), the continuous process is unfeasible because there is no intersection between the extractive and stripping section, but the batch process is feasible as the extractive and rectifying profiles intersect (Figure 3.7c). For Y_{U3} ($R=20$, $F_E/F=1$) no process is feasible: none of the section profiles intersect each other (Figure 3.7d). The corresponding detailed data can be found in Table 3.5.

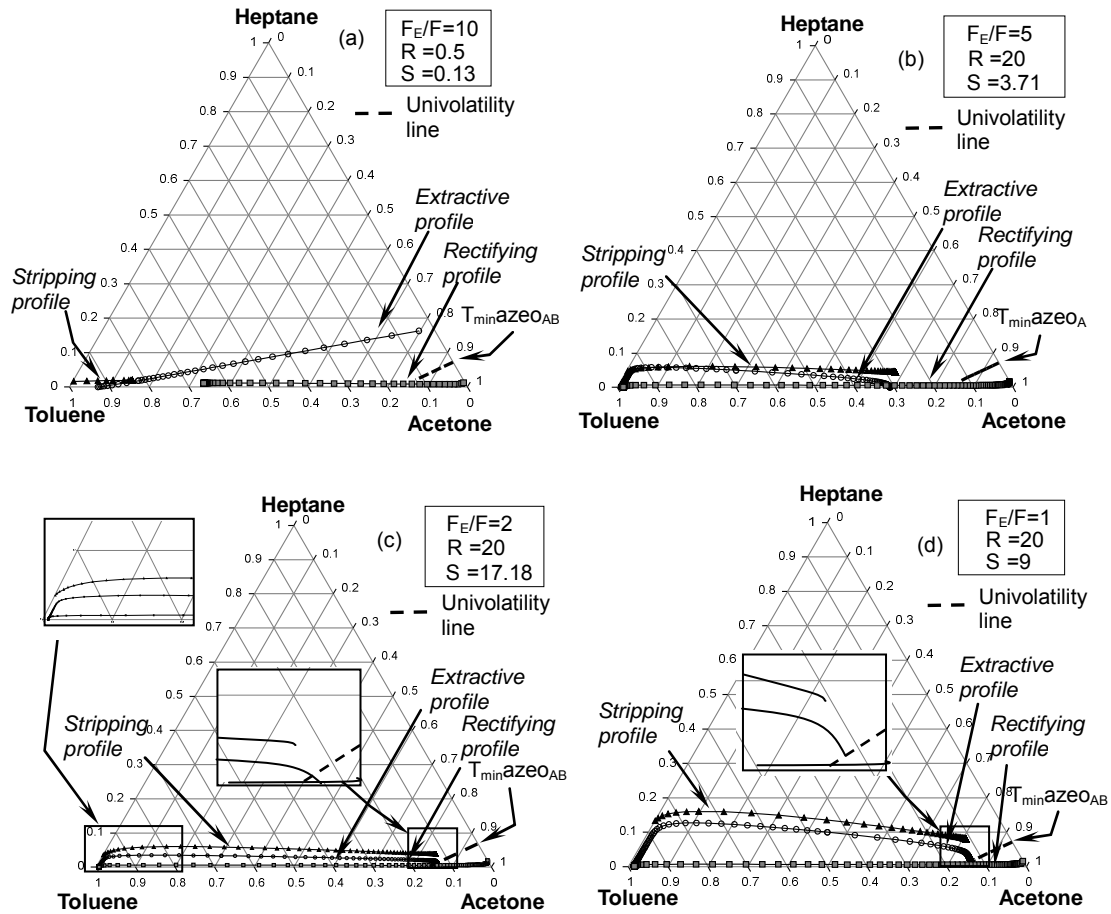


Figure 3.7 Rectifying, extractive and stripping composition for four operating parameter points taken from Figure 3.5 (b) point Y_{U1} , (b) point Y_{F1} , (c) point Y_{U2} and (d) point Y_{U3}

Table 3.5 Operating parameters corresponding to Figure 3.7a, b, c, d

Class 1.0-1a case A-E side with heavy entrainer							
Specification parameters for Figure 3.7(a)				Specification parameters for Figure 3.7(b)			
Apex	A	B	E	Apex	A	B	E
Name	acetone	heptane	Toluene	Name	acetone	heptane	Toluene
Boiling T(°C)	56.3	98.4	110.6	Boiling T(°C)	56.3	98.4	110.6
X _F	0.9	0.1	0	X _F	0.9	0.1	0
X _E	0	0	1	X _E	0	0	1
X _D	0.98	0.01	0.01	X _D	0.98	0.01	0.01
X _W	0.001782	0.00901	0.989208	X _W	0.003529	0.017843	0.978627
R	0.5			R	20		
F _E /F	10			F _E /F	5		
F	1			F	1		
D	0.9			D	0.9		
E	10			E	5		
W	10.1			W	5.1		
V	1.35			V	18.9		
η _B	0.98			η _B	0.98		
Reboil S	0.1337			Reboil S	3.7059		
F _E /V	7.4074			F _E /V	0.2646		
Specification parameters for Figure 3.7(c)				Specification parameters for Figure 3.7(d)			
Apex	A	B	E	Apex	A	B	E
Name	acetone	heptane	Toluene	Name	acetone	heptane	Toluene
Boiling T(°C)	56.3	98.4	110.6	Boiling T(°C)	56.3	98.4	110.6
X _F	0.9	0.1	0	X _F	0.9	0.1	0
X _E	0	0	1	X _E	0	0	1
X _D	0.98	0.01	0.01	X _D	0.98	0.01	0.01
X _W	0.016364	0.082727	0.900909	X _W	0.008571	0.043333	0.948095
R	20			R	20		
F _E /F	1			F _E /F	2		
F	1			F	1		
D	0.9			D	0.9		
E	1			E	2		
W	1.1			W	2.1		
V	18.9			V	18.9		
η _B	0.98			η _B	0.98		
Reboil S	17.1818			Reboil S	9		
F _E /V	0.0529			F _E /V	0.1058		

When concerns heptane (B) as the first product component separating from system acetone-heptane-toluene, the calculating result shows always unfeasible as it can be explained univolatility line $\alpha_{AB} = 1$ intersect at binary side A-E, all extractive profiles going in the direction to extractive stable node (A) instead of extractive stable node (B), makes it impossible to recover heptane in the whole operating parameter region.

In application of step 3, rigorous simulations are carried out with Aspen plus®, with thermodynamic model UNIFAC modified Dortmund 93 in an extractive column which features are displayed in Table 3.2. A feed F, $x_F = \{0.9; 0.1; 0.0\}$ close to the acetone– heptane azeotrope is separated with pure entrainer. Figure 3.8 shows simulation results under two operational parameter points: $F_E/F=1$, $R=20$ and $F_E/F=20$, $R=20$, and the rigorous simulation profiles in each section are compared to the approximate composition profile maps computed from Equations 3.6, 3.7 and 3.9.

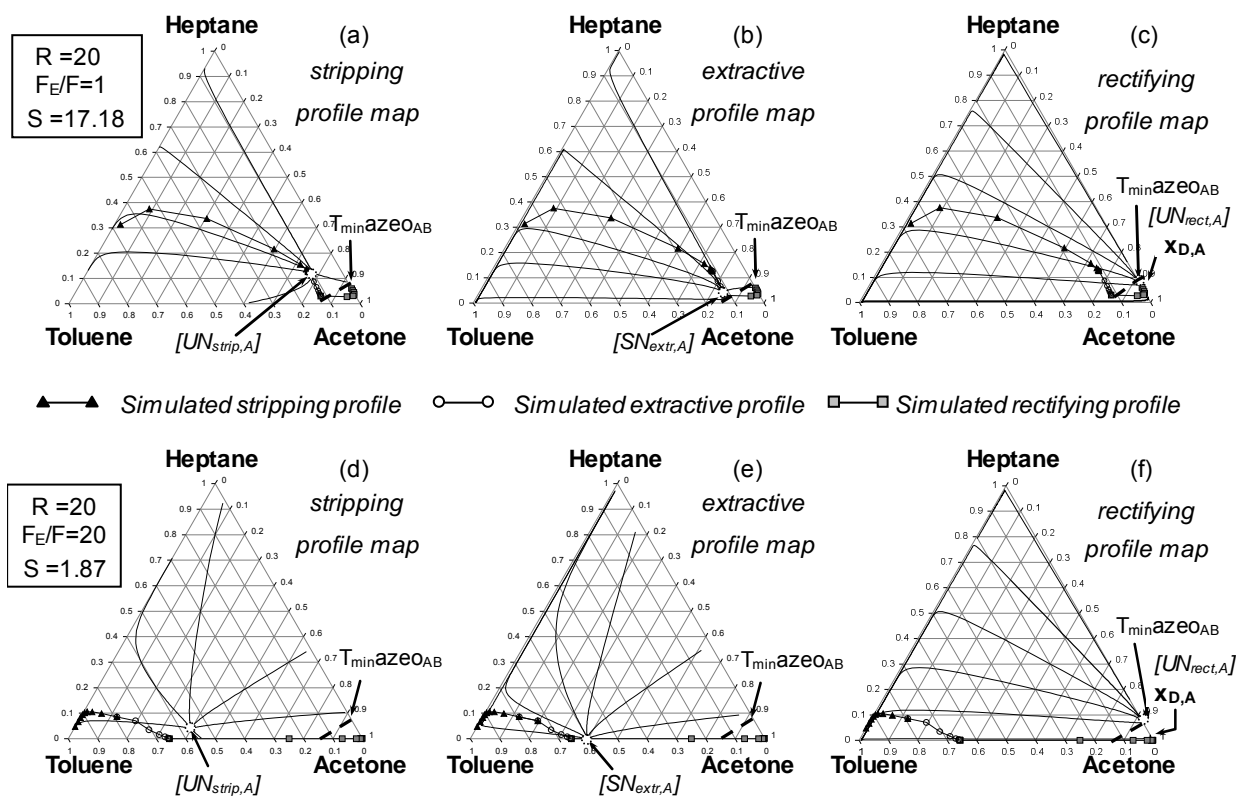


Figure 3.8 Rigorous simulation result to recover acetone at $F_E/F=1$, $R=20$ and $F_E/F=20$, $R=20$, compared with calculated profiles: (a-d) stripping section, (b-e) extractive section and (c-f) rectifying section.

At $F_E/F=1$, as predicted from Figure 3.7d, the rigorous simulation does not allow to recover acetone in the distillate with purity 0.98. Instead, $x_D=0.9468$ is obtained. At such a low entrainer - feed flow rate ratio, the F_E/V and the F_E/F values are lower than the minimal value for the batch and continuous processes (Figure 3.5). The extractive stable node $SN_{extr,A}$ lies on the univolatility curve (Figure 3.8c) and intersects a rectifying profile that cannot reach the targeted product purity (Figure 3.8e). Furthermore, the number of trays in the rectifying section is too large forcing the composition to turn away from the acetone vertex towards the azeotrope. At $F_E/F=20$, well within the feasible region in Figure 3.5, $SN_{extr,A}$ lies near the A-E edge. Distillate purity of rigorous simulation reaches 0.9965, well above the target purity. Moreover, the rigorous and approximate profiles shapes agree well but not strictly because rigorous profiles are computed from a fixed number of trays in each section when the approximate profile differential equations are not tray dependent but can be related to an infinite number of trays. Table and Table 3.7 list all the data corresponding to Figure 3.8.

Table 3.6 Operating parameters corresponding to Figure 3.8a, b, c.

Class 1.0-1a case A-E side with heavy entrainer($F_E/F=1$, $R=20$)									
Worksheet parameters			Rectifying section			Stripping section			
Specification	A	B	E	A	B	E	A	B	E
Name	acetone	heptane	Toluene	acetone	heptane	Toluene	acetone	heptane	Toluene
Boiling T(°C)	56.3	98.4	110.6	0.940169	0.0598	4.82E-05	0.757691	0.127262	0.115048
X_F	0.9	0.1	0	0.947888	0.0519	0.000192	0.754797	0.130026	0.115178
X_E	0	0	1	0.955306	0.044	0.000718	0.746387	0.136671	0.116943
X_D	0.98	0.01	0.01	0.960797	0.0366	0.002586	0.716357	0.15525	0.128393
R	20			0.960275	0.0306	0.009122	0.595835	0.215902	0.188263
F_E/F	1			0.940528	0.0271	0.032337	0.305418	0.336289	0.358293
F	1			0.84925	0.0296	0.121194	0.088589	0.375277	0.536133
D	0.9								
E	1			Extractive section					
W	1.1			A	B	E			
V	18.9			0.12119408	0.12119408	0.12119408			
η_B	0.98			0.12053856	0.12053856	0.12053856			
Reboil S	17.18			0.1197252	0.1197252	0.1197252			
F_E/V	0.0529			0.11868607	0.11868607	0.11868607			
Rigorous parameters				0.11733785	0.11733785	0.11733785			
X_F	0.9	0.1	0	0.11576276	0.11576276	0.11576276			
X_E	0	0	1	0.11522306	0.11522306	0.11522306			
X_D	0.98	0.01	0.01	0.11513531	0.11513531	0.11513531			
Num stages	22								
Solvent tray	7								
Feed tray	14								

Table 3.7 Operating parameters corresponding to Figure 3.8 d, e, f.

Class 1.0-1a case A-E side with heavy entrainer($F_E/F=20$, $R=20$)									
Worksheet parameters			Rectifying section			Stripping section			
Specification	A	B	E	A	B	E	A	B	E
Name	acetone	heptane	Toluene	acetone	heptane	Toluene	acetone	heptane	Toluene
Boiling T(°C)	56.3	98.4	110.6	0.998313	0.001074	0.000613	0.123069	0.086109	0.790821
X_F	0.9	0.1	0	0.997243	0.000748	0.00201	0.064322	0.098717	0.836961
X_E	0	0	1	0.993068	0.000538	0.006394	0.029028	0.105039	0.865932
X_D	0.98	0.01	0.01	0.979137	0.000413	0.02045	0.012034	0.105505	0.882462
R	20			0.931159	0.00037	0.06847	0.004779	0.101594	0.893627
F_E/F	20			0.750964	0.000459	0.248576	0.001853	0.094015	0.904132
F	1			0.343429	0.000553	0.656019	0.000701	0.082676	0.916623
D	0.9						8.03E-05	0.047568	0.932528
E	20			Extractive section					
W	10.1			A	B	E			
V	18.9			0.343429	0.000553	0.656019			
η_B	0.98			0.341597	0.001343	0.65706			
Reboil S	1.87			0.336675	0.003152	0.660173			
F_E/V	0.5291			0.32514	0.00724	0.66762			
				0.300835	0.016235	0.68293			
X_F	0.9	0.1	0	0.256756	0.034989	0.708254			
X_E	0	0	1	0.193505	0.070723	0.735772			
X_D	0.98	0.01	0.01	0.123069	0.086109	0.790821			
Num stages	22								
Solvent tray	7								
Feed tray	14								

3.4.1.2 Subcase Case (b): $\alpha_{AB}=1$ Curve Reaching the Binary Side B-E.

We use the separation of the minimum boiling azeotrope acetone-methanol with heavy entrainer chlorobenzene to illustrate the 1.0-1a class case (b), when the univolatility curve reaches the binary side B-E. As detailed in Rodriguez-Donis et al. (2009a), the expected behavior for batch extractive distillation is strictly identical to the previous case, except that (B), the intermediate boiling compound of the mixture is now the expected distillate instead of (A).

Figure 3.9 shows the residue curve map of the acetone (A) – methanol (B) – chlorobenzene (heavy E) mixture. The univolatility curve intersects the B-E side. Extractive profile maps are also displayed under infinite reflux ratio for $F_E/V=0.01 < (F_E/V)_{\min}$ and for $F_E/V=2 > (F_E/V)_{\min}$, with $(F_E/V)_{\min} \sim 0.4$. As in the 1.0-1a case (a), all extractive composition profiles end at $SN_{B,extr}$ close to the B-E edge for $F_E/V > (F_E/V)_{\min}$, indicating that the batch process is feasible. Under finite reflux ratio conditions (Figure 3.9d, $F_E/V=2$, $R=5$), the saddle $S_{A,extr}$ moves inside the triangle and drags along an extractive unstable boundary with other unstable extractive nodes. It generates an unfeasible composition region whose size grows as the reflux ratio decreases, where the extractive composition profile reaches $SN_{A,extr}$ instead of $SN_{B,extr}$.

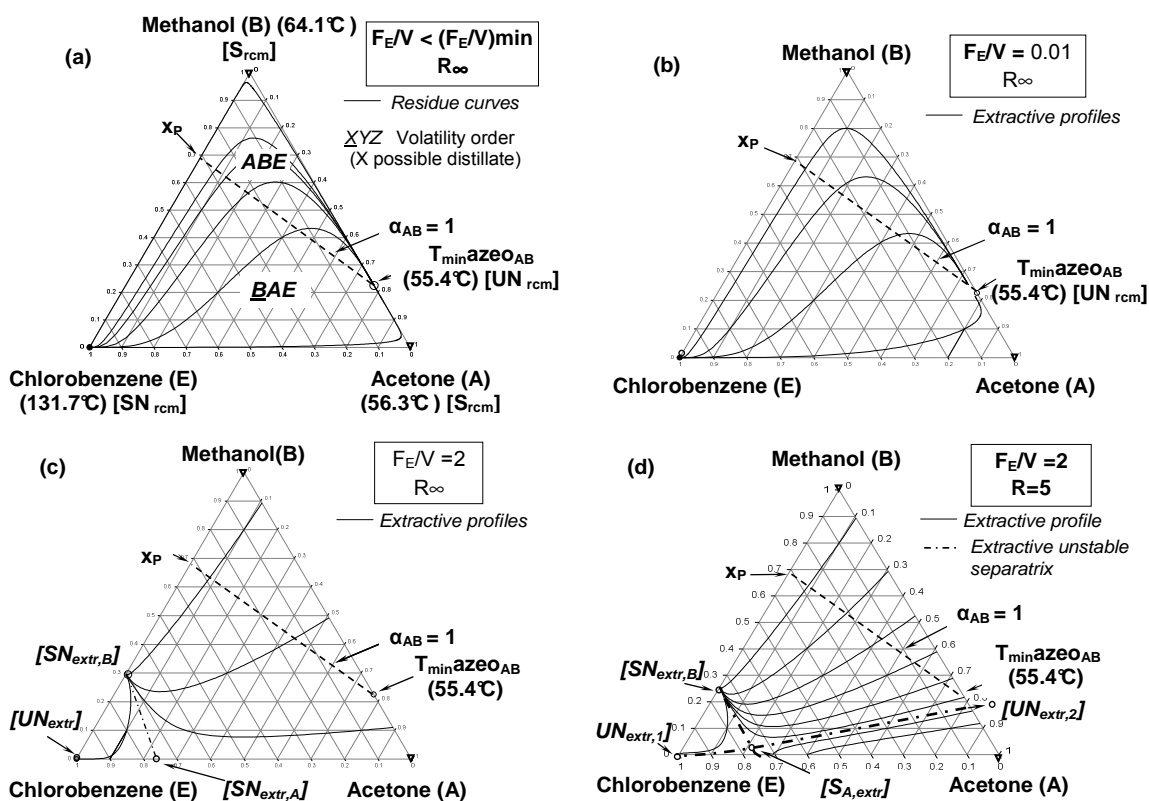


Figure 3.9 Separation of acetone-methanol using chlorobenzene: (a) 1.0-1a class residue curve map (rcm) and batch extractive profile map (b) ($F_E/V=0.01$, R_{∞}) (c) ($F_E/V=2$, R_{∞}) and (d) ($F_E/V=2$, $R=5$).

Figure 3.10 displays the feasible range of operating conditions as entrainer - feed flow rate ratio vs. reflux ratio to recover 98% mol methanol (B) as the univolatility line $\alpha_{AB} = 1$ intersects binary B-E side. Its shape is similar to the Figure 3.5 case to recover acetone (A) when the univolatility line $\alpha_{AB} = 1$ intersects binary A-E side. However, for this mixture, there is no larger region for the batch process than for the continuous process. Table 3.8 gathers all the data corresponding to Figure 3.10.

It is clear that there exists a minimum value for entrainer - feed flow rate ratio and this minimum values depend strongly on reflux ratio, it gets smaller as the function of reflux ratio gets smaller, until it reaches a minimum reflux ratio, in other words, if changing the X-axis reflux ratio with Y-axis reflux ratio, we can say the

desired product specification can be maintained over a wider range of reflux ratio as entrainer - feed flow rate ratio increase, the maximum values gradually reduces as reflux ratio gets smaller, until it reaches a minimum entrainer - feed flow rate ratio value. The reason is similar to former case a, extractive stable node (B) lies on x_p or lies along the univolatility line $\alpha_{AB} = 1$ when F_E/V value are below its minimum limitation, above minimum value, extractive stable node (B) becomes on the binary methanol-chlorobenene sides below x_p part, the $SN_{B,extr}$ generate an extractive stable region sets a minimum value for entrainer - feed flow rate ratio $(F_E/V)_{min}$ to recover methanol (B). There is also a minimum reflux ratio value, A detailed calculation of the profile map shows that the feasible rectifying section profiles region gets smaller when reflux ratio gets smaller until it can no longer intersect the extractive profile region. The same holds for the continuous mode because of a minimum F_E/V and reflux ratio in batch translates well into a minimum F_E/F and reflux ratio in continuous.

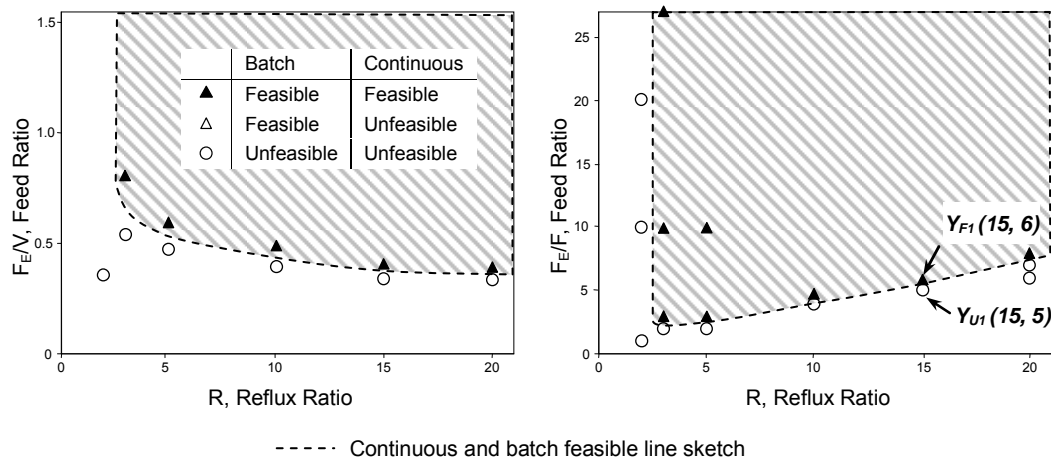


Figure 3.10 Extractive distillation of acetone – methanol with chlorobenzene (1.0-1a class). Entrainer - feed flow rate ratio as a function of the reflux ratio to recover 98%mol methanol (B).

Table 3.8 Operating parameters corresponding to Figure 3.10.

Specification	Class 1.0-1a case B-E side with heavy entrainer							Feasibility	
	A	B	E	Reflux ratio	Reboil ratio	F_E/F	F_E/V	Batch	Continuous
Name	acetone	methanol	chlorobenzene	20	2.33	8	0.42	yes	yes
Boiling T(°C)	56.3	64.5	131.7	20	3.09	6	0.32	no	no
X_F	0.1	0.9	0	20	2.66	7	0.37	no	no
X_E	0	0	1	15	2.36	6	0.42	yes	yes
X_D	0.01	0.98	0.01	15	2.82	5	0.35	no	no
Other Specification				10	1.94	5	0.51	yes	yes
F	1			10	2.41	4	0.41	no	no
D	0.8			5	1.74	3	0.56	yes	yes
η	0.98			5	0.53	10	1.85	yes	yes
				5	0.32	17	3.15	yes	yes
				5	2.57	2	0.37	no	no
				3	1.16	3	0.83	yes	yes
				3	1.71	2	0.56	no	no
				2	0.26	10	3.7	no	no
				2	2.45	1	0.37	no	no
				2	1.34	20	7.41	no	no

When concerns acetone (A) as the first product component from system acetone-heptane-toluene, the calculation results show the process always unfeasible as univolatility line $\alpha_{AB} = 1$ intersect at binary side B-E, all extractive profiles going in the direction to extractive stable node (B) instead of extractive stable node (A), makes it impossible to recover acetone (A) in the whole operating parameter region.

Figure 3.11 displays the composition profiles computed for all three sections at two critical operating parameter points in Figure 3.10b. For $Y_{F1}(R=15, F_E/F=6)$ the process is feasible for both batch and continuous process but it is not for $Y_{U1}(R=15, F_E/F=5)$, as both the extractive and the stripping profiles move in the opposite direction (Figure 3.10b). Unlike the previous 1.0-1a mixture, the batch and continuous feasible range are identical. The reason of this is that as the stripping section is located between the rectifying and extractive section, once the extractive profile no longer crosses the rectifying profile, it does not cross the stripping profile either. This is shown in Figure 3.10 for $R=15, F_E/F = 5$ and $F_E/F = 6$. When checking at $R=5, R=3$, we obtained similar graphs.

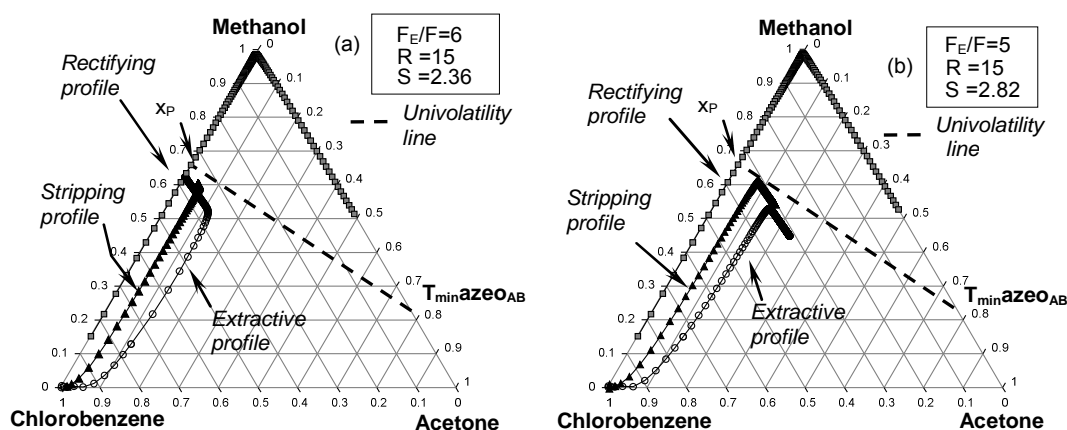


Figure 3.11 Rectifying, extractive and stripping composition for two operating parameter points taken from Figure 3.10 (b) point Y_{F1} and (b) point Y_{U1}

Similarly, for this case rigorous simulations were also carried out with Aspen Plus[®], with thermodynamic model UNIFAC. A feed F rich in methanol (B) with composition $x_F = \{0.1, 0.9, 0\}$ is used so as to distillate methanol as product. Under condition of very low reflux ratio ($R=1$) and entrainer - feed flow rate ratio ($F_E/F=10$), the process is unfeasible, product composition 0.9262 can not satisfy specified composition 0.98, meanwhile, under condition of very low entrainer - feed flow rate ratio ($F_E/F=1$) and reflux ratio ($R=20$), the product composition is only 0.7959, these two cases demonstrate the parameter lies in left and bottom blank sides(not lies in shade region) of graph Figure 3.10b will surely result in unfeasible process(Figure 3.12a-b). At the similar reason with case a, when choose two parameter ($R=20, F_E/F=10$) and ($R=20, F_E/F=20$) from shade region, the rigorous simulation results (Figure 3.12c.d) verified they are feasible for the reason of both specified distillated composition x_D can be obtained, satisfying the necessary and sufficient condition of the feasibility to have at least one possible column profile connecting bottoms composition x_w with the point x_D . Regarding purity, the first composition of distillate are $\{0.0108, 0.0069, 0.9823\}$ compared to bottom composition $\{0.9518, 0.0092, 0.0390\}$, the second composition of distillate $\{0.0113, 0.0002, 0.9885\}$ compared to residue composition $\{0.9753, 0.0049, 0.0198\}$.

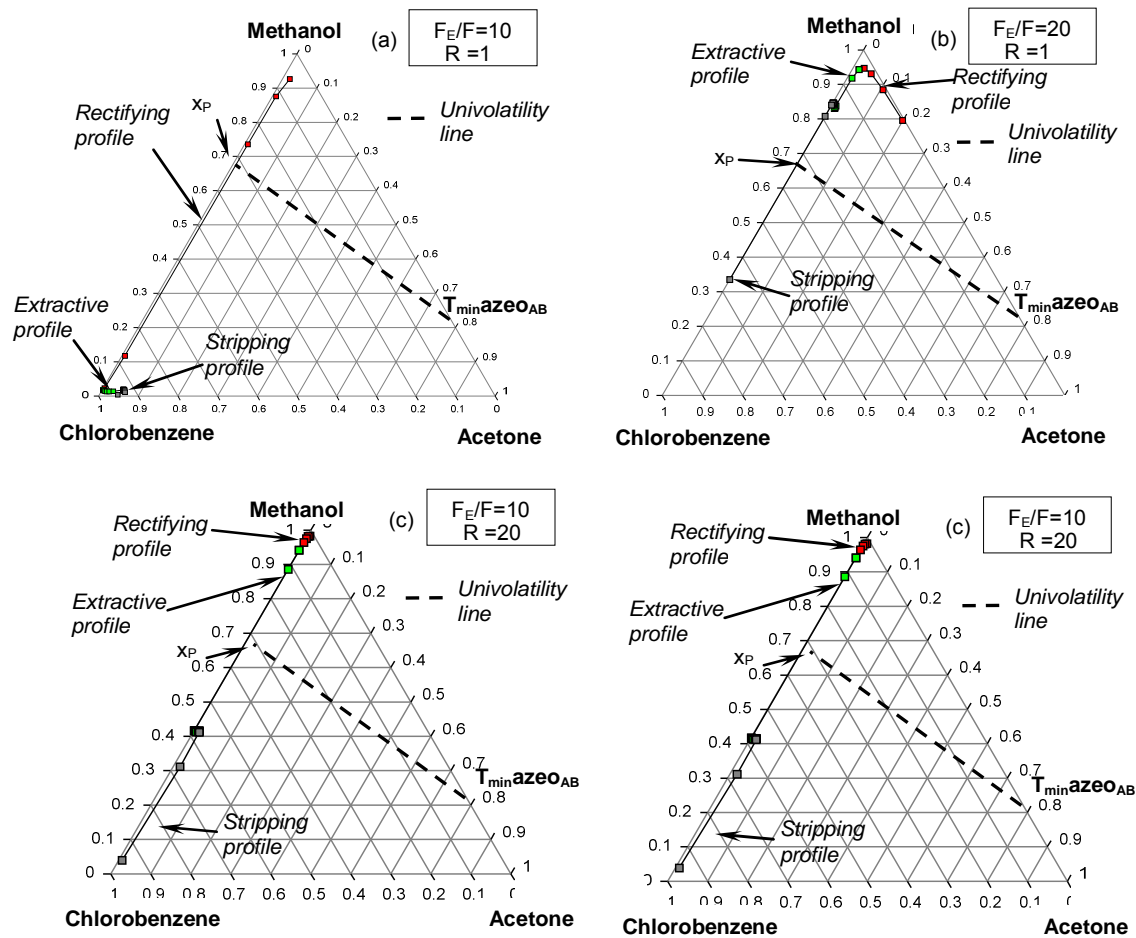


Figure 3.12 Rigorous simulation result to recover methanol at: (a) $R=1$, $F_E/F=10$; (b) $R=1$, $F_E/F=20$; (c) $R=20$, $F_E/F=10$ and (d) $R=20$, $F_E/F=20$.

3.4.2 Separation of maximum boiling azeotropes with heavy entrainers (class 1.0-2).

In this section, we consider the separation of a maximum boiling azeotrope with a heavy entrainer. The ternary mixture belongs to Serafimov's class 1.0-2. For the extractive process, two sub-cases arise, depending whether the univolatility curve $\alpha_{AB} = 1$ reaches the A-E or the B-E side (Rodriguez-Donis et al. 2009a).

3.4.2.1 Subcase 1.0-2case (a) univolatility line $\alpha_{AB}=1$ reaching the binary side A-E

Separation of the maximum boiling azeotrope chloroform (A) – vinyl acetate (B) by adding butyl acetate (heavy E) illustrates the case when $\alpha_{AB} = 1$ reaches the A-E side (Figure 3.13). Both original components A and B are unstable nodes, the entrainer (E) is the stable node, while the maximum boiling azeotrope $T_{max} azeo_{AB}$ is a saddle point. A rcm stable separatrix, links the azeotrope to E. According to the general feasibility criteria for extractive distillation under infinite reflux ratio (Rodriguez-Donis et al. 2009a),

both chloroform (A) and vinyl acetate (B) can be recovered as distillate depending on the global feed composition.

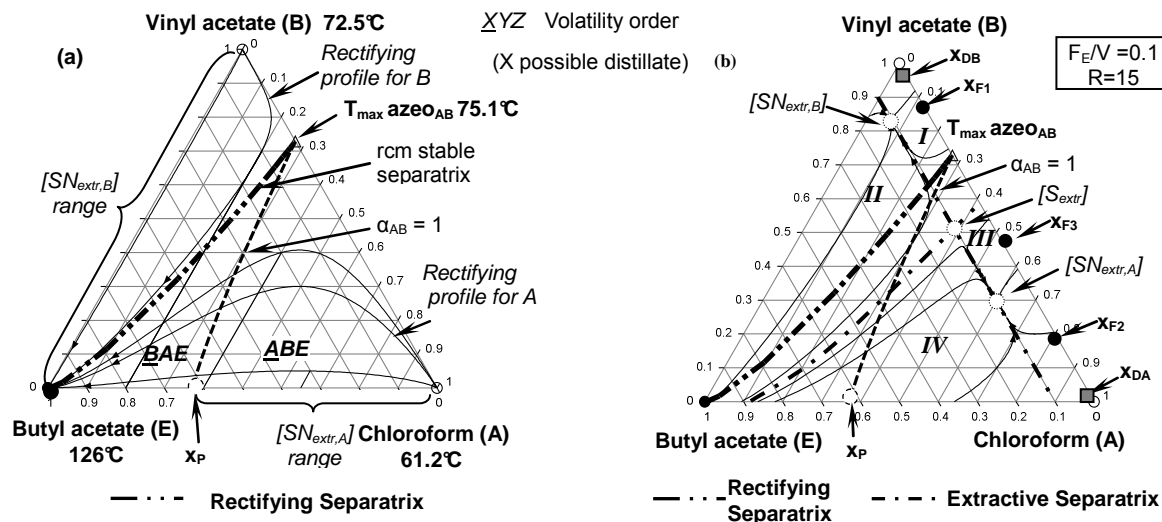


Figure 3.13 chloroform-vinyl acetate using butyl acetate: (a) 1.0-2 class residue curve map (rcm) and batch extractive profile map (b) ($F_E/V = 0.1 < (F_E/V)_{max}$, $R = 15$)

As the $[SN_{extr,A}]$ and $[SN_{extr,B}]$ range show (Figure 3.13a), there exists a maximum value $(F_E/V)_{max,A,R \rightarrow \infty}$ to recover component A but no entrainer limit restriction applies to recover component B at infinite reflux ratio (Rodriguez-Donis et al. 2009a). Under finite reflux ratio and for $(F_E/V) < (F_E/V)_{max,A}$ (Figure 3.13b), extractive separatrixes appear but they still allow to recover either A or B, depending on the global feed composition: pure A can be obtained from the initial charge composition x_{F2} by adding even a small quantity of E. Indeed, x_{F2} lies in the regions III and IV where extractive composition profiles reach $[SN_{extr,A}]$ which is able to cross a rectifying profile reaching the unstable rectifying node vertex A. Above $(F_E/V)_{max,A,R \rightarrow \infty}$, $[SN_{extr,A}]$ would disappear in the left of x_P . In contrast starting from x_{F1} in regions I and II, all extractive profiles reach $[SN_{extr,B}]$ whatever the entrainer - feed flow rate ratio and enable to recover distillate x_{DB} . Other cases for $F_E/V > (F_E/V)_{max,A}$ were detailed in Rodriguez-Donis et al. (2009a).

The feasible range of operating conditions as entrainer - feed flow rate ratio vs. reflux ratio to recover 98% mol of product is displayed in Figure 3.14 for chloroform (A). The corresponding operating parameters are shown in Table 3.9.

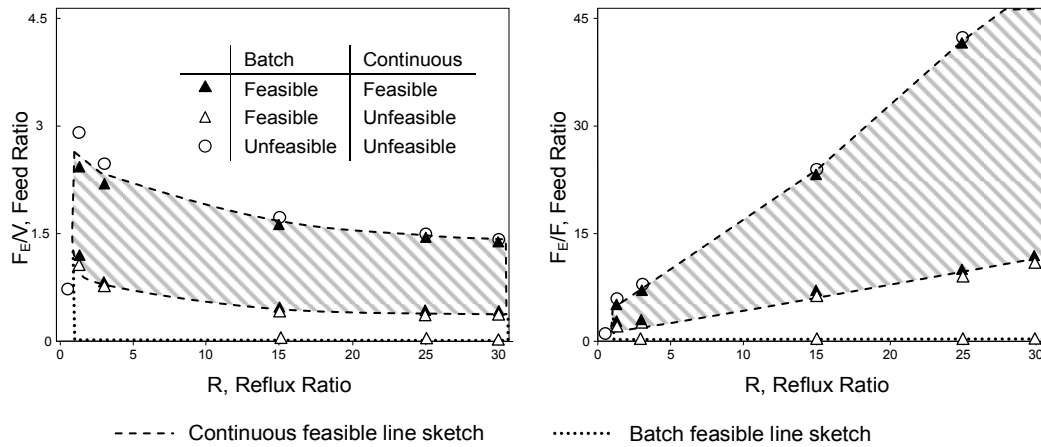


Figure 3.14 Extractive distillation of chloroform – vinyl acetate with butyl acetate (1.0-2 class). Entrainer - feed flow rate ratio as a function of the reflux ratio to recover 98%mol chloroform (A).

Table 3.9 Operating parameters corresponding to Figure 3.14.

Class 1.0-1a case A-E side with heavy entrainer								Feasibility	
Specification	A	B	E	Reflux ratio	Reboil ratio	F_E/F	F_E/V	Batch	Continuous
Name	chloroform	Vinyl acetate	Butyl acetate	30	0.55	51	1.3	yes	yes
Boiling T(°C)	61.2	72.5	126	25	0.57	41	1.41	yes	yes
X_F	0.9	0.1	0	15	0.62	23	1.59	yes	yes
X_E	0	0	1	30	2.31	12	0.42	yes	yes
X_D	0.98	0.01	0.01	25	2.32	10	0.45	yes	yes
F	1			3	0.51	7	1.94	yes	yes
D	0.9			15	2.03	7	0.49	yes	yes
η	0.98			1.3	0.41	5	2.41	yes	yes
				3	1.16	3	0.83	yes	yes
				1.3	0.8	2.5	1.2	yes	yes
				30	2.51	11	0.39	yes	no
				25	2.57	9	0.38	yes	no
				15	2.29	6.2	0.43	yes	no
				3	1.24	2.8	0.78	yes	no
				1.3	0.9	2.2	1.06	yes	no
				0.5	1.23	1	0.74	no	no
				30	279	0	0	yes	no
				25	234	0	0	yes	no
				15	144	0	0	yes	no
				30	0.54	52	1.4	no	no
				25	0.56	42	1.52	no	no
				15	0.6	24	1.66	no	no
				3	0.44	8	2.22	no	no
				1.3	0.34	6	2.89	no	no

When chloroform(A) is the distillate (Figure 3.14), there exists a maximum value for the entrainer - feed flow rate ratio above which the process is unfeasible both in batch and continuous. In continuous, the maximum gradually reduces as reflux ratio gets smaller, until a minimum R reflux ratio is reached. A detailed calculation of the profile map shows that the feasible rectifying section profiles region gets smaller until it can

no longer intersect the extractive profile. The batch (Figure 3.14a) and continuous mode (Figure 3.14b) feasible region are different, as an additional minimum value of the entrainer - feed flow rate ratio exists for the continuous mode, because under very low entrainer - feed flow rate ratio, the stripping section profile can no longer intersect the extractive section profile.

If the upper limit for the feed flow rate ratio is not a concern for industrial practice of continuous extractive distillation, the lower limit should be as low as possible for keeping the energy demand low. Figure 3.15 compares three different entrainers suitable to recover chloroform as distillate, under the 1.0-2 class. The location of the univolatility line is the closest to E for toluene, then for cyclohexane and finally for butyl acetate (Figure 3.15a). That expands the $SN_{\text{extr,A}}$ range and toluene has indeed the highest upper limit for the feed flow rate ratio (Figure 3.15b), followed by cyclohexane and butyl acetate. The opposite holds for the lowest feed flow rate ratio limit order. Concerning reflux ratio, toluene enables to operate at the lowest reflux ratio. A definite choice would require more process analysis and optimization. Overall, Figure 3.15 indicates that toluene exhibits the largest extractive feasible region, which can result in a better operational stability. That may become critical at low reflux ratio when the range of feasible feed flow rate ratio is narrowed.

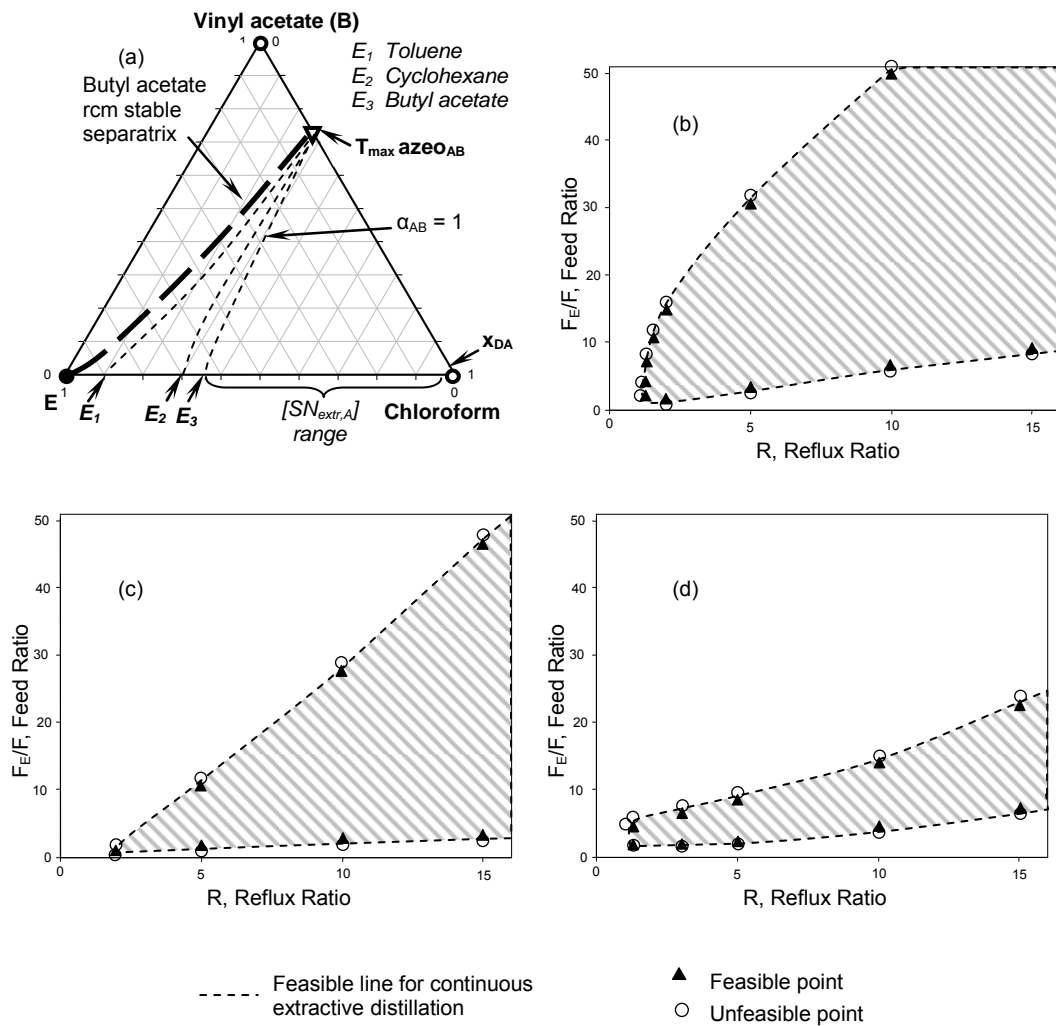


Figure 3.15 Comparison of three different entrainers to recover Chloroform from the mixture chloroform – vinyl acetate. (a) Univolatility curve location. (b) Toluene, (c) Cyclohexane and (d) Butyl acetate feasible regions.

When vinyl acetate(B) is the distillate, a behavior similar to the 1.0-1a case (a) is observed in Figure 3.16. Under infinite reflux ratio there is no limit for the entrainer - feed flow rate in batch process. Concerning the reflux ratio, an unstable extractive separatrix reduces the feasible region at low reflux ratio (Rodriguez-Donis et al., 2009a), thus defining an effective minimum feasible value for the reflux ratio, for both the batch and continuous modes. Overall, the continuous feasible region is again smaller than the batch one when the same purity is targeted, because of the limit set by the requirement of intersecting the stripping and extractive sections profiles (eg. below $F_E/F=0.2$). Table 3.10 displays operating parameters corresponding to Figure 3.16.

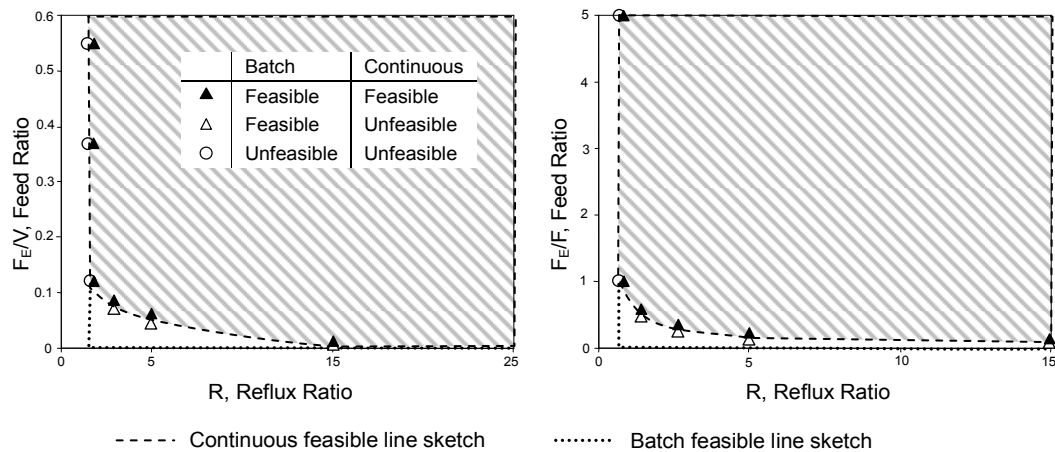


Figure 3.16 Extractive distillation of chloroform – vinyl acetate with butyl acetate (1.0-2 class). Entrainer - feed flow rate ratio as a function of the reflux ratio to recover 98%mol vinyl acetate (B).

Table 3.10 Operating parameters corresponding to Figure 3.16.

Specification	Class 1.0-2 case A-E side with heavy entrainer						Feasibility		
	A	B	E	Reflux ratio	Reboil ratio	F_E/F	F_E/V	Batch	Continuous
Name	chloroform	vinyl acetate	Butyl acetate	1	1.64	1	0.55	no	no
Boiling T(°C)	61.2	72.5	126	1	0.35	5	2.77	no	no
X_F	0.1	0.9	0	2	2.45	1	0.37	yes	yes
X_E	0	0	1	2	0.53	5	1.85	yes	yes
X_D	0.01	0.98	0.01	5	18	0.2	0.04	yes	no
F	1			5	13.5	0.3	0.06	yes	yes
D	0.8			15	48	0.2	0.01	yes	yes
η	0.98			15	72	0.1	0.007	yes	no

Rigorous simulations are carried out with ProsimPlus[®] in an extractive column whose features are displayed in Table 3.2. The rigorous profiles are then compared in Figure 3.17 to the approximate composition profile maps computed from Equations 3.6, 3.7 and 3.9, setting $x_D = 0.98$. As in the 1.0-1a case, approximate and rigorous profiles agree well. For the conditions ($F_E/F=5$; $R=5$) the process is feasible as the distillate purity reaches 0.982 in vinyl acetate. For the conditions ($F_E/F=5$; $R=0.1$) the process is unfeasible as the distillate purity can only reach 0.88 in vinyl acetate. The detailed information can be found in Tables 3.11- 3.12. Therefore, the approximate calculations are worthy to evaluate the feasibility of continuous extractive distillation processes under finite reflux ratio conditions.

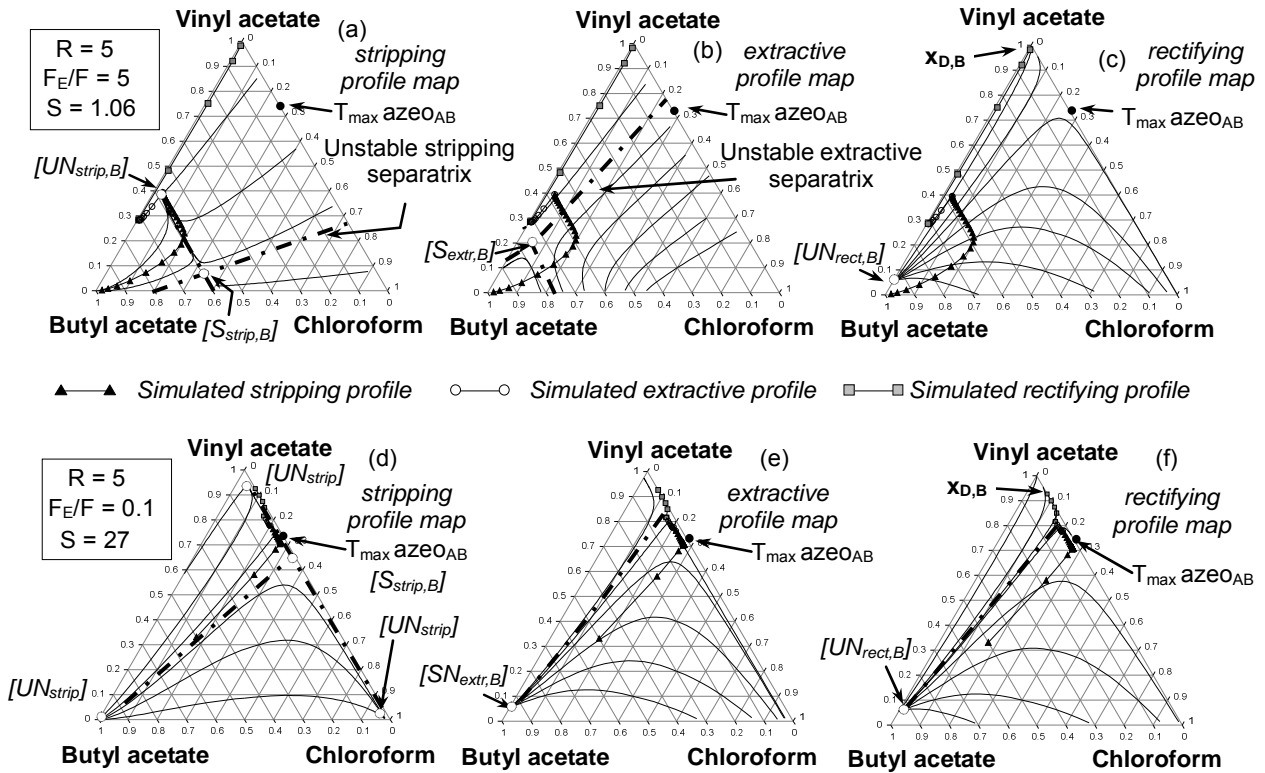


Table 3.11 Operating parameters corresponding to Figure 3.17a, b, c.

Class 1.0-2 case B-E side with heavy entrainer($F_E/F=5$, $R=5$)									
Worksheet parameters				Rectifying section			Stripping section		
Name	chloroform	vinyl acetate	Butyl acetate	A	B	E	A	B	E
Boiling T(°C)	61.2	72.5	126	chloroform	vinyl acetate	butyl acetate	chloroform	vinyl acetate	butyl acetate
X_F	0.1	0.9	0	5.07E-03	0.982132	0.0128	0.0317	0.394905	0.573442
X_E	0	0	1	8.06E-03	0.920564	0.0714	0.0333	0.393085	0.573641
X_D	0.01	0.98	0.01	9.11E-03	0.750609	0.240278	0.0355	0.390622	0.573893
X_W	0.017843	0.003529	0.978627	0.00682	0.482299	0.510877	0.0385	0.387329	0.574203
R	5			0.00393	0.284766	0.711306	0.0424	0.382989	0.574568
F_E/F	5			0.00496	0.284095	0.710945	0.0477	0.377372	0.574976
F	1						0.0543	0.370262	0.575398
D	0.9						0.0627	0.361495	0.575791
E	5			Extractive section			0.0729	0.351005	0.576103
W	5.1			A	B	E	0.0849	0.338859	0.57628
V	18.9			chloroform	vinyl acetate	butyl acetate	0.0984	0.325274	0.576287
η_B	0.98			0.00496	0.284095	0.710945	0.113284	0.310588	0.576128
Reboil S	1.06			0.00611	0.283681	0.710205	0.128929	0.2952	0.575871
F_E/V	0.9259			0.00741	0.283718	0.708874	0.144828	0.279478	0.575695
				0.00887	0.284506	0.706622	0.160387	0.263633	0.57598
				0.0106	0.286524	0.702923	0.174919	0.247561	0.577521
				0.0125	0.29057	0.696894	0.187465	0.230593	0.581942
				0.015	0.298057	0.686963	0.196413	0.211153	0.592434
				0.0182	0.311748	0.670036	0.198943	0.186542	0.614516
				0.023	0.337924	0.639062	0.190922	0.153888	0.65519
X_F	0.1	0.9	0	0.0317	0.394905	0.573442	0.168958	0.113633	0.717409
X_E	0	0	1	0.00496	0.284095	0.710945	0.134878	0.0727	0.792405
X_D	0.01	0.98	0.01	0.00496	0.284095	0.710945	0.0967	0.0402	0.863072
Num stages	40						0.0628	0.0196	0.917613
Solvent tray	5						0.0369	0.0085	0.954625
Feed tray	15						0.0187	0.00315	0.978134

Table 3.12 Operating parameters corresponding to Figure 3.17d, e, f.

Class 1.0-2 case B-E side with heavy entrainer($F_E/F=0.1$, $R=5$)									
Worksheet parameters				Rectifying section			Stripping section		
Name	chloroform	vinyl acetate	Butyl acetate	A	B	E	A	B	E
Boiling T(°C)	61.2	72.5	126	chloroform	vinyl acetate	butyl acetate	chloroform	vinyl acetate	butyl acetate
X_F	0.1	0.9	0	0.00497	0.885386	0.10964	0.0106	0.231015	0.758369
X_E	0	0	1	0.00515	0.583146	0.411702	0.0122	0.238958	0.748823
X_D	0.01	0.98	0.01	0.00365	0.354431	0.641917	0.0143	0.250749	0.734956
X_W	0.445	0.09	0.455	0.00265	0.25962	0.737729	0.0172	0.269218	0.713576
R	5			0.00223	0.228497	0.769269	0.0218	0.300968	0.677244
F_E/F	0.1			0.00208	0.218916	0.779	0.0306	0.366003	0.603436
F	1			Extractive section			0.0315	0.364945	0.603585
D	0.9			0.00203	0.216017	0.781951	0.0327	0.363459	0.603797
E	0.1			0.00202	0.215143	0.782841	0.0345	0.361375	0.604106
W	0.2			0.00201	0.21488	0.783109	0.037	0.358456	0.604578
V	5.4			0.00201	0.214801	0.78319	0.0403	0.354353	0.605356
η_B	0.98			0.00264	0.214514	0.782847	0.0447	0.348528	0.606758
Reboil S	27			0.0033	0.214404	0.782298	0.0504	0.340078	0.609531
F_E/V	0.0185			0.00399	0.214522	0.78149	0.0573	0.327378	0.61536
				0.00471	0.214932	0.780353	0.0647	0.307491	0.627823
X_F	0.1	0.9	0	0.00548	0.215716	0.7788	0.0709	0.275733	0.653391
X_E	0	0	1	0.00631	0.216981	0.776712	0.0725	0.227358	0.700112
X_D	0.01	0.98	0.01	0.0072	0.218877	0.773923	0.0662	0.164136	0.76965
Num stages	40			0.00819	0.221612	0.7702	0.052	0.0998	0.848202
Solvent tray	5			0.00931	0.225498	0.765196	0.0346	0.0503	0.915181
Feed tray	18						0.0187	0.0202	0.961044

3.4.2.2 Subcase 1.0-2 Case (b): univolatility line $\alpha_{AB}=1$ reaching the binary Side B-E.

Separation of the maximum boiling azeotrope acetone (A) – chloroform (B) by adding benzene (heavy E) illustrates the case when $\alpha_{AB} = 1$ reaches the B-E side (Figure 3.18). The 1.0-2 class diagram bears the same features as the previous chloroform-vinyl acetate-butyl acetate diagram, but for the location of the univolatility curve. As it now reaches the B-E edge, the batch extractive process criterion states that A can be distilled without any limit for the entrainer entrainer - feed flow rate ratio, whereas there exists a maximum entrainer entrainer - feed flow rate ratio to get B. Depending of the overall feed composition either A or B can be distilled: from x_{F1} B is the distillate product; from x_{F2} below the extractive separatrix, A is the distillate product.

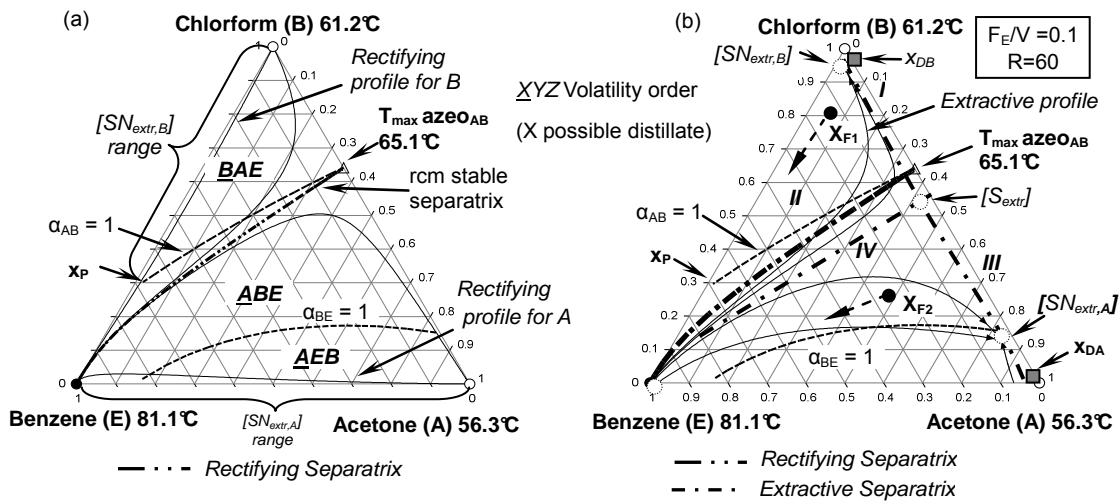


Figure 3.18 acetone-chloroform using benzene: (a) 1.0-2 class residue curve map (rcm) and batch extractive profile map (b) ($F_E/V=0.1 < (F_E/V)_{max}$, $R=60$).

As shown in Figure 3.18, both original components A and B are unstable nodes, the entrainer (E) is the stable node, while the maximum boiling azeotrope $T_{max\ azeoAB}$ is a saddle point, The rcm stable separatrix, so-called distillation boundary, links the azeotrope to E. The univolatility curve $\alpha_{AB} = 1$ starts at $T_{max\ azeoAB}$ until it intersects the B-E side at the so-called x_P point. Both acetone (A) and chloroform (B) are the most volatile in their respective region (see volatility order $B>A>E$ and $A>B>E$ in Fig.18a) where there exists a residue curve with decreasing temperature from E to their location. Therefore, either A or B are possible distillates of the extractive distillation process. As explained in Rodriguez-Donis et al. (2009a), there is a maximum value $(F_E/V)_{max,B,R\infty}$ to recover component B whereas no entrainer - feed flow rate ratio restriction applies to recover component A at infinite reflux ratio (See $[SN_{extr,A}]$ and $[SN_{extr,B}]$ range in Figure 3.18a). Figure 3.18b displays the extractive composition profile for $(F_E/V) < (F_E/V)_{max,B,R\infty}$, under infinite reflux ratio. Pure B can be obtained from the initial charge composition x_{F1} by adding even a small quantity of E.

Indeed, x_{F1} lies in the regions I and II where extractive composition profiles reach $[SN_{extr,B}]$ that are able to cross a rectifying profile reaching the unstable rectifying node vertex B, above $(F_E/V)_{max,B,R\infty}$, $[SN_{extr,B}]$ would disappear under composition x_p . In contrast starting from x_{S2} in regions III and IV, all extractive profiles reach $[SN_{extr,A}]$ whatever the entrainer - feed flow rate ratio and enable to recover distillate x_{DA} .

The feasible range of operating conditions as entrainer - feed flow rate ratio vs. reflux ratio to recover 98mol%mol of product is displayed in Figure 3.19 for acetone (A). It is similar to Figure 3.16 for the previous mixture. Again, the batch and continuous process feasible ranges are different because the continuous process requires that the stripping profile intersects the extractive profile when the same purity is targeted.

When distillate is acetone (A) (Figure 3.19), infinite reflux ratio analysis shows no limit for the entrainer - feed flow rate ratio. These results of Figure 3.19b in batch process agree well with the thermodynamics criteria analysis above. However, in continuous process of Figure 3.19a there exists additional minimum value F_E/F_{max} at any given reflux ratio $R > R_{min}$ or we can say at any given entrainer - feed flow rate ratio there exists minimum value of reflux ratio R_{min} , this minimum value remains nearly constant. This additional existence results from the stripping section profile can not intersect the extractive section in continuous process and its conditions limit feasibility, the operation requirement become more rigorous because all of parameters choice need occur over a more narrow range. Technically speaking in class 1.0-2, both component A and B can be recovered as they are unstable rectifying node UN_{rcm} , at the condition of $F_E = 0$ or infinite reflux ratio, this is similar to the theory of process azeotropic distillation, Figure 3.19b at the condition of infinite reflux ratio, verified this theory, obviously, in continuous process of Figure 3.19a, again, becomes unfeasible at this unlimited situation. Both continuous modes and batch modes display the same features for reflux ratio limitation. Similarly to Figure 3.16, there is a minimum reflux ratio value below which the separation becomes impossible no matter how big the amount entrainer feed given. The corresponding operating parameters are available in Table 3.13.

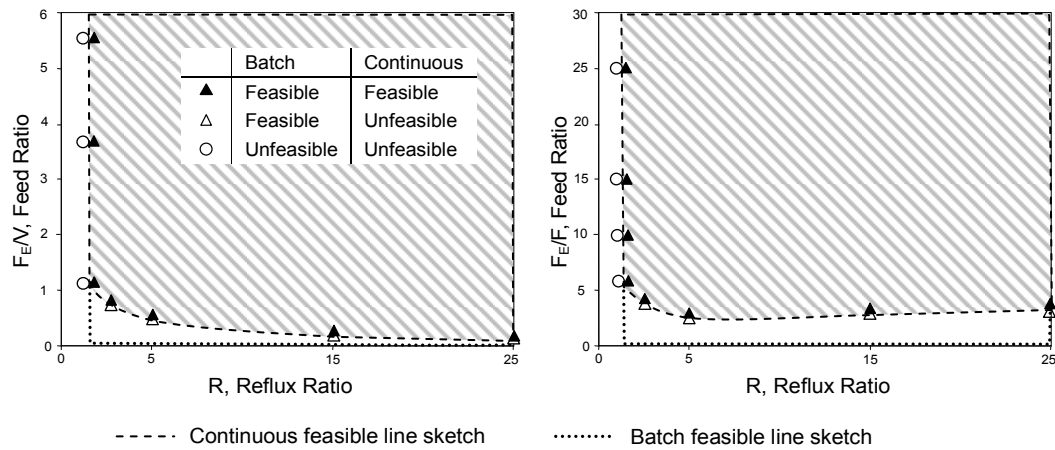


Figure 3.19 Extractive distillation of acetone – chloroform with benzene (1.0-2 class). Entrainer - feed flow rate ratio as a function of the reflux ratio to recover 98%mol acetone (A).

Table 3.13 Operating parameters corresponding to Figure 3.19.

Class 1.0-2 case B-E side with heavy entrainer								Feasibility	
Specification	A	B	E	Reflux ratio	Reboil ratio	F_E/F	F_E/V	Batch	Continuous
Name	acetone	chloroform	benzene	25	6.5	3.5	0.15	yes	no
Boiling T(°C)	56.3	61.2	81.1	25	5.7	4	0.17	yes	yes
X_F	0.9	0.1	0	15	4.65	3	0.21	yes	no
X_E	0	0	1	15	4	3.5	0.24	yes	yes
X_D	0.98	0.01	0.01	5	2.08	2.5	0.46	yes	no
F	1			5	1.74	3	0.56	yes	yes
D	0.9			2	0.27	10	3.7	yes	yes
η	0.98			2	0.18	15	5.56	yes	yes
				2	0.11	25	9.26	yes	yes
				1	0.18	10	5.56	no	no
				1	0.12	15	8.33	no	no
				1	0.17	25	13.89	no	no

The feasible range of operating conditions as entrainer - feed flow rate ratio vs. reflux ratio to recover 98%mol of product is displayed in Figure 3.20 for chloroform (B), showing the maximum entrainer entrainer - feed flow rate ratio value. It is slightly different from Figure 3.14 for the previous mixture as now the batch and continuous process feasible ranges are different. As expected from the infinite reflux ratio analysis there exists a maximum value for entrainer - feed flow rate ratio above which the process is unfeasible. This maximum value gradually reduces as reflux ratio gets smaller, until it reaches a minimum reflux ratio. A detailed calculation of the profile map shows that the feasible rectifying section profiles region gets smaller until it can no longer intersect the extractive profile region. The same holds for the continuous mode. However, the continuous (Figure 3.20a) and batch mode (Figure 3.20b) have a large difference as the existence of minimum value of the entrainer - feed flow rate ratio, because in continuous process the stripping section is now involved and its conditions can limit feasibility, the operations requirement become more rigorous because all of parameters choice need occur over more narrow range.

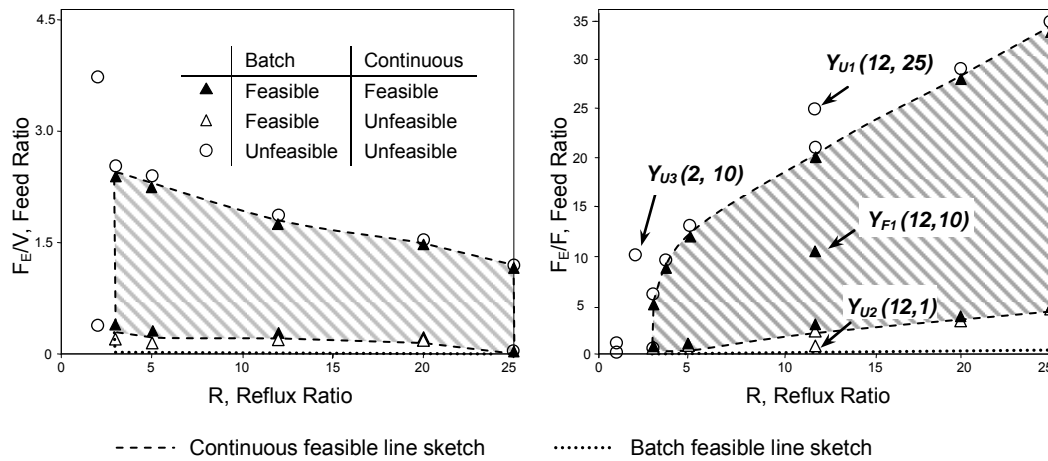


Figure 3.20 Extractive distillation of acetone – chloroform with benzene (1.0-2 class). Entrainer - feed flow rate ratio as a function of the reflux ratio to recover 98%mol chloroform (B).

Table 3.14. Operating parameters corresponding to Figure 3.20.

Class 1.0-2 case B-E side with heavy entrainer								Feasibility	
Specification	A	B	E	Reflux ratio	Reboil ratio	F_E/F	F_E/V	Batch	Continuous
Name	acetone	chloroform	benzene	20	4.6	4	0.21	yes	yes
Boiling T(°C)	56.3	61.2	81.1	20	0.67	28	1.48	yes	yes
X_F	0.1	0.9	0	20	6.1	3	0.16	yes	no
X_E	0	0	1	20	0.65	29	1.53	no	no
X_D	0.01	0.98	0.01	12	0.58	20	1.71	yes	yes
F	1			12	3.77	3	0.26	yes	yes
D	0.9			12	0.55	21	2.22	no	no
η	0.98			12	5.57	2	0.17	yes	no
				5	0.45	12	4.22	yes	yes
				5	6	0.8	0.15	yes	yes
				5	0.41	13	2.41	no	no
				5	6.75	0.7	0.13	yes	no
				3	0.71	5	0.39	yes	yes
				3	4.5	0.7	0.19	yes	yes
				3	0.59	9	2.60	no	no
				3	5.14	0.6	0.17	yes	no
				2	2.45	1	0.37	no	no
				2	0.27	10	3.7	no	no

Figure 3.21 displays the composition profiles computed to get $x_D = 0.98$, under four operating conditions reported in Figure 18b. For $Y_{U1}(R=12, F_E/F=25)$ the process is unfeasible as the rectifying profile cannot intersect the extractive section (Figure 3.21a). For $Y_{F1}(R=12, F_E/F=10)$, the process is feasible (Figure 3.21b). For $Y_{U2}(R=12, F_E/F=1)$ the batch process is feasible but not the continuous process as the stripping profile cannot intersect the extractive profile (Figure 3.21c). Figure 3.21d concerns the point Y_{U3} ($R=2, F_E/F=10$) which reflux ratio is lower than the minimum reflux ratio value: the rectifying profile is so short that it doesn't intersect the extractive section. Table 3.15 summarizes the operating parameters corresponding to Figure 3.21.

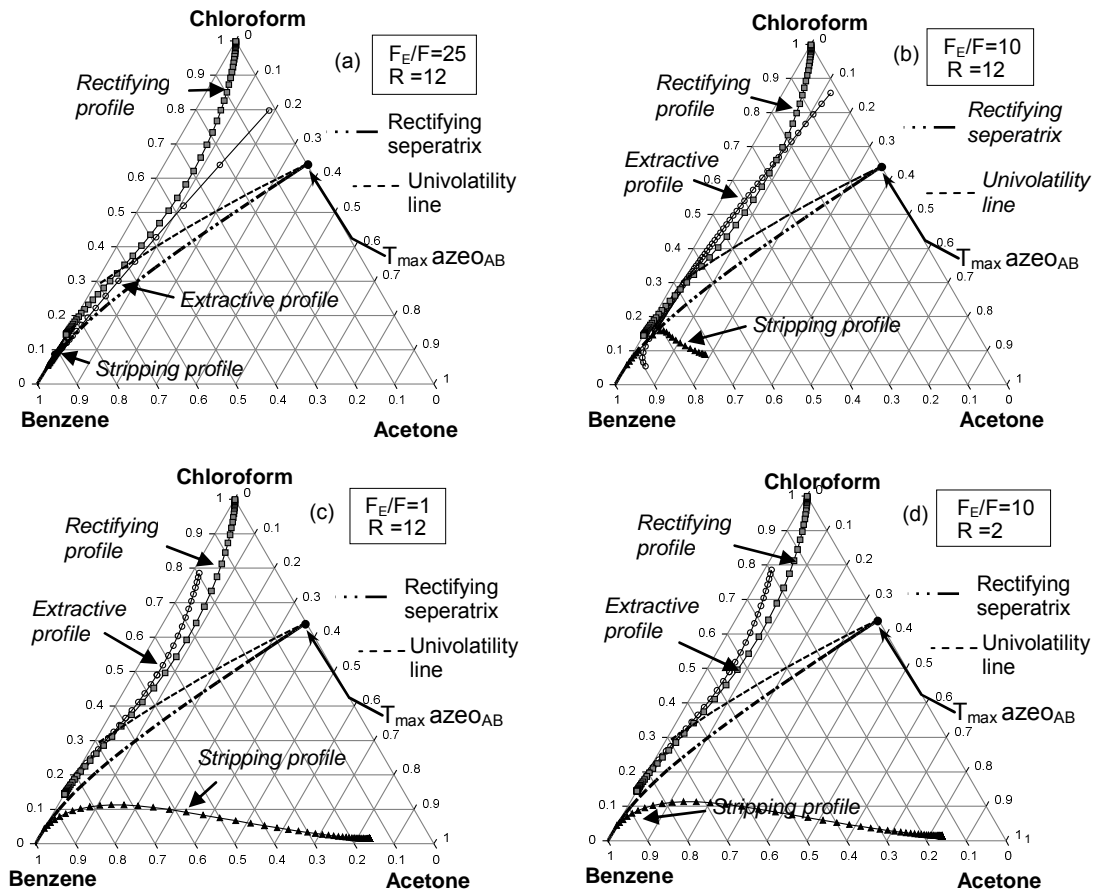


Figure 3.21 Rectifying, extractive and stripping composition for four operating parameter points taken from Figure 3.20 (a) point Y_{U1} , (b) point Y_{F1} , (c) point Y_{U2} and (d) point Y_{U3} .

Table 3.15. Operating parameters corresponding to Figure 3.21

Class 1.0-2 case B-E side with heavy entrainer							
Specification parameters for Figure 3.21(a)				Specification parameters for Figure 3.21(b)			
Apex	A	B	E	Apex	A	B	E
Name	acetone	chloroform	benzene	Name	acetone	chloroform	benzene
Boiling T(°C)	56.3	61.2	81.1	Boiling T(°C)	56.3	61.2	81.1
X _F	0.1	0.9	0	X _F	0.1	0.9	0
X _E	0	0	1	X _E	0	0	1
X _D	0.01	0.98	0.01	X _D	0.01	0.98	0.01
X _W	0.0036255	0.00071713	0.995657371	X _W	0.0090099	0.00178218	0.989207921
R	12			R	12		
F _E /F	25			F _E /F	10		
F	1			F	1		
D	0.9			D	0.9		
E	25			E	10		
W	25.1			W	10.1		
V	11.7			V	11.7		
η _B	0.98			η _B	0.98		
Reboil S	0.4661			Reboil S	1.1584		
F _E /V	2.1368			F _E /V	0.8547		
Specification parameters for Figure 3.21(c)				Specification parameters for Figure 3.21(d)			
Apex	A	B	E	Apex	A	B	E
Name	acetone	chloroform	benzene	Name	acetone	chloroform	benzene
Boiling T(°C)	56.3	61.2	81.1	Boiling T(°C)	56.3	61.2	81.1
X _F	0.1	0.9	0	X _F	0.1	0.9	0
X _E	0	0	1	X _E	0	0	1
X _D	0.01	0.98	0.01	X _D	0.01	0.98	0.01
X _W	0.08272727	0.01636364	0.900909091	X _W	0.0090099	0.00178218	0.989207921
R	12			R	2		
F _E /F	1			F _E /F	10		
F	1			F	1		
D	0.9			D	0.9		
E	1			E	10		
W	1.1			W	10.1		
V	18.9			V	2.7		
η _B	0.98			η _B	0.98		
Reboil S	10.6363			Reboil S	0.2673		
F _E /V	0.0855			F _E /V	3.7037		

3.5 CONCLUSIONS

A feasibility method built for the batch extractive distillation process was extended to investigate the range of operating parameters reflux ratio (R) and entrainer - feed flow rate ratio (F_E/F, F_E/V) for both continuous or batch process. It is shown that the feasibility under infinite reflux ratio conditions can be predicted from the general feasibility criterion enounced by Rodriguez-Donis et al. (2009a), which requires only the knowledge of the rcm topology and classification along with the computation of the univolatility line. The prediction is confirmed by the calculation of approximate composition profile in each column section, depending on reflux ratio and entrainer - feed flow rate ratio. Under finite reflux ratio conditions, the results at approximate calculations agree with those at the rigorous simulations of continuous extractive distillation processes, but also bring information about the location of pinch points and possible composition profiles separatrices that could impair the process feasibility.

For class 1.0-1a (minimum boiling azeotrope separation A-B by adding a heavy entrainer E), two sub cases arise depending on the univolatility line $\alpha_{AB} = 1$ location. Two azeotropic systems acetone-heptane with toluene (entrainer) and acetone-methanol with water (entrainer) are used to demonstrate the case when univolatility line $\alpha_{AB} = 1$ intersects the A-E edge (case a); an example acetone-methanol with heavy entrainer chlorobenzene is used to explain the case when univolatility line $\alpha_{AB} = 1$ intersects the B-E edge (case b).

At infinite reflux ratio for the batch process, the point x_p determines the minimal limit value for entrainer - feed flow rate ratio, the range of the extractive stable node $SN_{extr,A}$ and the expected product A (in class 1.0-1a case a), $SN_{extr,B}$ and the expected product B (in class 1.0-1a case b). Under finite reflux ratio, $SN_{extr,B}$ in class 1.0-1a case a) ($SN_{extr,A}$ in class 1.0-1a case b) moves inside the diagram and generates an extractive unstable separatrix that reduces the feasible region.

These results also translate well for continuous extractive distillation, regarding A as product component for the two examples of case a, the results show the expected feature: there is a minimum entrainer - feed flow rate ratio at any reflux ratio. Besides, there is maximum reflux ratio at any given entrainer entrainer - feed flow rate ratio. The maximum reflux ratio gets smaller as the entrainer entrainer - feed flow rate ratio reduces, in agreement with the result of Knapp and Doherty(1994). There is also a minimum reflux ratio value, below which the separation becomes impossible no matter how big is the entrainer to entrainer - feed flow rate ratio. The feasible regions of the two examples have the same shape but the limits are different because of the different properties of azeotrope and solvent performance.

The same shape of the operating parameter feasibility region holds for the continuous and batch mode, as the limitation F_E/V and reflux ratio in batch translates into a continuous value F_E/F . However, the minimum value F_E/V is smaller for the continuous than for the batch mode because the continuous profile sets stricter feasible conditions due to the necessary intersection between the stripping and the extractive profile.

Regarding case b aiming to produce acetone(A) as distillate from ternary system acetone (A)-methanol (B)-chlorobenzene(E), it bears symmetrical feature with case a, but then heptane(B) is the product as the univolatility curve $\alpha_{AB} = 1$ now reaches B-E edge.

For class 1.0-2 (separation of a maximum boiling azeotrope with a heavy entrainer) two sub cases also occur. Forth mixture chloroform (A) - vinyl acetate (B) using butyl acetate as entrainer(E), the univolatility curve $\alpha_{AB} = 1$ intersects the A-E edge (case a), while for the mixture acetone (A) – chloroform (B) using benzene (E) as entrainer, the univolatility curve $\alpha_{AB} = 1$ intersects the B-E edge (case b). The batch feasibility criterion under infinite reflux ratio then states that A or B can be distilled out, depending on the

starting composition. For case a (resp. case b), chloroform (A for case a) (resp. B for case b) can be a distillate product, provided that the entrainer entrainer - feed flow rate ratio lies below a maximal value $(F_E/V)_{\max}$ at a given reflux ratio. The continuous process also displays a corollary maximal value $(F_E/F)_{\max}$. But the continuous process also shows a minimum value F_E/F because of the necessary intersection between the stripping and the extractive section composition profiles. Under finite reflux ratio an extractive unstable separatrix moves inside the diagram and impacts the feasible composition region. In continuous mode, the minimum value F_E/F at a given reflux ratio gets smaller as reflux ratio reduces, and there also exists a minimum reflux ratio.

Regarding the distillation of vinyl acetate (B) when separating the mixture chloroform-vinyl acetate using butyl acetate as entrainer or acetone (A) when separating the mixture chloroform-acetone using benzene as entrainer, the batch extractive process analysis predicts no entrainer limitation under infinite reflux ratio. However there exists a minimum entrainer - feed flow rate ratio limit under finite reflux ratio for the continuous process because of the additional constraint that the stripping profile intersects the extractive profile. For both continuous and batch mode, there exist a minimum value for reflux ratio because of the reduction of the rectifying profile region as reflux ratio decreases.

Comparison of three entrainers leading to the same type of diagram and the same sub-case also shows that the feasible conditions ranges is entrainer dependent, in particular the minimum reflux ratio and the minimum entrainer entrainer - feed flow rate ratio, and that the methodology is suitable to compare entrainers in a preliminary step before optimizing the process with the entrainer regeneration column.

As these observations for the class 1.0-2 or 1.0-1a are corroborated by rigorous simulations, we demonstrate that feasibility analysis based on simple thermodynamic insight (the ternary class, the univolatility line intersect with the diagram) can be exploited to evaluate the feasibility under finite reflux ratio and both for batch and continuous operation.

Extension of Thermodynamic Insights on Batch Extractive
Distillation to Continuous Operation. Azeotropic Mixtures with a
light Entrainer

4.1 INTRODUCTION

In extractive distillation, the common industrial rule for selecting a suitable entrainer is to choose a miscible, heavy boiling, which forms no new azeotrope. It should interact differently with the components of the mixture causing their relative volatilities to either increase or reduce, and thereby ease the separation. However, there are some cases when its use is not recommended such as if a heat sensitive, high boiling component mixture to be separated. Different entrainers can cause different components to be recovered or recovered overhead in extractive distillation, Potential entrainers is critical since an economically optimal design made with an average design using best entrainer can be much less costly (Laroche et al, 1991). Theoretically, any candidate entrainer satisfying the feasibility and optimal criteria can be used no matter it is heavy, light, or intermediate entrainer. Literature studies on intermediate entrainer or light entrainer, even though not too much, validate this assumption. Laroche et al. (1991) investigated the use of heavy, intermediate and light boiling entrainer to separate minimum boiling azeotropes. In batch operation, Rodriguez-Donis et al, reviewed the use of these three kinds of entrainers to separate maximum boiling azeotropes and low relative volatility mixtures (Rodriguez-Donis et al., 2009a, 2009b, 2012a, 2012b). They also showed that entrainers forming azeotropes could also be used in extractive distillation (2010 DistAbs Proceedings), but that was not further tested for continuous operation.

In this chapter, we are here concerned by extending the thermodynamic insight on extractive distillation feasibility proven for batch distillation to continuous extractive distillation. In Chapter3, we have shown how the thermodynamic insight acquired on batch extractive distillation could be extended to the use of a heavy entrainer for separating minimum and maximum boiling azeotropes. Applying the general feasibility criterion for extractive distillation under infinite reflux ratio (Rodriguez-Donis et al., 2009a) which considered the volatility order regions of the ternary diagram, we pointed out how they could be extended to continuous extractive distillation and what differences occurred under finite reflux ratio. This chapter concerns the use of a light boiling entrainer for the separation of minimum and maximum boiling binary azeotropes.

After a brief state of the art section, we recall the essential features of the methodology, already described in chapter3, stress the specificities due to the use of a light entrainer. Then we investigate the two sub-cases process alternatives linked to the separation of a maximum boiling azeotrope with a light entrainer (class 1.0-1a) and of a minimum boiling azeotrope with a light entrainer (class 1.0-2) by applying the methodology. Through a systematic calculations of different section composition profiles, feasibility region for

two key parameters entrainer - entrainer - feed flow rate ratio and reboil ratio are determined and validated by rigorous simulation.

4.2 STATE OF THE ART WITH LIGHT ENTRAINER

In extractive distillation, a third component entrainer E is added to interact selectively with the original components A and B, to reinforce their relative volatility, thus enhancing the original separation. We refer to A as having a lower boiling point than B. It differs from azeotropic distillation by the fact that the third-body solvent E is fed continuously in another column position (either to the still, or to the column, or to the top) other than feed mixture. Entrainer design study has been rich in the literature, a potential candidate entrainer is often referred to three major property classes : (1) pure solvent properties such as boiling point, vapor pressure, molar volume, ... (Marrero and Gani, 2001; Chein-Hsiun, 1994); (2) process properties such as relative volatility, solvent solubility power, phase stability criterion performance index (Pretel et al., 1994) and univolatility and unidistribution curves (Laroche et al., 1992; Rodriguez-Donis et al. 2009a, 2009b, 2010, 2012a, 2012b); and (3) environment-related properties such as LC₅₀ (Song and Song, 2008), environmental waste, impact, health, and safety issues (Weis and Visco, 2010).

Literature studies on light entrainer for extractive distillation are scarce compared to the use of a heavy entrainer. Hunek et al. (1989) tested the separation of the minimum boiling azeotropic mixture ethanol (A)-water (B) with the light entrainer methanol by a pilot-plant experiment, calling this process reverse extractive distillation. Laroche et al. (1991) showed that the univolatility curve location could be used to determine the product obtained from extractive distillation of a minimum boiling azeotrope with a light entrainer: using acetone as a light entrainer, the separation of water ethanol (A) – water (B) gave water (B) as the bottom product of the extractive column; whereas the separation of methyl ethyl ketone (A) – water (B) gave methyl ethyl ketone (A) as the bottom product of the extractive column. The general criterion for extractive distillation feasibility under infinite reflux ratio (Rodriguez-Donis et al., 2009a) fully corroborates this analysis by combining simultaneously the relationship between the residue curve map and the location of the univolatility line.

Analyzing more than 400 binary azeotrope- entrainer system, for either azeotropic or extractive distillation, Laroche et al., (1992) concluded that: (1) light entrainers are common, almost as common as heavy entrainers; (2) light entrainers often represent the only viable alternative when a heavy entrainer cannot be used; and (3) light entrainers can perform as well or better than heavy entrainer. Further works have concerned batch extractive distillation. Lang et al. (1999a) assessed the feasibility of the extractive

distillation of ethanol (A)-water (B) with light entrainer methanol in batch rectifier and of mixture n-butanol (A) - n-butylacetate (B) with n-propylformate and di-propylether as light entrainer in a batch stripper. Considering a batch rectifier and a batch stripper, Varga (2006) studied the separation of three mixtures: ethanol-water (minimum boiling azeotrope) with light entrainer methanol, water - ethylene diamine (maximum boiling azeotrope) with light entrainer methanol, and chlorobenzene - ethylbenzene (close boiling mixture) with light entrainer 4-methylheptane. Feasibility, operating steps, limiting entrainer - feed flows, limiting reflux ratios, and limiting number of theoretical stages were then determined by parametric study on profiles maps, and verified by rigorous simulation. More recently, by the aid of thermodynamic insights on knowledge of the location of univolatility lines and residue curve analysis (Rodriguez-Donis et al. 2009a), Rodriguez-Donis et al. (2012) published a detailed study on the feasibility of homogeneous batch extractive distillation for all the possible sub-cases related to the separation of azeotropic mixtures with light entrainer which belongs to class 1.0-2 and 1.0-1a.. This paper aims to investigate that insight for the continuous extractive distillation process with a light entrainer.

From basic mass balance analysis, feasibility of an extractive distillation under finite reflux ratio (reboil ratio in revers extractive distillation) conditions requires that the top and bottom product composition are connected each other through the liquid composition profiles x_i in each sections. The calculation requires choosing a target product composition and depends on many parameters. In azeotropic distillation or common distillation process with two column sections, the relevant parameters to be considered are the heat condition of the feed variable q , the feed stage location, total number of stages, the column holdup, and the vapor flow rate ratio, the condenser cooling duty, the boiler heat duty and the reflux ratio. Not all are independent because the distillation column model has only two degrees of freedom (Widgado and Seider, 1996). Extractive distillation further adds the entrainer feed flow rate ratio to the list of the parameters as another degree of freedom. Like a previous study in this series, we focus only on the influence of the reboil ratio and entrainer - feed flow rate ratio on feasibility. Finding the ranges of reboil ratio and entrainer - feed flow rate ratio values that enable a feasible extractive distillation is the main issue of extractive distillation.

Upon the feasibility study on separation a maximum (minimum) boiling azeotrope with the entrainer forming no new azeotrope which belongs to the 1.0-1a of Serafimov's class (occurrence 21.6%), most literature focus on a heavy entrainer. The study with light entrainer, which is of equal importance, was not studied in continuous operation but was in batch by using composition profiles. In contrast, applying light entrainer for separating a maximum boiling azeotrope, the corresponding ternary diagram belongs to the 1.0-

1a Serafimov's class (occurrence 21.6%). The separation of a minimum boiling azeotrope with a light entrainer corresponds to the 1.0-2 class (occurrence 8.5%).

Knapp et al (1994) investigated the limit quantities of both reflux ratio and entrainer - feed flows for a conventional

case of ternary mixture which belongs to class 1.0-1a, where a heavy entrainer is added to separate an azeotropic mixture with minimum azeotrope and other literature merely focus on batch case 1.0-2 with heavy entrainer (Lang et al., 2000), case 1.0-1a,1.0-2 and 0.01 with light entrainer (Lang et al., 1999b),1.0-1b heavy entrainer with intermediate(Lelkes et al., 2002,Rév et al., 2003) were also published. The extension of thermodynamic insight to other mixture classes with light entrainer was systematically studied by (Rodriguez-Donis et al., 2012a) who combined knowledge of the thermodynamic properties of residue curve maps and of the univolatility and unidistribution curves location. As a continue work of this series, this Chapter aims to identify how the thermodynamic insight underlying the general feasibility criterion can be transposed to continuous operation of extractive distillation with light entrainer, not only for the 1.0-1a class so far well studied but for all the classes found feasible in batch. For all suitable classes, the general criterion under infinite reboil ratio could explain the product to be recovered and the possible existence of limiting values for the entrainer - feed flow rate ratio for batch operation: a minimum value for the class 1.0-1a, a maximum value for the class 1.0-2, etc... The behavior at finite reboil ratio could be deduced from the infinite behavior and properties of the residue curve maps, and some limits on the reboil ratio were found. However precise finding of the limiting values of reboil ratio or of the entrainer - feed flow rate ratio required other techniques, summarized as following parts.

4.3 COLUMN CONFIGURATION AND OPERATION

Extractive distillation can be operated either in batch or in continuous mode. The batch mode is usually used for separating small quantities of mixture varying composition, besides the conventional batch rectifier (Lelkes, Lang, Benadda, and Moszkowicz, 1998a,Stéger et al., 2005), both batch stripper (Lang et al., 1999b, Varga, 2006) and middle vessel columns (Davidyan et al., 1994)have also been suggested and discussed in the literature, even though the use of a light entrainer would recommend to use a batch stripper, as the product being expected to be a heavy boiler could be removed from the boiler still (Varga et al., 2006).Varga (2006) studied four configurations for extractive distillation using light entrainer premixed to the charge in the still before distillation (SBD), fed continuously into the still (BED-B) at the top (BED-T) or at an intermediate location BED-I and provided recommendations for separating minimum and maximum

azeotropes and close-boiling mixtures. In the present Chapter, we consider a continuous column with the original binary mixture (A+B) initially charged into the column top vessel and it is fed to the first top tray as boiling liquid (L_T), light entrainer (F_E) fed at an intermediate location below the main feed (A+B), according to Figure 4.1b. It gives rise to three column sections, the extractive and stripping section, as in the batch column (Figure 4.1a), partial evaporation of the liquid phase reaching the column bottom gives the vapor flow rate ratio (V_S). The remaining liquid is drawn as bottom product (W) in order to maintain the liquid amount into the boiler. For continuous configuration, as we consider a light entrainer (boiling temperature below that of both A and B), the entrainer stream is fed below the main feed in continuous (b), these two feeds leading to three column sections, stages above azeotropic mixture feed named rectifying section, stages between azeotropic mixture feed and entrainer feed named extractive section, stages below is stripping section (see Figure 4.1b).

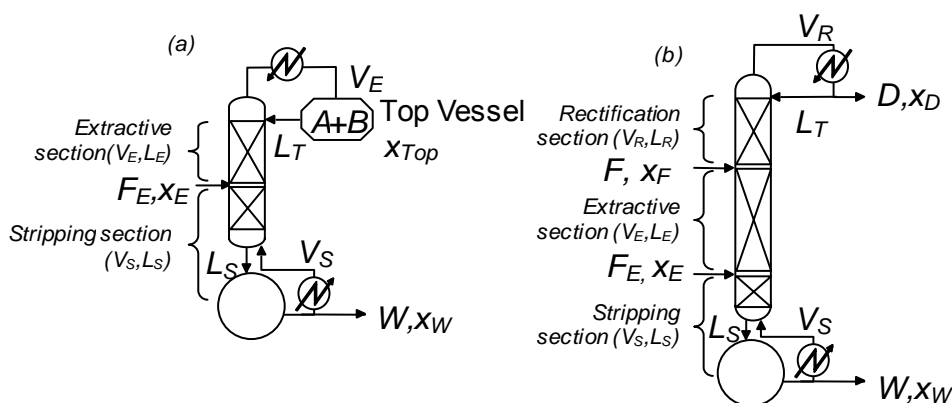


Figure 4.1 Configurations of extractive distillation column: (a) batch (b) continuous.

4.4 EXTRACTIVE DISTILLATION FEASIBILITY ASSESSMENT

According to Serafimov's classification of ternary diagrams (Kiva et al; 2003) the separation of a minimum boiling azeotrope with a light entrainer gives rise to a 1.0-2 class diagram (8.5% occurrence among ternary azeotropic mixtures) and the separation of a maximum boiling azeotrope gives rise to a 1.0-1a class diagram (21.6% occurrence).

Chapter 2 gave an overview of the state of the art on the feasibility assessment of continuous extractive distillation when a heavy entrainer is used. Many classical tools used for azeotropic distillation are valid for extractive distillation: residue curve map analysis, composition profiles.... A key parameter is the reflux ratio, which should be as low as possible for economic reasons, as it governs the internal liquid flow into the column. But, the occurrence of the middle / extractive section sets new challenges for extractive distillation. The ratio of the entrainer / main feeds becomes a variable as important as the reflux ratio.

Besides, feasibility in terms of composition profiles now requires that all three sections intersect together as was highlighted with the work on double feed columns of Levy and Doherty (1986). Laroche et al. (1992) further brought attention to univolatility curves and volatility order regions for the 1.0-1a class with a heavy entrainer, explaining that depending on the location of the univolatility curve intersection with the A-B-E triangle, product can be either A or, less intuitive, B the intermediate boiler. Explanation also came from the study of the middle section composition profile map topology and singular points for the 1.0-1a class (Knapp and Doherty, 1994, Lelkes et al. 1998, Brüggemann and Marquardt, 2004, Frits et al. 2006) as feasibility of the extractive distillation process required the stable node of the extractive section to be near the triangle edge, so as to intersect a rectifying section curve reaching the desired distillate. As the stable node moves along the univolatility curve for the 1.0-1a class when the entrainer - feed flow rate ratio increases below a minimum entrainer - feed flow rate ratio value, the process becomes feasible above that limit value (Lelkes et al., 1998).

Rodriguez-Donis and her colleagues extended systematically that analysis for the separation of minimum or maximum boiling azeotropes and of low relative volatility mixtures, considering light, intermediate or heavy entrainer, by batch extractive distillation (2009a, 2009b, 2010, 2012a, 2012b). Combining knowledge of the thermodynamic properties of residue curve maps and of the univolatility and unidistribution curves location, they expressed a general feasibility criterion for extractive distillation under infinite reflux ratio. Serafimov's classes covering up to 53% of azeotropic mixtures can match the criterion and are suited for extractive distillation : 0.0-1 (low relative volatility mixtures) (Rodriguez-Donis et al. 2009b), 1.0-1a, 1.0-1b, 1.0-2 (azeotropic mixtures with light, intermediate or heavy entrainers forming no new azeotrope) (Rodriguez-Donis et al. 2009a, 2012a, 2012b), 2.0-1, 2.0-2a, 2.0-2b and 2.0-2c (azeotropic mixtures with an entrainer forming one new azeotrope) (Rodriguez-Donis et al. 2010). For all suitable classes, the general criterion under infinite reflux ratio could explain the product to be recovered and the possible existence of limiting values for the entrainer - feed flow rate ratio for batch operation: a minimum value for the class 1.0-1a, a maximum value for the class 1.0-2, etc...

The behavior at finite reflux ratio could be deduced from the infinite behavior and properties of the residue curve maps, and some limits on the reflux ratio were found. However precise finding of the limiting values of reflux ratio or of the entrainer - feed flow rate ratio requires other techniques, like the intersection of composition profiles, either discrete, tray by tray ones (Levy and Doherty, 1986, Julka and Doherty, 1993) or continuous ones from a differential model (Lelkes et al. 1998). Pinch point analysis also allows to find these values, either by using an algebraic criteria (Levy et al. 1986) or with mathematical approaches, like

bifurcation theory (Knapp and Doherty, 2004), interval arithmetics (Frits et al. 2006) or by a combined bifurcation-short cut rectification body method (Brüggemann and Marquardt, 2008).

Then theoretical validation is performed by simulation with a rigorous model including both mass and energy balances.

4.5 FEASIBILITY STUDY METHODOLOGY

Our methodology aims at extending thermodynamic insight for batch extractive distillation to continuous. The main difference lies in the existence of a stripping section for the continuous column configuration, compared to the batch column configuration (see Figure 4.1), whereas the key parameters remain the reboil ratio S and the solvent to feed flow-rate ratio F_E/F for continuous operation mode or F_E/V , where V is the vapor flow-rate going up from the boiler, for the batch process.

4.5.1 Thermodynamic feasibility criterion for 1.0-1a and 1.0-2 ternary diagram classes.

Rodriguez-Donis et al. (2012a) reformulated for light entrainers the general criterion for extractive distillation enounced by Rodriguez-Donis et al., 2009a: *Component A or B can be drawn as first bottom product using a stripper configuration if there is a residue curve going from the entrainer E towards A or B and following an increasing temperature in the region in which A or B is the least volatile component of the ternary mixture*, Figure 4.2 and Figure 4.3 summarize the topological features (singular points, univolatility lines $\alpha_{AB}=1$ and volatility order regions) and the products achievable for the class 1.0-1a (maximum boiling azeotrope with a light entrainer) and 1.0-2 (minimum boiling azeotrope with a light entrainer) diagrams.

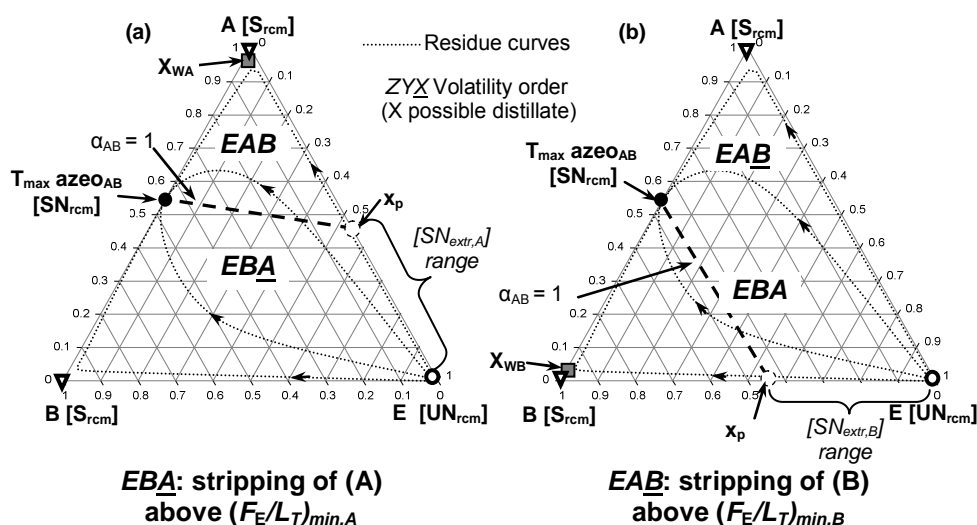


Figure 4.2. Thermodynamic features of 1.0-1a mixtures with respect to batch extractive distillation. Separation of a maximum boiling azeotrope with a light entrainer.

For class 1.0-1a (Figure 4.2) the entrainer is the residue curve unstable node UN_{rcm} (open circle), apex A and B are residue curve saddle point S_{rcm} (open triangle down) while maximum boiling azeotrope is stable node SN_{rcm} (filled circle). By using azeotropic distillation It is impossible to recover A or B but a maxT azeotrope at the column bottom in a batch stripper or in the continuous column bottom since A and B are both saddle points. By using extractive distillation, either A or B can removed as product thanks to the univolatility line $\alpha_{AB}=1$ that starts from the maximum boiling azeotrope and intersects one triangle side at x_p . The univolatility line divides the composition graph into two volatility order regions. The x_p location decides which possible product A or B can be recovered from bottom: A when x_p lies on the A-E side (Figure 4.2a), B when x_p lies on the B-E side (Figure 4.2b) because the general criterion is fulfilled: A (in Figure 4.2a) (B in Figure 4.2b) is the most volatile in the region $E\bar{B}A$ ($E\bar{A}B$ in Figure 4.2b) where it is connected to E by a residue curve of increasing temperature from E to A (B), equivalent to the stripping section profile under infinite reboil ratio.

The feasibility related to entrainer - feed flow rate ratio by the fact of the extractive profile map, under infinitely reboil ratio and an infinitesimal entrainer - feed flow rate ratio (Figure 4.2), with a stripping configuration, the singular point and stabilities of the extractive profile map are the same with residue curve map in shape and directions, because the ending point of the extractive composition profile SN_{extr} , lies at the residue curve stable node SN_{rcm} , apexes A and B become extractive saddle node S_{extr} while maximum boiling azeotrope become stable node SN_{extr} . As the entrainer - feed flow rate ratio increases, extractive singular points move towards the entrainer vertex, with extractive saddle node moving along the triangle B-E and A-E edge, whereas minT azeo $_{AB}$ SN_{extr} move along the univolatility curve $\alpha_{AB}=1$. Ultimately UN_{extr} and S_{extr} may merge at the sacrifice of the extractive singular point S_{extr} being on the triangle edge (Rodriguez-Donis et al., 2009a, Lang et al., 1999a). As the SN_{extr} must be present near the triangle edge to enable intersection of stripping and extractive section profiles and thus for the process to be feasible, thus a minimum entrainer - feed flow rate ratio $(F_E/F)_{min,A}$ (resp. $(F_E/F)_{min,B}$) is required for the process to be feasible and recover the feasible product A (resp. B) when the $\alpha_{AB}=1$ intersects the A-E (resp. B-E) edge.

The separation of the maximum boiling azeotrope ($x_{azeo,A}=0.4$ @434.2K, 1atm) propanoic acid (414.4K) (A) – DMF (425.2K) (B) using MIBK (389.7K) (E) illustrates Figure 4.2a, as $\alpha_{AB}=1$ intersects the binary side A-E; and the separation of the maximum boiling azeotrope ($x_{azeo,A}=0.35$ @393K) water (373.2K) (A) – ethylenediamine EDA (390.4K) (B) using acetone (E) (329.3K) illustrates Figure 4.2b as $\alpha_{AB}=1$ curve intersects the binary side B-E.

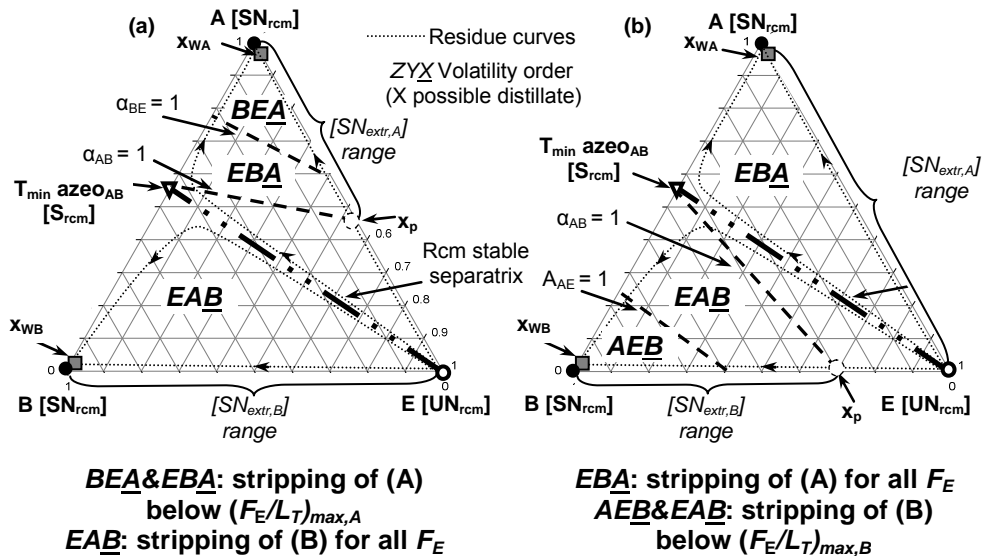


Figure 4.3. Thermodynamic features of 1.0-2 mixtures with respect to batch extractive distillation. Separation of a maximum boiling azeotrope with a light entrainer.

Figure 4.3 summarizes the topological features of the ternary diagrams 1.0-2 with a light entrainer. The entrainer is the residue curve unstable node UN_{rcm} (open circle), apex A and B are stable node SN_{rcm} (filled circle) while minimum boiling azeotrope are residue curve saddle point S_{rcm} (open triangle down).

Even though both apex A and B are $[SN_{rcm}]$ but lie in two different distillation regions. Therefore, unless the distillation boundary is highly curved, they cannot be recovered sequentially in a batch stripper by azeotropic distillation process (Bernot et al., 1990), however, extractive distillation is a worthy alternative process, as the feeding of the entrainer at an intermediate column tray generates extractive profiles able to cross the distillation boundary of the residue curve map.

As the residue curve map is split in two distillation regions by a distillation boundary. The univolatility lines $\alpha_{AB}=1$ that starts from the minimum boiling azeotrope and intersects one triangle side at x_p , which result in two case to consider, both components A and B can be recovered as bottom products as they satisfy the general feasibility criterion: in volatility order region BEA and EBA , A is the least volatile component and connected to entrainer E by a residue curve in the direction of increasing temperature and is a product (denoted in Figure 4.3as \underline{A}). In volatility order region AEB and EAB , the same occurs for B which is the bottom product. Univolatility curves α_{EA} and α_{EB} do not affect the (A) vs. (B) volatility order and therefore the expected product.

Under infinite reboil ratio and an infinitesimal entrainer - feed flow rate ratio (Figure 4.3), similarly, extractive profile map the same shape and directions with residue curve map, as the ending point of the extractive composition profile, SN_{extr} , lies at the residue curve stable node, SN_{rcm} , apexes A and B become

stable node SN_{extr} while minimum boiling azeotrope becomes extractive saddle S_{extr} . There is no limit entrainer - feed flow rate ratio for recovery component B (resp. A) but existing $(F_E/F)_{max,A}$ for component A (resp. $(F_E/F)_{max,B}$ for B) because the extractive unstable node $UN_{extr,B}$ (resp. $UN_{extr,A}$) can be located at any position on the edge B-E (resp. A-E), The same event was observed in the separation of maxT with heavy entrainer and discussed in detail in Rodriguez-Donis et al.(2009b).

Illustration is done for the separation of the minimum boiling azeotrope ethanol A -water B with methanol E, so that $\alpha_{AB} = 1$ curve intersects the binary side A-E (Figure 4.3a); and for the separation of the minimum boiling azeotrope methyl ethyl ketone – benzene B with acetone (329.3K) E, so that $\alpha_{AB} = 1$ curve intersects the binary side B-E.

The separation of the minimum boiling azeotrope ($x_{azeo,A}=0.88$ @351.1K) ethanol (A)(351.5k)- water (373.1K) (B) with methanol(337.6K) (E) illustrates Figure 4.3a, as the $\alpha_{AB} = 1$ curve intersects the binary side A-E; and for the separation of the minimum boiling azeotrope ($x_{azeo,A}=0.50$ @351.2K) methyl ethyl ketone (352.5K) (A) – benzene (353.2K) (B) with acetone (E) illustrates Figure 4.3b, as the $\alpha_{AB} = 1$ curve intersects the binary side B-E.

More details about the topology changes of the extractive section composition profile map with the reboil ratio and the entrainer - feed flow rate ratio in the case of a light entrainer are discussed in Rodriguez-Donis et al. (2012a).

4.5.2 Calculation of reboil ratio vs. entrainer - feed flow rate ratio diagrams.

As recalled in the literature (Knapp and Doherty, 1994; Brüggeman and Marquardt, 2004), extractive distillation processes studies require assessing reflux ratio vs. entrainer - feed flow rate ratio diagrams when using a heavy entrainer. Initial studies of this kind of method in embryo appeared in Knight and Doherty, (1986) by finding of pinch points for each section profiles allowed determining the limiting values of the operating parameters from single feed azeotropic distillation columns to double (Levy and Doherty, 1986), (Wahnschafft and Westerberg, 1993b). later works (Levy et al., 1985, Levy and Doherty, 1986, Julka and Doherty, 1993) relied upon plate by plate calculations, which required setting tray numbers in each section. In chapter 3, we showed that thermodynamic insight validated for batch distillation could help draw these diagrams because the general feasibility criterion used to generate that insight held for the intersection of the extractive and rectifying section of the continuous distillation column. With a light entrainer we shall compute

reboil ratio vs. entrainer - feed flow rate ratio diagrams and expect the general criterion to explain the feasible conditions under which the extractive and the stripping section can intersect.

The methodology of checking the extractive distillation feasibility is then carried out in three steps:

1. Sketch of the reboil ratio vs. entrainer - entrainer - feed flow rate ratio diagram features, from the knowledge of limiting values for the entrainer - feed flow rate ratio in batch mode, namely a value for F_E/L_T transformed into a limiting entrainer - feed flow rate ratio value for continuous mode F_E/F , with the help of the following equation:

$$\left(\frac{F_E}{F}\right) = \left(\frac{F_E}{L_T}\right) \cdot \left(\frac{(S+1) \cdot \frac{W}{F} - q'}{1 + q' \cdot \left(\frac{F_E}{L_T}\right)}\right) \quad (4.1)$$

where we use the notations given in Figure 4.1b for the continuous extractive column. We have considered the general case of partially vaporized feeds F ($q'=1$ for boiling liquid; $q'=0$ for saturated vapour) and F_E ($q=1$ for boiling liquid; $q=0$ for saturated vapour). Below, we use “entrainer - feed flow rate ratio” as a short name for both F_E/L_T and F_E/F .

2. Completion of the reboil vs. entrainer - feed flow rate ratio diagram, by checking the intersection of composition profiles maps computed for all three rectifying, extractive and stripping sections, for a given product purity. The rectifying section is expected to make a distinction between the continuous and the batch modes.
3. Rigorous simulation with a MESH equilibrium distillation column model either with ProSimPlus 3.1 (Prosim SA, 2009) or Aspen 11.1 (Aspentech, 2001) software is run to check the feasibility. For all illustrating mixtures, the thermodynamic model UNIFAC modified Dortmund version 1993 (Gmehling et al., 1993, Weidlich and Gmehling, 1987) is used. Considering the reboil and the entrainer - feed flow rate ratio and composition, those simulations provide the exact distillate and bottom compositions along with the stage compositions and flows of liquid and vapour and temperatures. Additionally, these simulations consider energy balances, which do not play a significant role in feasibility.

In Step 1, we refer to the F_E/L_T ratio since in a batch stripper (Figure 4.1a), the original binary mixture (A+B) is initially charged into the column top vessel and it is fed to the first top tray as boiling liquid (L_T), which is equivalent with L_R in a continuous column. Partial evaporation of the liquid phase reaching the column bottom gives the vapor flow rate ratio (V_S). The remaining liquid is drawn as bottom product (W). The

reboil ratio is V_S/W . As the distillate composition x_w is chosen to compute the composition profiles, we set a distillate recovery yield to allow computing W from mass balance, given values for the main and entrainer feed composition and flow rate ratio.

The investigation of the batch extractive process feasibility rely on a short-cut method to compute the extractive distillation liquid column profiles, deriving from differential Equation(4.2)(Lelkeset al., 1998b) published the extractive and rectifying profiles, together with Equation(4.3), model for predicting the still-path of composition x_S and holdup U .

$$\frac{dx_i}{dh} = x_i - y_i^* \quad (4.2)$$

$$\frac{d(Ux_S)}{dt} = F_Z \cdot x_Z - F_D \cdot X_D \quad (4.3)$$

These two equations are solved as an initial value problem during feasibility study (Varga et al., 2006). Rodriguez-Donis et al. (2007) studied the feasibility of heterogeneous extractive distillation process in a continuous column considering several feed point strategies for the entrainer recycle stream and for the main azeotropic feed, the operating policy composed by a single or both decanted liquid phases is considered as well as the external feeding influence on the composition of the top column liquid stream.

In Equation (4.1), y_i^* and y_i are the equilibrium composition with x_i and the operating composition computed from material balance for a given tray, respectively. Depending on the section, Equations (4.4), (4.5) and (4.6) are labeled with subscript R (rectifying) E (extractive) or S (stripping). The model to calculate the liquid composition profile in each column section based on the following assumptions: (1) theoretical plates, (2) saturated liquid feed of mixture to separated, (3) saturated vapor entrainer feed, (4) constant molar flow rate ratio of liquid and vapor in three respective sections of the column, (5) liquid is incompressible fluid.

In a batch column, we recall the work of Rodriguez-Donis et al., (2011), considering the feed physical state for mixture to be separated as saturated liquid ($q=1$) and entrainer feed as saturated vapor ($q=0$), one obtains:

$$L_s = L_E = L_R + F \quad (4.4)$$

$$V_r = V_E = V_s + F_E \quad (4.5)$$

$$V_r = D \cdot (R + 1) \quad (4.6)$$

To get the expected product in the bottom a composition x_W has been chosen. Bottom flow rate ratio can be get with a give bottom recovery rate, distillate rate and flow rate ratio correspondingly calculated based on mass balances. The relationship between reflux ratio and reboil ratios can be established by the Equations (4.5) and (4.6).

Note that Rodriguez-Donis et al.(2011) have published the extractive liquid Equation(4.7),(4.8),(4.9) and(4.10) in a batch stripping by considering the feed physical state by the variable q ($q=1$ or $q=0$) and defining the reboil ratio S .

For y and V/L with a boiling liquid F_E ($q=1$):

$$y|_{q=1} = \frac{x + \left(\frac{F_E}{L_T}\right) \cdot x_E - \left(\frac{S}{S+1}\right) \cdot \left(1 + \frac{F_E}{L_T}\right) \cdot x_W}{\left(\frac{S}{S+1}\right) \cdot \left(1 + \frac{F_E}{L_T}\right)} \quad (4.7)$$

$$\frac{V}{L}|_{q=1} = \left(\frac{S}{S+1}\right) \cdot \left(1 + \frac{F_E}{L_T}\right) \quad (4.8)$$

For y and V/L with for a saturated vapor F_E ($q=0$):

$$y|_{q=0} = \frac{x + \left(\frac{F_E}{L_T}\right) \cdot x_E - \left(\frac{1}{S+1}\right) \cdot x_W}{\left(\frac{S}{S+1} + \frac{F_E}{L_T}\right)} \quad (4.9)$$

$$\frac{V}{L}|_{q=0} = \left(\frac{S}{S+1} + \frac{F_E}{L_T}\right) \quad (4.10)$$

Under infinite reboil ratio, Equations (4.7), (4.8), (4.9) and (4.10) become identical whatever the feed state is. Therefore, the extractive liquid composition maps are similar and the process limiting entrainer - feed flow rate ratio is identical considering the entrainer as saturated liquid or vapor. The stripping composition profiles are computed by setting $F_E=0$. Under infinite reboil ratio S , they become equivalent to the residue curve Equation 4.2.

Considering the liquid profile of the extractive section starts at the composition of the top vessel (x_{Top}) and ends at an unstable extractive node UN_{extr} . The stripping profile then, makes connection between UN_{extr} and the liquid composition in the boiler x_W . A set of operating conditions that provide a continuous liquid profile in the column from x_{Top} to x_W is considered as a feasible extractive batch distillation process. Under

feasible conditions, the composition profile $\{x_{Top}-x_W\}$ for the stripping column configuration (Figure 4.1a) combines an extractive section composition profile $\{x_{Top}-[UN_{extr}]\}$, $[UN_{extr}]$ located at the entrainer feeding plate, and a stripping section composition profile $\{[UN_{extr}]-x_W\}$, assimilated to a residue curve at S_∞ .

For step 2, the liquid composition profile in each column section is computed by using the general differential model of Lelkes et al (Lelkes et al., 1998). With constant molar overflow assumptions, once a composition of the bottom product x_W has been chosen.

$$\frac{dx_i}{dh} = \frac{V}{L}(y_i - y_i^*) \quad (4.11)$$

Assuming constant molar overflow, we can write for the vapour internal flow rate ratio:

$$V_S = S \cdot W \quad (4.12)$$

$$V_E = V_S + (1-q) \cdot F_E = S \cdot W + (1-q) \cdot F_E \quad (4.13)$$

$$\begin{aligned} V_R &= V_E + (1-q') \cdot F \\ &= S \cdot W + (1-q) \cdot F_E + (1-q') \cdot F = L_T + D \end{aligned} \quad (4.14)$$

and for the internal liquid flow rate ratio:

$$L_R = L_T \quad (4.15)$$

$$L_E = L_R + q' \cdot F = L_T + q' \cdot F \quad (4.16)$$

$$L_S = V_S + W = (S+1) \cdot W = L_E + q \cdot F_E = L_T + q' \cdot F + q \cdot F_E \quad (4.17)$$

Then, the expressions for y are obtained from partial mass balances in each section.

The general expressions for y and V/L in the rectifying section are

$$y = \frac{1}{S + (1-q)\frac{F_E}{W} + (1-q')\frac{F}{W}} \left(\frac{F_E}{W} x_E + \left(S - q' \frac{F}{W} - q \frac{F_E}{W} + 1 \right) x_i + \frac{F}{W} x_F - x_W \right) \quad (4.18)$$

$$\frac{V_R}{L_R} = \frac{S \cdot W + (1-q) \cdot F_E + (1-q') \cdot F}{(S+1) \cdot W - q \cdot F_E - q' \cdot F} \quad (4.19)$$

To get the equations relevant to the extractive section, one should set $F=0$ in Equations 4.18 and 4.19.

To get the relevant equation for the stripping section, one should set $F_E=0$ and $F=0$ in Equation 4.18 and 4.19.

For the continuous column, supposing a boiling liquid main feed F , the rectifying profile becomes for $q=0$ (saturated vapor entrainer):

$$\frac{dx_i}{dh} = \frac{S + \frac{F_E}{W}}{(S+1) - \frac{F}{W}} \cdot \left[\frac{1}{S + \frac{F_E}{W}} \left(\frac{F_E}{W} \cdot x_E + \left(S - \frac{F}{W} + 1 \right) x_i + \frac{F}{W} \cdot x_F - x_W \right) - y_i^* \right] \quad (4.20)$$

For $q=1$ (boiling liquid entrainer)

$$\frac{dx_i}{dh} = \frac{S}{(S+1) - \frac{F_E}{W} - \frac{F}{W}} \cdot \left[\frac{1}{S} \left(\frac{F_E}{W} x_E + \left(S - \frac{F}{W} - \frac{F_E}{W} + 1 \right) x_i + \frac{F}{W} x_F - x_W \right) - y_i^* \right] \quad (4.21)$$

and the extractive profile:

For $q=0$ (saturated vapor entrainer)

$$\frac{dx_i}{dh} = \frac{S + \frac{F_E}{W}}{S+1} * \left[\frac{1}{S + \frac{F_E}{W}} \left[(1+S) \cdot x_i + \left(\frac{F_E}{W} \right) \cdot x_E - x_W \right] - y_i^* \right] \quad (4.22)$$

For $q=1$ (boiling liquid entrainer)

$$\frac{dx_i}{dh} = \frac{S}{(S+1) - \frac{F_E}{W}} * \left[\frac{1}{S} \left(\frac{F_E}{W} \cdot x_E + \left(1 + S - \frac{F_E}{W} \right) x_i - x_W \right) - y_i^* \right] \quad (4.23)$$

Finally, for the stripping profile:

$$\frac{dx_i}{dh} = \frac{S}{S+1} \cdot \left[\left(1 + \frac{1}{S} \right) \cdot x_i - \frac{1}{S} \cdot x_w - y_i^* \right] \quad (4.24)$$

Under infinite reboil ratio, the equations are identical whatever the entrainer feed state q value is as was recalled by Rodriguez-Donis et al. (2012): “the extractive liquid composition maps are similar and the process limiting entrainer - feed flow rate ratio under infinite reboil ratio is identical considering the entrainer as a saturated liquid or vapor”. This will hold for the assessment of the limiting flow rate ratio values in step 1. For step 2, small differences may arise but we choose to feed the entrainer as a saturated vapor ($q=0$). Then, as the entrainer is fed below the main feed (Figure 4.1b), all the entrainer readily goes up into the extractive section. Consequently, we use Equations 4.20, 4.22 and 4.24 to compute the section composition profiles. Table 4.1 displays some data of the flow rate ratio and composition for the mixtures used as illustration.

Table 4.1. operating parameters for all case study involving possible products.

Case study		A	B	E		
Class1.0-1a case (a): A(propanoic acid) – B(DMF)+ E(MIBK)						
<i>product.</i> A (propanoic acid)	Feed x_F	0.9	0.1	0	Distillate flow rate ratio,D	1.1
	Entrainer x_E	0	0	1	Bottom flow rate ratio,W	0.9
	Bottom, x_w	0.98	0.01	0.01	Feed flow rate ratio,F	1
	Distillate x_D	0.0164	0.0827	0.9009	Entrainer - feed flow rate ratio, F_E/F	1
	Product recovery, η_b	0.98	0	0	Reboil up ratio,S	10
	Global feed $x_F + x_E$	0.45	0.05	0.5	Reflux ratio, R	8.09
Class1.0-1a case (b): A (water) - B (EDA) + E (acetone)						
<i>product.</i> B (EDA)	x_F	0.1	0.9	0	D	10.02
	x_E	0	0	1	W	0.98
	x_w	0.01	0.98	0.01	F	1
	x_D	0.002	0.98	0.018	F_E/F	10
	η_b	0	0.98	0	S	15
	$x_F + x_E$	0.082	0.98	0.9090	R	1.47
Class1.0-2 case (a): A (ethanol) – B (water) + E (methanol)						
<i>product.</i> A (ethanol)	x_F	0.9	0.1	0	D	10.1
	x_E	0	0	1	W	0.9
	x_w	0.99	0.005	0.005	F	1
	x_D	0.0018	0.0094	0.9888	F_E/F	10
	η_b	0.98	0	0	S	10
	$x_F + x_E$	0.0818	0.0091	0.9091	R	0.88
<i>product.</i> B (water)	x_F	0.1	0.9	0	D	10.1
	x_E	0	0	1	W	0.9
	x_w	0.005	0.99	0.005	F	1
	x_D	0.0094	0.0018	0.9888	F_E/F	10
	η_b	0	0.98	0	S	10
	$x_F + x_E$	0.0091	0.0818	0.9091	R	0.88
Class1.0-2 case (b): A (MEK) – B (benzene) + E (acetone)						
<i>product.</i> A(MEK)	x_F	0.9	0.1	0	D	5.1
	x_E	0	0	1	W	0.9
	x_w	0.98	0.01	0.01	F	1
	x_D	0.0035	0.0179	0.9786	F_E/F	5
	η_b	0.98	0	0	S	5
	$x_F + x_E$	0.15	0.0167	0.8333	R	0.86
<i>product.</i> B(benzene)	x_F	0.1	0.9	0	D	5.1
	x_E	0	0	1	W	0.9
	x_w	0.01	0.98	0.01	F	1
	x_D	0.0179	0.0035	0.9786	F_E/F	5
	η_b	0	0.98	0	S	5
	$x_F + x_E$	0.0167	0.15	0.8333	R	0.86

Table 4.2 displays the extractive distillation column features used in step 3. Rigorous simulation with a MESH equilibrium distillation column model either with ProSim Plus 3.1 (Prosim SA, 2009) or Aspen 11.1

(Aspentech, 2001) software is run to check the feasibility. Optimisation of the separation is not performed, in particular with respect to reboil ratio, energy demand, entrainer feed flow rate ratio or the number of trays in each section as such an optimisation is out of our scope and should be done for a column sequence with both the extractive distillation and the entrainer regeneration column. The number of trays in the extractive section is set at a proper value so that the terminal point of the extractive section composition profile reaches near to the extractive section stable node.

Table 4.2. Column operating specifications for rigorous simulation

Specifications	Class1.0.1-a	Class1.0.2
Tray number, N	40	50
Entrainer tray, N_{FE}	15	30
Feed tray, N_F	5	15
x_F , mole fraction (A,B,E)	{0.9; 0.1; 0.0}	{0.1; 0.9; 0.0}
x_E , mole fraction (A,B,E)	{0.0; 0.0; 1.0}	{0.0; 0.0; 1.0}

Results are displayed in terms of entrainer entrainer - feed flow rate ratio vs. reboil ratio S (diagrams F_E/F vs. S) in continuous mode and F_E/V vs. S in batch mode.

4.6 RESULTS

4.6.1 Separation of Maximum Boiling Temperature Azeotropes with light Entrainers (Class 1.0-1a).

4.6.1.1 Case (a): $\alpha_{AB}=1$ Curve Reaching the Binary Side A-E.

The separation of the maximum boiling azeotrope propanoic acid (414.4K) (A) – DMF (425.2K) (B) ($x_{azeo,A}=0.4$ @434.2K, 1atm) using MIBK (389.7K) as a light entrainer (E) is taken from Rodriguez-Donis et al (2012a). Propanoic acid is used as a food preservative, intermediate in the production polymers, pesticides and pharmaceuticals. The ternary diagram belongs to the class 1.0-1a and is the antipodal of the 1.0-1a diagram (Kiva et al., 2003) referring to the separation of a minimum-boiling azeotrope using a heavy entrainer, described in Chapter3.

The univolatility line $\alpha_{AB}=1$ ends at the A - E sides at about 90mol% MIBK, defining two different volatility regions. From the feasibility criterion enounced above for batch extractive distillation, feasible region EBA lies below the univolatility line, propanoic acid (A) can be recovered as bottom product above a minimum entrainer - feed flow rate ratio so that $SN_{ext,A}$ lies near the A-E edge where it can intersect a stripping profile which can reach $x_{W,A}$. whereas no $SN_{ext,B}$ appear makes to recover B unfeasible. The point

where univolatility line intercept the benzene-acetone edge is near to a MIBK corner, as show in Figure 4.4, this location point is at $x_E=0.9$ (90% MIBK). There is a minimum entrainer flow rate ratio which correspond to $SN_{ext,A}$, below it the stable extractive node $SN_{ext,A}$ is located on the univolatility line, thus the extractive profile cannot reach a stripping profile that reaches the expected product A.

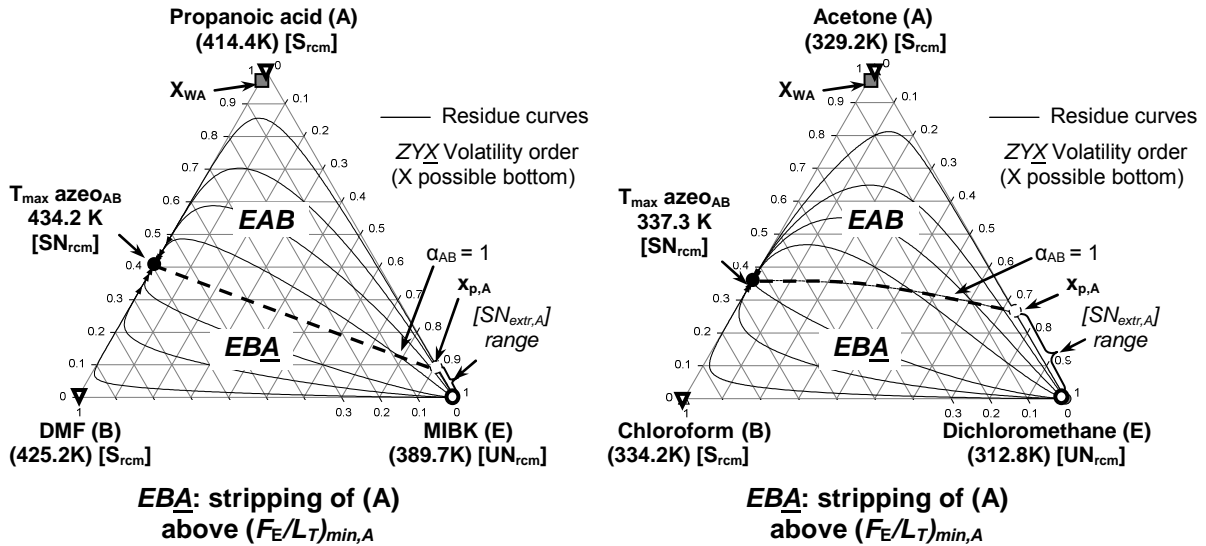


Figure 4.4. Propanoic acid – DMF maximum boiling azeotrope separation using light entrainer MIBK and (b) acetone – chloroform using dichloromethane. 1.0-1a class residue curve map and extractive distillation

When considering a continuous column, the feasibility requires that the extractive and the rectifying profiles intersect as well. Checking the intersection of all three column section profiles computed with equations Equations 4.20, 4.22 and 4.24, the F_E/F vs. S reboil ratio diagram displays in Figure 4.5 the feasible operating condition range to obtain a bottom product with a 98% purity. The results are summarized in following graph. Feasible regions (shaded) are sketched by drawing these series of points (filled triangle up represents a feasible point; open circle represents an unfeasible point).

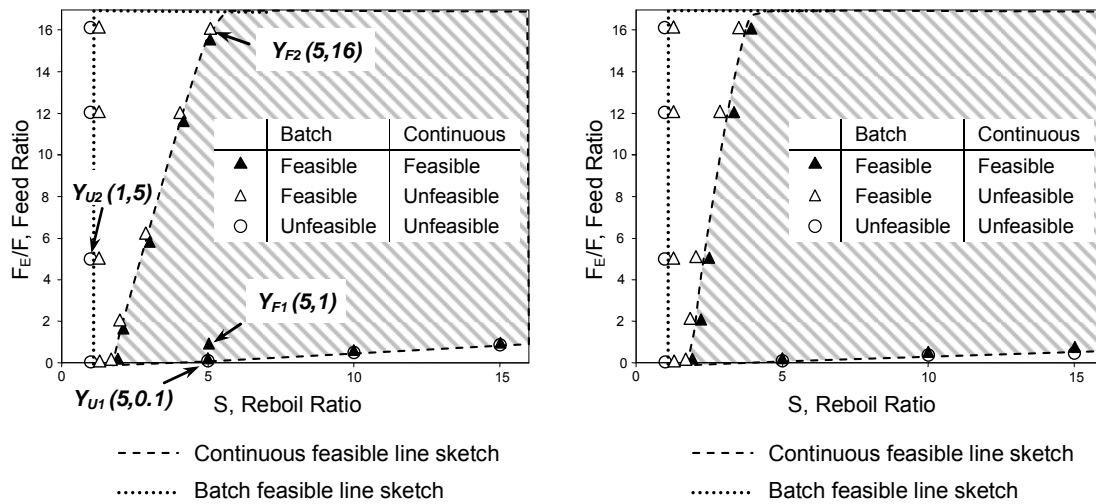


Figure 4.5. Entrainer – feed flow rate ratio F_E/F as a function of the reboil ratio S . (a) Propanoic acid – MIBK using DMF Separation to recover propanoic acid and (b) Acetone – chloroform separation using dichloromethane to recover acetone

Table 4.3 gives the data corresponding to Figure 4.5.

Table 4.3 Operating parameters corresponding to Figure 4.5.

Class 1.0-1a case A-E side with light entrainer to recover A							Feasibility	
Specification	A	B	E	Reboil ratio	Reflux ratio	FE/F	Batch	Continuous
Name	Propanoic acid	DMF	MIBK	15	12.18	1	yes	yes
Boiling T(K)	414.4	425.2	389.7	15	0.33	40	yes	yes
X_F	0.9	0.1	0	15	13.4	0.9	no	no
X_E	0	0	1	15	0.32	41	yes	no
X_W	0.98	0.01	0.01	10	12.71	0.6	yes	yes
F	1			10	1.75	5	yes	yes
W	0.9			10	0.32	28	yes	yes
η	0.98			10	14.83	0.5	no	no
				10	0.3	30	yes	no
				5	11	0.3	yes	yes
				5	0.29	15	yes	yes
				5	14.67	0.2	no	no
				5	0.27	16	yes	no
				2	1.55	1	yes	yes
				2	0.81	2	no	no
				1	0.16	5	no	no
				1	7.27	0.01	no	no
				0.5	0.32	1	no	no
				0.5	0.07	5	no	no

Figure 4.5 concerns a propanoic acid (A) distillate from ternary system propanoic acid –DMF separation with entrainer MIBK, minimum entrainer - feed flow rate ratio occurs along with reboil ratio changes, the minimum entrainer - feed flow rate ratio occurs at a higher value as reboil ratio increases, the minimum entrainer - feed flow rate ratio value can also be explained by the using polarity argument (Robinson and Gilliland, 1950): “the general rule is if the added entrainer is more polar than the components of original mixture, it will increase the relative volatility of the less polar component relative to

the more polar, and if the added entrainer is less polar, the reverse will be true”, because of nature difference in vapor pressure between the azeotropic constituents, an entrainer which enhance the natural volatility difference (increase γ_1 relative to γ_2) is favored over one which increase γ_2 relative to γ_1 . In this latter case, adding small quantities of entrainer actually makes the separation more difficult, and quantities large enough must be used to reverse the volatility order, this makes different entrainers may have different minimum value of entrainer - feed flow rate ratio and limitation value slope.

The graph exhibits minimum reboil ratio value, below which the desired separation is impossible no matter how big the amount entrainer feed given, like reflux ratio situation, for any specified bottom composition, the location and orientation of the stripping profile is determined by reboil ratio, as the reboil ratio increased, the rectifying profile moves away from the bottom composition and increases in size, as well. As (Rodriguez-Donis et al., 2009b) expatiated, “under finite reflux ratio, an extractive unstable separatrix formed by node of UN_{extr} and $S_{B,extr}$ moves inside the diagram, an unfeasible composition region happens as all extractive composition profile on the left of this separatrix cannot reach the right side to get the $SN_{A,extr}$, and still pass cannot go through it to reach expected distillate near A, either. This extractive unstable separatrix sets a boundary prevent the still pass go through it”, A detailed calculation of the profile map when reboil ratio gets smaller also shows that the feasible stripping section profiles region gets smaller until it can no longer intersect the extractive profile region. This is shown in Figure 4.6. Figure 4.6a displays three stripping profiles computed for $x_{WA} = \{. . 0.01; .\}$ and changing the expected purity in component A from 0.98 to 0.7. Figure 4.6b shows the evolution of the stripping profile computed from x_{WA} with a purity of 98% in A, while changing the other component concentration under various reboil ratios.

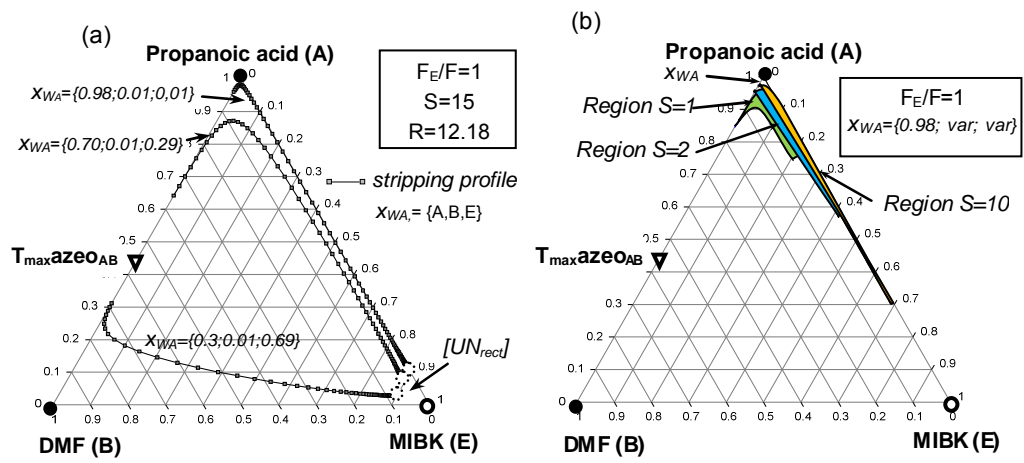


Figure 4.6. The influence of the reboil ratio on stripping section composition profiles.

In *Figure 4.6a*, the shape of the stripping profiles follows that of the residue curves typical for a 1.0-1a mixture (*Figure 4.4*). For A purity of 98 mole% or 70 mole%, the profiles go near the AE edge. For A purity of 30 mole%, it goes to the BE edge.

Under entrainer - feed flow rate ratio $F_E/F=1$, the shaded region in *Figure 4.6b* show that the stripping profile gets smaller in length as the reboil ratio decreases from 10 to 1. This will affect the feasibility as a smaller stripping profile may not intersect an extractive profile.

The same holds for the continuous mode because of a minimum F_E/V and reboil ratio in batch translates well into a minimum F_E/V and reboil ratio in continuous. The main difference lies in additional maximum entrainer - feed flow rate ratio occurs resulting from a too short rectifying section profile, but the influence of the rectifying in lower maximum value as reboil ratio diminishes as the stripping section becomes to control the unfeasibility. When concerns a DMF (B) as distillate, the result shows process exhibiting unfeasible feature for any given reboil ratio or entrainer - feed flow rate ratio.

In conclusion, firstly, the minimum entrainer - feed flow rate ratio value gets smaller along with the reboil ratio. In other word, switching the X-axis reboil ratio with Y-axis entrainer - feed flow rate ratio, we can state that the desired product specification can be maintained over a wider range of reboil ratio as the entrainer - feed flow rate ratio increases. Secondly, a maximum entrainer–entrainer - feed flow rate ratio exists and gradually reduces as the reboil ratio gets smaller, until it reaches a minimum value.

Figure 4.7a-d demonstrate that the three section profile behaviors along with the transition between feasible and unfeasible regions in *Figure 4.5b*. The minimum entrainer - feed flow rate ratio is the same for both the batch and the continuous processes, as it comes from the shared intersection condition between the stripping and the extractive profile. *Figure 4.7a* and *Figure 4.7b* illustrate that: for point Y_{F1} , all three profiles intersect, whereas for point Y_{U1} below the minimum entrainer - feed flow rate ratio, the stripping section composition profile cannot intersect with the extractive profile, leading to an unfeasible process for both the batch and continuous processes. *Figure 4.7c* (point Y_{F2}) illustrates the case when the batch process is feasible whereas the continuous process is not (open triangle) because the rectifying profile does not intersect the extractive profile. At very low reboil ratio, none of the process is feasible as illustrated in *Figure 4.7d*: then the stripping profile is too short. Similar results were obtained in batch distillation (Varga, 2006). The value of S at this point can be regarded as the minimum reboil ratio, with which the minimum amount of vapors returned to the column. Thus, this point also corresponds to the minimum reboiler heat duty and

condenser cooling capacity required for the separation. More detailed information of data can be seen in Table 4.4.

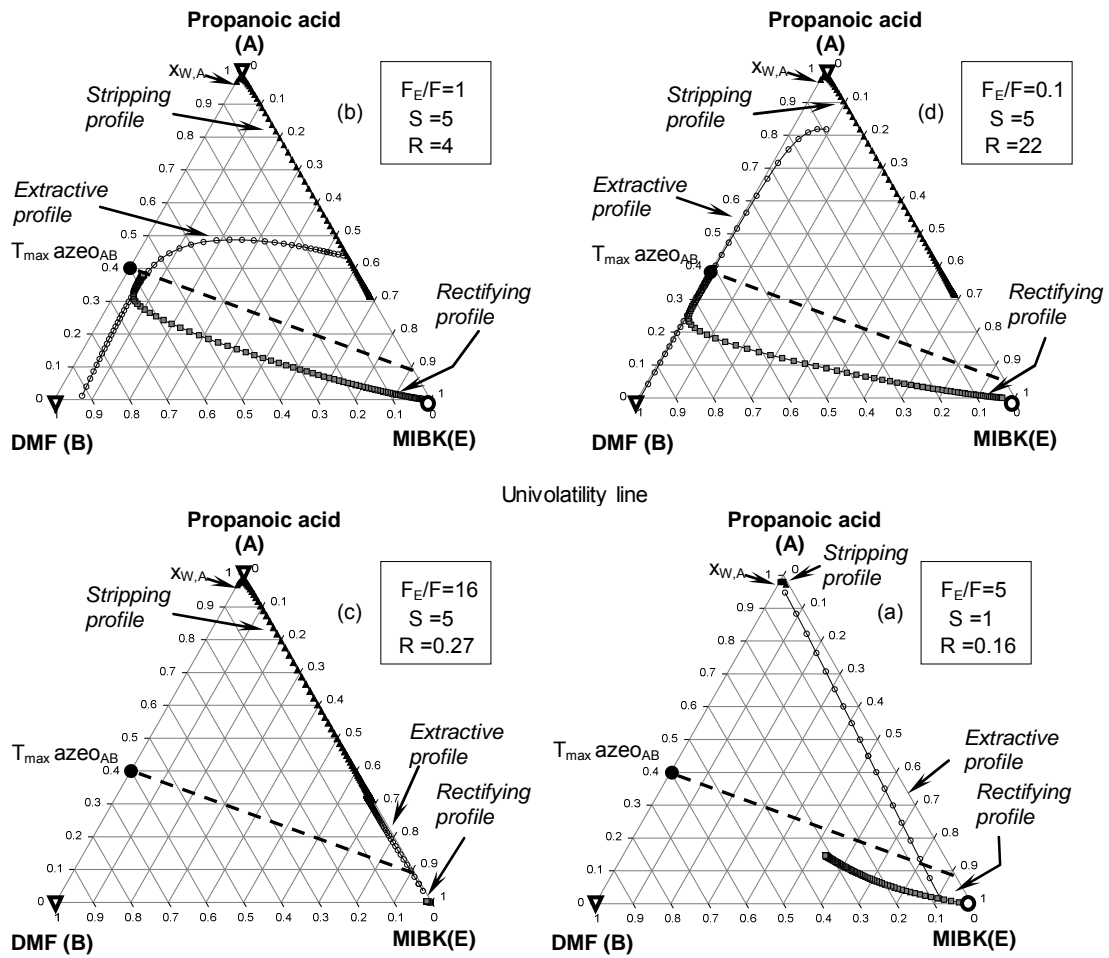


Figure 4.7. Operating parameter scene explanation. Points taken from Figure 4.5: (b) point Y_{F1} , (a) point Y_{U1} , (c) point Y_{F2} and (d) point Y_{U2} .

Table 4.4 Operating parameters corresponding to Figure 4.7.

Class 1.0-1a case A-E side with light entrainer to recover A							
Specification parameters for Figure 4.7(a)				Specification parameters for Figure 4.7(b)			
Apex	A	B	E	Apex	A	B	E
Name	Propanoic acid	DMF	MIBK	Name	Propanoic acid	DMF	MIBK
Boiling T(K)	414.4	425.2	389.7	Boiling T(K)	414.4	425.2	389.7
X_F	0.9	0.1	0	X_F	0.9	0.1	0
X_E	0	0	1	X_E	0	0	1
X_W	0.98	0.01	0.01	X_W	0.98	0.01	0.01
X_D	0.003529412	0.017843137	0.978627451	X_D	0.016363636	0.082727273	0.900909091
Reboil S	1			Reboil S	5		
F_E/F	5			F_E/F	1		
F	1			F	1		
W	0.9			W	0.9		
E	5			E	1		
D	5.1			D	1.1		
V	5.9			V	5.5		
η_B	0.98			η_B	0.98		
R	0.16			R	4		
Specification parameters for Figure 4.7(c)				Specification parameters for Figure 4.7(d)			
Apex	A	B	E	Apex	A	B	E
Name	Propanoic acid	DMF	MIBK	Name	Propanoic acid	DMF	MIBK
Boiling T(K)	414.4	425.2	389.7	Boiling T(K)	414.4	425.2	389.7
X_F	0.9	0.1	0	X_F	0.9	0.1	0
X_E	0	0	1	X_E	0	0	1
X_W	0.98	0.01	0.01	X_W	0.98	0.01	0.01
X_D	0.001118012	0.005652174	0.993229814	X_D	0.09	0.455	0.455
Reboil S	5			Reboil S	5		
F_E/F	16			F_E/F	0.1		
F	1			F	1		
W	0.9			W	0.9		
E	16			E	0.1		
D	16.1			D	0.2		
V	20.5			V	4.6		
η_B	0.98			η_B	0.98		
R	0.27			R	22		

A closer look at the profile map topology shows that under finite reboil ratio, the stripping profile gets smaller (Figure 4.7d). Besides, the feasible extractive profile region shrinks because of an extractive profile separatrix that moves inside the triangle and reduces the size of the feasible region. This combination prevents the profiles to intersect each other and the process is unfeasible.

In step 3, in order to verify step 2 predictions, rigorous simulation is performed for the acetone – chloroform – dichloromethane mixture with parameter values reported in Table 4.1 and Table 4.2, but for $S=20$ and $F_E/F=20$. The rigorous composition profile is shown in Figure 4.8 along with the simplified stripping, extractive and rectifying profile maps from equations 4.20, 4.22 and 4.24. We feed the feed mixture as a boiling liquid state and the entrainer as a saturated vapor.

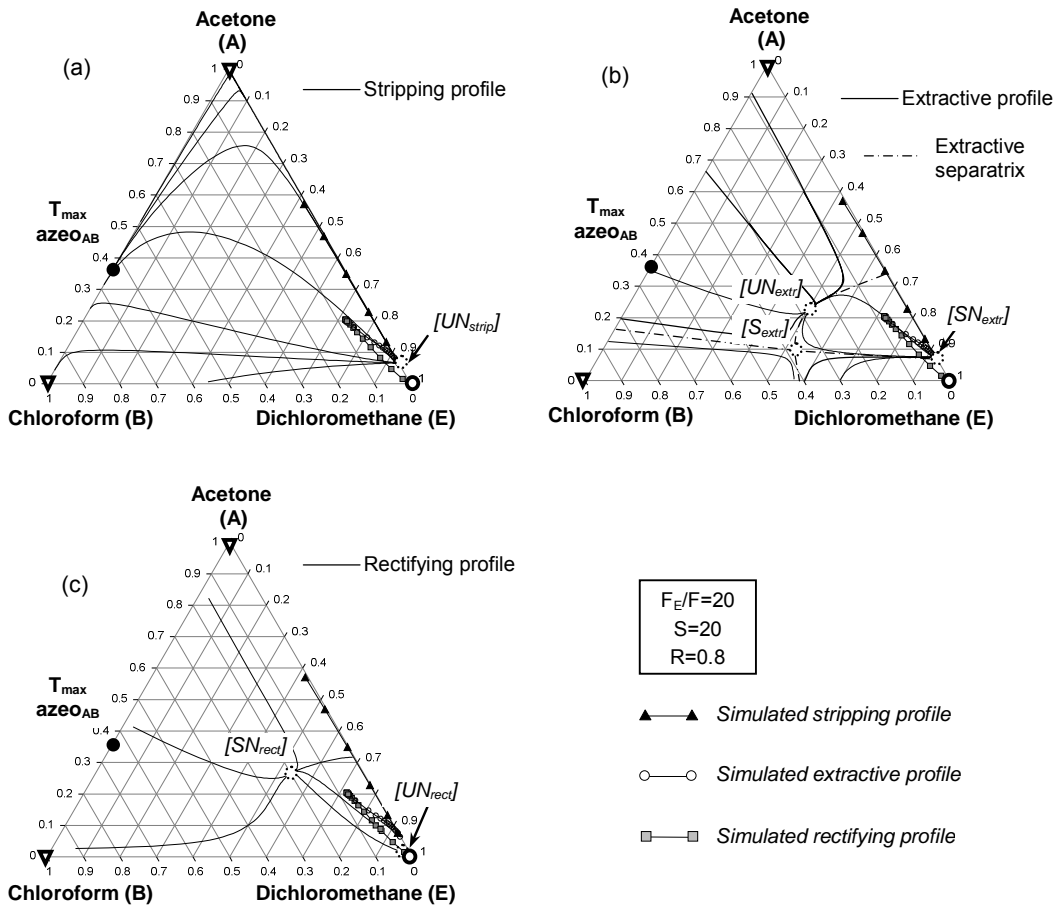


Figure 4.8. Rigorous simulation result to recover A (acetone) at $F_E/F=20$, $S=20$, compared with calculated profiles: (a) rectifying section, (b) extractive section and (c) stripping section.

Table 4.5 Operating parameters corresponding to Figure 4.8a, b, c.

Class 1.0-1a case A-E side with light entrainer($F_E/F=1$, $S=15$) to recover A									
Worksheet parameters				Rectifying section			Stripping section		
Specification	A	B	E	A	B	E	A	B	E
Name	Propanoic acid	DMF	MIBK	Propanoic acid	DMF	MIBK	Propanoic acid	DMF	MIBK
Boiling T(°C)	414.4	425.2	389.7	0.11762895	1.81E-05	0.88235294	0.93391962	0.007579	0.05850137
X_F	0.9	0.1	0	0.2091853	5.64E-05	0.79075829	0.96156179	0.00753565	0.03090256
X_E	0	0	1	0.34668243	0.00023459	0.65308297	0.97635947	0.0075126	0.01612792
X_W	0.98	0.01	0.01	0.51458544	0.00130371	0.48411084	0.98413069	0.0075005	0.0083688
X_D	0.016363636	0.082727273	0.900909091	0.6698993	0.00868987	0.32141083	0.98817372	0.00749412	0.00433214
Reboil S	15			Extractive section			0.99026818	0.00749074	0.00224108
F_E/F	1			A	B	E	0.99135147	0.00748889	0.00115962
F	1			Propanoic acid	DMF	MIBK	0.99191169	0.00748784	0.00060046
W	1.1			0.6698993	0.00868987	0.32141083	0.99220158	0.0074872	0.00031121
E	1			0.76992091	0.00849532	0.22158377	0.99235175	0.00748676	0.00016147
D	0.9			0.83813996	0.00836969	0.15349034	0.99242968	0.00748644	8.39E-05
V	14.5			0.88019169	0.00829477	0.11151354	0.99247021	0.00748617	4.36E-05
η_B	0.98			0.90457503	0.00825228	0.08717268	0.99249136	0.00748593	2.27E-05
R	12.18			0.91821368	0.00822885	0.07355746	0.99250246	0.0074857	1.18E-05
				0.92567387	0.00821604	0.06611009	0.99250835	0.00748547	6.18E-06
				0.92968607	0.00820823	0.0621057	0.99251152	0.00748525	3.23E-06
Rigorous parameters									
X_F	0.9	0.1	0	0.9318091	0.00819699	0.05999391	0.99251328	0.00748503	1.69E-06
X_E	0	0	1	0.93294495	0.00813665	0.0589184	0.9925143	0.00748481	8.84E-07
X_D	0.98	0.01	0.01	0.93391962	0.007579	0.05850137	0.99251493	0.00748461	4.63E-07
Num stages	40						0.99251516	0.00748459	2.43E-07
Solvent tray	15						0.99251335	0.00748652	1.28E-07
Feed tray	5						0.99249212	0.00750781	6.70E-08
							0.99227797	0.00772199	3.51E-08
							0.99017745	0.00982253	1.83E-08

Rigorous calculation was performed for a 40 tray tower(including the reboiler) to distil a saturated liquid stream mixture containing 90 mol% of propanoic acid and 10 mol% of DMF fed on tray 5 and the pure saturated vapour entrainer MIBK fed on tray 15. The simulation is based on thermodynamic model UNIFAC modified Dortmund version 1993(Gmehling et al., 1993, Weidlich and Gmehling, 1987), and follows the assumption of no significant pressure gradients in the adiabatic column and constant molar flow of vapor-liquid.

In state variables settings, set the operate saturated liquid temperature 423K for feed mixture and saturated vapor temperature 389.3K for entrainer at 1 atm, The specification for this column is somewhat unusual, as reboil ratio and reboil rate are fixed instead of the common tray used reflux ratio and distillate rate. The extractive column has two design degrees of freedom left once the total number of stages and feed plate location are fixed: reboil ratio and entrainer - feed flow rate ratio. The reboil rate is given by mass balance calculation 395kmol/h when the feed flow rate ratio is set for 400kmol/h.

The extractive distillation column enables to obtain propanoic acid, a saddle point of the residue curve map (Figure 4.4), as the bottom product and a binary mixture DMF-MIBK from the top. The top composition can then be further processed in a regeneration column to obtain high purity DMF and regenerate the

entrainer MIBK. The results of the simulation composition are compared to the approximate section composition profiles in Figure 4.8. The process under conditions of reboil ratio ($S=15$) and entrainer - entrainer - feed flow rate ratio ($F_E/F=1$) is feasible, because starting from the charge of given composition (x_F) under the given operation conditions the specified distilled composition x_W can be obtained satisfying the necessary and sufficient condition of the feasibility to have at least one possible column profile connecting still path with the point x_W .

The results show singular points which are different from those of the residue curve map (under infinite condition) in Figure 4.4, as under finite reboil ratio, the singular points move inside the triangle and generate a new shape, in fact, the singular points for each column match each other by rigorous with Aspen and method in this article, they have a close agreement on profile shape and the location of singular point for three column sections. Supplementary data are available in Table 4.5.

4.6.1.2 Case (b): $\alpha_{AB}=1$ Curve Reaching the Binary Side B-E.

For the separation of the maximum boiling azeotrope water (373.2K)(A) – ethylene diamine EDA (390.4K) (B) ($x_{azeo,A}=0.35$ @393K) with acetone (329.3K) as light entrainer (E), the ternary diagram belongs to the 1.0-1a class but now the univolatility curve $\alpha_{AB}=1$ intersects the binary side B-E near 70mol% of acetone (Figure 4.9).

Ethylenediamine is widely used in large quantities in the chemical industry, as chelating agent and precursor to other ligands, a precursor to pharmaceuticals, agrochemicals, and various polymers, a corrosion inhibitor in paints and coolants, a common organic additive, and chemical for color photography developing. By using the example of the separation of water–ethylenediamine with a heterogeneous entrainer light benzene (353.2K), Lang and Modla (2006) made an exposition of generalized method for calculation of residue curves and determination of heterogeneous batch distillation regions, takes into consideration the possibility of the withdrawal of any fraction of either liquid phase from the decanter as distillate, and the simplified and rigorous simulation calculations were carried out for this system. Rodriguez-Donis et al. (2011) published thermodynamic insights on the feasibility of homogeneous batch extractive distillation for water-ethylenediamine separation with methanol (337.6K).

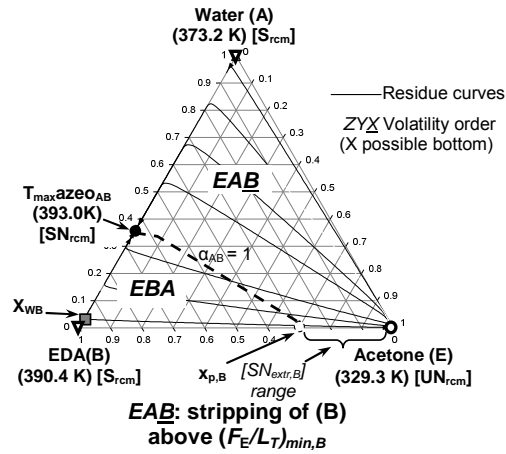


Figure 4.9. Water– ethylene diamine maximum boiling azeotrope separation using light entrainer acetone: 1.0-1a class residue curve map and extractive distillation process insights

The case when the univolatility line $\alpha_{AB} = 1$ reaches the binary side B-E to recover B (EDA) as bottom product is symmetric to the previous one when $\alpha_{AB} = 1$ reaches the binary side A-E to recover A. This feature has been verified with detail by varying the entrainer - feed flow rate ratio and the reflux ratio in the first part of this series of articles.

Univolatility line $\alpha_{AB} = 1$ ends at the binary EDA (390.4K) B - acetone (329.3K) E side at about 70mol% acetone give birth to a $SN_{ext,B}$. Following our methodology, the batch process analysis (step 1) states that B is recovered above a minimal value for the entrainer - feed flow rate ratio F_E/L_T so that the extractive section stable nodes $SN_{ext,B}$ lies near the B-E edge. Then the extractive profile can reach $SN_{ext,B}$ and cross a stripping profile reaching near the apex B (EDA).

By computing approximate composition profiles in each column section (step2), the F_E/F vs. S reboil ratio diagram displays in Figure 4.9 the feasible operating condition range (triangle symbols) to obtain a residue with a 98 mol% purity.

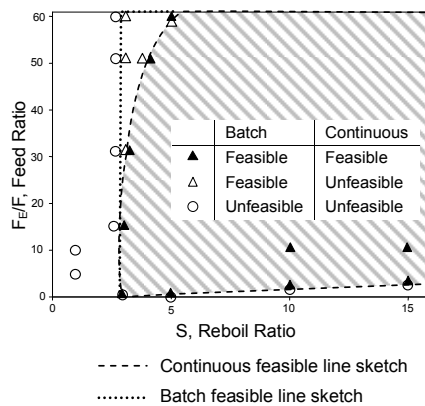


Figure 4.10. Entrainer - entrainer - feed flow rate ratio F_E/F as a function of the reboil ratio S. Water – EDA – acetone separation to recover 98 mol% EDA as bottom product.

Table 4.6 Operating parameters corresponding to Figure 4.10.

Specification	Class 1.0-1a case B-E side with light entrainer to recover B						Feasibility	
	A	B	E	Reboil ratio	F_E/F	Reflux ratio	Batch	Continuous
Name	Water	EDA	Acetone	15	3	4.86	yes	yes
Boiling T(K)	373.2	390.4	329.3	15	10	1.47	yes	yes
X_F	0.1	0.9	0	15	2	7.27	no	no
X_E	0	0	1	10	2	4.84	yes	yes
X_W	0.01	0.98	0.01	10	30	0.33	yes	yes
F	1			10	0.1	81.5	no	no
W	0.9			10	1	9.59	no	no
η	0.98			5	1	4.78	yes	yes
				5	0.1	40.67	no	no
				3	0.8	3.56	yes	yes
				3	1	2.86	yes	yes
				3	30	0.1	yes	yes
				3	39	0.07	yes	yes
				3	0.6	4.71	no	no
				3	40	0.07	yes	no
				1	10	0.09	no	no
				1	5	0.19	no	no

Figure 4.10 concerns an EDA (B) as bottom product shows the same qualitative features as Figure 4.5. It is clear that there exists a minimum value for entrainer - feed flow rate ratio and this minimum value depends strongly on the reboil ratio, it gets smaller as the function of reboil ratio gets smaller, until it reaches a minimum reboil ratio, in other words, if changing the X-axis reboil ratio with Y-axis feed ratio, we can say that the desired product specification can be maintained over a wider range of reboil ratio as entrainer - feed flow rate ratio increases, the maximum value gradually reduces as reboil ratio gets smaller, until it reaches a minimum entrainer - feed flow rate ratio value. There is also a minimum reboil ratio value. A detailed calculation of the profile map shows that the feasible stripping section profiles region gets smaller when reboil ratio gets smaller until it can no longer intersect the extractive profile region. The same holds for the continuous mode because of a minimum F_E/V and reboil ratio in batch translates well into a minimum F_E/V and reboil ratio in continuous. The main difference between two graphs lies there is an additional maximum entrainer - feed flow rate ratio F_E/V .

When water (A) is the first product, the calculation results show that the process is always unfeasible as univolatility line $\alpha_{AB} = 1$ intersect binary side B-E, all extractive going in to the direction of extractive stable node (B) instead of extractive stable node (A), which makes impossible to recover water (A) in the whole operation parameter region. Corresponding information is supplied in Table 4.6.

4.6.2 Separation of Minimum Boiling Temperature Azeotropes with Light Entrainers (class 1.0-2).

The separation of a minimum boiling temperature azeotrope A-B with a light entrainer E gives rise to a ternary diagram ABE that belongs to the 1.0-2 class. The azeotrope is a saddle point of the residue curve map and is connected to the unstable node light entrainer by a distillation boundary. Both A and B are stable

nodes and so they can be obtained, either one or the other, as a bottom product by azeotropic distillation in their respective distillation region. By using extractive distillation one gets an enlarged feasible region to recover the bottom product as was noticed by Lang et al., (1999). Depending on the univolatility curve location and intersection with either the A-E side or the B-E side, two sub cases arise.

4.6.2.1 Case (a) univolatility curve $\alpha_{AB}=1$ reaching the Binary Side A-E

The separation of the minimum boiling azeotrope ethanol (351.5K)(A)-water (373.1K) (B)($x_{azeo,A}=0.88$ at 351.1K) with light entrainer methanol (337.6K) (E) gives rise to a 1.0-2 class ternary diagram where the univolatility curve $\alpha_{AB}=1$ reaches the A-E side near 63mol% in methanol. Both original components ethanol (A) and water (B) are stable nodes, the entrainer methanol (E) is the unstable node, while the minimum boiling azeotrope $T_{min,azeo_{AB}}$ (351.1K) is a saddle point. The rcm stable separatrix links the azeotrope to E and divides the composition diagram into two distinct distillation regions, each of which shares the same features. The definition of distillation region was given by Ewell and Welch(1945): any initial condition that is taken in a given batch distillation region leads to the same sequence of cuts. Bernot et al. (1990) explained the rule of how the node and separatrices constitute a distillation boundary, and the essential requirement of recovering A or B from this system sequentially in a batch stripper by an azeotropic distillation process unless this distillation boundary is highly curved. Hence extractive distillation is necessary, as it adds another solvent from the middle part of column can make the extractive profile cross the distillation boundary of residue curve map.

The location where univolatility line intersects the ethanol-methanol edge of the triangle is important in determining if methanol is an effective entrainer. The closer the intersection point ($x_{p,A}$) is to the methanol corner, the less entrainer is required, which means lower operating and capital costs. As shown in Figure 4.11, this location point is at $x_E=0.7$ (70mol% methanol).

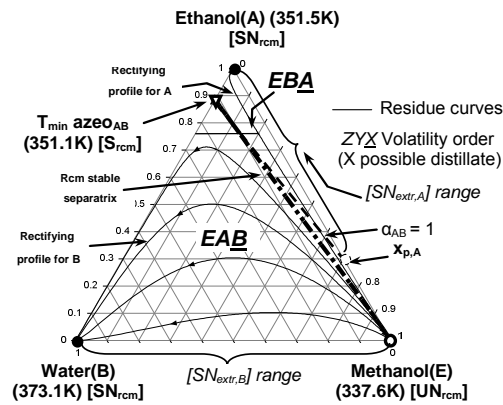


Figure 4.11. Ethanol-water minimum boiling azeotrope separation using light entrainer methanol. 1.0-2 class residue curve map and extractive distillation process insights

According to the extractive feasibility general criterion, both A and B can be recovered as bottom products. Ethanol (A) can only be recovered in the small volatility order region EBA , provided that the entrainer - feed flow rate ratio value stays below a maximum limit. Water (B) can be recovered by batch extractive stripping under infinite reboil ratio in region EAB . In that volatility order region, extractive composition profiles reach $[SN_{extr,B}]$ which connects to the stripping liquid profile running from (E) to (B) near to the edge (E-B). Temperature increases along the extractive profile.

Figure 4.12 displays the feasible parameter ranges to recover either ethanol (A) (Figure 4.12a) or water (B) (Figure 4.12b) in terms of entrainer - feed flow rate ratio F_E/F vs reboil ratio S.

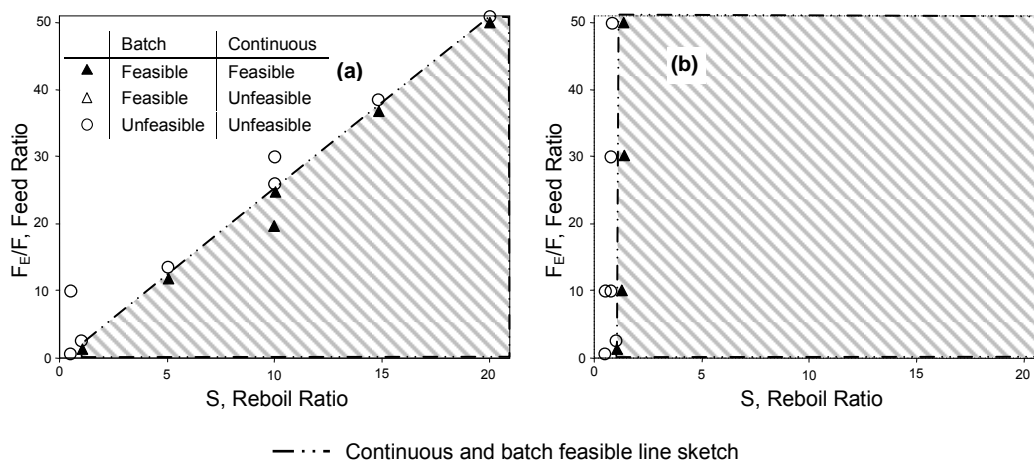


Figure 4.12. Entrainer - entrainer - feed flow rate ratio F_E/F as a function of the reboil ratio S. Ethanol-water-methanol separation: (a) to recover 98 mol% ethanol (A) (b) to recover 98 mol% water (B).

As expected from the batch thermodynamic insight, there exists a maximum value for F_E/V to recover ethanol which translates for the continuous process into F_E/F , above which the process is unfeasible. That maximum gradually reduces as reboil ratio gets smaller, until reaching a minimum reboil ratio. A detailed

calculation of the profile map (not shown) demonstrated that the feasible stripping section profiles region gets smaller and smaller until it can no longer intersect the extractive profile region. The same holds for the continuous mode as a maximum in batch translates into a maximum in continuous, as well.

When the bottom product is water (B), Figure 4.12b shows no limit for the entrainer - feed flow rate ratio in batch as expected and in continuous mode as well. There exists a minimum reboil ratio as an unstable extractive separatrix reduces the feasible region, as an unstable extractive separatrix reduces the feasible region when the reboil ratio decreases. Continuous modes display the same features with batch process; there is a minimum reboil ratio value below which the separation becomes impossible no matter how big the amount entrainer feed given. Table 4.7 gives corresponding information needed for the above conclusion.

Table 4.7 Operating parameters corresponding to Figure 4.12.

Class 1.0-2 case A-E side with light entrainer							Feasibility	
Ethanol (A) as bottom product								
Specification	A	B	E	Reboil ratio	Reflux ratio	FE/F	Batch	Continuous
Name	Ethanol	Water	Methanol	1.1	1	0.81	yes	yes
Boiling T(K)	351.5	373.2	337.6	1.1	2	0.42	no	no
X_F	0.9	0.1	0	10	22	0.4	yes	yes
X_E	0	0	1	10	23	0.39	no	no
X_W	0.98	0.01	0.01	20	49	0.36	yes	yes
F	1			20	50	0.35	no	no
W	0.9			0.5	10	0.03	no	no
η	0.98			1	10	0.08	no	no
Water (B) as bottom product								
Specification	A	B	E	Reboil ratio	Reflux ratio	FE/F	Batch	Continuous
Name	Ethanol	Water	Methanol	1.1	1	0.81	yes	yes
Boiling T(K)	351.5	373.2	337.6	1.1	2	0.42	yes	yes
X_F	0.1	0.9	0	10	22	0.4	yes	yes
X_E	0	0	1	10	23	0.39	yes	yes
X_W	0.01	0.98	0.01	20	49	0.36	yes	yes
F	1			20	50	0.35	yes	yes
W	0.9			0.5	10	0.08	no	no
η	0.98			1	10	0.08	no	no

4.6.2.2 Case (b) univolatility curve $\alpha_{AB}=1$ reaching the Binary Side B-E.

The separation of the minimum boiling azeotrope methyl ethyl ketone (352.5K) (A) – benzene (353.2K) (B) ($x_{azeo,A}=0.50$ @351.3K) with acetone (329.3K) (E) illustrates the subcase for class 1.0-2 with a univolatility curve $\alpha_{AB} = 1$ that reaches the B-E edge around 36 mol% in acetone (Figure 4.13). This separation has once been studied by (Donald and Ridgway, 1958). MEK have extensive application refer to as a solvent, as a welding agent, a precursor to methyl ethyl ketone peroxide, and a catalyst for some polymerization reactions.

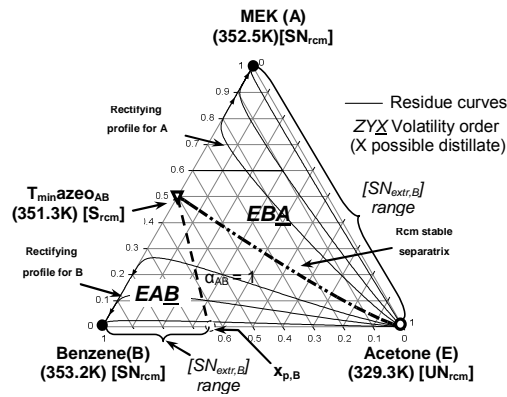


Figure 4.13. MEK – benzene minimum boiling azeotrope separation using light entrainer acetone. 1.0-2 class residue curve map and extractive distillation process insights

Univolatility line $\alpha_{AB}=1$ end at the binary side MEK-benzene sides at about 50% MEK defines two feasible regions. Because both MEK (A) and Benzene(B) are the most volatile in respective region, where there exists a residue curve with increasing temperature from E to their locations, either of components A and B is possible distillate of the extractive distillation process. The rectifying stable separatrix is slightly curved in the region that contains component A, it makes possible to get MEK as a bottom product, Nevertheless, the rectifying stable separatrix curvature is small and does not provide a sufficient recovery of component B via azeotropic distillation, which leads to a greater opportunity of applying the extractive distillation process. A batch extractive stripper will improve the recovery because the extractive feasible region EBA is much greater than the simple distillation region defined by the distillation boundary of the residue curve map.

The location point where univolatility line intersect the benzene-acetone edge is far to the acetone corner, as shown in Figure 4.13, this location point is at $x_E=0.35$ (35mol% acetone).Benzene can be recovered in small region EAB above univolatility line $\alpha_{AB}=1$.There exists a maximum $(F_E/F)_{max,B}$ to get product (B) under infinite reboil ratio if the initial composition lies in the volatility order region EAB . However MEK (A) can be recovered by batch extractive stripping under infinite reboil ratio in regions EBA , as in the region below the stable extractive separatrix, extractive composition profiles reach $[UN_{extr,A}]$ which links the stripping liquid profile (residue curves) running from (E) to (A) near to the acetone(E)-MEK(A) edge.

The extractive process behaves as in the previous 1.0-2 sub-case, but now the maximum entrainer - feed flow rate ratio exists to recover bottom product B (benzene) whereas there are no limit to recover A (MEK) as a bottom product. This is seen in Figure 4.14 that displays the entrainer - feed flow rate ratio vs. reboil ratio feasible ranges.

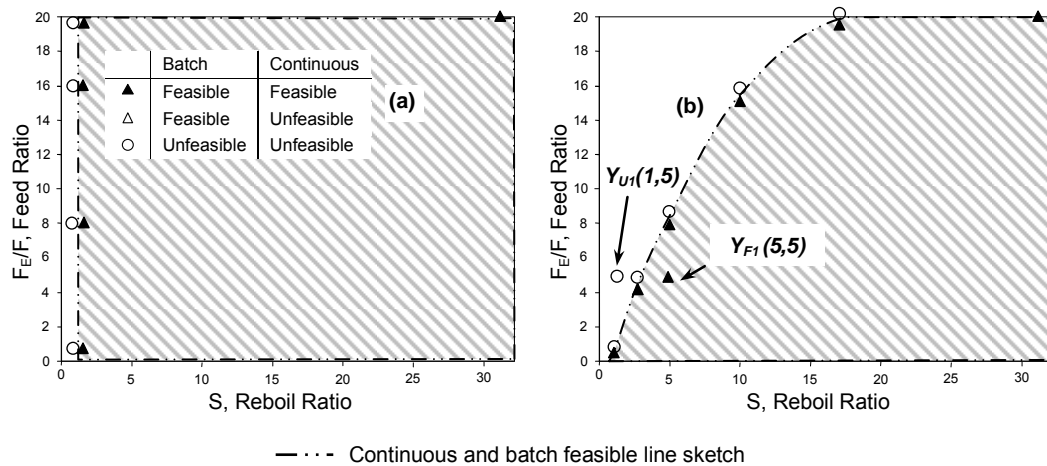


Figure 4.14. Entrainer - entrainer - feed flow rate ratio F_E/F as a function of the reboil ratio S . MEK-benzene-acetone separation: (a) to recover 98 mol% MEK (A) (b) to recover 98 mol% benzene (B).

Figure 4.14a concerns a benzene (B) distillate. As expected from the infinite reboil ratio analysis there exists a maximum value for entrainer - feed flow rate ratio above which the process is unfeasible. That maximum value gradually reduces as reboil ratio gets smaller, until it reaches a minimum reboil ratio. The same holds for the continuous mode as a maximum in batch can translate into a maximum in continuous.

When distillate is MEK (A), infinite reboil ratio analysis shows no limit for the entrainer - feed flow rate ratio. These results of Figure 4.14b in batch process agree well with the thermodynamics criteria analysis. Both continuous modes and batch modes display the same features for reboil ratio limitation. Similarly to Figure 4.12b, there is a minimum reboil ratio value below which the separation becomes impossible no matter how big is the amount entrainer feed given. Table 4.8 gives corresponding data related to Figure 4.14a.

Table 4.8 Operating parameters corresponding to Figure 4.14a.

Class 1.0-2 case B-E side with light entrainer							Feasibility	
Benzene (B) as bottom product								
Specification	A	B	E	Reboil ratio	Reflux ratio	FE/F	Batch	Continuous
Name	MEK	Benzene	Acetone	30	20	1.34	yes	yes
Boiling T(K)	352.5	353.2	329.3	10	15	0.59	yes	yes
X_F	0.9	0.1	0	10	16	0.55	no	no
X_E	0	0	1	5	8	0.54	yes	yes
X_W	0.98	0.01	0.01	5	9	0.48	no	no
F	1			3	4	0.63	yes	yes
W	0.9			3	5	0.51	no	no
η	0.98			1	0.5	1.33	yes	yes
				1	0.8	0.89	no	no
MEK (A) as bottom product								
Specification	A	B	E	Reboil ratio	Reflux ratio	FE/F	Batch	Continuous
Name	MEK	Benzene	Acetone	30	20	1.34	yes	yes
Boiling T(K)	352.5	353.2	329.3	10	15	0.59	yes	yes
X_F	0.1	0.9	0	10	16	0.55	yes	yes
X_E	0	0	1	5	8	0.54	yes	yes
X_W	0.01	0.98	0.01	5	9	0.48	yes	yes
F	1			3	4	0.63	yes	yes
W	0.9			3	5	0.51	yes	yes
η	0.98			1	0.5	1.33	yes	yes
				0.5	10	0.03	no	no

Figure 4.15 shows the simplified profiles for a feasible and an unfeasible point taken from Figure 4.14b. Under conditions $F_E/F=5$ and $S=5$, the process is feasible as all three column sections composition profiles intersect. For $F_E/F=5$ and $S=1$, the process is unfeasible because the stripping and the rectifying profiles are too short and neither one nor the other intersect with the extractive profile. Corresponding data can be seen in Table 4.9.

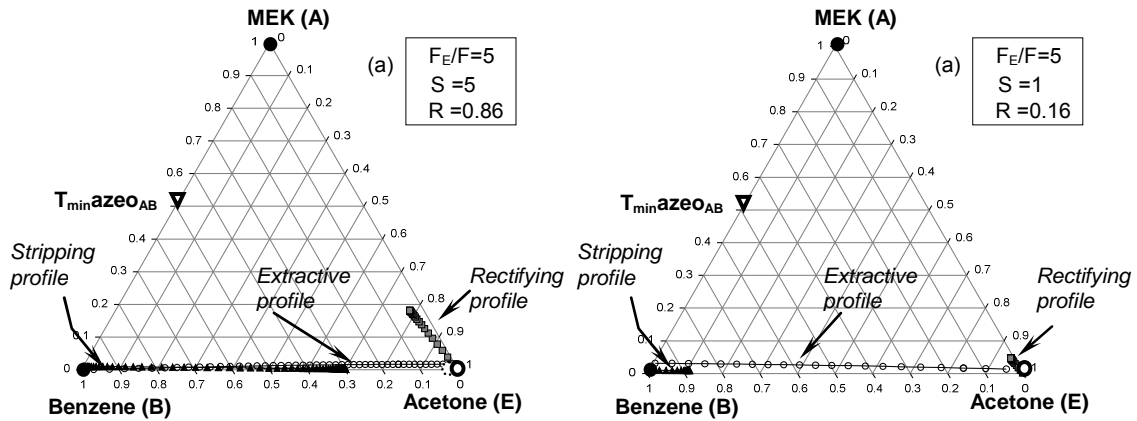


Figure 4.15. Operating parameter scene explanation. Points taken from Figure 13b: (a) point Y_{F1} , (b) point Y_{U1}

Table 4.9 Operating parameters corresponding to Figure 4.15a,b.

Class 1.0-2 case B-E side with light entrainer to recover B							
Specification parameters for Figure 4.15(a)				Specification parameters for Figure 4.15(b)			
Apex	A	B	E	Apex	A	B	E
Name	MEK	Benzene	Acetone	Name	MEK	Benzene	Acetone
Boiling T(K)	414.4	425.2	389.7	Boiling T(K)	414.4	425.2	389.7
X_F	0.1	0.9	0	X_F	0.1	0.9	0
X_E	0	0	1	X_E	0	0	1
X_W	0.01	0.98	0.01	X_W	0.01	0.98	0.01
X_D	0.017843137	0.003529412	0.978627451	X_D	0.017843137	0.003529412	0.978627451
Reboil S	5			Reboil S	1		
F_E/F	5			F_E/F	5		
F	1			F	1		
W	0.9			W	0.9		
E	5			E	5		
D	5.1			D	5.1		
V	9.5			V	5.9		
η_B	0.98			η_B	0.98		
R	0.86			R	0.16		

The extractive section composition profile shows drastically changes under the influence of reboil ratio, the effects of reboil ratio is studied for the same entrainer - feed flow rate ratio $F_E/F=1$ and $S=1, 15, 30$ in Figure 4.15.

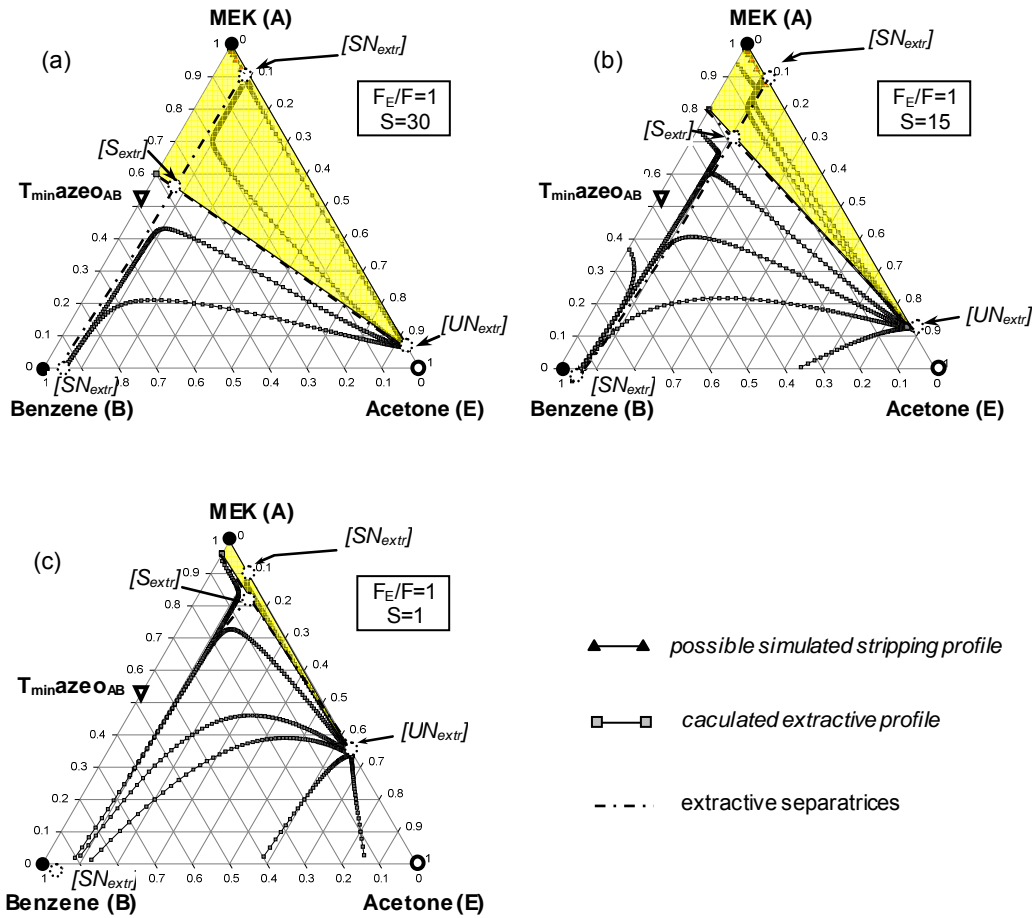


Figure 4.16. Influence of the reboil ratio on the extractive section composition profiles.

The Figure 4.16a, b, c illustrates clearly the evolution of the fixed points and separatrixes location as S decreases. The extractive unstable node UN_{extr} moves toward apex A parallel to the binary edge AB. The saddle node S_{extr} moves toward the $SN_{extr,A}$ on the extractive separatrix, which results in the shrinking of extractive feasible region when S decreases from 30 to 1. The extractive separatrix location remains the same in the meanwhile. At $S=1$, this stresses the need for a large reboil ratio for the process to be feasible, whose consequence is a large heat duty.

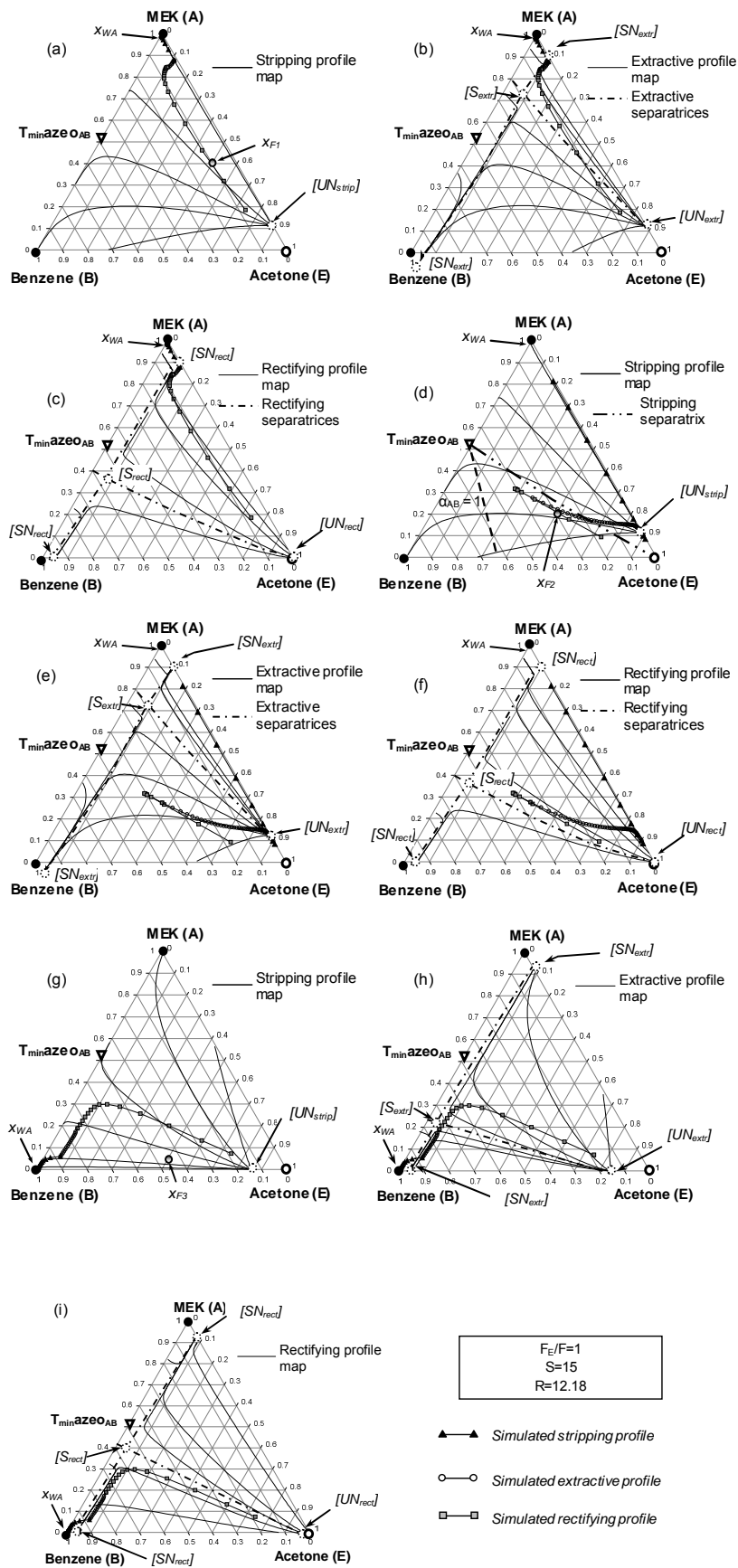


Figure 4.17. Rigorous simulation result to recover MEK (a-f) or Benzene (g-i) at $S=15$, $F_E/F=1$ compared with simplified composition profiles: (a, d, g) stripping section, (b, e, h) extractive section and (c, f, i) rectifying section.

The methodology step 3 relies upon rigorous simulations. Figure 4.17 shows how the rigorous profiles match well the simplified composition profile maps for the stripping, extractive and rectifying sections. Rigorous simulation for continuous distillation separation of MEK-benzene with acetone also based on thermodynamic model UNIFAC modified Dortmund version 1993 (Gmehling et al., 1993, Weidlich and Gmehling, 1987). A saturated liquid fresh feed with composition 10 mol% MEK and 90 mol% benzene is fed into a 50 tray tower (including the reboiler) on tray 15 and the pure saturated vapour entrainer acetone feed on tray 30, in state variable settings, set feed mixture vapor fraction as 0 for and set entrainer feed vapor fraction as 1 at 1 atm, The reboil rate is given by mass balance calculation 65 kmol/h when the feed flow rate ratio is 100 kmol/h. Reboil ratio and reboil rate are chosen instead of commonly used reflux ratio and distillate rate, the extractive column has two design degrees of freedom once the total stages and feed location are fixed: reboil ratio and entrainer - feed flow rate ratio.

The stable node (benzene) is expected as the bottom product and the MEK are distillate from the top by the second distillate column. A briefly optimization for stage number is carried out by comparison of product purity and profile feature. The continuous simulation results along with profiles calculated based on Equations 4.20, 4.22 and 4.24 in part 4.5.2 are summarized in Figure 4.17.

Under conditions $F_E/F=1$ and $S=15$, one notices that most profile maps display separatrices inside the triangle and singular points that are no longer pure components or azeotropes, as was the case for infinite conditions (residue curve map). In particular, the extractive profile maps depend on the targeted bottom product and the feed composition as it is shown in Figure 4.17b to recover A (product x_{WA} from x_{F1}) and Figure 4.17e to recover B (product x_{WB} from x_{F2}): the stable nodes are inverted and the saddle point location is different.

Overall, each section of the rigorous profiles matches well with the simplified profiles. The rigorous simulation enables to recover MEK with a purity of 0.99901 or Benzene with a purity of 0.99903. One notices that the rectifying and the extractive separatrices have close locations. However the composition profiles in these two sections have different curvature. For both cases, the rectifying profile is bounded on its left by the rectifying separatrix. Then the extractive section profile is bounded on its right by the extractive separatrix. The corresponding operating parameters are showed in Table 4.10.

Analyzing the azeotropic and extractive processes for 1.0-2 class, we can conclude that both are eligible to get A or B as products because A and B are stable nodes of the residue curve map. In batch mode, it was shown in the literature that the extractive process could enable to cross the rcm distillation

boundary of the MEK-benzene mixture with acetone and thus offer a larger composition region to obtain MEK as a product. However we could not verify nor invalidate this in continuous mode by rigorous simulation which is subject to the lever rule and to an additional requirement for the process to be feasible.

Table 4.10 Operating parameters corresponding to Figure 4.17a, b, c.

Class 1.0-2 case B-E side with light entrainer($F_E/F=1$, $S=15$) to recover B									
Worksheet parameters				Rectifying section			Stripping section		
Specification	A	B	E	A	B	E	A	B	E
Name	MEK	Benzene	Acetone	MEK	Benzene	Acetone	MEK	Benzene	Acetone
Boiling T(°C)	414.4	425.2	389.7	0.740741	0.073587	0.185672	0.025553	0.0567	0.917746
X_F	0.1	0.9	0	0.593343	0.133199	0.273457	0.009898	0.049298	0.940804
X_E	0	0	1	0.428894	0.200382	0.370724	0.003763	0.041998	0.954239
X_W	0.01	0.98	0.01	0.285681	0.255818	0.458501	0.001416	0.035383	0.963201
X_D	0.082727273	0.016363636	0.900909091	0.187362	0.288206	0.524433	0.00053	0.029599	0.969872
S	15	W	0.9	0.130557	0.299755	0.569688	0.000197	0.024631	0.975172
F_E/F	1	V	14.5	0.100841	0.297778	0.601381	7.32E-05	0.020411	0.979516
F	1	η_B	0.98	0.085921	0.28828	0.6258	2.71E-05	0.016852	0.983121
D	1.1	R	12.18	0.07837	0.274822	0.646808	1.00E-05	0.013869	0.986121
Rigorous parameters				0.07431	0.259283	0.666407	3.69E-06	0.011381	0.988616
X_F	0.1	0.9	0	0.071851	0.242647	0.685502	1.36E-06	0.009312	0.990686
X_E	0	0	1	0.07011	0.225479	0.704412	5.00E-07	0.007599	0.9924
X_D	0.01	0.98	0.01	0.068685	0.208168	0.723147	1.84E-07	0.006184	0.993816
Num stages	50	Feed tray	15	0.067406	0.191027	0.741567	6.76E-08	0.005017	0.994983
Solvent tray	30			0.066971	0.175211	0.757819	2.48E-08	0.004057	0.995943
Extractive section							9.11E-09	0.003269	0.996731
	0.069315	0.167953	0.762732	0.066864	0.103002	0.830134	3.34E-09	0.002622	0.997378
	0.070156	0.160674	0.769169	0.066153	0.094394	0.839453	1.23E-09	0.002092	0.997908
	0.070252	0.153169	0.77658	0.06545	0.08596	0.84859	4.49E-10	0.001657	0.998343
	0.06997	0.145366	0.784664	0.064763	0.077791	0.857447	1.63E-10	0.001302	0.998698
	0.069491	0.137264	0.793245	0.0641	0.069968	0.865932	5.87E-11	0.001012	0.998988
	0.068902	0.128905	0.802193	0.063468	0.062562	0.87397			
	0.068252	0.120352	0.811396	0.025553	0.0567	0.917746			
	0.067567	0.111687	0.820746						

4.7 CONCLUSIONS

A feasibility method to study the separation with a light boiling entrainer E of maximum (1.0-1a Serafimov's class) and minimum (1.0-2 Serafimov's class) boiling temperature azeotropic mixtures by using a batch stripper has been extended to extractive distillation operated in continuous mode so as to investigate the potential feasible region of the operating parameters reboil ratio (S) and entrainer - feed flow rate ratio (F_E/F , F_E/L_T) for both continuous and batch processes. We have considered for the continuous process a column configuration with the entrainer fed below the main azeotropic mixture feed, giving rise to three column sections, namely stripping, extractive and rectifying.

A feasibility methodology has been proposed. It proceeds in three steps. Firstly, prediction under infinite reboil ratio conditions is based on the general feasibility criterion enounced by Rodriguez-Donis et al. (2009a) and detailed when using a light entrainer by Rodriguez-Donis et al. (2012a). It relies upon the knowledge of the residue curve map topology and classification along with the computation of the univolatility

line and enables to predict possible products and the limiting values of the entrainer - feed flow rate ratio. Secondly, the process operation under finite reboil ratio requires checking the intersection of the approximate composition profile in each column section, depending on the reboil ratio and entrainer - feed flow rate ratio, and a target product composition and recovery. This gives rise to entrainer - feed flow rate ratio vs. reboil ratio diagrams where the feasible ranges of the parameters are highlighted. The approximate composition profiles also bring information about the location of pinch points and possible composition profiles separatrices that could impair the process feasibility. Third, the approximate calculations are compared with rigorous simulations of continuous extractive distillation processes, providing rigorous values of the product composition and recovery.

The design equations for the three section columns of extractive distillation process have been derived based on the bottom product recovery and composition, on the azeotropic mixture feed composition, and the reboil ratio and entrainer - feed flow rate ratio. Both feeds state (boiling liquid or saturated vapor) are considered. The further analysis has been made assuming that the mixture is fed as boiling liquid and the entrainer is fed as saturated vapor.

Under infinite reboil ratio, the univolatility line $\alpha_{AB}=1$ ends at the binary sides, gives birth to the point x_p . This determines two different volatility order regions. According to the general feasibility criterion enounced above, there exist limiting values for the entrainer - feed flow rate ratio for some products in the batch extractive process.

For the class 1.0-1a, corresponding to the separation of a maximum boiling azeotropic mixture A-B using a light entrainer E, two sub cases arise, whether the univolatility line $\alpha_{AB} = 1$ intersects the A-E edge (case a) or B-E edge (case b). The system propanoic acid– dimethyl formamide (DMF) with light entrainer methyl isobutyl ketone (MIBK) is used to demonstrate the case when the univolatility line $\alpha_{AB} = 1$ intersects the A-E edge (case a). The system water – ethylene diamine (EDA) with light entrainer acetone is an example of the case when the univolatility line $\alpha_{AB} = 1$ intersects the B-E edge (case b). The separation of a maximum boiling azeotropic mixture using a light entrainer shows antipodal feature with the separation of a minimum boiling azeotrope using a heavy entrainer as they both belong to the same Serafimov's class 1.0-1a.

For the 1.0-1a class, above a minimal limit entrainer - feed flow rate ratio value, the extractive stable node $SN_{ext,A}$ (respectively $SN_{ext,B}$ for case b) is located in the region where it can intersect a stripping profile which can reach the expected product A (in class 1.0-1a case a), or the expected product B (in class 1.0-1a

case b). Under finite reboil ratio, $SN_{extr,B}$ (class 1.0-1a, case a) , $SN_{extr,A}$ (class 1.0-1a, case b) moves inside the diagram and generates an extractive unstable separatrix that reduces the feasible region. These results also translate well for continuous extractive distillation when we apply our methodology. Regarding propanoic acid (A) as a bottom product for case a, there exists a minimum value F_E/V at given reboil ratio, that gets smaller as the reboil ratio reduces. The minimum entrainer - feed flow rate ratio is the same for both the batch and the continuous process, as it comes from the shared intersection condition between the stripping and the extractive profile. The main difference lies in the occurrence of an additional maximum entrainer - feed flow rate ratio for the continuous process, which results from a too short rectifying section profile that cannot intersect the extractive section composition profile. At very low reboil ratio, none of the processes is feasible because the stripping profile is too short. The value of S at this point can be regarded as the minimum reboil ratio, with which the minimum amount of vapor is returned to the column. Regarding case b aiming to produce EDA (B) as bottom product, it bears symmetrical feature with case a aiming to produce product propanoic acid (A).

For the class 1.0-2, corresponding to the separation of a minimum boiling temperature, two examples are considered: the separation of the azeotrope ethanol (A) - water (B) with light entrainer methanol gives rise to the 1.0-2 class case a where the univolatility curve $\alpha_{AB} = 1$ reaches the A-E side. The mixture methyl ethyl ketone (A) – benzene (B) using acetone as entrainer illustrates the subcase b, the univolatility curve $\alpha_{AB} = 1$ intersects the B-E edge. Both belonging to the 1.0-2 class, the separation of a minimum boiling azeotropic mixture using a light entrainer and the separation of a maximum boiling azeotrope using a heavy entrainer are antipodal ternary diagrams.

The batch feasibility criterion under infinite reflux ratio states that A or B can be distilled out, depending on the starting composition. Depending on the univolatility line $\alpha_{AB} = 1$ location, for case a (resp. case b), component B (resp. A) can be a bottom product, provided that the entrainer entrainer - feed flow rate ratio lies below a maximal value $(F_E/L_T)_{max}$ at a given reboil ratio. Under finite reboil ratio an extractive unstable separatrix moves inside the diagram and impacts the feasible composition region. For continuous extractive distillation, these results translate well. The $(F_E/L_T)_{max}$ translates into a maximum value F_E/F at a given reboil ratio gets smaller as reboil ratio reduce, and there also exists a minimal reboil ratio S . Regarding the distillation of ethanol(A) when separating the mixture ethanol - water, the results show the following feature: There is no limit entrainer - feed flow rate ratio for recovery component water(B) but existing $(F_E/F)_{max,A}$ for component ethanol(A) because the extractive stable node to get B $SN_{extr,B}$ can be located at any position on the edge B-E (resp. A-E) whereas the extractive stable node $SN_{extr,A}$ needs to be located in

the region where A is the least volatile. That maximum gradually reduces as reboil ratio gets smaller, until it reaches a minimum reboil ratio. A detailed calculation of the profile map (not shown) demonstrated that the feasible stripping section profiles region gets smaller until it can no longer intersect the extractive profile region. When aiming to get water (B) as bottom product, the results show no limit for the entrainer - feed flow rate ratio in batch as expected and in continuous mode as well. For both products, there exists a minimum reboil ratio as an unstable extractive separatrix reduces the feasible region when the reboil ratio decreases. The continuous mode displays the same features than the batch process.

Regarding case b illustrated with the ternary system methyl ethyl ketone (A) – benzene (B) using entrainer acetone, the behavior is symmetrical. The aiming to have bottom product methyl ethyl ketone (A) bears symmetrical feature with case a aiming to recover water (B) at the bottom, but then aiming to benzene (B) has a $(F_E/F)_{max,B}$ as the univolatility curve $\alpha_{AB} = 1$ now reaches B-E edge.

Analyzing the azeotropic and extractive processes for 1.0-2 class, both are eligible to get A or B as product because A and B are stable nodes of the residue curve map. In batch mode, it was shown in the literature that the extractive process could enable to cross the rcm distillation boundary of the MEK-benzene mixture with acetone and thus offers a larger composition region than the azeotropic one to obtain MEK as a product. However we could not verify nor invalidate this in continuous mode by rigorous simulation which is subject to the lever rule and to an additional requirement for the process to be feasible.

The possible advantage of using a light entrainer is to give more opportunities for separating minT and maxT azeotropic mixtures when it is not easy to find an appropriate heavy or intermediate entrainer. In perspective, it could be interesting to evaluate the possible energy gain of the whole system (extractive and regeneration columns), compared to the use of a heavy entrainer.

CHAPTER

5

Conclusions, Perspective

5.1 CONCLUSIONS

The operational stability of separation processes is a crucial factor to the economic success of such processes. This is especially true for extractive distillation columns that often show counterintuitive operational properties. It is sometimes useful to sacrifice cost-optimality of a steady-state design in favor of better operational stability. Thus, exploring a feasible region based on the two key parameters for the extractive distillation process, reflux ratio and entrainer - feed flow rate ratio, is an important issue when that chemical process is designed. Feasibility studies also contribute to a better understanding of such complex unit operations as both minimum solvent flow rate ratio and minimum reflux ratios can be used as indicators of a flowsheet's energy requirements. The limitations of entrainer - feed flows and operating reflux ratios give essential guidance for design and operation of extractive distillations.

Our objective concerns the extension of thermodynamic insights gathered on batch distillation studied by Rodriguez-Donis et al (2009a, 2009b, 2010, 2012a, 2012b) to the continuous extractive distillation process. Those authors combined knowledge of the thermodynamic properties of residue curve maps and of the univolatility and unidistribution curves location. They expressed a general feasibility criterion for extractive distillation under infinite reflux ratio (reboil ratio) and showed how it could apply to separate minimum or maximum boiling azeotropes or low relative volatility mixtures, by using heavy, light or intermediate entrainers, even when a new azeotrope was formed. Nevertheless, it was never systematically checked for continuous operation, which was our main focus. We focus in chapter 3 on the separation of minimum and maximum azeotropic mixtures A-B with a heavy entrainer E and in chapter 4 on the separation of maximum and minimum azeotropic mixtures A-B with a light entrainer E. All those mixtures A-B-E refers to the 1.0-1a (occurrence 21.6%) and 1.0-2 (occurrence 8.5%) Serafimov's classes respectively.

We use a methodology in three steps: firstly, we use the batch extractive distillation criterion to identify possible products and limiting parameter values. As they are based on thermodynamic and topological features of the ternary diagram, the batch thermodynamic insight are also valid concepts for continuous distillation as well. The second step of our methodology concern operation under finite reflux ratio or reboil ratio as these conditions are required to obtain either a distillate or a bottom product in continuous operation. Systematic calculations of rectifying, extractive, stripping section composition profiles and checking of their intersection enables to identify the feasibility region for the two key parameters, entrainer - feed flow rate ratio and reflux ratio/reboil ratio. During step 2, the product composition and recovery yield is assumed. Under finite reflux ratio conditions, the approximate calculations agree with the rigorous simulations of

continuous extractive distillation processes, but also bring information about the location of pinch points and possible composition profiles separatrices that could impair the process feasibility. Step 3 relies upon rigorous simulations that are used to verify the approximate profile predictions and obtain rigorous values of the product composition and recovery.

Chapter 3 concerns the use of a heavy entrainer fed as a boiling liquid above the main azeotropic mixture feed. The continuous column has then three sections, stripping below the main feed, extractive between the two feeds and rectifying above the entrainer feed. Application of our methodology enables to investigate the range of operating parameters reflux ratio (R) and entrainer - feed flow rate ratio (F_E/F , F_E/V) for both continuous or batch process.

For class 1.0-1a (minimum boiling azeotrope separation A-B by adding a heavy entrainer E), two sub cases arise depending on the univolatility line $\alpha_{AB} = 1$ location. Two azeotropic systems acetone-heptane with toluene (entrainer) and acetone-methanol with water (entrainer) are used to demonstrate the case when univolatility line $\alpha_{AB} = 1$ intersects the A-E edge (we call it case a); an example acetone-methanol with heavy entrainer chlorobenzene is used to explain the case when univolatility line $\alpha_{AB} = 1$ intersects the B-E edge (we call it case b).

At infinite reflux ratio for the batch process, the point x_p determines the minimal limit value for entrainer - feed flow rate ratio, the range of the extractive stable node $SN_{extr,A}$ and the expected product A (in class 1.0-1a case a), $SN_{extr,B}$ and the expected product B (in class 1.0-1a case b). Under finite reflux ratio, the $SN_{extr,B}$ in class 1.0-1a case a) ($SN_{extr,A}$ in class 1.0-1a case b) moves inside the diagram and generates an extractive unstable separatrix that reduces the feasible region.

These results also translate well for continuous extractive distillation, regarding A as product component for the two example of case a, the result show the expected feature: there is a minimum entrainer - feed flow rate ratio at any reflux ratio. Besides, there is maximum reflux ratio at any given entrainer entrainer - feed flow rate ratio. The maximum reflux ratio gets smaller as the entrainer entrainer - feed flow rate ratio reduces, in agreement with Knapp and Doherty, (1994)result. There is also a minimum reflux ratio value, below which the separation becomes impossible no matter how big is the value of entrainer to entrainer - feed flow rate ratio. The two examples have the same type of shape but different limits because of the different properties of azeotrope and solvent performance.

The same shape of the operating parameter feasibility region holds for the continuous and batch mode, as the limitation F_E/V and reflux ratio in batch translates into a continuous value F_E/F . However, the minimum

value F_E/V is smaller for the continuous than for the batch mode because the continuous profile sets stricter feasible conditions due to the necessary intersection between the stripping and the extractive profile.

Regarding case b aiming to produce acetone(A) as distillate from ternary system acetone (A)-methanol (B)-chlorobenzene(E), it bears symmetrical feature with case a, but then heptane(B) is the product as the univolatility curve $\alpha_{AB} = 1$ now reaches B-E edge.

For class 1.0-2 (separation of a maximum boiling azeotrope with a heavy entrainer) two sub cases also occur. Forth mixture chloroform (A) - vinyl acetate (B) using butyl acetate as entrainer(E), the univolatility curve $\alpha_{AB} = 1$ intersects the A-E edge (case a), while for the mixture acetone (A) – chloroform (B) using benzene (E) as entrainer, the univolatility curve $\alpha_{AB} = 1$ intersects the B-E edge (case b). The batch feasibility criterion under infinite reflux ratio then states that A or B can be distilled out, depending on the starting composition. For case a (resp. case b), chloroform (A for case a) (resp. B for case b) can be a distillate product, provided that the entrainer entrainer - feed flow rate ratio lies below a maximal value $(F_E/V)_{max}$ at a given reflux ratio. The continuous process also displays a corollary maximal value $(F_E/F)_{max}$. But the continuous process also shows a minimum value F_E/F because of the necessary intersection between the stripping and the extractive section composition profiles. Under finite reflux ratio an extractive unstable separatrix moves inside the diagram and impacts the feasible composition region. In continuous mode, the minimum value F_E/F at a given reflux ratio gets smaller as reflux ratio reduces, and there also exists a minimum reflux ratio.

Regarding the distillation of vinyl acetate (B) when separating the mixture chloroform-vinyl acetate using butyl acetate as entrainer or acetone (A) when separating the mixture chloroform-acetone using benzene as entrainer, the batch extractive process analysis predicts no entrainer limitation under infinite reflux ratio, but there exists a minimum entrainer - feed flow rate ratio limit under finite reflux ratio for the continuous process because of the additional constraint that the stripping profile intersects the extractive profile. For both continuous and batch mode, there exist a minimum value for reflux ratio as the reduction of the rectifying profile region as reflux ratio decreases.

Comparison of three entrainers leading to the same type of diagram and sub-case also shows that the feasible conditions ranges is entrainer dependent, in particular the minimum reflux ratio and the minimum entrainer entrainer - feed flow rate ratio, and that the methodology is suitable to compare entrainers in a preliminary step before optimizing the process with the entrainer regeneration column.

Chapter 4 concerns the use of a light entrainer fed as a saturated vapor below the main azeotropic mixture feed. A feasibility method to study the separation of maximum (1.0-1a Serafimov's class) and minimum (1.0-2 Serafimov's class) boiling temperature azeotropic mixtures with a light boiling entrainer E by using a batch stripper has been extended to extractive distillation operated in continuous mode so as to investigate the potential feasible region of the operating parameters reboil ratio (S) and entrainer - feed flow rate ratio (F_E/F , F_E/L_T) for both continuous and batch processes. We have considered for the continuous process a column configuration with the entrainer fed below the main azeotropic mixture feed, giving rise to three column sections, namely stripping, extractive and rectifying.

A feasibility methodology has been proposed. It proceeds in three steps. Firstly, prediction under infinite reboil ratio conditions is based on the general feasibility criterion enounced by Rodriguez-Donis et al. (2009a) and detailed when using a light entrainer by Rodriguez-Donis et al. (2012a). It relies upon the knowledge of the residue curve map topology and classification along with the computation of the univolatility line and enables to predict possible products and the limiting values of the entrainer - feed flow rate ratio. Secondly, the process operation under finite reboil ratio requires checking the intersection of the approximate composition profile in each column section, depending on the reboil ratio and entrainer - feed flow rate ratio, and a target product composition and recovery. This gives rise to entrainer - feed flow rate ratio vs. reboil ratio diagrams where the feasible ranges of the parameters are highlighted. The approximate composition profiles also bring information about the location of pinch points and possible composition profiles separatrices that could impair the process feasibility. Third, the approximate calculations are compared with rigorous simulations of continuous extractive distillation processes, providing rigorous values of the product composition and recovery.

The design equations for the three section columns of extractive distillation process have been derived based on the bottom product recovery and composition, on the azeotropic mixture feed composition, and the reboil ratio and entrainer - feed flow rate ratio. Both feeds state (boiling liquid or saturated vapor) are considered. The further analysis has been made assuming that the mixture is fed as boiling liquid and the entrainer is fed as saturated vapor.

Under infinite reboil ratio, the univolatility line $\alpha_{AB}=1$ ends at the binary sides, gives birth to the point x_p . This determines two different volatility order regions. According to the general feasibility criterion enounced above, there exist limiting values for the entrainer - feed flow rate ratio for some products in the batch extractive process.

For the class 1.0-1a, corresponding to the separation of a maximum boiling azeotropic mixture A-B using a light entrainer E, two sub cases arise, whether the univolatility line $\alpha_{AB} = 1$ intersects the A-E edge (case a) or B-E edge (case b). The system propanoic acid– dimethyl formamide (DMF) with light entrainer methyl isobutyl ketone (MIBK) is used to demonstrate the case a when the univolatility line $\alpha_{AB} = 1$ intersects the A-E edge. The system water – ethylene diamine (EDA) with light entrainer acetone is an example of the case b, when the univolatility line $\alpha_{AB} = 1$ intersects the B-E edge. The separation of a maximum boiling azeotropic mixture using a light entrainer shows antipodal feature with the separation of a minimum boiling azeotrope using a heavy entrainer as they both belong to the same Serafimov's class 1.0-1a.

For the 1.0-1a class, above a minimal limit entrainer - feed flow rate ratio value, the extractive stable node $SN_{extr,A}$ (respectively $SN_{extr,B}$ for case b) is located in the region where it can intersect a stripping profile which can reach the expected product A (in class 1.0-1a case a), or the expected product B (in class 1.0-1a case b). Under finite reboil ratio, $SN_{extr,B}$ (class 1.0-1a case a), $SN_{extr,A}$ (class 1.0-1a case b) move inside the diagram and generate an extractive unstable separatrix that reduces the feasible region. These results also translate well for continuous extractive distillation when we apply our methodology. Regarding propanoic acid (A) as a bottom product for case a, there exists a minimum value F_E/V at a given reboil ratio, that gets smaller as the reboil ratio reduces. The minimum entrainer - feed flow rate ratio is the same for both the batch and the continuous process, as it comes from the shared intersection condition between the stripping and the extractive profile. The main difference lies in the occurrence of an additional maximum entrainer - feed flow rate ratio for the continuous process, which results from a too short rectifying section profile that cannot intersect the extractive section composition profile. At a very low reboil ratio, none of the processes is feasible because the stripping profile is too short. The value of S at this point can be regarded as the minimum reboil ratio, with which the minimum amount of vapor is returned to the column. Regarding case b aiming to produce EDA (B) as bottom product, it bears symmetrical feature with case a aiming to produce product propanoic acid (A).

For the class 1.0-2, corresponding to the separation of a minimum boiling temperature. Two examples are considered: the separation of the azeotrope ethanol (A) - water (B) with light entrainer methanol gives rise to the 1.0-2 class case a where the univolatility curve $\alpha_{AB} = 1$ reaches the A-E side. while the case of the mixture methyl ethyl ketone (A) – benzene (B) using acetone as entrainer illustrates the subcase b, the univolatility curve $\alpha_{AB} = 1$ intersects the B-E edge. Both belonging to the 1.0-2 class, the separation of a minimum boiling azeotropic mixture using a light entrainer and the separation of a maximum boiling azeotrope using a heavy entrainer are antipodal ternary diagrams.

The batch feasibility criterion under infinite reflux ratio states that A or B can be distilled out, depending on the starting composition. Depending on the univolatility line $\alpha_{AB}=1$ location, for case a (resp. case b), component B (resp. A) can be a bottom product, provided that the entrainer entrainer - feed flow rate ratio lies below a maximal value $(F_E/L_T)_{max}$ at a given reboil ratio. Under finite reboil ratio an extractive unstable separatrix moves inside the diagram and impacts the feasible composition region. For continuous extractive distillation, these results translate well. The $(F_E/L_T)_{max}$ translates into a maximum value F_E/F at a given reboil ratio gets smaller as reboil ratio reduce, and there also exists a minimal reboil ratio S . Regarding the distillation of ethanol(A) when separating the mixture ethanol - water, the result show the following feature: There is no limit entrainer - feed flow rate ratio for recovery of component water(B)but existing $(F_E/F)_{max,A}$ for component ethanol(A) because the extractive stable node to get B ($SN_{extr,B}$) can be located at any position on the edge B-E (resp. A-E) whereas the extractive stable node $SN_{extr,A}$ needs to be located in the region where A is the least volatile. That maximum gradually reduces as reboil ratio gets smaller, until it reaches a minimum reboil ratio. A detailed calculation of the profile map (not shown) demonstrated that the feasible stripping section profiles region gets smaller until it can no longer intersect the extractive profile region. When aiming to get water (B) as bottom product, the result shows no limit for the entrainer - feed flow rate ratio in batch as expected and in continuous mode as well. For both products, there exists a minimum reboil ratio as an unstable extractive separatrix reduces the feasible region when the reboil ratio decreases. The continuous mode displays the same features than the batch process.

Regarding case b illustrated with the ternary system methyl ethyl ketone (A) – benzene (B) using entrainer acetone, the behavior is symmetrical the aiming to have bottom product methyl ethyl ketone (A) bears symmetrical feature with case a aiming to recover water (B) at the bottom, but then aiming to benzene (B) has a $(F_E/F)_{max,B}$ as the univolatility curve $\alpha_{AB} = 1$ now reaches B-E edge.

Analyzing the azeotropic and extractive processes for 1.0-2 class, we can state that both are eligible to get A or B as products because A and B are stable nodes of the residue curve map. In batch mode, it was shown in the literature that the extractive process could enable to cross the rcm distillation boundary of the MEK-benzene mixture with acetone and thus offer a larger composition region to obtain MEK as a product. However we could not verify nor invalidate this in continuous mode by rigorous simulation which is subject to the lever rule and to an additional requirement for the process to be feasible.

A possible advantage of using a light entrainer is to give more opportunities to separating minT and maxT azeotropic mixtures when it may be not easy to find a heavy or intermediate entrainer. In perspective,

it could be interesting to evaluate the possible energy gain of the whole process, the extractive distillation column and the regeneration column, compared to the use of a heavy entrainer.

As these observations for the class 1.0-2 or 1.0-1a are corroborated by rigorous simulations, we demonstrate that feasibility analysis based on simple thermodynamic insight (the ternary class, the univolatility line intersect with the diagram) can be exploited to evaluate the feasibility under finite reflux ratio and both for batch and continuous operation.

5.2 PERSPECTIVE

A future work in the area of feasibility study on extractive distillation may treat some of the following topics:

1. The batch extractive process insight to the continuous process could be extended to other Serafimov's topological Classes that were found feasible in batch mode (1.0-1b, 0.0-1, 2.0-1, 2.0-2a, 2.02b, 2.02c, and 3.1-2). Heterogeneous extractive distillation could also be considered, first in batch then in continuous.
2. The experimental validation of the ternary system separating process results described in chapter 3 and 4 for both batch and continuous column could provide insight into more practical issues regarding to the operation of the columns. In that case one should undertake preliminary validation of the thermodynamic properties predicted in this work by using the UNIFAC model.
3. The optimization of the process should also provide a more comprehensive overview of the advantages and drawbacks for each column configuration. More specifically, it would be interesting to investigate more systematically during the feasibility analysis of the continuous process the effect of other parameters like the feed composition location, the feed physical state.
4. The optimization of the continuous process sequence, including both the extractive distillation column and the entrainer regeneration column should be considered to study the overall process energy consumption. This should be related to the entrainer design issue as the entrainer should not only make the process of extractive column feasible but also be easily regenerated from the non-product component in the regeneration column.

CHAPTER

APPENDIX

Appendix: nomenclature, reference

6.1 NOMENCLATURE

A	light original component
\underline{ABE}	Volatility orders, A is possible distillate
AzAB	binary azeotrope of the two original components A and B
AzEA	binary azeotrope of the entrainer and the original component A
AzEAB	ternary azeotrope of the entrainer and the original components A and B
B	heavy original Component
BED	batch extractive distillation column
BED-B	batch extractive distillation column supply solvent to bottom section
BED-I	batch extractive distillation column supply solvent to intermediate section
BED-T	batch extractive distillation column supply solvent to top vessel
BES	batch extractive distillation in a batch stripper
BES-B	batch extractive distillation in a batch stripper supply solvent to bottom section
BES-I	batch extractive distillation in a batch stripper solvent to intermediate section
BES-T	batch extractive distillation in a batch stripper solvent to top vessel
C	the third parameter C of the relationship of Antoine [mmHg °C]
D	distillate flow [mol / h]
DWC	dividing wall column
DMF	dimethylformamide
E	entrainer
EDA	ethylenediamine
EtOH	ethanol
Extr	extraction section
F	feed flow rate ratio [mol / h]
F_E	entrainer - feed flow rate ratio
F_E/F	entrainer - feed flow rate ratio, continuous process
F_E/V	entrainer - feed flow rate ratio, batch process
$(F_E/V)_{\min}$	minimum entrainer - feed flow rate ratio, batch process
$(F_E/V)_{\max}$	maximum entrainer - feed flow rate ratio, batch process
H^v	vapor enthalpy
h^l	liquid enthalpy
HIDiC	highly integrated distillation columns
K_i	distribution coefficient
L	liquid flow rate ratio [mol / h]
L_e	extractive section liquid flow rate ratio
L_s	stripping extractive section liquid flow rate ratio
L_T	boiling liquid at top vessel
MIBK	methyl isobutyl ketone
MEK	methyl ethyl ketone

MESH	material, equilibrium, summation and enthalpy equation
MeAC	methyl acetate
MeOH	methanol
N	number of theoretical stages
N_{FE}	entrainer feed stages
N_F	original mixture feed stages
p	pressure [Hgmm] [atm]
Q_n	heat input [kW]
R	reflux ratio
R_{max}	maximum reflux ratio
R_{min}	minimum reflux ratio
RCM	residue curve map
RD	reactive distillation
$[SN_{extr}]$	extractive node feasible range
S	reboil ratio
S_1	saddle originating at the "product" vertex
S_2	saddle originating at the "nonproduct" vertex
SBD	solvent- enhanced batch distillation
SN	stable node originating at the azeotrope
SN'	stable node originating outside the composition simplex
Str	stripping section
T	temperature [°C]
$T_{maxazeAB}$	the maximum azeotrope point of mixture AB
$T_{minazeAB}$	the minimum azeotrope point of mixture AB
UN	unstable node originating at the entrainer vertex
UN'	unstable node originating outside the composition simplex
V	vapors flows [kmol h ⁻¹]
W	bottom product flow rate ratio [mol / h]
$x_{azeo,A}$	composition of A in azeotrope mixture
x_D	distillate fraction
x_i	liquid mole fraction of component i
x_F	original mixture liquid mole fraction
x_E	entrainer liquid mole fraction
x_F+x_E	original mixture and entrainer mass balance point
x_p	intersection point between univolatility curve and residue curve passing through the distillate product
x_W	residue mole fraction
$Y_{u,n}$	unfeasible operating parameter point
$Y_{f,n}$	feasible operating parameter point
y^*	vapor phase composition in equilibrium with x
y_i	vapor mole fraction of component i

Greek letters

α_{ij}	volatility of component i relative to component j
γ_i	activity coefficient of component i
τ	binary interaction parameter in NRTL model
η	recovery rate [%]

Subscripts

i	stage index
j	component index
min	minimum value
T	top (decanter) vessel
m	middle section or middle section map
r	rectifying section or rectifying map
s	stripping section or stripping map
Heavy	heavy (least volatile) component
light	light (most volatile) component
N	section stages

Explanation of Figures

●	stable node of the distillation line map
○	unstable node of the distillation line map
Δ	saddle point of the distillation line map
————	composition profile
-----	continuous feasible line
-----	batch feasible line
—■—■—	simulated rectifying composition profile
—○—○—	simulated extractive composition profile
—▲—▲—	simulated stripping composition profile
— . . .	extractive and stripping separatrix
— . —	residue curve map separatrix
- - -	univolatility line

6.2 REFERENCES

A

Aspen Plus 11.1 User Guide, 2001. Available at <http://www.aspentech.com> (last accessed Feb. 2012), 2010.

B

Barreto A. A., I. Rodriguez-Donis, V. Gerbaud, and X. Joulia, Optimization of heterogeneous batch extractive distillation. In press available at <http://pubs.acs.org/doi/abs/10.1021/ie101965f>.

Barreto, A.A., Rodriguez-Donis, I., Gerbaud, V., Joulia, X., 2011. Optimization of Heterogeneous Batch Extractive Distillation. *Industrial & Engineering Chemistry Research* 50, 5204–5217.

Bausa, J., Watzdorf, R., Marquardt, W., 1998. Shortcut methods for non ideal multicomponent distillation: I. Simple columns. *AIChE Journal* 44, 2181–2198.

Berg, L., Station, M.S.C.E.E., 1948. Azeotropic distillation. Montana State College.

Bernot, C., Doherty, M.F., Malone, M.F., 1990. Patterns of composition change in multicomponent batch distillation. *Chemical Engineering Science* 45, 1207–1221.

Bernot, C., Doherty, M.F., Malone, M.F., 1991. Feasibility and separation sequencing in multicomponent batch distillation. *Chemical engineering science* 46, 1311–1326.

Brüggemann, S., Marquardt, W., 2002. Shortcut design of extractive distillation columns. *Distillation and Absorption, Baden-Baden, September 30-October 2*.

Brüggemann, S., Marquardt, W., 2004. Shortcut methods for non ideal multicomponent distillation: 3. Extractive distillation columns. *AIChE Journal* 50, 1129–1149.

C

Chein-Hsiun, T., 1994. Group-contribution method for the estimation of vapor pressures. *Fluid Phase Equilibria* 99, 105–120.

Cheong, W., Barton; P., 1999. Azeotropic Distillation in a Middle Vessel Batch Column. 1. Model Formulation and Linear Separation Boundaries. *Industrial & Engineering Chemistry Research* 38, 1504–1530.

D

Davidyan, A.G., Kiva, V.N., Meski, G.A., Morari, M., 1994. Batch distillation in a column with a middle vessel. *Chemical engineering science* 49, 3033–3051.

Demicoli, D., Stichlmair, J., 2003. Novel operational strategy for the separation of ternary mixtures via cyclic operation of a batch distillation column with side withdrawal. *Computer Aided Chemical Engineering* 14, 629–634.

Denes, F., Lang, P., Modla, G., Joulia, X., 2009. New double column system for heteroazeotropic batch distillation.

Computers & Chemical Engineering 33, 1631–1643.

Doherty, M.F., Calderola, G.A., 1985. Design and synthesis of homogeneous azeotropic distillations. 3. The sequencing of columns for azeotropic and extractive distillations. *Industrial & engineering chemistry fundamentals* 24, 474–485.

Doherty, Michael F., Malone, M.F., 2001. *Conceptual Design of Distillation Systems*, Available at: <http://148.201.96.14/dc/ver.aspx?ns=000157102> [Accessed February 10, 2012].

Donald, M.B., Ridgway, K., 1958. The binary systems benzene-ethyl methyl ketone and benzene-cyclohexane. *Journal of Applied Chemistry* 8, 403–407.

Düssel, R., Stichlmair, J., 1995. Separation of azeotropic mixtures by batch distillation using an entrainer. *Computers & Chemical Engineering* 19, Supplement 1, 113–118.

E

Ewell, R., Harrison, J., Berg, L., 1944. Azeotropic distillation. *Industrial & Engineering Chemistry* 36, 871–875.

F

Fidkowski, Z., Doherty, M.F., Malone, M.F., 1993. Feasibility of separations for distillation of non ideal ternary mixtures. *AIChE Journal* 39, 1303–1321.

Fien, G.-J.A.F., Liu, Y.A., 1994. Heuristic synthesis and shortcut design of separation processes using residue curve maps: a review. *Ind. Eng. Chem. Res.* 33, 2505–2522.

Forbes, R.J., 1970. *A short history of the art of distillation: from the beginnings up to the death of Cellier Blumenthal*, BRILL.

Foucher, E.R., Doherty, M.F., Malone, M.F., 1991. Automatic screening of entrainers for homogeneous azeotropic distillation. *Industrial & Engineering Chemistry Research* 30, 760–772.

Frits, E.R., Lelkes, Z., Fonyó, Z., Rév, E., Markót, M.C., Csendes, T., 2006. Finding limiting flows of batch extractive distillation with interval arithmetic. *AIChE Journal* 52, 3100–3108.

Fukushima, T., Kano, M., Hasebe, S., 2006. Dynamics and Control of Heat Integrated Distillation Column (HIDiC). *Journal of Chemical Engineering of Japan* 39, 1096–1103.

G

Geankoplis, C. 2003. *Transport Processes and Separation Process Principles*, 4th Edition. Prentice Hall.

Gerbaud, V., I. Rodriguez-Donis I., 2010, *Distillation de mélanges non idéaux. Courbes de résidu et autres outils de conception*. Dossier J2 611. de la collection “Techniques de l’ingénieur”, Procédés chimie - bio – agro. Opérations unitaires. Génie de la réaction chimique. Opérations Unitaires. Distillation et absorption. Ed. Tissot, Paris, 2010

Gerbaud, V., I. Rodriguez-Donis I., 2010, *Distillation de mélanges non idéaux. Distillation azéotropique et distillation extractive. Choix de l’entraîneur* Dossier J2 612. de la collection “Techniques de l’ingénieur” Procédés chimie - bio – agro. Opérations unitaires. Génie de la réaction chimique. Opérations Unitaires. Distillation et

absorption. Ed. Tissot, Paris.

Gmehling, J., Li, J., Schiller, M., 1993. A modified UNIFAC model. 2. Present parameter matrix and results for different thermodynamic properties. *Industrial & Engineering Chemistry Research* 32, 178–193.

Gmehling, J., Onken, U., Rarey-Nies, J.R., 1978. Vapor-liquid equilibrium data collection. Dechema.

Gmehling, J., Menke, J., Krafczyk, J., Fischer K. Azeotropic data, 2004, 1992 pages, Wiley VCH.

H

Halvorsen, I.J., Skogestad, S., 2011. Energy efficient distillation. *Journal of Natural Gas Science and Engineering* 3, 571–580.

Hilmen, E., Kiva, V., Skogestad, S., 2003. Topology of ternary VLE diagrams: elementary cells. *AIChE Journal* 48, 752–759.

Hilmen, E.K., 2000. Separation of azeotropic mixtures: tools for analysis and studies on batch distillation operation. Norwegian University of Science and Technology: PhD Thesis.

Hua, C., Li, X., Xu, S., Bai, P., 2007. Design and operation of batch extractive distillation with two reboilers. *Chinese Journal of Chemical Engineering* 15, 286–290.

Hunek, J., Gal, S., Posel, F., Glavič, P., 1989. Separation of an azeotropic mixture by reverse extractive distillation. *AIChE Journal* 35, 1207–1210.

J

Jiménez, L., Wanhschafft, O., Julka, V., 2001. Analysis of residue curve maps of reactive and extractive distillation units. *Computers & Chemical Engineering* 25, 635–642.

Jogwar, S.S., Daoutidis, P., 2009. Dynamics and control of vapor recompression distillation. *Journal of Process Control* 19, 1737–1750.

Jogwar, S.S., Baldea, M., Daoutidis, P., 2009. Dynamics and Control of Process Networks with Large Energy Recycle. *Industrial & Engineering Chemistry Research* 48, 6087–6097.

Julka, V., Doherty, M. F. 1993. Geometric nonlinear analysis of multicomponent non ideal distillation: a simple computer-aided design procedure. *Chemical Engineering Science* 48, 1367–1391. doi:10.1016/0009-2509(93)80045-R.

K

Kaibel, G., 1987. Distillation columns with vertical partitions. *Chemical Engineering & Technology* 10, 92–98.

Kiva, V., Hilmen, E., Skogestad, S., 2003. Azeotropic phase equilibrium diagrams: a survey. *Chemical Engineering Science* 58, 1903–1953.

Knapp, J.P., Doherty, M.F., 1990. Thermal integration of homogeneous azeotropic distillation sequences. *AIChE Journal*, 36, 969-983.

Knapp, J.P., Doherty, M.F., 1992. A new pressure-swing-distillation process for separating homogeneous

azeotropic mixtures. *Industrial & engineering chemistry research* 31, 346–357.

Knapp, J.P., Doherty, M.F., 1994. Minimum entrainer - feed flows for extractive distillation: A bifurcation theoretic approach. *AIChE Journal* 40, 243–268.

Kontogeorgis, G.M., Folas, G.K., 2010. *Thermodynamic Models for Industrial Applications: From Classical and Advanced Mixing Rules to Association Theories*. John Wiley & Sons.

Kossack, S., Kraemer, K., Gani, R., Marquardt, W., 2008. A systematic synthesis framework for extractive distillation processes. *Chemical Engineering Research and Design* 86, 781–792.

L

Lang, P., Yatim, H., Moszkowicz, P., Otterbein, M., 1994. Batch extractive distillation under constant reflux ratio. *Computers & chemical engineering* 18, 1057–1069.

Lang, P., Lelkes, Z., Otterbein, M., Benadda, B., Modla, G., 1999. Feasibility studies for batch extractive distillation with a light entrainer. *Computers & Chemical Engineering* 23, S93–S96.

Lang, P., Modla, G., Benadda, B., Lelkes, Z., 2000a. Homoazeotropic distillation of maximum azeotropes in a batch rectifier with continuous entrainer feeding I. Feasibility studies. *Computers & Chemical Engineering* 24, 1665–1671.

Lang, P., Modla, G., Kotai, B., Lelkes, Z., Moszkowicz, P., 2000b. Homoazeotropic distillation of maximum azeotropes in a batch rectifier with continuous entrainer feeding II. Rigorous simulation results. *Computers & Chemical Engineering* 24, 1429–1435.

Lang, P., Modla, G., 2006. Generalised method for the determination of heterogeneous batch distillation regions. *Chemical engineering science* 61, 4262–4270.

Laroche, L., Bekiaris, N., Andersen, H.W., Morari, M., 1992. The curious behavior of homogeneous azeotropic distillation—implications for entrainer selection. *AIChE Journal* 38, 1309–1328.

Lei, Z., Chen, B., Ding, Z., 2005. *Special distillation processes*, Elsevier.

Lelkes, Z., Lang, P., Benadda, B., Moszkowicz, P., 1998. Feasibility of extractive distillation in a batch rectifier. *AIChE Journal* 44, 810–822.

Lelkes, Z., Lang, P., Moszkowicz, P., Benadda, B., Otterbein, M., 1998. Batch extractive distillation: the process and the operational policies. *Chemical Engineering Science* 53, 1331–1348.

Lelkes, Z., Rev, E., Steger, C., Fonyo, Z., 2002. Batch extractive distillation of maximal azeotrope with middle boiling entrainer. *AIChE Journal* 48, 2524–2536.

Lelkes, Z., Rev, E., Steger, C., Varga, V., Fonyo, Z., Horvath, L., 2003. Batch extractive distillation with intermediate boiling entrainer, in: *European Symposium on Computer Aided Process Engineering-13 36th European Symposium of the Working Party on Computer Aided Process Engineering*. Elsevier, pp. 197–202.

Levy, S.G., Van Dongen, D.B., Doherty, M.F., 1985. Design and synthesis of homogeneous azeotropic distillations. 2. Minimum reflux ratio calculations for non ideal and azeotropic columns. *Ind. Eng. Chem. Fund.* 24, 463–474.

Levy, S.G., Doherty, M.F., 1986. Design and synthesis of homogeneous azeotropic distillations. 4. Minimum reflux

ratio calculations for multiple-feed columns. *Industrial & engineering chemistry fundamentals*. 25, 269–279.

Lewis, G.N., Cornish, R.E., 1933. Separation of the isotopic forms of water by fractional distillation. *Journal of the American Chemical Society* 55, 2616–2617.

Lucia, A., Amale, A., Taylor, R., 2008. Distillation pinch points and more. *Computers & Chemical Engineering* 32, 1342–1364.

Luyben, W.L. & Chien, I.L., 2001a. Design and control of distillation systems for separating azeotropes, Wiley Online Library.

Luyben, W.L., 2008a. Effect of solvent on controllability in extractive distillation. *Industrial & Engineering Chemistry Research* 47, 4425–4439.

Luyben, W.L., 2008b. Comparison of extractive distillation and pressure-swing distillation for acetone-methanol separation. *Industrial & Engineering Chemistry Research* 47, 2696–2707.

Luyben, W.L., 2008c. Control of the maximum-boiling acetone/chloroform azeotropic distillation system. *Industrial & Engineering Chemistry Research* 47, 6140–6149.

Luyben, W.L., Yu, C.-C., 2009. *Reactive Distillation Design and Control*. John Wiley & Son.

Luyben, W.L., Chien, I.L., 2010. Design and control of distillation systems for separating azeotropes. Wiley Online Library.

M

Malone, M.F., Doherty, M.F., 2000. Reactive distillation. *Industrial & Engineering Chemistry Research* 39, 3953–3957.

Marrero, J., Gani, R., 2001. Group-contribution based estimation of pure component properties. *Fluid Phase Equilibria* 183–184, 183–208.

Matsuyama H., Nishimura, H., 1977. Topological and thermodynamic classification of ternary vapor-liquid equilibria. *Journal of Chemical Engineering of Japan* 10.

Modla, G., Lang, P., 2008. Feasibility of new pressure swing batch distillation methods. *Chemical Engineering Science* 63, 2856–2874.

Modla, G., Lang, P., Denes, F., 2010. Feasibility of separation of ternary mixtures by pressure swing batch distillation. *Chemical Engineering Science* 65, 870–881.

Modla, G., 2010. Pressure swing batch distillation by double column systems in closed mode. *Computers & Chemical Engineering* 34, 1640–1654.

Modla, G., 2011. Separation of a Chloroform-Acetone-Toluene mixture by pressure-swing batch distillation in different column configurations. *Industrial & Engineering Chemistry Research*.

Muhrer, C.A., Collura, M.A., Luyben, W.L., 1990. Control of vapor recompression distillation columns. *Industrial & Engineering Chemistry Research* 29, 59–71.

N

Naito K., Nakaiwa M., Huang K., Endo A., Aso K., Nakanishi T., Nakamura T., Noda H., Takamatsu T., 2000. Operation of a bench-scale ideal heat integrated distillation column (HIDiC): an experimental study. *Computers and Chemical Engineering* 24, 495–499.

Nakaiwa, M., Huang, K., Naito, K., Endo, A., Owa, M., Akiya, T., Nakane, T., Takamatsu, T., 2000. Parameter analysis and optimization of ideal heat integrated distillation columns (HIDiC), *European Symposium on Computer Aided Process Engineering-10*. Elsevier, 661–666.

Nakaiwa M., Huang K., Naito K., Endo A., Akiya T., Nakane T., Takamatsu T., 2001. Parameter analysis and optimization of ideal heat integrated distillation columns. *Computers & Chemical Engineering* 25, 737-744.

Nakaiwa M., Huang K., Endo A., Ohmori T., Akiya T., Takamatsu T., 2003. Internally heat-integrated distillation columns: a review. *Chemical Engineering Research and Design*. 81(1), 162-177.

P

Petlyuck F.B. 2004. *Distillation Theory and Its Application to Optimal Design of Separation Units*. Cambridge University Press, Cambridge, ISBN 978-0-521-82092-8.

Petlyuk F., Danilov R., Skouras S., Skogestad S., 2011. Identification and analysis of possible splits for azeotropic mixtures. 2. Method for column sections. *Chemical Engineering Science* 66, 2512-2522.

Petlyuk, F., Danilov, R., Skouras, S., Skogestad, S., 2012. Identification and analysis of possible splits for azeotropic mixtures. 2. Method for simple columns. *Chemical Engineering Science* 69, 159–169.

Pham, H.N., Ryan, P.J., Doherty, M.F., 1989. Design and minimum reflux ratio for heterogeneous azeotropic distillation columns. *AIChE Journal* 35, 1585–1591.

Pham, H.N., Doherty, M.F., 1990a. Design and synthesis of heterogeneous azeotropic distillations—II. Residue curve maps. *Chemical Engineering Science* 45, 1837–1843.

Pham, H.N., Doherty, M.F., 1990b. Design and synthesis of heterogeneous azeotropic distillations—III. Column sequences. *Chemical Engineering Science* 45, 1845–1854.

Phimister, J.R., Seider, W.D., 2000. Semicontinuous, pressure-swing distillation. *Industrial & engineering chemistry research* 39, 122–130.

Poellmann, P., Blass, E., 1994. Best products of homogeneous azeotropic distillations. *Gas separation & purification* 8, 194–228.

Pommier, S., Massebeuf, S., Kotai, B., Lang, P., Baudouin, O., Floquet, P., Gerbaud, V., 2008. Heterogeneous batch distillation processes: Real system optimisation. *Chemical Engineering and Processing: Process Intensification* 47, 408–419.

Pretel, E.J., Lopez, P.A., Bottini, S.B., Brignole, E.A., 1994. Computer-aided molecular design of solvents for separation processes. *AIChE Journal* 40, 1349–1360.

Prosim Plus 3.1 User guide available at <http://www.prosim.net> (last accessed Feb. 2012), 2009.

R

Repke, J.-U., Klein, A., Bogle, D., Wozny, G., 2007. Pressure Swing Batch Distillation for Homogeneous Azeotropic Separation. *Chemical Engineering Research and Design* 85, 492–501.

Reshetov, S.A., Kravchenko, S.V., 2007. Statistics of liquid-vapor phase equilibrium diagrams for various ternary zeotropic mixtures. *Theoretical Foundations of Chemical Engineering* 41, 451–453.

Rév, E., Lelkes, Z., Varga, V., Stéger, C., Fonyo, Z., 2003. Separation of a minimum-boiling azeotrope in a batch extractive rectifier with an intermediate-boiling entrainer. *Industrial & engineering chemistry research* 42, 162–174.

Robbins, L., 2011. *Distillation control, optimization, and tuning : fundamentals and strategies*. CRC Press, Boca Raton, FL.

Robinson, C.S., Gilliland, E.R., 1950. *Elements of fractional Distillation*. McGra-Hill New York.

Rodríguez-Donis, I., Gerbaud, V., Joulia, X., 2001a. Entrainer selection rules for the separation of azeotropic and close-boiling-temperature mixtures by homogeneous batch distillation process. *Industrial & engineering chemistry research* 40, 2729–2741.

Rodríguez-Donis, I., Gerbaud, V., Joulia, X., 2001b. Heterogeneous entrainer selection for the separation of azeotropic and close boiling temperature mixtures by heterogeneous batch distillation. *Industrial & engineering chemistry research* 40, 4935–4950.

Rodríguez Donis, I., Gerbaud, V., Joulia, X., 2002. Feasibility of heterogeneous batch distillation processes. *AIChE Journal* 48, 1168–1178.

Rodríguez-Donis, I., Esquijarosa, J.A., Gerbaud, V., Joulia, X., 2003. Heterogeneous batch-extractive distillation of minimum boiling azeotropic mixtures. *AIChE Journal* 49, 3074–3083.

Rodríguez-Donis, I., Papp, K., Rev, E., Lelkes, Z., Gerbaud, V., Joulia, X., 2007. Column configurations of continuous heterogeneous extractive distillation. *AIChE Journal* 53, 1982–1993.

Rodríguez-Donis, I., Gerbaud, V., Joulia, X., 2009a. Thermodynamic Insights on the Feasibility of Homogeneous Batch Extractive Distillation, 1. Azeotropic Mixtures with a Heavy Entrainer. *Industrial & Engineering Chemistry Research* 48, 3544–3559.

Rodríguez-Donis, I., Gerbaud, V., Joulia, X., 2009b. Thermodynamic Insights on the Feasibility of Homogeneous Batch Extractive Distillation, 2. Low-Relative-Volatility Binary Mixtures with a Heavy Entrainer. *Industrial & Engineering Chemistry Research* 4, 3560–3572.

Rodríguez-Donis, I., Gerbaud, V., Joulia, X., 2010. Thermodynamic insight on extractive distillation with entrainer forming new azeotropes. In *Proceedings of Distillation & absorption 2010*, Eindhoven, Holland, September 12-15, 431436.

Rodríguez-Donis, I., Gerbaud, V., Joulia, X., 2012a. Thermodynamic Insights on the Feasibility of Homogeneous Batch Extractive Distillation. 3. Azeotropic Mixtures with Light Entrainer. *Industrial & engineering chemistry research* 51, 4643-4660.

Rodríguez-Donis, I., Gerbaud, V., Joulia, X., 2012b. Thermodynamic Insights on the Feasibility of Homogeneous. Batch Extractive Distillation. 4. Azeotropic Mixtures with Intermediate Boiling Entrainer. *Industrial & engineering*

chemistry research 51, 6489–6501.

S

S.E., A., 1984. Energy savings in distillation plants by using vapor thermo-compression. *Desalination* 49, 37–56.

Seader, J. D., Henley, Ernest J., Seader, J.D., 1998. *Separation Process Principles*. Wiley, New York.

Serafimov, L., 1970a. General Principles of the Course of Unidistribution Lines in Vapor-Liquid Equilibrium Diagrams of Ternary Mixtures. *Physical-Chemical Foundations of Rectification, Collection of papers by Moscow Lomonosov Institute of Fine Chemical Technology, MITChT, Moscow* 20–30.

Serafimov, L., 1970b. The azeotropic rule and the classification of multicomponent mixtures VII. Diagrams for ternary mixtures. *Russ. J. Phys. Chem* 44, 567–571.

Serafimov, L., Gol'berg, Y.E., Vitman, T., Kiva, V., 1972. Properties of univolatility sets and its location in the concentration space In *Chemistry. Collection of the Scientific Works of Ivanovo Energetic Institute, Ivanovo-Vladimir* 166–179.

Serafimov, L., Timofeev, V., Balashov, M., 1973. Rectification of Multicomponent Mixtures II. Local and General Characteristics of the Trajectories of Rectification Processes at Infinite Reflux ratio. *Acta Chemica Acad. Sci. Hung* 75, 193–211.

Serafimov, L., 1996. Thermodynamic and Topological Analysis of Liquid-Vapor Phase Equilibrium Diagrams and Problems of Rectification of Multicomponent Mixtures. *Mathematical methods in contemporary chemistry* 557.

Simulis Thermodynamics, Documentation available at <http://www.prosim.net>

Skouras, S., Kiva, V., Skogestad, S., 2005. Feasible separations and entrainer selection rules for heteroazeotropic batch distillation. *Chemical engineering science* 60, 2895–2909.

Skouras, S., Skogestad, S., Kiva, V., 2005. Analysis and control of heteroazeotropic batch distillation. *AIChE Journal* 51, 1144–1157.

Song, J., Song, H.-H., 2008. Computer-Aided Molecular Design of Environmentally Friendly Solvents for Separation Processes. *Chemical Engineering & Technology* 31, 177–187.

Sorensen, E., 1999. A cyclic operating policy for batch distillation-theory and practice. *Computers & chemical engineering* 23, 533–542.

Stéger, C., Varga, V., Horvath, L., Rev, E., Fonyo, Z., Meyer, M., Lelkes, Z., 2005. Feasibility of extractive distillation process variants in batch rectifier column. *Chemical engineering and processing* 44, 1237–1256.

Szanyi, A., Mizsey, P., Fonyo, Z., 2004. Novel hybrid separation processes for solvent recovery based on positioning the extractive heterogeneous-azeotropic distillation. *Chemical engineering and processing* 43, 327–338.

T

Tamayo-Galván, V.E., Segovia-Hernández, J.G., Hernández, S., Hernández, H., 2008. Controllability analysis of

modified Petlyuk structures. *The Canadian Journal of Chemical Engineering* 86, 62–71.

Thomas, B., Karl Hans, S., 1994. Knowledge integrating system for the selection of solvents for extractive and azeotropic distillation. *Computers & Chemical Engineering* 18, Supplement 1, 25–29.

U

Ulrich, J., Morari, M., 2003. Operation of Homogeneous Azeotropic Distillation Column Sequences. *Industrial & Engineering Chemistry Research* 42, 4512–4534.

Underwood, A., 1949. Fractional distillation of multicomponent mixtures. *Industrial & Engineering Chemistry* 41, 2844–2847.

Urdaneta, R.Y., Bausa, J., Brüggemann, S., Marquardt, W., 2002. Analysis and conceptual design of ternary heterogeneous azeotropic distillation processes. *Industrial & engineering chemistry research* 41, 3849–3866.

V

Van Dongen, D.B., Doherty, M.F., 1985. On the dynamics of distillation processes–VI. Batch distillation. *Chemical engineering science* 40, 2087–2093.

Van Dyk, B., Nieuwoudt, I., 2000. Design of Solvents for Extractive Distillation. *Industrial & Engineering Chemistry Research* 39, 1423–1429.

Van Kaam, R., Rodriguez-Donis, I., Gerbaud, V., 2008. Heterogeneous extractive batch distillation of chloroform-methanol-water: Feasibility and experiments. *Chemical engineering science* 63, 78–94.

Varga, V. 2006. *Distillation Extractive Discontinue dans une Colonne de Rectification et dans une Colonne Inverse*. Ph.D. Thesis, Toulouse.

Varga, V., Rev, E., Gerbaud, V., Fonyo, Z., Joulia, X., 2006. Batch extractive distillation with light entrainer. *Chemical Biochemical Engineering Quarterly* 20, 1–23.

Vidal, J., 2003. *Thermodynamics: Applications in Chemical Engineering and the Petroleum Industry*. Editions OPHRYS.

W

Wahnschafft, O.M., Koehler, J., Blass, E., Westerberg, A.W., 1992. The product composition regions of single-feed azeotropic distillation columns. *Industrial & engineering chemistry research* 31, 2345–2362.

Wahnschafft, O.M., Westerberg, A.W., 1993. The product composition regions of azeotropic distillation columns. 2. Separability in two-feed columns and entrainer selection. *Industrial & engineering chemistry research* 32, 1108–1120.

Weidlich, U., Gmehling, J., 1987. A modified UNIFAC model. 1. Prediction of VLE, hE, and γ_{∞} . *Industrial & engineering chemistry research* 26, 1372–1381.

Weis, D.C., Visco, D.P., 2010. Computer-aided molecular design using the Signature molecular descriptor: Application to solvent selection. *Computers & Chemical Engineering* 34, 1018–1029.

Widagdo S. and Seider W.D. 1996. Azeotropic distillation. *AIChE Journal*, 42, 96-146.

Repke, J.-U., A. Klein, D. Bogle, G. Wozny. 2007. Pressure Swing Batch Distillation for Homogeneous Azeotropic Separation. *Chemical Engineering Research and Design* 85, 492-501.

Y

Yao, J.Y., Lin, S.Y., Chien, I., 2007. Operation and control of batch extractive distillation for the separation of mixtures with minimum-boiling azeotrope. *Journal of the Chinese Institute of Chemical Engineers* 38, 371–383.

Yatim, H., Moszkowicz, P., Otterbein, M., Lang, P., 1993. Dynamic simulation of a batch extractive distillation process. *Computers & chemical engineering* 17, 57–62.

Abstract

We study the continuous extractive distillation of minimum and maximum boiling azeotropic mixtures A-B with a heavy or a light entrainer E, intending to assess its feasibility based on thermodynamic insights. The ternary mixtures belong to the common 1.0-1a and 1.0-2 class ternary diagrams, each with two sub-cases depending on the univolatility line location. The column has three sections, rectifying, extractive and stripping. Differential equations are derived for each section composition, depending on operating parameters: distillate product purity and recovery, reflux ratio R and entrainer – feed flow rate ratio F_E/F for the heavy case; bottom product purity and recovery, reboil ratio and entrainer – feed flow rate ratio for the light entrainer case. For the case with a heavy entrainer fed as a boiling liquid above the main feed, the feasible product and operating parameters R and F_E/F ranges are assessed under infinite reflux ratio conditions by using the general feasibility criterion enounced by Rodriguez-Donis et al. (Ind. Eng. Chem. Res, 2009, 48(7), 3544–3559). For the 1.0-1a class, there exists a minimum entrainer - feed flow rate ratio to recover the product, and also a minimum reflux ratio. The minimum entrainer - feed flow rate ratio is higher for the continuous process than for the batch because of the additional requirement in continuous mode that the stripping profile intersects with the extractive profile. For the 1.0-2 class both A and B can be distilled. For one of them there exists a maximum entrainer - feed flow rate ratio. The continuous process also has a minimum entrainer - feed flow rate ratio limit for a given feasible reflux ratio.

For the case with a light entrainer fed as saturated vapor below the main feed, the feasible product and operating parameters S and F_E/F ranges are assessed under infinite reflux ratio conditions by using the general feasibility criterion enounced by Rodriguez-Donis et al. (Ind. Eng. Chem. Res, 2012, 51, 4643–4660), Compared to the heavy entrainer case, the main product is removed from the column bottom. Similar results are obtained for the 1.0-1a and 1.0-2 class mixtures whether the entrainer is light or heavy. With a light entrainer, the batch insight about the process feasibility holds for the stripping and extractive sections. Now, an additional constraint in continuous mode comes from the necessary intersection between the rectifying and the extractive sections.

This work validates the proposed methodology for assessing the feasibility of continuous extractive distillation processes and enables to compare entrainers in terms of minimum reflux ratio and minimum entrainer feed flow rate ratio.

Key word

Extractive distillation – feasibility – thermodynamic insight – univolatility line - unidistribution line - reflux ratio – entrainer - feed flow rate ratio – reboil ratio – heavy entrainer – light entrainer

Résumé

Nous étudions la faisabilité du procédé de distillation extractive continue pour séparer des mélanges azéotropiques A-B à température de bulle minimale ou maximale, avec un tiers corps E lourd ou léger. Les mélanges ternaires A-B-E appartiennent aux classes 1.0-1-a et 1.0-2 qui se subdivisent chacune en deux sous-cas selon la position de la courbe d'univolatilité. La colonne de distillation a trois sections, rectification, extractive, épuisement. Nous établissons les équations décrivant les profils de composition liquide dans chaque section en fonction des paramètres opératoires: pureté et taux de récupération du distillat, taux de reflux ratio R et rapport des débits d'alimentation F_E/F dans le cas d'un tiers corps lourd; pureté et taux de récupération du produit de pied, taux de rebouillage S et rapport des débits d'alimentation F_E/F dans le cas d'un tiers corps léger.

Avec un tiers corps lourd alimenté comme liquide bouillant au dessus de l'étage d'alimentation du mélange A-B, nous identifions le distillat atteignable et les plages de valeurs faisables des paramètres R et F_E/F à partir du critère général de faisabilité énoncé par Rodriguez-Donis et al. (Ind. Eng. Chem. Res, 2009, 48(7), 3544–3559). Pour la classe 1.0-1a, il existe des rapport F_E/F et reflux ratio minimum. Le rapport F_E/F est plus important pour le procédé continu que pour le procédé discontinu parce que la faisabilité du procédé continu nécessite que les profils d'épuisement et extractifs s'intersectent. Pour la classe 1.0-2, les deux constituants A et B sont des distillats potentiels, l'un sous réserve que le rapport F_E/F reste inférieur à une valeur limite maximale. Le procédé continu exhibe également une valeur minimale de F_E/F à un taux de reflux ratio donné, contrairement au procédé discontinu.

Avec un tiers corps léger alimenté comme vapeur saturante sous l'étage d'alimentation du mélange A-B, nous identifions le produit de pied atteignable et les plages de valeurs faisables des paramètres S et F_E/F à partir du critère général de faisabilité énoncé par Rodriguez-Donis et al. (Ind. Eng. Chem. Res, 2012, 51, 4643–4660). Comparé au cas des tiers corps lourds, le produit principal est obtenu en pied. Autrement, les comportements des classes 1.0-1a et 1.0-2 sont analogues entre les tiers corps léger et lourd. Avec un tiers corps léger, le procédé continu ajoute la contrainte que les profils de rectification et extractifs s'intersectent. La contrainte d'intersection des profils d'épuisement et extractif est partagée par les deux modes opératoires continu et discontinu.

Ce travail valide la méthodologie proposée pour évaluer la faisabilité du procédé de distillation extractive continue et permet de comparer les tiers entre eux en termes de taux de reflux ratio minimum et de rapport de débit d'alimentation minimal.

Mots-clés

Distillation extractive - courbes d'univolatilité - taux de reflux ratio - taux de solvant - entraîneur lourde - entraîneurlégerère